

THE WILD GOOSE ASSOCIATION



PROCEEDINGS OF THE
TWELFTH ANNUAL TECHNICAL SYMPOSIUM
12-14 OCTOBER 1983
WASHINGTON, D.C.



PUBLISHED BY
THE WILD GOOSE ASSOCIATION
P.O. BOX 556
BEDFORD, MASSACHUSETTS 01730

THE WILD GOOSE ASSOCIATION

The Wild Goose Association (WGA) is a professional organization of individuals and organizations having an interest in loran (long range navigation). It is named after the majestic birds that navigate thousands of miles with unerring accuracy. The WGA was organized in 1972 and its membership now includes hundreds of professional engineers, program managers, scientists and operational personnel from all segments of government industry, and the user community throughout the world, working for the advancement of loran.

CONVENTION COMMITTEE

R. Schellhase Chairman
R. Orr Administration
H. T. Sherman Technical Chairman
R. V. McKeown Hospitality

BOARD OF DIRECTORS 1982-83

C. S. Andren President
E. L. McGann Vice President
L. F. Fehlner Secretary
D. A. Carter Treasurer

J. Alexander
B. Ambroseno
J. Beukers
J. Culbertson
W. Dean
L. Higginbotham
J. Illgen
V. Johnson
J. Van Etten
V. Weihe

BOARD OF DIRECTORS 1983-84

C. S. Andren President
E. L. McGann Vice President
L. F. Fehlner Secretary
D. A. Carter Treasurer

J. Alexander
B. Ambroseno
J. Culbertson
W. Dean
L. Higginbotham
J. Illgen
V. Johnson
A. W. Marchal
J. Van Etten
V. Weihe

TABLE OF CONTENTS

	<u>PAGE</u>
The Session Chairmen	1
Technical Sessions	
Session One	2
Speakers	69
Session Two	70
Speakers	133
Session Three	134
Speakers	147
Session Four	148
Speakers	212
Session Five - Panel Discussion	
Calibration, ASF & Predictability	213
Convention Scene and Awards	215
Registered Attendees	219
Acknowledgements	224

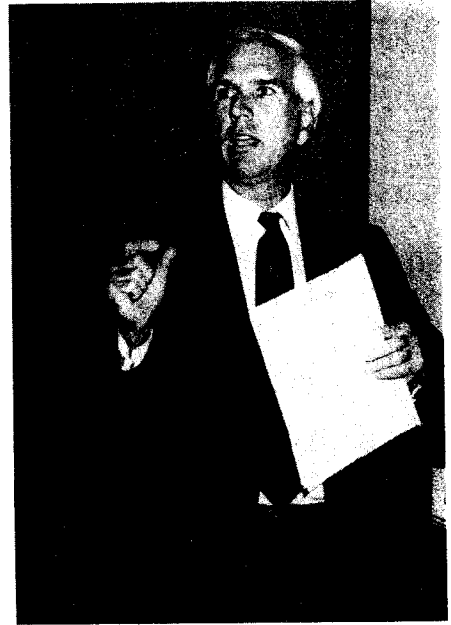
OVER FORTY YEARS OF LORAN-HOW WE GOT TO WHERE WE ARE Walter N. Dean	3
THE U.S. COAST GUARD R&D LORAN-C STABILITY STUDY LT D.S. Taggart	10
A FIRST LOOK AT LORAN-C CALIBRATION DATA IN THE GULF OF MEXICO James R. McCullough, B. Irwin, R. Hayward and R. Bowles	25
VIEWNAV - PRECISION NAVIGATION, PLANNING, AND TACTICAL CONTROL Mortimer Rogoff	68
A QUARTER CENTURY OF LORAN-C Larry Sartin	NA
CONTROL ALGORITHM FOR A RHO-RHO LORAN-C SYSTEM Dr. P. Enge & Mr. M. Poppe	71
DIFFERENTIAL LORAN-C FOR DUOY POSITION CHECKING David Wells & James Rennie	79
OBSERVATIONS OF THE PERFORMANCE OF THE SOUTHEAST U.S. LORAN CHAIN L. Fehlner & T. Jerardi	87
SAUDI ARABIA LORAN-C CHAINS Vernon L. Johnson	119
LORAN-C THE PRESENT AND THE FUTURE CDR N. A. Pealer	126
DESLOT: AN ACCEPTABLE ALTERNATIVE? LTJG R. Orr	135
REMOTE OPERATING SYSTEM - ITS PROMISE; ITS RISK Ens B. Serinis	NA
LORAN-C IN-BAND NOTCH FILTER Ed Bregstone	NA
A FAST UPDATE LORAN RECEIVER USING LOCAL AREA CONVERSION Gerald F. Sage	NA
AUTOMATIC AIRCRAFT/VESSEL TRACKING SYSTEMS William Marchal	137
EVOLUTION OF LORAN-C TIMING TECHNIQUES Laura G. Charron & Carl Lukac	141
LORAN-C SYSTEM MANAGEMENT INFORMATION DATA BASE LT J. R. Iverson	NA
NAVIGATION AVIONICS INTEGRATION WITH LORAN-C J. Leighton & R. Warren	149
THE HISTORY OF LORAN-C CHARTING AT THE NATIONAL OCEAN SERVICE Jeffery Stuart	158
FREQUENCY AND TIME DOMAIN CHARACTERIZATION OF LORAN-C SIGNALS IN THE NEAR FAR FIELD F. W. Mooney & A. D. Frost	186
U.S. BUREAU OF THE CENSUS INVESTIGATION OF LORAN-C APPLICATION TO THE 1990 CENSUS P. Angus, D. Burnham & A. D. Frost	196
LORAN-C: 1983 AND BEYOND LCDR W. J. Thrall	202
LORAN-C CALIBRATION Jack Ligon	206

NA - NOT AVAILABLE FOR PUBLICATION

THE SESSION CHAIRMEN



Dr. Carl Faflick



Bill Marchal



CDR Dave Clememts



Larry Sartin

SESSION ONE

CHAIRMAN

Dr. Carl Faflick
Megapulse

Walter N. Dean
ARNAV Systems, Inc.
4740 Ridge Drive N.E.
Salem, Oregon 97303

ABSTRACT

This paper is a review of the history of Loran-C from the author's point of view. It covers the sometimes devious routes the development of loran and its derivative systems have taken since the inception in 1940.

LORAN ORIGINS

Loran was developed just before World War II, at M.I.T. Radiation Lab, starting in 1942. It was originally conceived as an HF system, similar to British GEE. The designers soon decided that the groundwave propagation necessary for long range navigation could be better obtained at MF. The result was that they took over 160 meter ham band and set up business at 1850 KC.

During the war, loran was used for both sea and air navigation. A typical production shipboard receiver was the DAS-3, and airborne receivers the AN/APN-4 and later AN/APN-9. All these were manually operated, matching pulses on a scope and then counting timing markers to get time differences. Installed in all bombers ferried to Britain, receivers had cabling identical to British GEE, so that loran could be removed and GEE installed easily. Starting in the North Atlantic area, the system was quickly expanded to the Pacific when needed to help air and sea operations there.

Loran was soon providing navigation across most of the North Atlantic and Pacific. Figure 1 shows the groundwave and skywave coverage which was available from about 1945 until

Loran-C took over in the 1970's. Figure 2 shows a commercial Loran-A receiver in 1950 which had the great advance of using a veeder-root counter to read time differences.

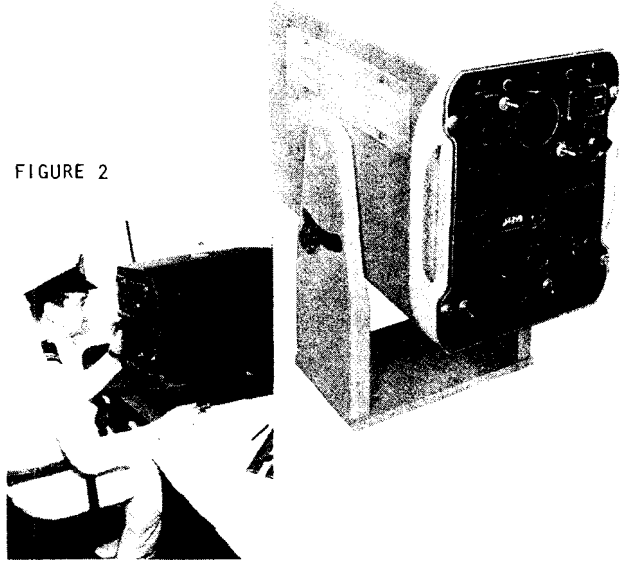


FIGURE 2

Loran has fostered a considerable family of systems, as illustrated by the family tree, Figure 3. A brief description of some of the descendants is in order.



FIGURE 1 Loran-A world coverage map

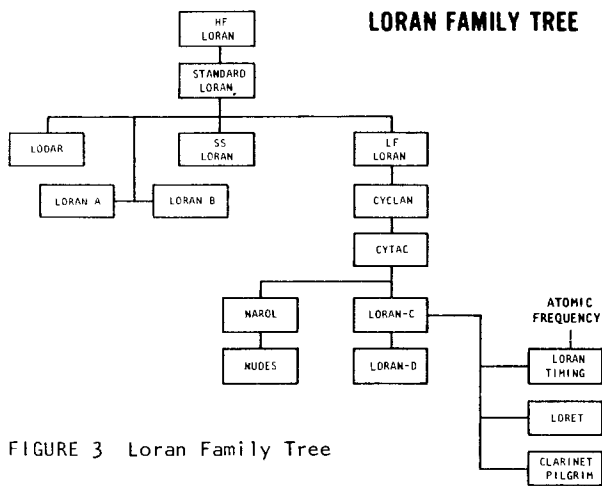


FIGURE 3 Loran Family Tree

Lodar was an experimental use of loran for direction finding. A major problem with HF DF systems was the skywave error, produced by the angular displacement of the skywave. Direction finding on the groundwave loran pulses was considerably more accurate, but use of the system in an angle measuring mode never caught on.

Skywave Synchronized (SS) loran was used to guide bombers over Germany in the later years of WW II. See Figure 4. The transmissions from

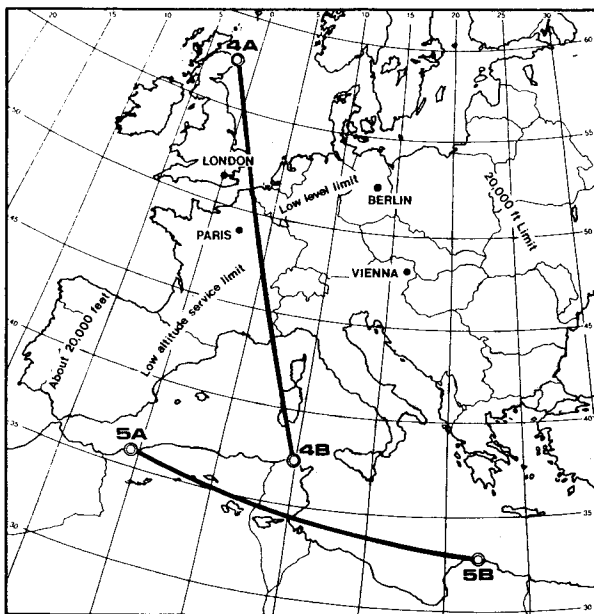


FIGURE 4 Area over which SS Loran was available for air navigation during the winter of 1944-1945 at low level and at 20,000 ft.

Scotland were synchronized by first-hop E skywaves with transmissions from Bizerte, Tunisia. Transmissions from Oran, Algeria, on a different rate, were synched with Appolonia, Libya. Transmission was maintained from about an hour before dusk to an hour before dawn. It is said that the Germans never recognized this use of the loran, and did not try to jam it.

Loran-A is merely a new name for standard loran. Loran-B was an attempt to achieve precise positioning by cycle matching Loran-A. The relatively slow rise time of the pulses made cycle identification too difficult, and the system was abandoned.

Narol, inverse loran, was the technique used for nudes, the nuclear detonation evaluation system, to be described in more detail later.

Loret, loran retransmission, was experimented with at some length, and is used for windfinding.

Other systems on the chart will be discussed in their chronological order.

The fundamental reason for usefulness of standard loran over sea and a reason for the development of LF loran are seen in Figures 5 and 6 which show the field strength versus distance for 2MHz as well as 180 and 100 KHz. Over seawater the practical range of the 2 MHz signals is about 500 nm, compared to 1000 to 1400 for the lower frequencies. Over land, the differences are dramatic - under 100 nm for 2 MHz, vs. 700 to 1000 nm for the lower frequencies.

FIGURE 5 Ground-wave field strength over sea water from 25 kw transmitter

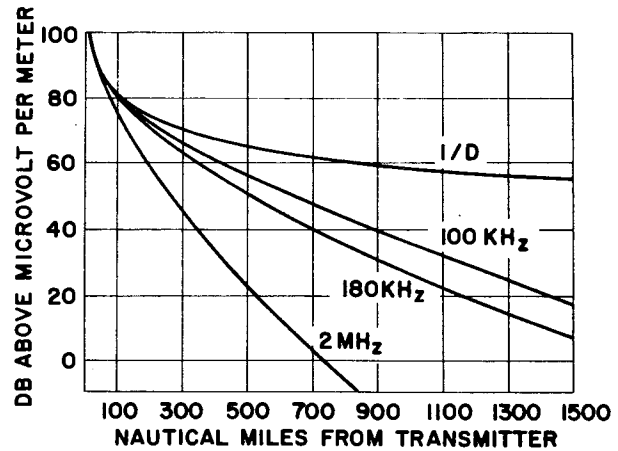
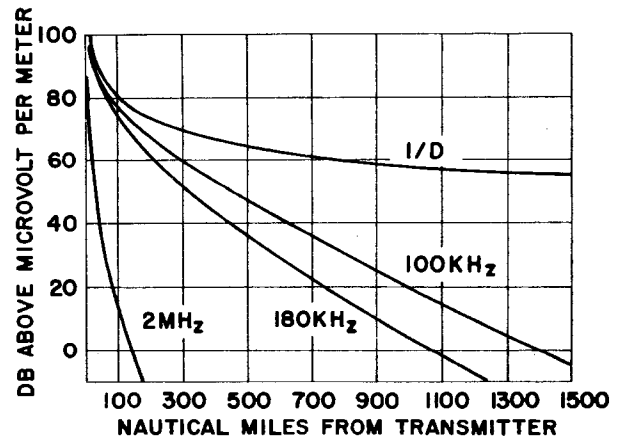


FIGURE 6 Ground-wave field strength over poor earth from 25 kw transmitter



LOW FREQUENCY LORAN

First experiments - better overland ground-wave propagation at LF prompted experimentation with LF loran at 180 KC in 1945. A three station chain was set up on the East Coast of the U.S. and extensive field testing conducted. Attempts were made to obtain accurate time differences by phase matching pulses, but these were troubled by cycle selection errors.

Canadian and Arctic LF loran - USAF operations Musk Ox and Musk Calf in 1946-47 used balloon-supported antennas for transmitters in Canada. Some practical navigation information was obtained. Operation Beetle on the North Arctic coast in 1948 used three transmitters with 625 FT self-supporting towers. Miscalculation of poor conductivity or arctic tundra resulted in inability to sync the slaves at Skull Cliff, Alaska and Cambridge Bay, NWT, from the master at Kittigazuit, NWT. The project was an expensive study of logistics and low frequency propagation in the Arctic.

CYCLAN

In an attempt to circumvent the cycle selection errors of LF loran, Win Palmer in 1946 invented the Cyclan system. This was a 2-frequency system transmitting pulses on 180 and 200 KC which resolved the cycle selection problem by envelope matching on both frequencies. Two dual transmitters were built under USAF sponsorship, and set up at Mackay radio stations at Palo Alto, California and Hillsboro, Oregon, with 10 KW pulse power. For receiving at the stations we used beverage antennas, because the distance between stations made reception marginal. The towers were grounded, and had to be driven through a coupler at the top connected to the top loading elements. The original system used severe band limiting on the transmissions.



FIGURE 7 The receiving equipment in this truck was used to check signals from the first experimental Cyclan system, tested on the Pacific coast.

We were unable to synch at night because of the low power, so 100-KW amplifiers were procured by the Air Force, and the 200 KC output changed to 160 KC to avoid interference. The monitor receiver occupied most of a truck (Figure 7) and performed a number of firsts, including measuring time differences with 23 NS RMS fluctuations at Reno. The Cytac program was also the first time the need for wide bandwidth

to avoid skywave interference was recognized. All the field operations led to a proposal for developing a single frequency cycle matching system at 100 KC. But the USAF terminated Cyclan in favor of WHYN, an FM-CW system under development which self-destructed a year later.

CYTAC

In 1952 Air Force decided they needed a ground based all weather long range tactical bombing system. Sperry proposed Cytac, which introduced the concept of multiple pulsing and phase coding. The 8-phase code was classified secret, and was not used during nearly all of the testing. Near the end of the test period it was used long enough to verify the presence of multi-hop skywaves at 900 miles and the ability of the phase coding to reject them. Ground and

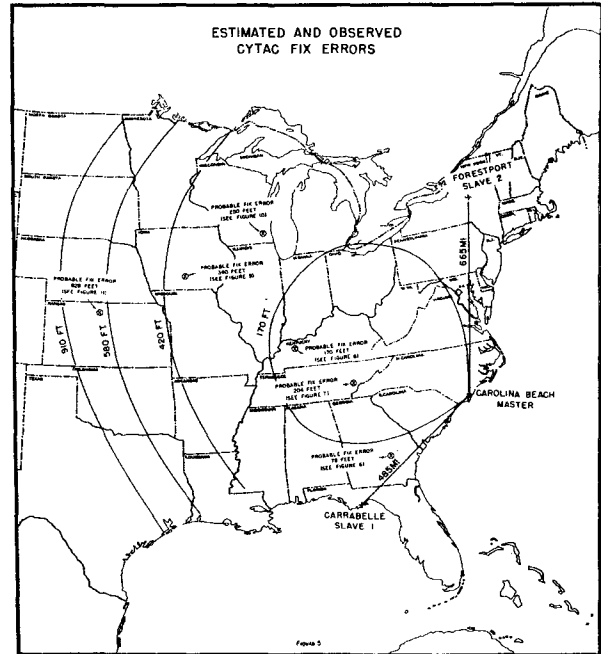


FIGURE 8 Estimated and observed Cytac fix errors

air testing were conducted over land with transmitters at Forestport, NY Carolina Beach, NC and Carrabelle, Fl. Figure 8 shows the chain and a number of the monitor sites. Figure 9 shows a balloon which supported an experimental

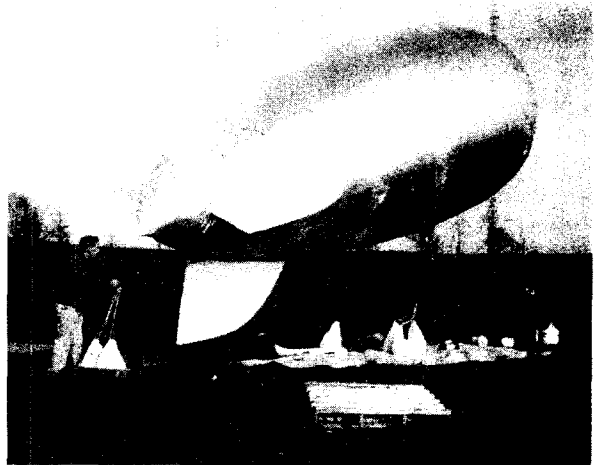


FIGURE 9

antenna at Forestport. It was a full quarter wave, 750 meters high, and, not surprisingly, put out an excellent signal.

Five ground monitor trailers, one NBS monitor, one DC-3 and one B-29 had Cytac receivers. Figure 10 shows one of the GMR trailers and the shiny NBS monitor. The airborne receiver/computer was planned to fit in a pod on an F-84, as shown in Figure 11. The combined experimental airborne receiver (E.A.R.) and computer was finally fitted into a B-29. Figure 12 shows the E.A.R. in the bomb bay of the B-29. It was put there because the computer took up all the fuselage space. The system finally flew and operated just before the Air Force cancelled the program, having concluded that a need no longer existed for the system.

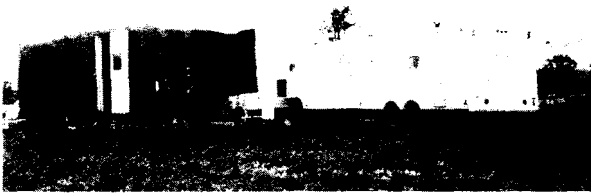


FIGURE 10

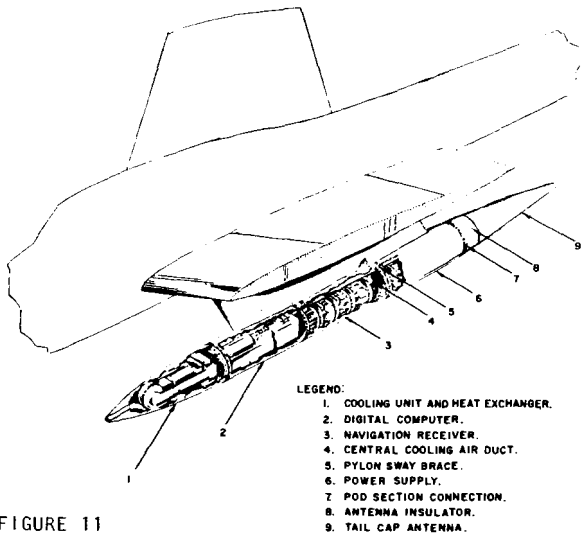


FIGURE 11

NUDETS TESTS

Just when the Cytac program was ending in 1955, Operation Teapot, a series of atmospheric nuclear tests took place in Nevada. Three of the GMR's in the field were used to provide timing for measurements on the VLF pulse in an inverse loran technique to locate the nuclear explosions. Then for Operation Redwing in '56, a Cytac transmitter was moved to Haiku, Hawaii and GMRS's to Maui, Midway and Palmyra. Figure 13 shows a full front view of a Cytac ground monitor receiver located in a shack on Palmyra. The system used the Cytac time base to get an inverse hyperbolic fix on the MEP from the nuclear explosions. The signals, put on oscilloscopes and recorded on continuous strip

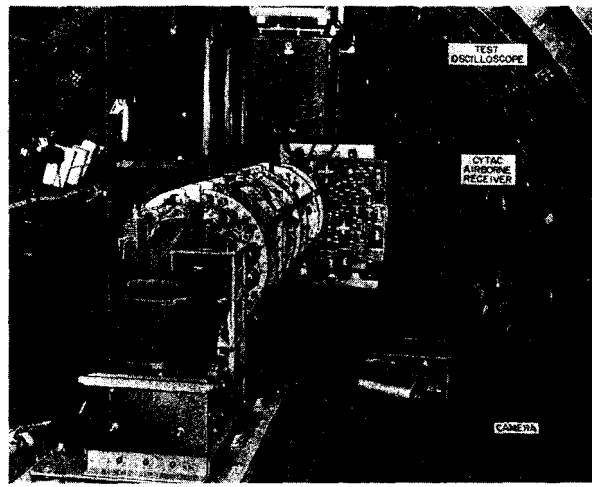


FIGURE 12

cameras, were timing pulses from Cytac receiver along with VLF wideband signals.

LORAN-C

In 1957, the Navy was concerned with the problem of accurate navigation of the Polaris submarines. Their plan was to make a sonar map of the ocean bottom, and use that as a reference for the subs. To do the mapping, they had three survey ships, aptly named the Bowditch, the Dutton and the Michaelson. These ships were prepared to map bottom contours with sonar, but they had one problem - they had no accurate positioning system. Cytac could do the job, but since it had just been discarded by the Air Force, it obviously could not be used as is. Enter the Coast Guard and the re-naming of the loran systems. The old "standard" loran became Loran-A and the converted Cytac became Loran-C. The GRI was changed from the oddball rate of Cytac to rates compatible with loran standards. The multiple pulsing was retained and a new phase code developed by Bob Frank and friends. The new East Coast chain was formed by moving the Forestport transmitter to Martha's Vineyard and the Carrabelle transmitter to Jupiter, Florida. Modules of an airborne receiver which had been under development were stuffed into a shipboard package and christened the AN/SPN-28, and Loran-C was off and running.

Coast Guard management of the Loran-C program was started under Capt. Pete Colmar, who was succeeded as head of EEE by Capt. Zeke

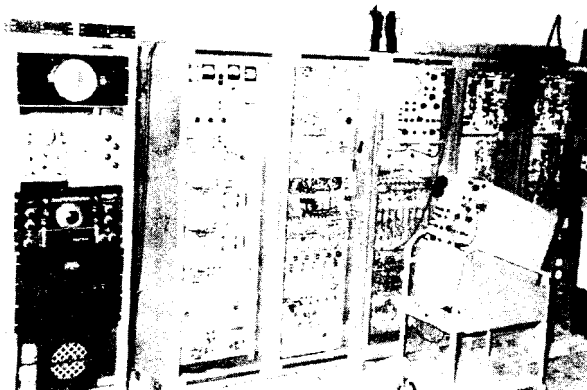


FIGURE 13



FIGURE 14

Bruner. The first long range skywave measurements were made in 1958. Two flights were made in Coast Guard R5D measuring skywaves from the East Coast. The first went as far as Natal, Brazil, and got good nighttime skywave data all the way. The second went to Iceland, Scotland, Europe and Africa, measuring transatlantic skywaves even when night paths lasted only a half hour.

The first overseas chain, nicknamed "Tack", was the Mediterranean, with the master at Simeri Cricchi, Italy, X at Marble Arch, Libya, and Y at Targabarun, Turkey. Figure 14 shows the AN/FPN-39 transmitter, with CDR Helmer Pearson, CDR Dick Pascuiti and Lt. Al Manning. A monitor using AN/SPN-30 receivers was first set up on the Island of Rhodes (Figure 15).

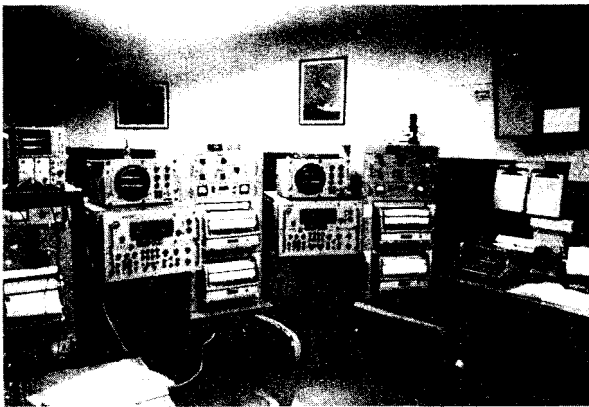


FIGURE 15

The second overseas chain, called "Rail", was the Norwegian Sea Chain, the Master at Ejde, Faeroes, and secondaries at Bo, Norway, Man Mayen and Sandur, Iceland.

The Navy decided to use loran receivers aboard the submarines, so they ordered the AN/WPN-3 (Figure 16) and AN/WPN-4. The difference between the two was that the WPN-4 included a Loran-A channel which was consistently unused. This was still in the era of mechanical phase shifters and veeder-root counters to measure time delays.

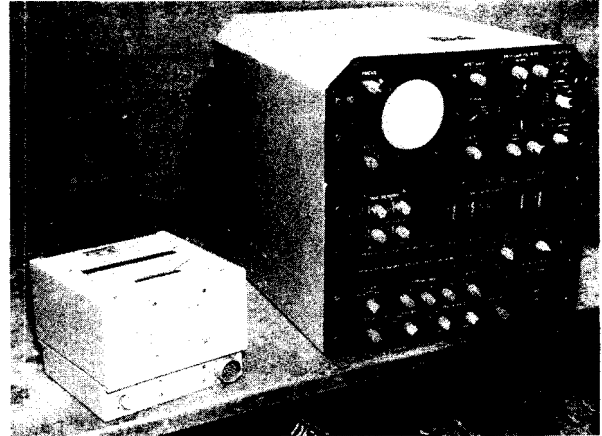


FIGURE 16

HIGH ALTITUDE NUCLEAR EXPLOSIONS

1962 was the year of Operation Fishbowl, a series of high altitude nuclear explosions above Johnston Island. Loran signal measurements were made in Hawaii, Alaska, and Eastern U.S. These showed that the D layer, which reflects 100 KHz, was affected, even on the U.S. East Coast, at distances of over 5000 miles.

NUDES

In the early 1960's the Air Force was still interested in inverse loran (Narol) for locating nuclear explosions, and ordered the AN/GSQ-44 nuclear detonation evaluation system (Nudes). Three monitors were built and installed in Germany, and an additional secondary was added to the Norwegian Sea chain at Sylt to provide good sync signals. The system has since been decommissioned.

LORAN-D

In the middle 1960's the Air Force suddenly revived an interest in loran as a weapon delivery system and sponsored development of Loran-D. New airborne receivers were also designed, the first using microcircuits being the AN/ARN-78 (Figure 17). This led to development of the AN/ARN-85 (Figure 18), an integrated airborne loran navigator, which was superseded by the AN/ARN-92.

CLARINET PILGRIM

Also in the middle 1960's, Elmer Lipsey and Arnold Swagerty at Coast Guard had the idea of using pulse position modulation of loran pulses for communication. This developed into the Clarinet Pilgrim System, which was installed in

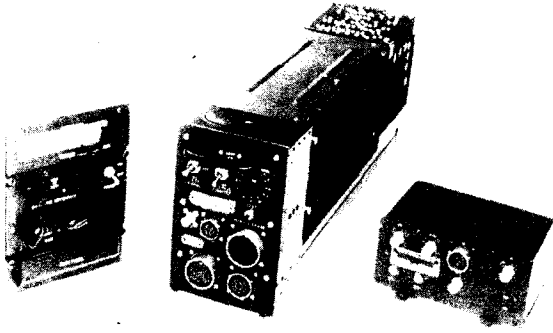


FIGURE 17

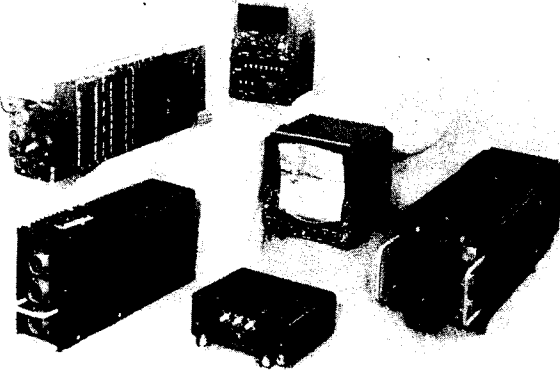


FIGURE 18

the Wespac chain to relay fleet broadcasts. Figure 19 shows a transmitter control unit installed at each of the five Wespac stations. It receives the fleet broadcast on communication receivers and converts it to pulse position modulation of the last six pulses of the loran group. The system also included interstation teletype using modulation of the first two pulses.

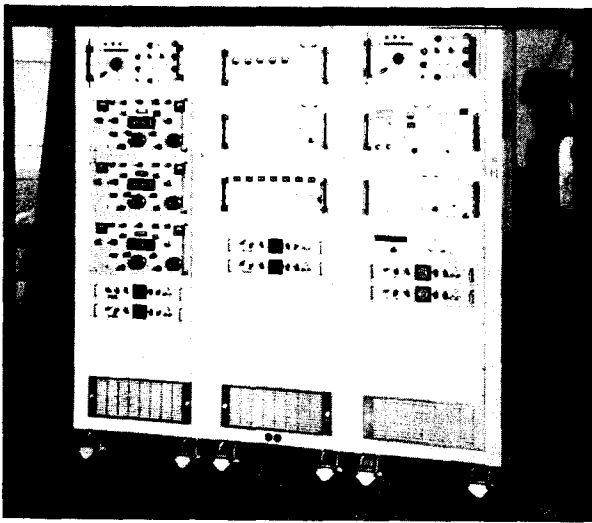


FIGURE 19

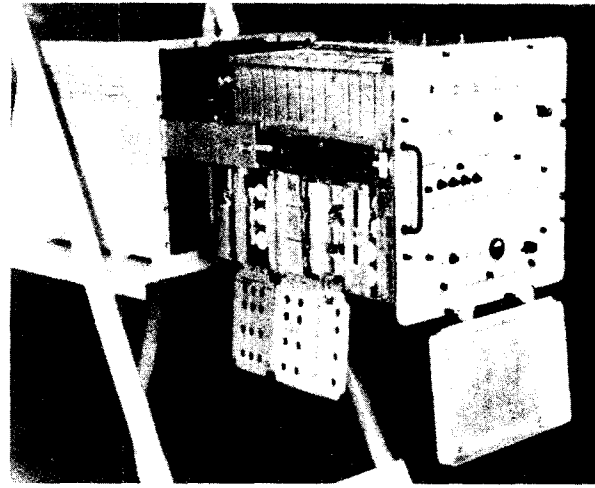


FIGURE 20

RECEIVER DEVELOPMENT

Microcircuits were slow coming to the submarine loran users. It finally did, and Figure 20 illustrates the technology of 1970 in an expensive Navy loran sensor - the AN/BRN-5, built for the FBM submarines to replace the WPN-3. Just for contrast, Figure 21 is a view of an airborne receiver of the 80's - the AVA-1000. It is interesting to note that, in many ways, this receiver and computer has more capability than the Cytac receiver/computer that occupied most of a B-29 thirty years ago.

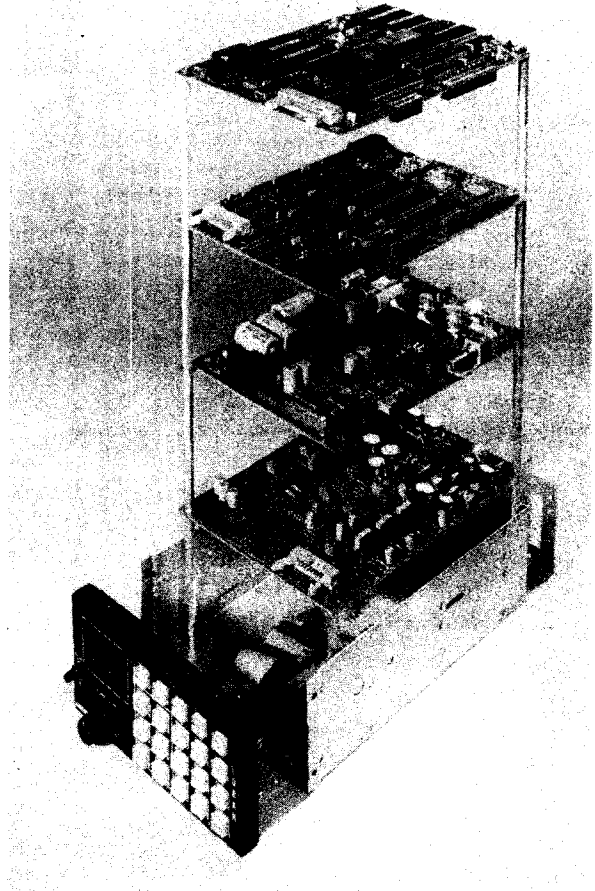


FIGURE 21

CONCLUSIONS

This has been a rather parochial view of the past history of Loran. Others will present some different incidents in Loran history, particularly from more recent years. The history of Loran, however, shows one basic characteristic - durability. Cyclan was terminated because an untested competitor had not yet failed. Cytac was terminated because the Air Force couldn't foresee the need for such a system, which they actually used in Southeast Asia a little over ten years later. Today Loran-C has shown much of what it can do, but its future again is challenged by proponents of another promising system. The critical area of the challenge is in the political and public relations arena.

U.S. COAST GUARD R&D
LORAN-C STABILITY STUDY

LT DOUGLAS S. TAGGART
USCG R&D CENTER
AVERY POINT
GROTON, CONNECTICUT 06340

ABSTRACT

For the past two years, the U.S. Coast Guard Research and Development Center (R&DC) has been collecting Loran-C time difference data to determine Loran-C signal stability in the navigable waters of various U.S. and Canadian harbors and harbor entrances. This data is being collected, automatically, by remote, computer-based Harbor Monitor Sets that were developed by the R&DC Electronics Branch. Presently, there are 28 remote equipment sites that monitor 36 different locations. Twice weekly, a R&DC computer automatically retrieves data from the Harbor Monitor Sets over commercial-grade telephone lines.

Processed data is presented to Coast Guard Research and Development Headquarters in Quarterly Status Review Reports. This report presents time difference plots and elliptical error plots for each site; and includes a section dedicated to the modeling of each monitored chain secondary. The mathematical model assumes a uniform propagation velocity throughout the coverage area. The key element of this uniform propagation model is the double range difference that is computed for each site. The study's ultimate goal is the prediction of Loran-C repeatable accuracy throughout the year, at all locations within the model limits.

BACKGROUND

Since 1976 the U.S. Coast Guard has been conducting studies on the feasibility of using Loran-C as a precision aid for navigation in the Harbor-Harbor Entrance (HHE) areas of the continental United States. In the mid 1970's, the St. Marys River mini-chain was established and a number of R&D projects were conducted using this experimental, low power, small coverage area chain. Reference (1) contains information on the mini-chain operation and the various R&D efforts that were conducted in that area. These projects were concerned with Loran-C guidance equipment (PILOT), trackline surveying techniques (visual and micro-wave) and the evaluation of time difference (TD) grid stability of a short baseline system.

The R&D PILOT program and development of the trackline survey were essentially

completed on the St. Marys River during 1980/81. It was during this period that the mini-chain project was terminated and the St. Marys River was re-surveyed and performance of the PILOT system was evaluated on the Great Lakes Loran-C chain. Since 1981, additional surveys and demonstrations of PILOT have been conducted throughout the United States. Specific details on the trackline survey and the PILOT system can be found in References (2) through (6).

During the operation of the mini-chain, one of the tasks undertaken by the U.S. Coast Guard's Research and Development program was the collection of Loran-C time difference (TD) data to evaluate the accuracy of chain control. Even though it was initially assumed that large temporal effects would not be present for the short baseline mini-chain, the ability of the system area monitor (SAM) to successfully control the chain for precision navigation was questioned. To verify this, a number of monitor sites were established along the St. Marys River. Prior to 1981, a typical data collection unit (DCU) consisted of an Internav Loran-C receiver (initially a Model 101 and later a Model 204), an interface unit and a Texas Instrument Model 733 data terminal. DCUs of this nature were initially used for the St. Marys River mini-chain. These units often resulted in poor data quality primarily caused by the absence of automatic receiver control. In 1977 the LC-204s were modified by Internav to provide for more reliable unattended operation. Also a Magnavox AN/BRN-5 receiver was added to the DCU. Later in the DCU development stage a microprocessor and telephone modem were added to allow for remote access of stored data.

One of the more common modes of data collection incorporated by these DCUs was as follows. The LC-204 provided 1000 averaged data samples every 49.3 seconds (1000 GRIs for rate 4930) while the AN/BRN-5 receiver output instantaneous data every 50 seconds. The data from each receiver was then independently averaged and stored in 15 minute intervals. The data used to analyze the chain control effects presented in Reference (1) consisted of twice daily system samples. These samples were computed from one hour averages of the 15 minute samples taken at noon and midnight. In July 1981, the DCUs were retired from service and replaced with the first generation Harbor Monitor Set.

HARBOR MONITOR SET

It should be pointed out that the present Loran-C Signal Stability Study was initiated as a result of the chain control evaluation conducted on the mini-chain. As previously

noted, seasonal fluctuations on the small scale mini-chain were not expected. However, gathered data actually showed significant variations of this type. To further investigate the characteristics of Loran-C stability on an operational chain the R&D Signal Stability project was initiated.

In the fall of 1979, the Statement of Work (S.O.W.) for the Harbor Monitor project was received by the USCG R&D Center. This S.O.W. called for the development and deployment of a remote computer, interfaced to an Internav LC-404 receiver with the ability to automatically collect Loran-C data and store it for retrieval via commercial grade telephone line. This mode of "automatic" operation was desired so that the data quality could be improved and the "post data edit process" (quite common with the DCUs) could be eliminated.

In September of 1980, a prototype installation was accomplished at Point Allerton, Massachusetts. After several months of field tests and software improvements the system hardware/software design was complete and the true Harbor Monitor Set (HMS) came to be. A block diagram of this unit is shown in Figure 1. This unit was given the name; "Type-C Harbor Monitor Set". Between February and April of 1981, five monitor sites were installed in the St. Marys River area.

During the Type-C development stage, an additional HMS was designed for data retrieval of USCG Loran-C chain control data. This device, known as the Type-A monitor, collects Loran-C TD data from the A1 and A2 Austron 5000 control sites. This system consists of a PCM-12 microcomputer and phone modem. The Type-A system is located at the chain control station with all connections made on a "not to interfere" basis with the chain control data lines. The first of these sites was the Seneca, New York monitor. This site was installed in September 1980.

In the summer of 1981, four additional Type-C monitor sets were installed outside the St. Marys River area. These four monitors were located at: Lewes, Delaware; Gloucester, New Jersey; Yorktown, Virginia and Nahant, Massachusetts. These monitors were used to collect data from the North East U.S. Loran-C Chain (GRI 9960). In October of 1981, due to budget cuts, it was announced that the Coast Guard would close the R&D Center in May 1982. At this point, the Coast Guard's R&D Signal Stability study had been underway for approximately two years. The first year had been spent almost entirely on the R&D Center's development of a workable collection unit. During the second year,

data was collected almost exclusively from the Great Lakes chain, limited of course to the St. Marys River area. Rather than a "wind the project down" approach, Coast Guard Headquarters stressed the need for additional spare Type-C units. In the event that the Center did close, Headquarters wanted to have the ability to obtain Loran-C data (on additional Loran-C chains) with monitors installed by Headquarters personnel.

During the "close down phase" of the R&D Center it became clear that support of the "custom built" Type-A and Type-C hardware/software would not be possible at the Headquarters level. To eliminate this problem it was decided that a new "off the shelf" monitor would be built. Development of this new monitor began in February of 1982; R&D personnel that were previously involved with guidance equipment (PILOT) and the trackline survey were assigned to this task.

In April of 1982, it was announced that the plans to close the R&D Center in May were cancelled. The new closing date was moved back to September of 1982.

The construction of the new HMS monitor continued. Development was completed in May 1982. This new monitor was later dubbed the "Type-D" set. The initial Type-D monitor consisted of a Hewlett-Packard 9915 microprocessor, an Internav LC-404 receiver and a small power distribution/interface system (PDIS). Although the unit was not entirely "off the shelf", it was considerably less complicated than the Type-C monitor. The first Type-D monitor was installed at Bristol, Rhode Island in June of 1982. Figure 2 is a picture of the present day Type-D monitor.

One major improvement of the Type-D system was the automatic control and monitoring of the Internav LC-404 receiver. The Type-C monitor did allow for limited manual control of the receiver; however, this was only possible during telephone calls to the site. If the receiver lost "lock" for whatever reasons, no data was collected until the problem was discovered and manually corrected during the next scheduled phone call. This fact resulted in a considerable number of "extra" calls to check operations. The Type-D monitor eliminated this costly (both monetarily and with regard to precious periods of lost data) error.

DATA COLLECTION MODES

As previously mentioned, the collection modes of the DCUs varied considerably. Methods and formats for collection of data were dependent on the type of receiver used

as well as the storage capabilities of the logging device. In the S.O.W. for the development of the Type-A and Type-C monitor it was clearly stated that "on-site" magnetic tape was not a satisfactory method of storing data. The PCM-12 microcomputer possesses the capability of preprocessing the data and storing the results in RAM. The memory size is determined by the number of memory cards installed in the machine. Initially, on-site storage was in the area of 7k to 8k bytes. To allow for data retrieval through the use of telephone lines, it was decided that the frequency of data collection would be limited in such a way as to result in a two to three day period between phone calls. This allowed for non-polling of sites by R&D personnel over weekends and holidays.

It should be pointed out that the S.O.W. was deviated from with regard to the Type-D monitor development. The primary means of data storage within the HP-9915 (other than the available 32k bytes of memory space dedicated to the program and variable space) is a magnetic cassette tape.

The periods and intervals of data collection agreed upon to satisfy the above stated requirements were as follows. The sites were configured for two collection periods spaced 12 hours apart. Each collection period lasted for one hour. During this one hour period, the on-site computer interrogates the LC-404 every 40 seconds for TD data. This 40 second interval was chosen based on simulator tests that showed under conditions encountered at harbor monitor sites, the LC-404 has a "servo loop time constant" of 6-8 seconds. Using the 40 second sample interval, the receiver outputs were assumed to be statistically independent. The hour periods were set to begin at noon and midnight. The noon sample period was consistent with the Great Lakes Chain system sample period between 12:00 and 1:00 p.m. local time. During these periods, chain control procedures called for minimal control effects initiated by chain monitor personnel.

A typical line of preprocessed stored data contains the following information; Julian day, sample hour, number of samples (90 during an hour), maximum and minimum TD encountered in decimal values of microseconds, the average TD and the standard deviation. After the Type-D monitor was developed, the data line was modified to include the average signal to noise ratio. In November of 1982, the number of one hour sample periods obtained at each site was increased to four. These four one hour periods are spaced six hours apart. East coast (GRI 9960, 8970 and 7980) sample

periods begin at 0400Z, 1000Z, 1600Z and 2200Z. West coast (GRI 9940 and 5990) sample periods begin at 0300Z, 0900Z, 1500Z and 2100Z.

The mode of data collection previously described has been labeled as "low-density" data. During the construction of the Type-D monitor, an additional "high-density" mode of data collection was developed. It should be noted that the original S.O.W. did not address this additional mode; however, it was a desired feature of the R&D Loran-C Survey project. A standard procedure adopted during development of trackline survey techniques was the placement of a centrally located monitor to record any TD fluctuations that may occur during the course of a survey. These fluctuations were then removed from the surveyed data to obtain the unbiased estimates for waypoints. Usually these monitors consisted of LC-404 receivers and Texas Instrument Model 733 data recorders. These semi-automatic monitors were not reliable.

Returning to the discussion of the high-density mode; data is taken from the receiver every 40 seconds and the statistics of 22 samples are calculated and stored for 15 minute intervals. During a 24 hour period, 96 data lines are created for each monitored TD. The maximum number of data lines that can be stored prior to filling the allotted storage space is 767. Operating with two monitored TDs, this equates to approximately 4 days.

In order to clarify the terms associated with data collection the following terminology has been adopted; "data collection" refers to the collection of data at the HMS site, "data retrieval" is the process of obtaining that collected data, via telephone line, for analysis and storage at the R&D Center.

During the data retrieval process (when the site is transferring data back to R&DC) the high-density data collection routine is interrupted. The data retrieval process takes approximately 20 minutes at 300 baud. In an effort to time correlate the data from various sites, all sites operating in the high-density mode are programmed to begin a new sample period each day at 0000Z (GMT). The first Type-D monitor deployed in Bristol, Rhode Island, during June of 1982, was operated in the high-density mode and initially used as a trackline survey monitor. In September 1982, six Type-D sites operating in the high-density mode were installed along the St. Lawrence Seaway.

DATA RETRIEVAL AND MANAGEMENT SYSTEM

During the development of the Type-A and Type-C systems the problem of retrieving the collected data was also addressed. The system that was developed utilized a PCM-12 microprocessor and a Racal-Vadic auto dialer. This system was dubbed the Microprocessor Auto Dial system (MAD). There were a number of versions of this system. Later, a PDP-8 based Scientific Information Processing System (SIPS) was added for storage of data on hard disk removable platters with long term storage on 9 track tape. The main problem with this retrieval system was making the data available to Coast Guard Headquarters for data analysis.

In January of 1982, at the same time development of the Type-D monitor began, development of a Hewlett-Packard 9845 based Data Retrieval and Management System was initiated. The HP-9845 was chosen due to the availability and the familiarity that R&DC personnel had with this machine. Previous R&D projects, specifically the PILOT tape generation project and the trackline survey data collection and analysis effort, had used the HP-9845 exclusively. As was the case with the Type-D monitor, this new retrieval system was to be designed for easy "handoff" to Headquarters once the Center closed.

A block diagram of the resulting system is shown in Figure 3. This system was given the name "Data Retrieval and Management System" (DRAMS). This system can be operated in the automatic or manual mode. In the automatic mode, the seven day, 24 hour timer turns the system on at 1:00 a.m. every Monday and Thursday, the autostart feature of the HP-9845 loads and executes the retrieval program. All sites are sequentially called and data is retrieved, sorted and stored in the correct data files. During this operation, each site's status is evaluated and results are logged on the internal paper printer. With the present number of sites (28), the entire process takes approximately 2 hours to complete. In the event that there are problems noted at any particular site, the same program can be used to call sites in the manual mode.

The data management portion of this system is dedicated to the correct storage and filing of each site's data files. Data files can be individually accessed and copied to compatible HP-9845 mass storage devices for transfer to Headquarters. The data files are divided into 366 records. Each record is equivalent to the corresponding julian day of the calendar year. Each 160 character record contains the "four sample a day" data statistics. There are individual data files

for each monitored site TD.

DRAMS was completed and placed into full operation in July of 1982.

QUARTERLY REPORTS

The present status of the HMS network is shown in Figure 4. The data base that is being generated by these monitors is constantly growing. With the announcement in the fall of 1982 that the R&D Center would not close, the HMS network was expanded to the Gulf and West coast chains.

Until September of 1983, the R&D Center's main function in the Harbor Monitor project had been the development of the monitors and the acquisition and editing of the collected data. To date, all of the Stability Studies (to be covered in a later section of this paper) have been written at the Headquarters level. Data used to generate these reports was furnished to Headquarters by the Center.

In addition to the actual computer data files that were supplied to the Headquarters project officer, a quarterly hard copy report produced by the R&D Center was initiated. This quarterly report, which has been dubbed, "The Harbor Monitor System Loran-C Signal Analysis Quarterly Status Review" or simply the "HMS Quarterly Review", details the data collected over three month periods. These reviews are generated at the end of each fiscal quarter. The reviews are divided into four or five sections.

Section I of this review outlines quarterly activity with regard to HMS site installations and de-installations. Section II details the data collection methods (low-density/high-density). Section III presents the TD plots for each site's quarterly and yearly data base as well as quarterly elliptical error plots for the various triad combinations that are monitored at each site. An example of a standard TD plot and an elliptical error plot are shown in Figures 5 and 6, respectively. Section IV is dedicated to the presentation of the various Uniform Propagation Model "runs" that are completed for the various chains and their associated secondaries. This model will be explained in the following section of this paper. Section V, when included, presents high-density data that is collected from those sites operating in that particular mode. This section is broken down into seven day periods. One page of plots presents TD, SNR, and standard deviation plots. An additional page shows elliptical/radial error plots and a final page, when appropriate, shows the effects of using a single monitor as a differential correction source. This

differential plot concept was adopted during the one year, St. Lawrence River, high-density data collection phase. Examples of these three plots are shown in Figures 7, 8 and 9.

UNIFORM PROPAGATION MODEL

To predict the repeatability of the Loran-C system, a Uniform Propagation Model has been developed. This model was introduced in the St. Marys River Loran-C Mini-Chain report (Reference 1). Subsequent stability reports (which will be covered in the next section of this paper) have made improvements to the model. For this discussion, the model will be simply defined for a single baseline as follows:

$$\underline{z}(n) = \underline{A} \begin{bmatrix} \widehat{dTD(n)} \\ \underline{C}(n) \end{bmatrix} + \underline{e}(n)$$

In this model, $z_1(n)$ is the data record from site 1, $z_2(n)$ is the data record from site 2, etc. The A matrix, which operates on the dTD(n) term, is comprised of the double range differences as defined in Reference (7). The dTD(n) vector represents the changes in the uniform propagation velocity in units of nanoseconds per kilometer. The C(n) vector represents the common error terms that are introduced by controlling the chain with a receiver (Austron 5000) that is different from the HMS receiver (Internav LC-404). The e(n) vector includes all remaining TD variations that the model does not account for.

Using the minimum mean square error estimation process, the estimated dTD(n) and C(n) vectors are as follows:

$$\begin{bmatrix} \widehat{dTD(n)} \\ \underline{C}(n) \end{bmatrix} = (\underline{A}^T \underline{A})^{-1} \underline{A}^T \underline{z}(n)$$

The model residuals (r(n)) are then computed as follows:

$$\underline{r}(n) = \underline{z}(n) - \underline{A} \begin{bmatrix} \widehat{dTD(n)} \\ \underline{C}(n) \end{bmatrix}$$

More details on this model can be found in References 1, 7, 8 and 9.

LORAN-C SIGNAL STABILITY STUDIES

If the question were asked, "What contribution has the Loran-C R&D Project made to the Loran-C community?", the answer would be the Loran-C Signal Stability Reports. These reports, of which there are presently

three, are available to the public in the National Technical Information System (NTIS). These reports are listed in the reference section of this paper as References 7, 8 and 9.

The first stability report addresses the usefulness of Loran-C for precision navigation on the St. Lawrence River. The East Coast Loran-C chain was monitored in this area. It should be noted that the one year St. Lawrence high-density collection effort (previously referred to in this paper) was initiated because of this stability report. The second report to be published covered the use of the Great Lake Loran-C chain for precision navigation on the St. Marys River. The most recent report, the Northeast/Southeast (NEUS/SEUS), was the first stability report to address an entire coverage area. In fact, this report presents findings for the entire East and Gulf coast. The contour diagram shown in Figure 10 is taken from this report (Reference 9).

Future Loran-C Signal Stability Study reports will be completed for the U.S. West Coast, Canadian West Coast and Great Lakes Loran-C chains. Present funding for this Coast Guard R&D project is planned through FY87. These future reports will continue to expand on the Uniform Propagation Model and will include repeatability contour charts.

FUTURE ACTIVITY

In addition to the previously mentioned stability reports, the Loran-C Signal Stability project will approach the concept of "differential Loran-C". Present project plans call for a demonstration of a real time system in early FY85. Results obtained during this demonstration may be used to establish the format for differential corrections. The means of communicating corrections will be investigated, formats of both voice and digital messages will be experimented with, and the addition of differential information to nautical charts will be considered. The nautical chart information may include items such as reference TDs, waypoint TDs, methods of receiving differential messages, etc.

Recent discussions with the Federal Aviation Administration indicate the need for information regarding the repeatability of Loran-C throughout coverage areas. As Figure 4 clearly shows, the present HMS network is concentrated along the coastal areas of the country. To expand the present network inland will require an interagency agreement. Recent discussions between the FAA and Coast Guard R&D Headquarters indicated that this may occur in the near

future.

Finally, with regard to the Department of Defense's Global Positioning System (GPS), knowledge gained concerning the repeatable accuracies of Loran-C may influence the degree of accuracy/repeatability made available to the non-military GPS user.

REFERENCES

1. Olsen, D.L., "St. Marys River Loran-C Mini Chain Final Report", July 1981. U.S. Coast Guard Report No. CG-D-11-82. Available from the National Technical Information Service, Springfield, Virginia 22161 as PB82-255183.
2. Lewicki, J.P., Milne, T.J., and Sedlock, A.J., "Time Difference Survey System", April 1981. Published as U.S. Coast Guard Report No. CG-D-72-81. Available from the National Technical Information Service, Springfield, Virginia 22161 as AD-A115588.
3. Sedlock, A.J., "HHE Loran-C Time Difference Surveying, Final Report", November 1982. Published as U.S. Coast Guard Report No. CG-D-54-82. Available from the National Technical Information Service, Springfield, Virginia 22161 as AD-A124343.
4. Edwards, C.R., "PILOT, A Precision Intercoastal Loran Translocator, Volume 1 - Users Manual", The John Hopkins University Applied Physics Laboratory Report No. SDO 5699 September 1980.
5. Tarr, J.E., Eifert, J.W., and Starkes, J.H., "PILOT, A Precision Intercoastal Loran Translocator, Volume 2 - Hardware", The John Hopkins University Applied Physics Laboratory Report No. SDO 5699.1 July 1980.
6. Baer, G.E. and Harrison, J.F., Jr., "PILOT, A Precision Intercoastal Loran Translocator, Volume 3 - Software", The John Hopkins University Applied Physics Laboratory March 1982. Published as U.S. Coast Guard Report No. CG-D-21-81, III. Available from the National Technical Information Service, Springfield, Virginia 22161 as AD-A121759.
7. Slagle, D.C., and Wenzel, R.J., "Loran-C Signal Stability Study: St. Lawrence Seaway", July 1982. Published as U.S. Coast Guard Report No. CG-D-39-82. Available through the National Technical Information Service, Springfield, Virginia 22161 as AD-A126093.
8. Slagle, D.C., and Wenzel, R.J., "Loran-C Signal Stability Study: St. Marys River", December 1982. Published as U.S. Coast Guard Report No. CG-D-43-82. Available from the National Technical Information Service, Springfield, Virginia 22161 as AD-A130609.
9. Slagle, D.C., and Wenzel, R.J., "Loran-C Signal Stability Study: NEUS/SEUS", August 1983. Published as U.S. Coast Guard Report No. CG-D-28-83. Available from the National Technical Information Service, Springfield, Virginia 22161 as AD-A137628.

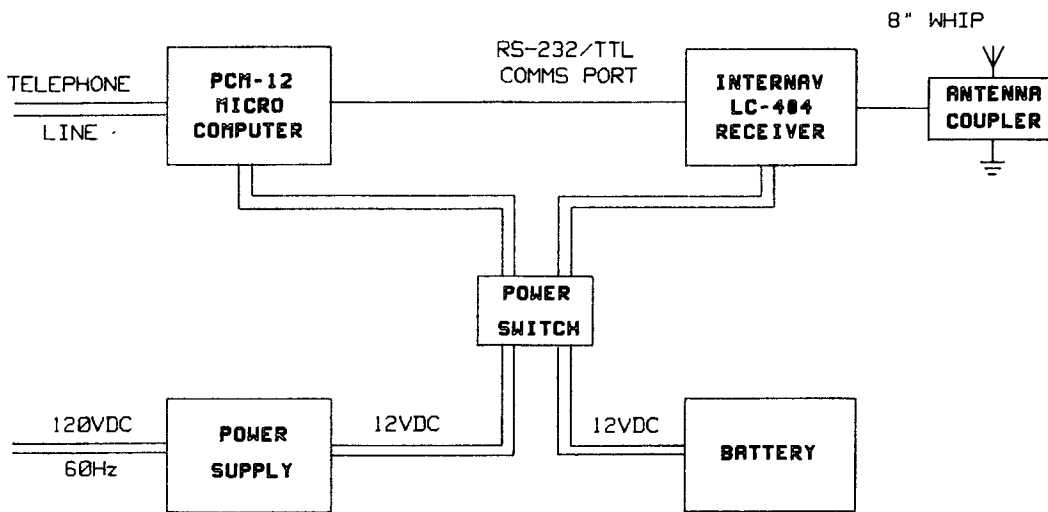


Figure 1. Block Diagram Type-C HMS Monitor.

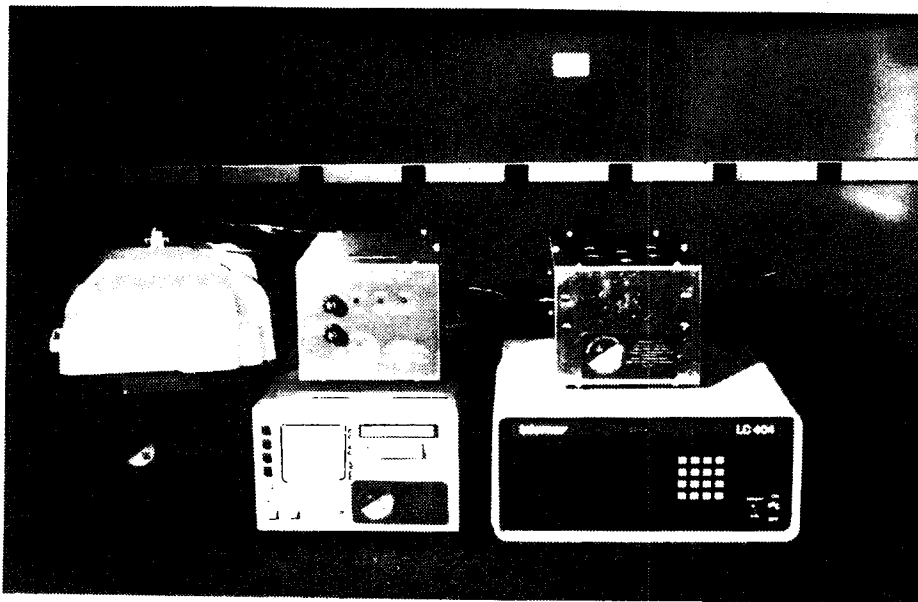


Figure 2. Type-D HMS Monitor.

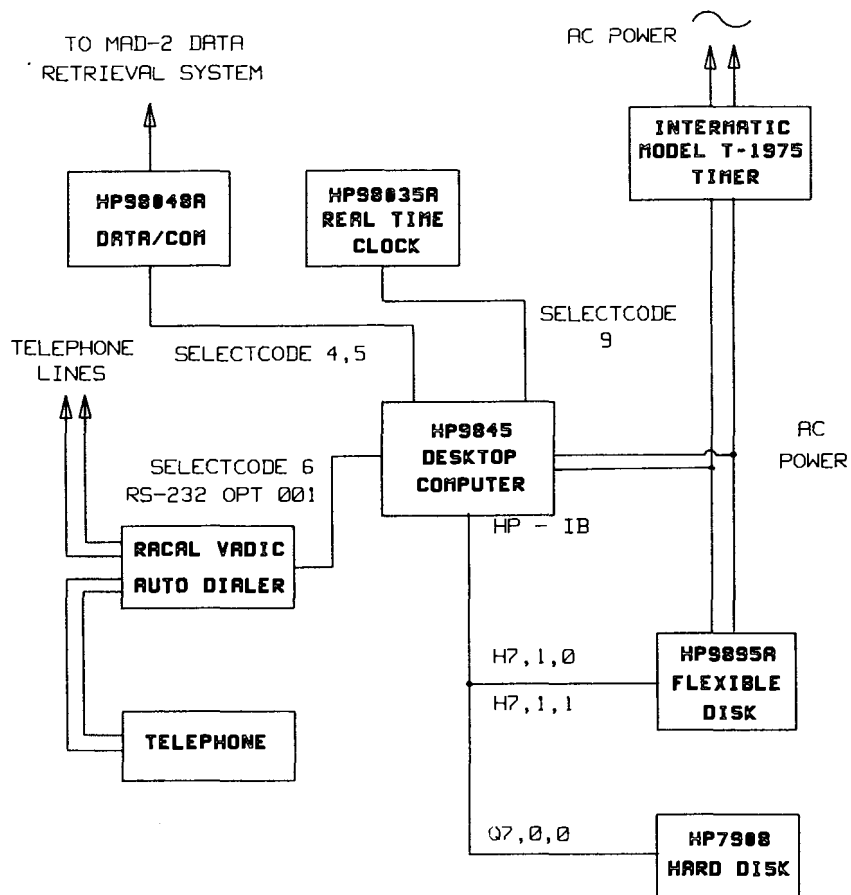


Figure 3. Data Retrieval and Management System (DRAMS).

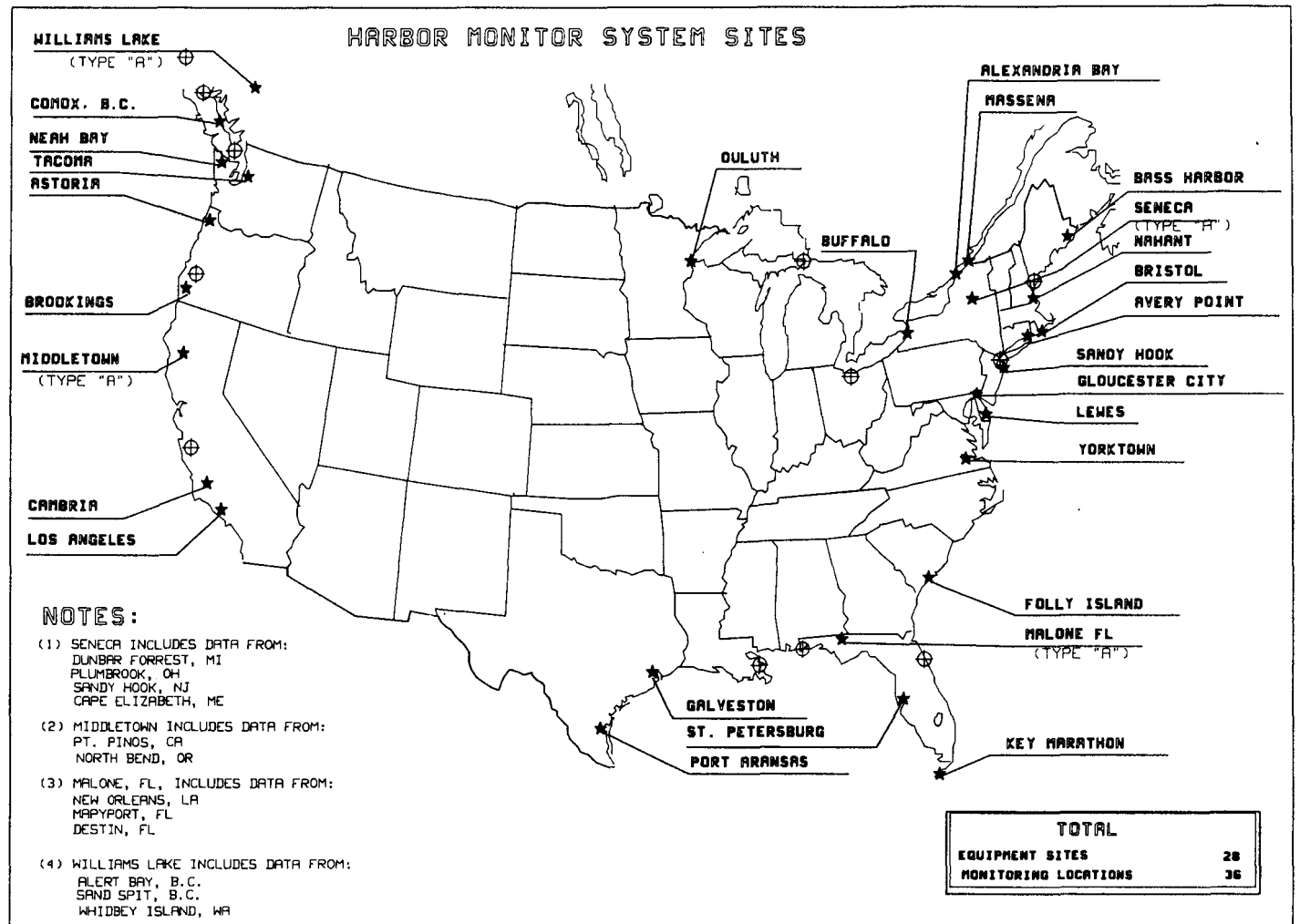


Figure 4. Harbor Monitor Network.

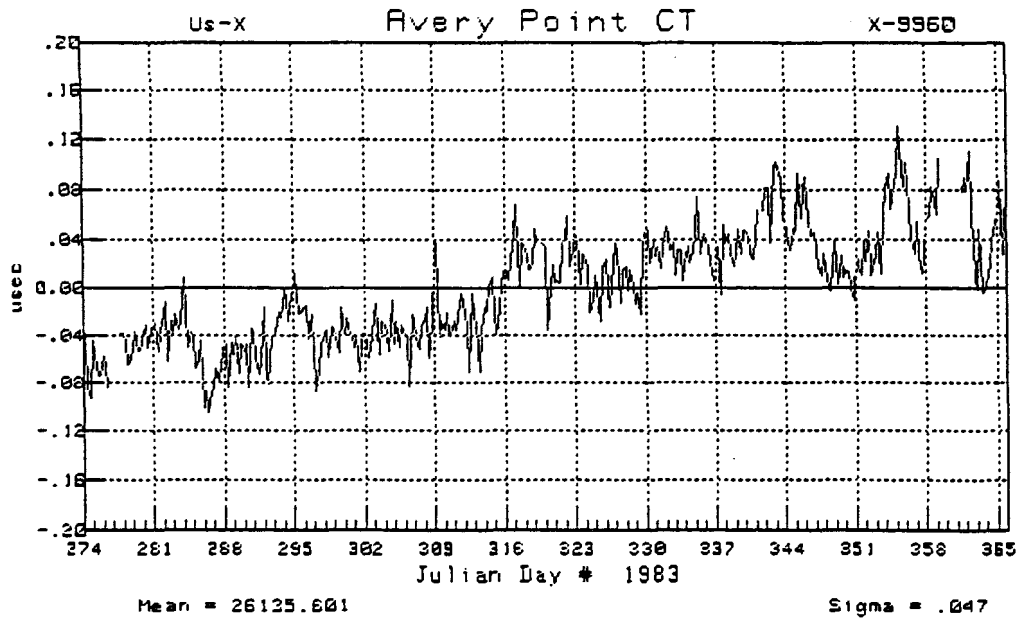
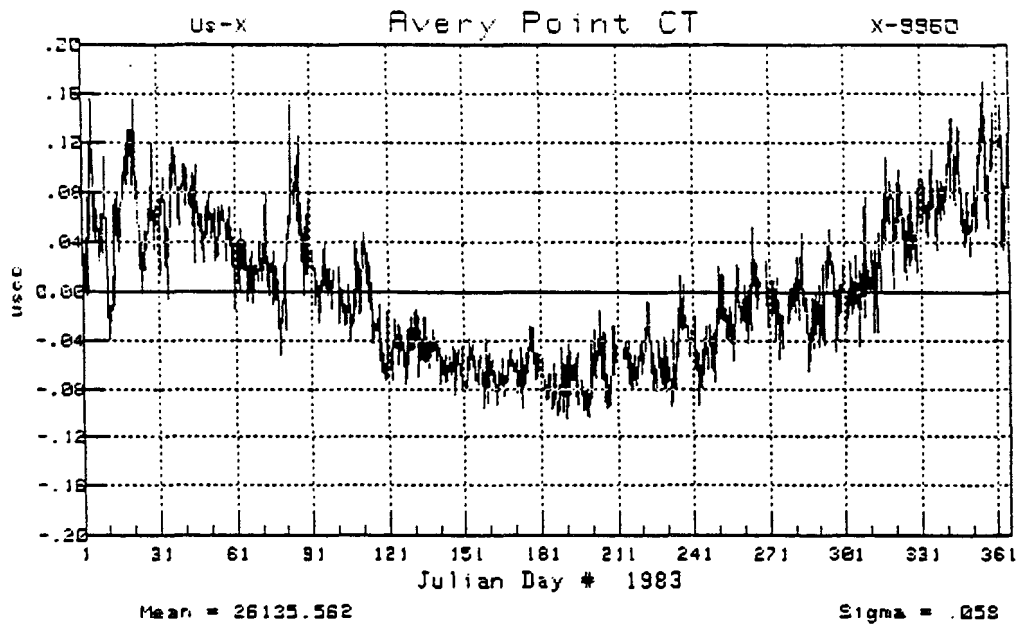
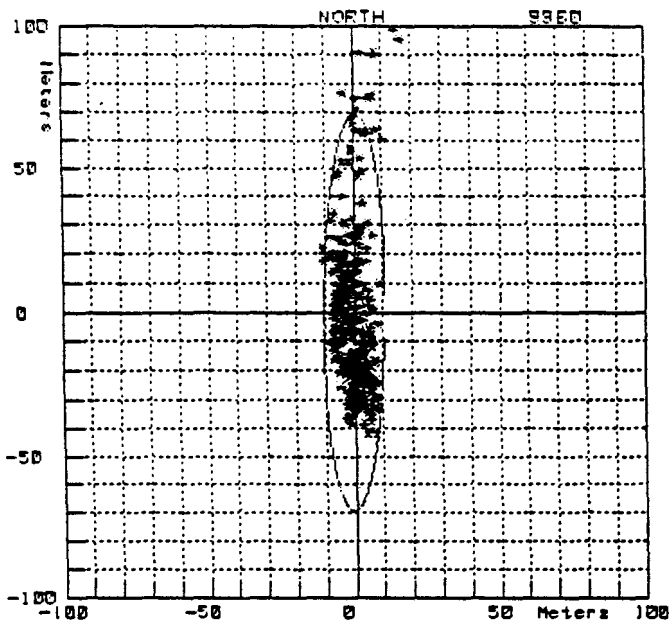


Figure 5. Time Difference (TD) Plots for 9960 Xray at Avery Point.
 Top: One Year; Bottom: 90 Day (Last Quarter).



2-D Elliptical Error

Inclusive Julian Dates:
274 to 365 1963

Probability of 95 %

Rho XY = .831

Sigma X = .047 msec

Sigma Y = .115 msec

X-Y Position Computed
using Mean TD's:

X = 26135.681

Y = 43995.159

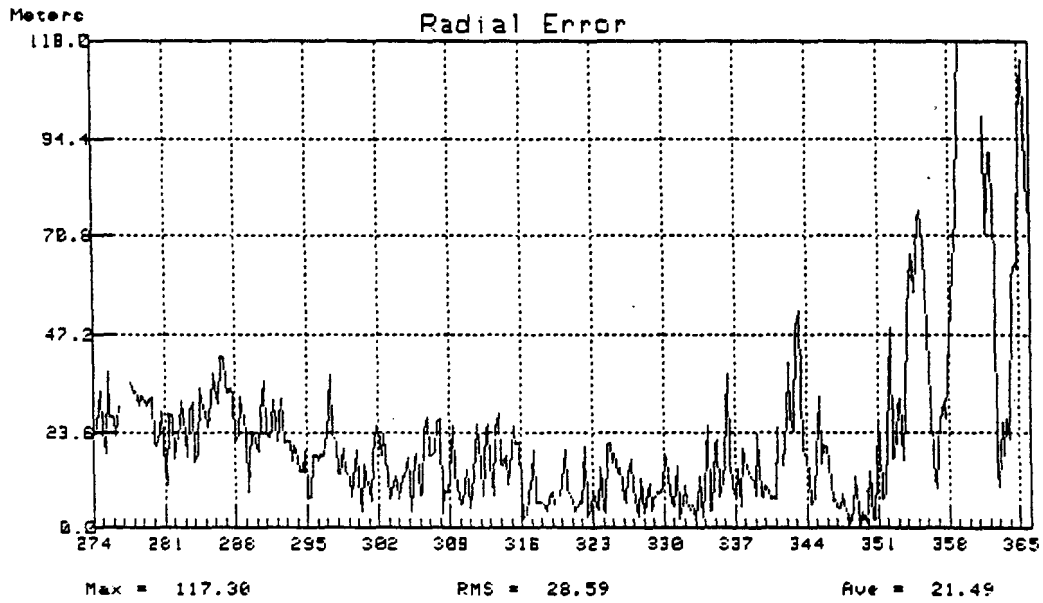


Figure 6. Elliptical Error and Radial Error Plots for 9960 X-ray and Yankee at Avery Point.

ALEX BAY N.Y.

Plot of TD, SNR and STD
0000Z on day 133 to 2345Z day 139

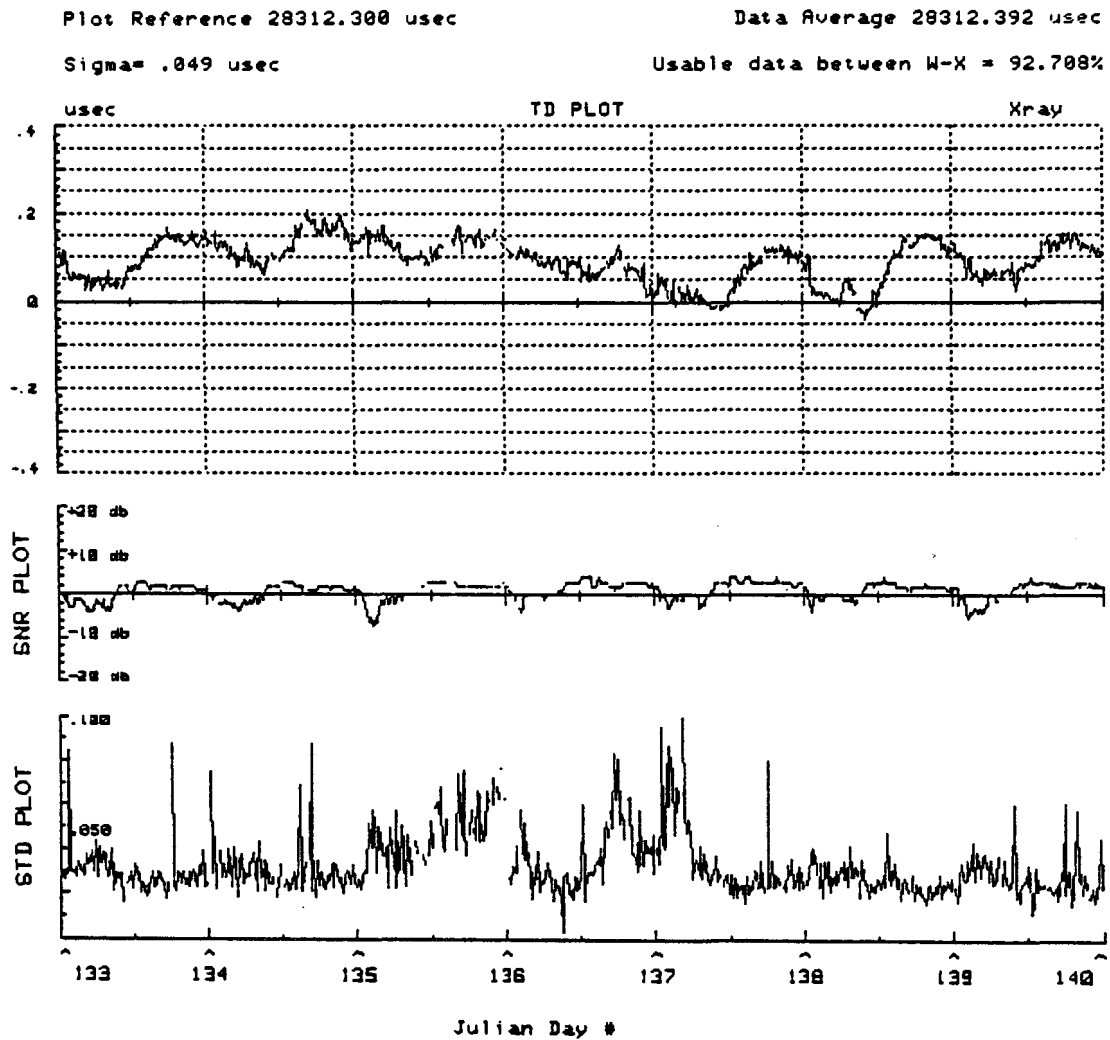
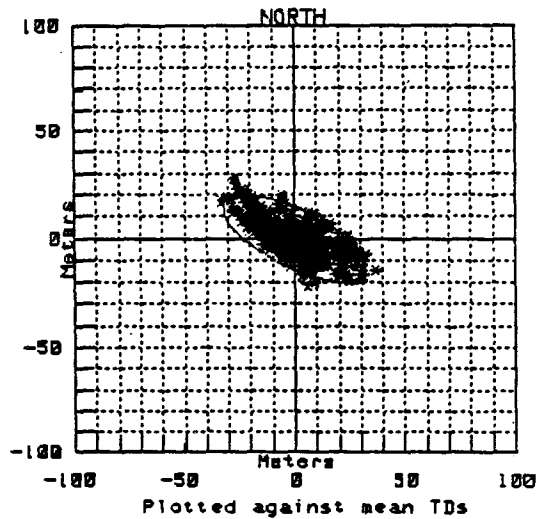
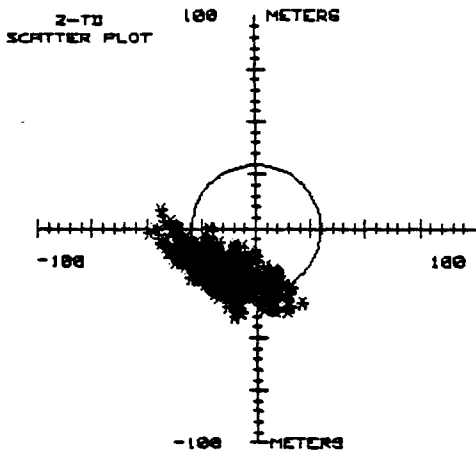
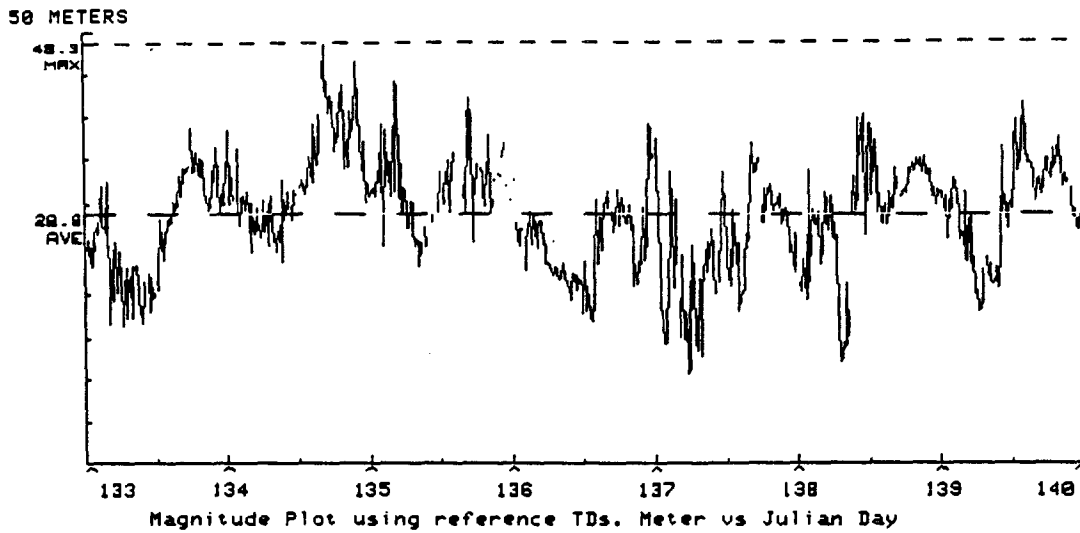


Figure 7. TD, SNR and Standard Deviation Plots for 9960 Xray at Alexandria Bay, New York. High-density 15 minute average data for a seven day period

ALEX BAY N.Y. (W-X) 2-TD RADIAL/ELLIPTICAL ERROR PLOT
 0000Z on day 133 to 2345Z day 139



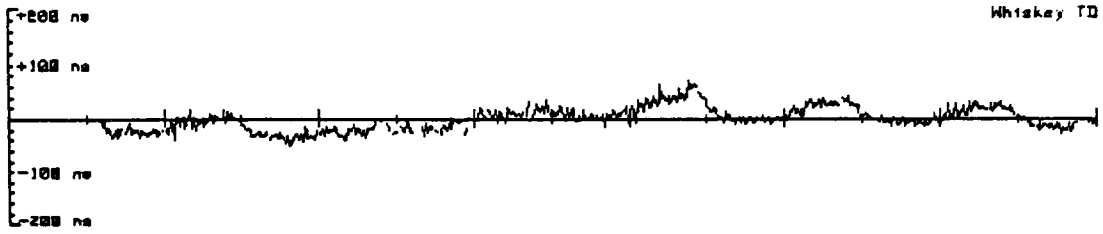
Plotted against AUG 82 reference TDs

AVE RADIAL ERROR (METERS) = 28.76
 RMS RADIAL ERROR (METERS) = 29.42
 MAX RADIAL ERROR (METERS) = 48.86

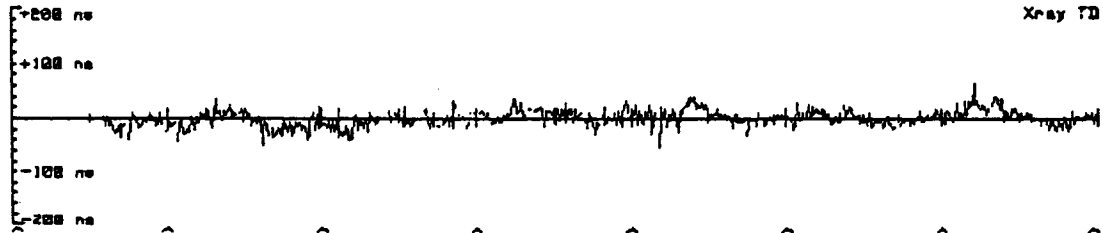
rho WX .848 95% error ellipse
 sigma W .042 Mean TD 15431.358
 sigma X .049 Mean TD 28312.392

Figure 8. 9960 Whiskey and Xray 2-TD Radial/Elliptical Error Plots for Alexandria Bay, New York. Obtained using high-density data.

DIFFERENTIAL PLOT
ALEX BAY N.Y. referenced to Massena N.Y.



Mean = -709.557 usec Sigma = .021 usec Rho = .896



133 134 135 136 137 138 139 140
Julian Day

Mean = -420.738 usec Sigma = .016 usec Rho = .955

Error Ellipse at ALEX BAY N.Y.
using Massena N.Y. as the reference.

Differential calculated by subtracting 100
Massena N.Y. TDs from
ALEX BAY N.Y.'s TDs.

Rho .510
Sigma W .021 usec
Sigma X .015 usec

Note: The error ellipse orientation and
the change in magnitude when compared
to the uncorrected error ellipse for
ALEX BAY N.Y. are the
important features of this plot.

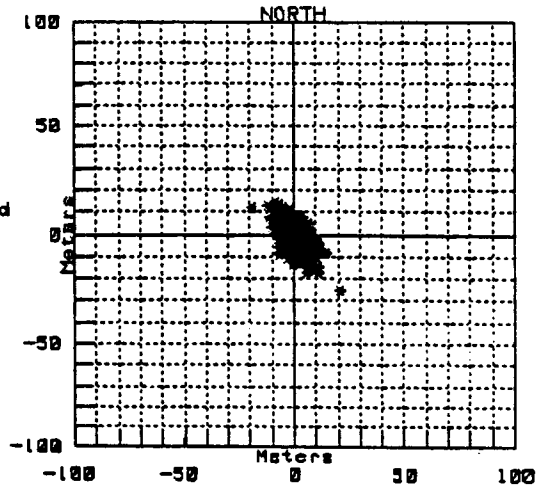


Figure 9. Differential Plot at Alexandria Bay, New York using Massena, New York as the reference. Obtained using high-density data.

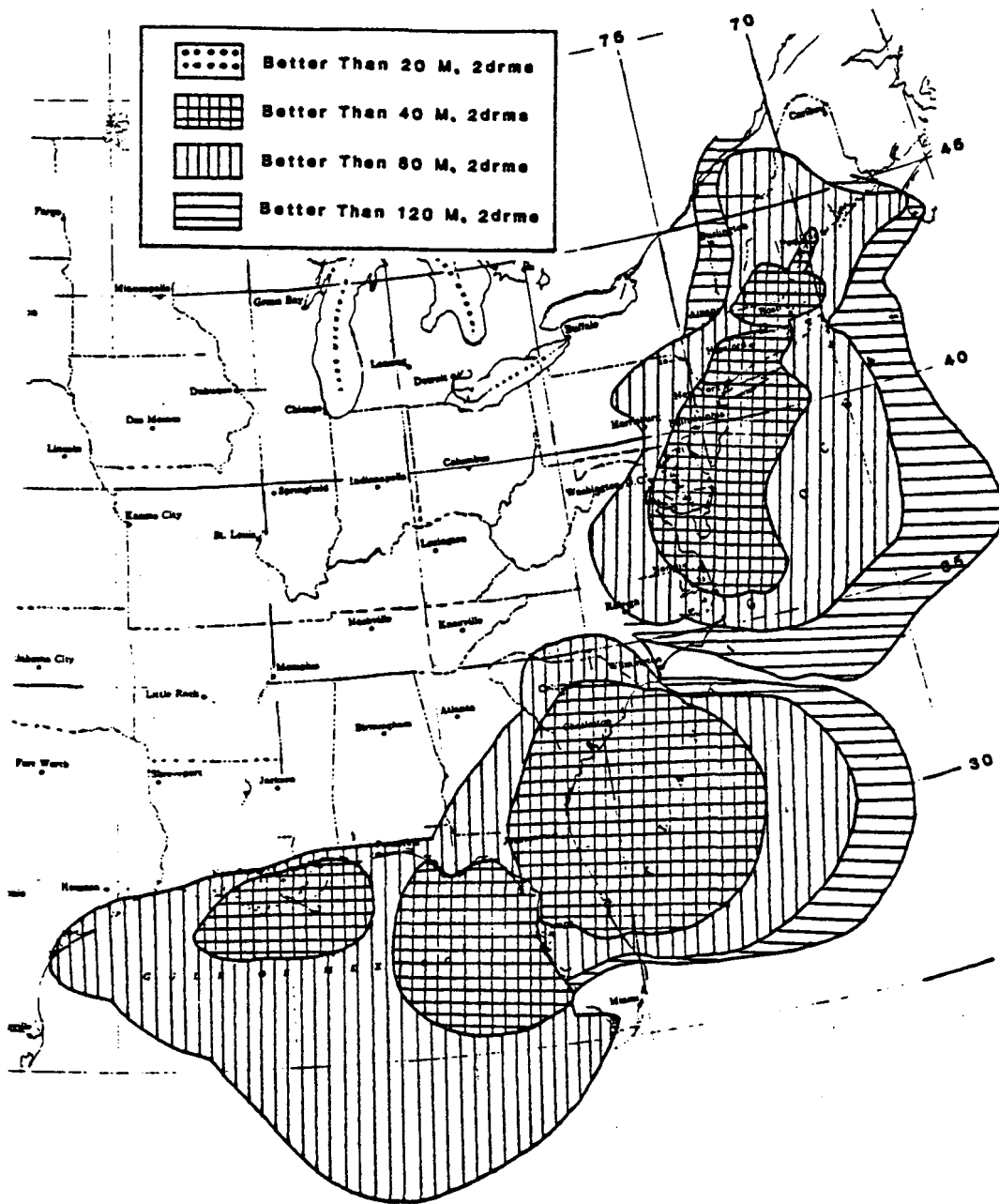


Figure 10. NEUS/SEUS Composite Repeatability Contour Diagram.

A FIRST LOOK AT LORAN-C CALIBRATION DATA IN THE GULF OF MEXICO

J. R. McCullough
Woods Hole Oceanographic Institution
Woods Hole, Massachusetts 02543

B. J. Irwin, R. C. Hayward, and R. M. Bowles
U.S. Geological Survey
Woods Hole, Massachusetts 02543

ABSTRACT

Observed LORAN-C calibrations in the northern Gulf of Mexico are analyzed and compared with Millington model predictions. Provisional charts of Additional Secondary Phase Factor (ASF) and Time Delay (TD) anomalies are derived. The potential impact of ASF charts on the evolution of LORAN accuracy and coverage is discussed, as are suggestions for improvements in current calibration methods. Some advantages of using the Global Positioning System (GPS) for LORAN calibration are presented.

Eight appendixes provide background information and a LORAN glossary. They describe a new method for remotely determining land conductivities using baseline TD observations and tomography, discuss ASF's and emission delays, show ASF contours in lowlands, and compare derived conductivity estimates with earlier AM broadcast band estimates. Error sources and suggestions for future surveys are discussed. Scatter plots of unedited verification cruise data are shown.

INTRODUCTION

LORAN-C geodetic accuracy is presently restricted by overland propagation delays which, if not considered, can cause fix errors as large as 2.5 kilometers in the Gulf of Mexico. Changes in the LORAN ground-wave velocity arises from altered electromagnetic boundary conditions at the earth's surface and associated propagation in the atmosphere. Because LORAN has low signal variance at great range (order 10 m at 10^6 m), mean propagation speeds need to be predictable to about one part in 10^5 to fully utilize the capabilities inherent in the system.

The speed of electromagnetic radiation in a vacuum is now so well established (± 4 parts in 10^9) that it, together with the definition of the second (time),

defines the standard of length--the meter (Pipkins and Ritter, 1983). Without direct calibration, however, the mean speed of LORAN ground-wave propagation is only predictable to a few parts in 10^4 overland and a few parts in 10^5 over salt water. (For recent reviews see McCullough, Irwin, and Bowles 1982; and Frank, 1983.)

Models used to estimate LORAN propagation are typically organized into three terms:

1. A fixed parameter, range dependent, nonlinear model of propagation over idealized salt-water conditions. This term accounts for most of the propagation travel time over land and sea and is referred to here as the "SALT-model."
2. A locally fixed offset or bias due to the presence of land segments in the propagation path, the ASF.
3. Variations due to seasonal and weather-related changes along the propagation path.

McCullough and others, 1982, discuss the overall problem and provide ASF data for the U.S. East Coast; this current paper provides ASF corrections for the Gulf of Mexico and encourages publication of ASF charts. Our goal in presenting these first Gulf of Mexico results is to stimulate interest in the development of:

- o Charts of land-sea ASF's.
- o Charts of seasonal variability.
- o Charts of TD anomalies.
- o Computer oriented forms of the chart data.

With ASF information, LORAN geodetic accuracy can be improved by as much as an order of magnitude: Coverage can be extended beyond that of conventional LORAN charts and fixes can be made automatically without human intervention.

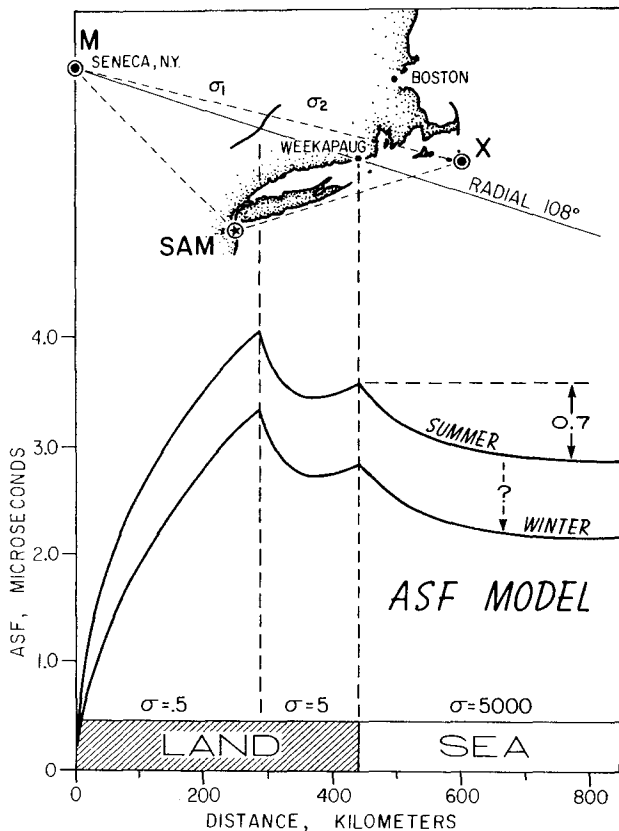


Figure 1. Model ASF predictions for the Seneca transmitter in summer and winter conditions. Note the abrupt changes, called phase recoveries, at the conductivity boundaries near the Hudson River valley and at the shore.

TECHNICAL BACKGROUND

ASF and Seasonal Variations

Figure 1 shows the cumulative ASF's along the 108° azimuth radial from the Master Rate-9960 transmitter at Seneca, New York. The modeled ASF's rise rapidly at first, taper off with range, and then actually decrease at boundaries with increasing conductivity, such as those at the Hudson River valley and the coast. Such ASF reversals, called phase recoveries, play an important part in LORAN calibration. (See McCullough and others, 1982, for experimental evidence of the sea phase recovery.) The abrupt overland phase recovery at the Hudson River Valley is the result of assuming a step function increase of ten in conductivity at that boundary. ASF's are nonlinear, reversing functions of conductivity and range. The winter curve,

sketched below that for summer (fig. 1), has smaller cumulative values because LORAN pulses travel slightly faster in winter than in summer.

Figure 2 (adapted from Slagle and Wenzel, 1982, p. B-11) illustrates seasonal variations suggested by time-interval-number (TINO) observations from the Seneca and Nantucket transmitters of Rate-9960 for the calendar year 1981. TINO's measure the interval between the start of the group-repetition interval (GRI) of the local transmitter timer and the arrival time of a pulse transmitted from another station in the chain. TINO measurements are routinely made using a dedicated Austron-2000 receiver and a special timing circuit that blocks the powerful local transmission. TINO trends are used to monitor chain performance. In addition, they can provide a time history of the sum of several delay variations. These include the relative clock drifts between the two transmitter timers, the baseline travel time variations, the antenna coupler delay variations, and the receiver delay variations.

By differencing TINO's from two transmitters, such as those of Seneca and Nantucket (M-X, Figure 2, top), the relative clock variations at the transmitters can be removed, leaving the two-way propagation-time variations and the sum of all coupler and receiver delay variations. Receiver and coupler variations can be determined directly or estimated from the difference of simultaneous TD observations available near some of the baseline extremes. To the extent that the coupler-receiver delays can be determined or ignored, such TINO differences can provide information about the two-way travel time variations along the baseline -- a variable of fundamental importance to LORAN navigation.

The peak-to-peak range of the TINO differences shown in Figure 2 (top), is typically 1.4 microsec suggesting the one-way propagation on the 590 km MX baseline may vary by as much as 0.7 microsec from summer to winter or about 1.2 microsec per 1000 km. (A winter LORAN pulse from M would be 210 m ahead of an equivalent summer pulse at Nantucket Island.) In the figure, peak winter variations, associated with large atmospheric temperature changes, cause 1.0 microsec TINO variations in as few as five days. Summer conditions are considerably more stable. Together, Figures 1 and 2 indicate the nonlinear, range-dependent nature of ASF's and illustrate seasonal and weather-induced fluctuations of ASF's in New England.

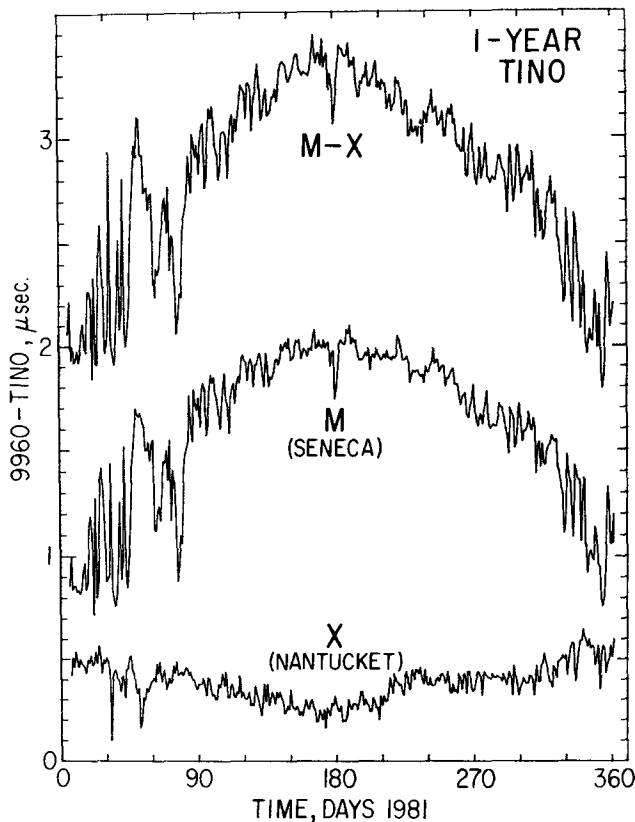


Figure 2. Observed seasonal ASF variations shown by time interval number (TINO) records at Seneca (M) of the arrival times of Nantucket transmissions, and at Nantucket (X) of the arrival times of Seneca transmissions, during 1981. TINO variations give the sum of: the relative clock drift between the two transmitter timers, propagation travel time variations, and delay variations in the TINO receiver and its antenna coupler. The TINO difference (M-X), shown above, removes the clock drift leaving only the sum of the variations in the two-way propagation travel time, and delay variations of the two receivers and their antenna couplers.

Extreme weather variations cause large rapid TINO variations between days 30 and 90. Summer TINO conditions are more stable. Nantucket TINO's vary less than those of Seneca because variations are largely compensated by the system area monitor (SAM), which receives X over a relatively stable ocean propagation path.

Gulf Data Sources and ASF Predictions

The Gulf of Mexico data stations and cruises used are shown in Figure 3. The USCG cruises used Austron-5000 wide-band receivers and shore-based navigation; the USGS cruises used Northstar-6000 narrow-band receivers and LORAN velocity-aided Transit Satellite navigation. Miscellaneous observations from drilling platforms, USCG land stations, APL LONARS sites, and USAF flight lines are included in Figure 3 and in Table 1. See Appendices A through H for discussion of related topics.

ASF predictions were made by the Defense Mapping Agency Hydrographic/Topographic Center (DMA). Observations were made by the U.S. Coast Guard (USCG), the U.S. Geological Survey (USGS), the U.S. Air Force (USAF), the Applied Physics Laboratory of the Johns Hopkins University (APL), and John E. Chance and Associates, Inc. The SALT-model used is from McCullough and others, 1982; the nominal emission delays (NED's) are from USCG (1981). Estimates of the seasonal variations were based on historical records (no direct observations were taken as part of the ASF surveys). Similarly, weather effects and broadcast emission delay (BED) variations were not monitored and were treated as noise.

The Millington model ASF contours in the Gulf of Mexico (fig. 4) have been computed using the assumed conductivity zones (5 and 30 mmho/m) shown in Figure 3. These provisional conductivity assumptions and model computations were provided by DMA. The radial structure of the contours at sea, such as those seen in the M-Range-ASF chart in the western Gulf (fig. 4), are due to azimuthal variations of the land lengths. Near shore ASF components tend to more nearly follow the shore line due to off-shore recovery effects.

The Delta-Range-ASF's (fig. 5), which represent differences of the Range-ASF's (fig. 4) for M-W, M-X, and M-Y, are numerically noisy due to subtraction roundoff to 0.1 microsec. Direct model predictions at full precision would appear smooth. The Delta-Range-ASF's represent TD predictions less the nominal emission delay (NED) bias (see Appendix D).

Gulf LORAN Geometry

LORAN geometric parameters in the Gulf are summarized in Table 2. Shown on a two by two degree latitude/longitude grid are: the W, X, and Y TD lane widths (meters per microsec); the TD crossing angles (degrees); and the one D-rms values

Table 1
Data Sources

#	Dates	Group	Loc.	Ship	Cruise	Control	Datum & Surveyor
1	1-14 Oct 1978	USCG	Gulf	BIBB	Tampa to Brownsville	Raydist + 30 m	NAD-27, R.J. Christian
2	5-17 Jul 1980	USCG	W.Gulf	ACUSHNET	Western Gulf	Raydist + 30 m	WGS-72 J.F.Weseman
3	1-7 Jan 1981	USCG	E.Gulf	INGHAM	Tampa to Norfolk	Maxiran + 30 m	WGS-72 E.F.Nuzman
4	28-30 May 1981	USGS	E.Gulf	GYRE 81-9	Tampa to Boothbay	Transit (BE)	WGS-72 (BE) B.J.Irwin
5	11-14 Oct 1983	USGS	E.Gulf	GYRE 83-13	Miami to Pensacola	Transit (BE)	WGS-72 (BE) B.J.Irwin
6	4-20 Nov 1983	USGS	W.Gulf	GYRE 83-14	Galveston to Galveston	Transit (BE)	WGS-72 (BE) B.J.Irwin

#	Dates	Group	Loc.	Station Type	Control	Datum & Surveyor
7	26 Sept - Dec 1, 1978	USCG	Gulf	Land Stations (22)	JMR-1	WGS-72 --
8	Mar-Apr 1980	APL	E.FLA	Lonars (4)	Transit (PE)	WGS-72 Fehlner
9	Dec 1981	US Air Force	Miss. to Fla.	Aircraft (Eglin A.F.B)	Cubic Western	WGS-72 (?) R.E.Voigt
10	1982-1983	John Chance	W.Gulf	Drilling Platform (13)	Transit	WGS-72 (BE) K.L.Maynard

GULF CALIBRATION CRUISES and FIXED STATIONS

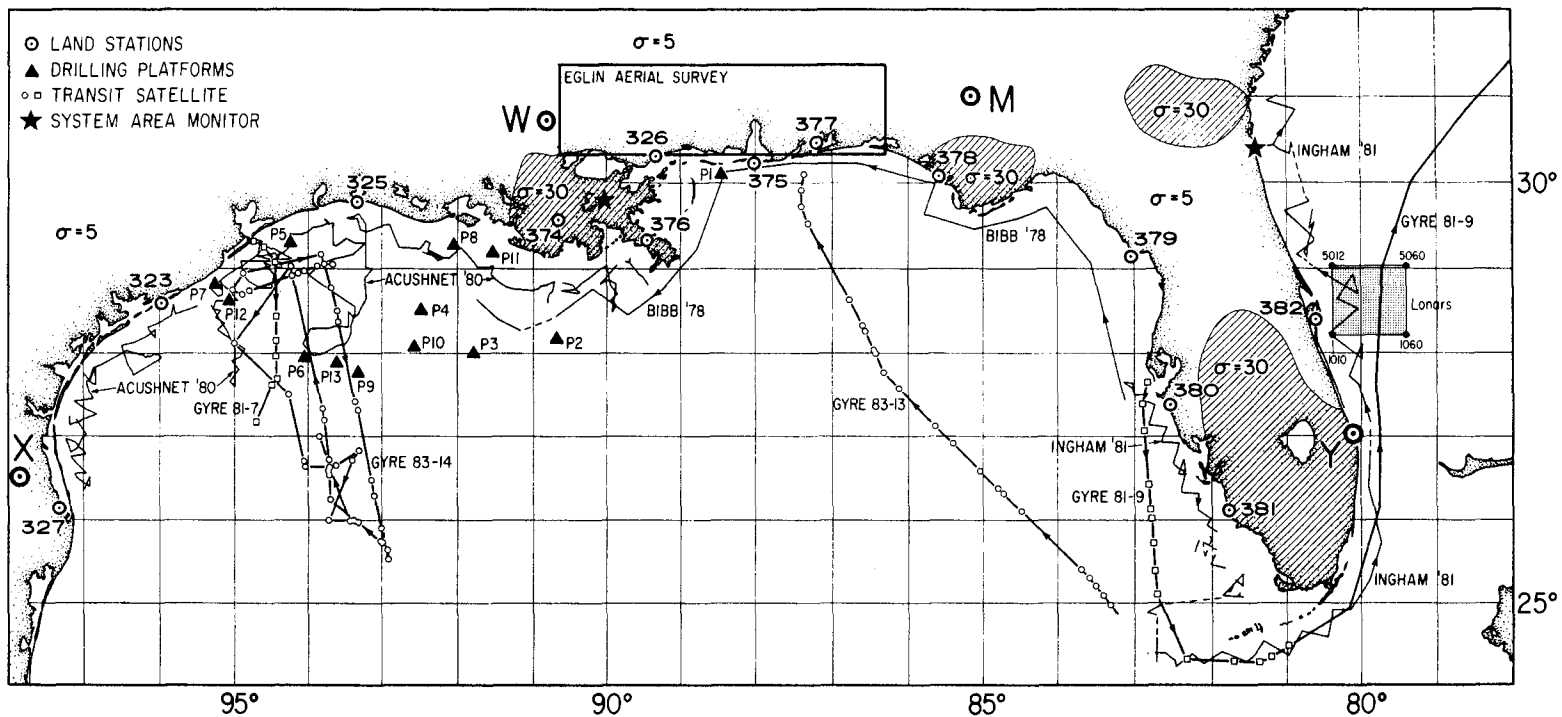


Figure 3. ASF calibration cruise chart for the Gulf of Mexico. Ship tracks include one BIBB, one ACUSHNET, one INGHAM, and four GYRE cruises. Also shown are thirteen USCG land stations, thirteen drilling platform sites, the Eglin AFB aerial survey region, the LONARS area, the 7980 M-W-X-Y transmitters, the two 7980 SAM's, and the DMA land conductivity zones ($\sigma = 5$ and 30 mmho/m).

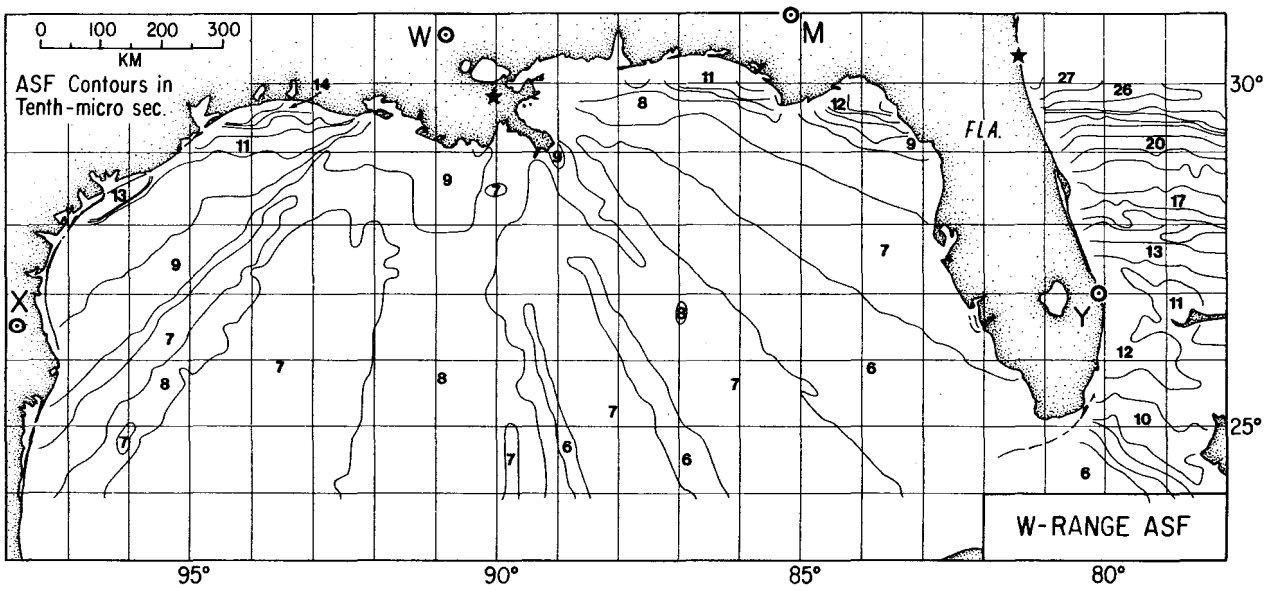
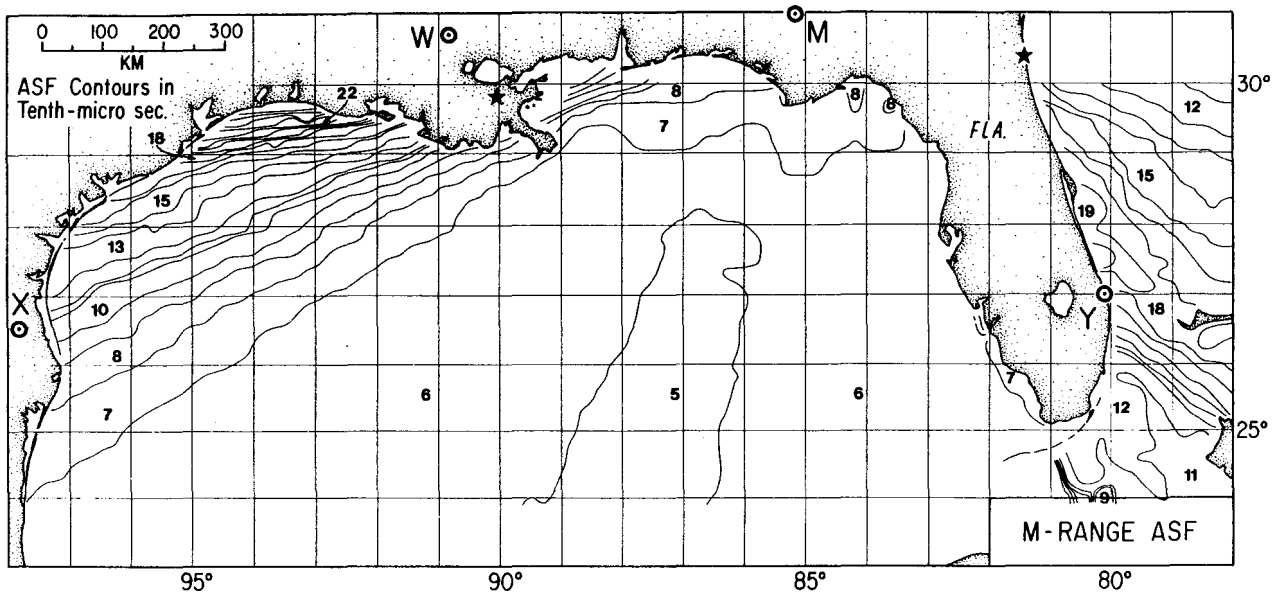


Figure 4. (Continued next page.)

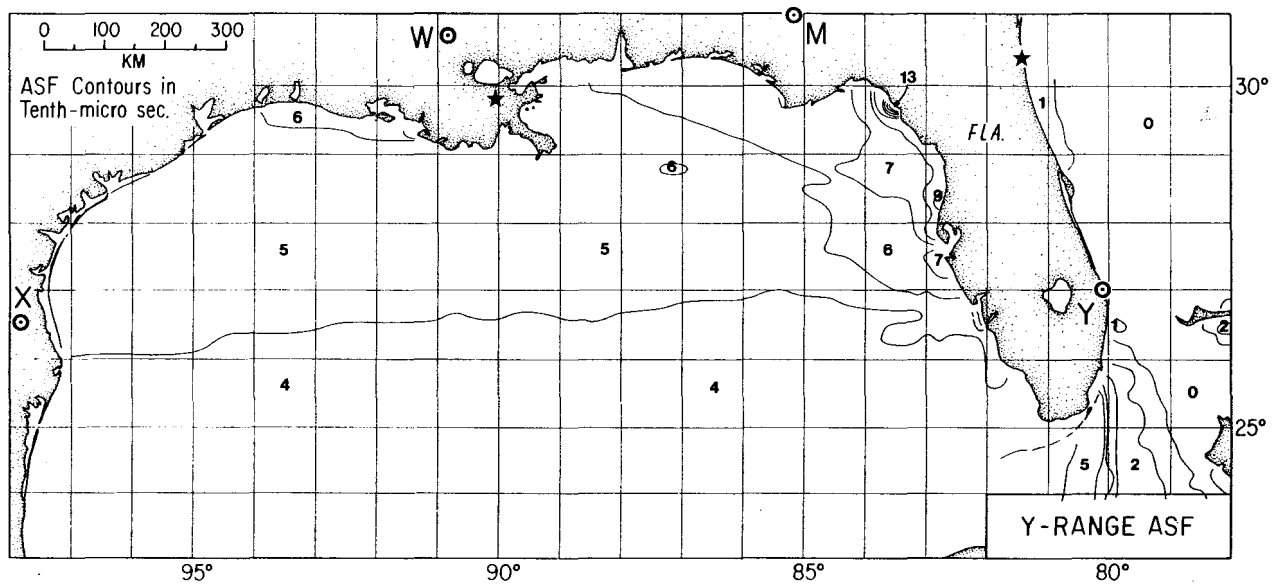
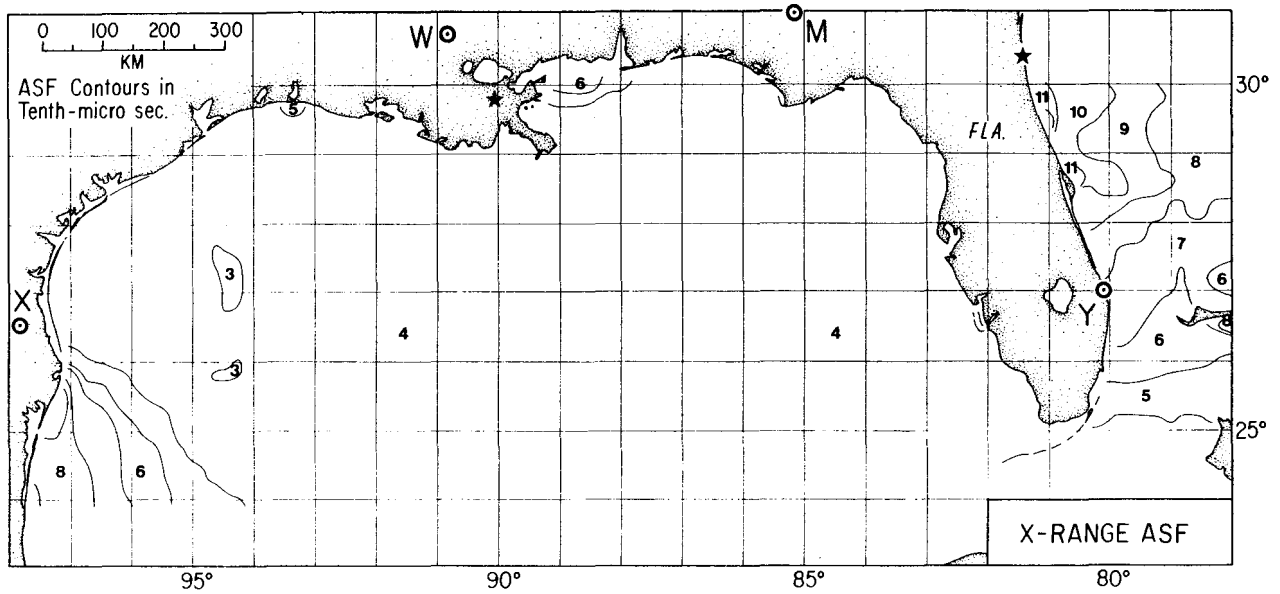


Figure 4. Model Range-ASF contours in the Gulf for the M, W, X, and Y transmitters of LORAN chain 7980. Featureless contours such as those for X are desired. Contours far from shore approach great circle radial paths; contours near shore more nearly parallel the shore due to offshore phase recovery effects. The large gradients in M in the western Gulf, and in M and W east of Florida, are caused by land lengths variations of M and W with azimuth.

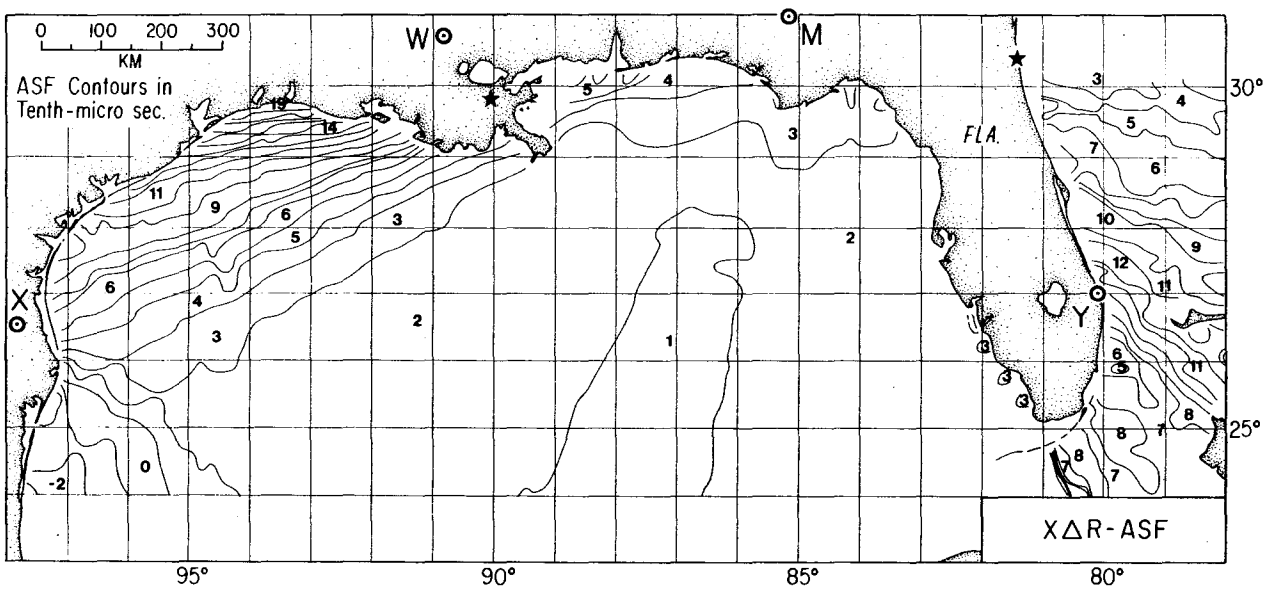
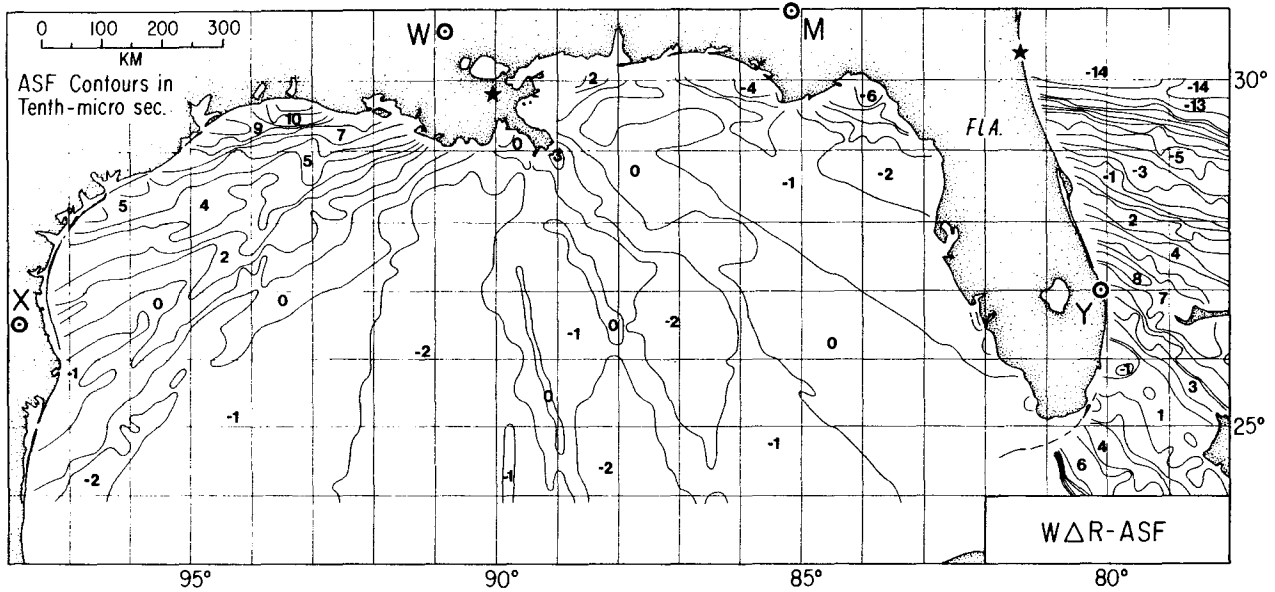


Figure 5. (Continued next page.)

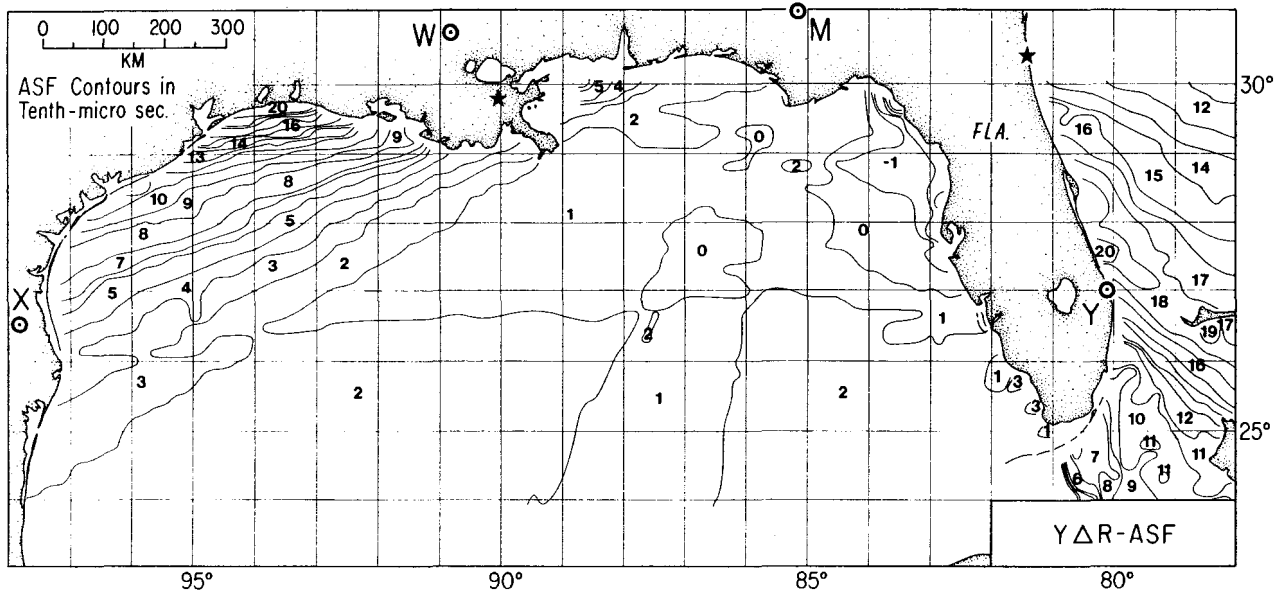


Figure 5. Model Delta-Range-ASF contours in the Gulf, constructed from the data of Figure 4. The contour shape shown represent the predicted shape of TD-ASF contours, but the values assigned have not been adjusted to represent TD-ASF's at this stage. Small scale contour features are due to round-off error and grid size in the DMA tabulated predictions; direct model calculations would be smoother.

Table 2.
LORAN Geometric and 1D-rms parameters in the Gulf of Mexico.

Long.	96°	94°	92°	90°	88°	86°	84°
Lat. 30°	10006	2885	W LANES, m per microsec		159	178	484
28	1418	789	704	173	232	263	389
26	1010	682	424	267	334	360	449
24	939	712	476	368	447	467	563
Lat. 30°X LANES, m per microsec....				...Y.LANES, m/microsec..		
28	170	157	153	150	400	227	150
26	153	150	151	154	314	221	170
24	164	162	164	170	330	263	224
	223	196	192	197	382	334	316
	CROSSING ANGLE, deg.						
Lat. 30°	(W-X)			 (W-Y)		
28	63	76	88	35	88	81	74
26	85	79	62	43	69	78	84
24	57	55	47	38	54	59	62
	33	38	36	31	43	45	45
Lat. 30°	1D-RMS, m per (tenth microsec each TD)						
28	1123	299	72	40	43	29	53
26	143	82	51	45	42	35	43
24	122	85	68	66	58	52	57
	177	121	101	99	87	81	88

(meters) assuming one tenth microsec rms for each TD. Typical D-rms values are in the range 30 to 100 meters except in the Galveston area where large lane widths and poor crossing angles cause significant deterioration of the LORAN geometry. The proposed transmitter near Waco Texas would correct this problem. Note that the planned degraded-GPS accuracy of 50m 1D-rms (100 m 2D-rms) is comparable to LORAN 0.1 microsec rms for most of the Gulf, i.e., LORAN geodetic accuracy becomes equal to that of degraded-GPS at about the 0.1 microsec rms TD accuracy in the Gulf.

Seasonal Variations

Stations	Dist. km	P-P micro sec. per1000 km	Ref.
Seneca and Nantucket	590	1.2	Fig. 2
Dana and Carolina beach	1061	0.7	Frank (1974)
Gulf of Mexico MWXY	about 1000	0.36	Fig. 6

LORAN Seasonal Propagation Variations

The seasonal variations in the Gulf of Mexico are relatively small in comparison with the seasonal propagation variations in New England (fig. 2). Figure 6 shows one-year TD histories for monitors at Galveston (G), Destin (D), and St. Petersburg (P) (from Wenzel and Slagle, 1983). Each of the six TD records shows variations in mean propagation speed along four paths determined by the observation point, the system area monitor (SAM), and Master-Secondary pair. The geometry involved is illustrated by the quadrilateral MSYPM (top right, fig. 6) that connects the Master (M) at Malone, Fla., the SAM (S) at Mayport, the Y-Secondary (Y) at Jupiter, and the receiving monitor (P) at St. Petersburg. The net TD variation (DELTA.TD) at the monitor is:

$$\text{DELTA.TD} = \text{MS} - \text{SY} + \text{YP} - \text{PM}$$

where MS, SY, YP, and PM are the propagation travel time changes contributed by each of the sides of the quadrilateral MSYPM.

Various double range difference (DRD) models, based on this geometry are discussed by Slagle and Wenzel (1982). The correlation of the DRD-distances and signed seasonal peak-to-peak TD variations in the Gulf is illustrated in Figure 6 (bottom). The much smaller slope (0.36 versus 1.2 microsec/1000 km mentioned earlier for New England) together with the small range of DRD-distances encountered offshore, predict seasonal variations of typically 0.2 microsec peak to peak for most of the Gulf between Texas and Florida, (see also Wenzel and Slagle, 1983, pp. 5-15). In some areas, such as the LONARS area, the DRD distances are too small for seasonal, weather, and diurnal bias effects to be detectable (Fehlner and Jerardi, 1983).

OBSERVATIONS

Common Properties

Figures 7 through 10 summarize the primary observational data used in this study. Figure 7 shows the W Secondary TD-ASF's as a function of azimuth at W. In like manner, Figures 8 and 9 show the Y and X summaries. In Figure 10, which presents a similar summary for W in the western Gulf of Mexico, the reference transmitter used is X instead of M. In each of the four figures, DMA Millington model predictions and an arbitrary fit to the USCG data are shown for reference. The observed ASF's were computed using the SALT-model (McCullough and others, 1982) and the USCG published nominal emission delays (NED's). Any change in the NED of a Secondary causes an equal change in the zero-point of its observed TD-ASF. Thus the levels of all the W, X, and Y TD-ASF observations are set by the assumed Secondary NED's.

Appendices C, D, and F discuss the 7980 NED's, the TD-ASF's of Figures 7-10 (Eqs. D-6 through D-10), and observational error sources in the LORAN surveys.

W-TD-ASF's, Eastern Gulf

Figure 7 summarizes the W-TD-ASF observations in the eastern Gulf of Mexico as a function of azimuth at the W (Grangeville, La.) transmitter. In both data frames, the trend of the USGS data is indicated by the arbitrary line A. The USGS 1981 and 1983 cruise data (lower frame) are consistent over the 20-degree arc from the Florida Keys to Tampa; the USCG data agree near the Keys, but are 0.4 microsec larger north of the Keys. There is also a difference in slope of the line A and the DMA prediction (dashed line). Factors contributing to the bias difference may include seasonal variations, conductivity variations in the M transmitter overland paths, shore

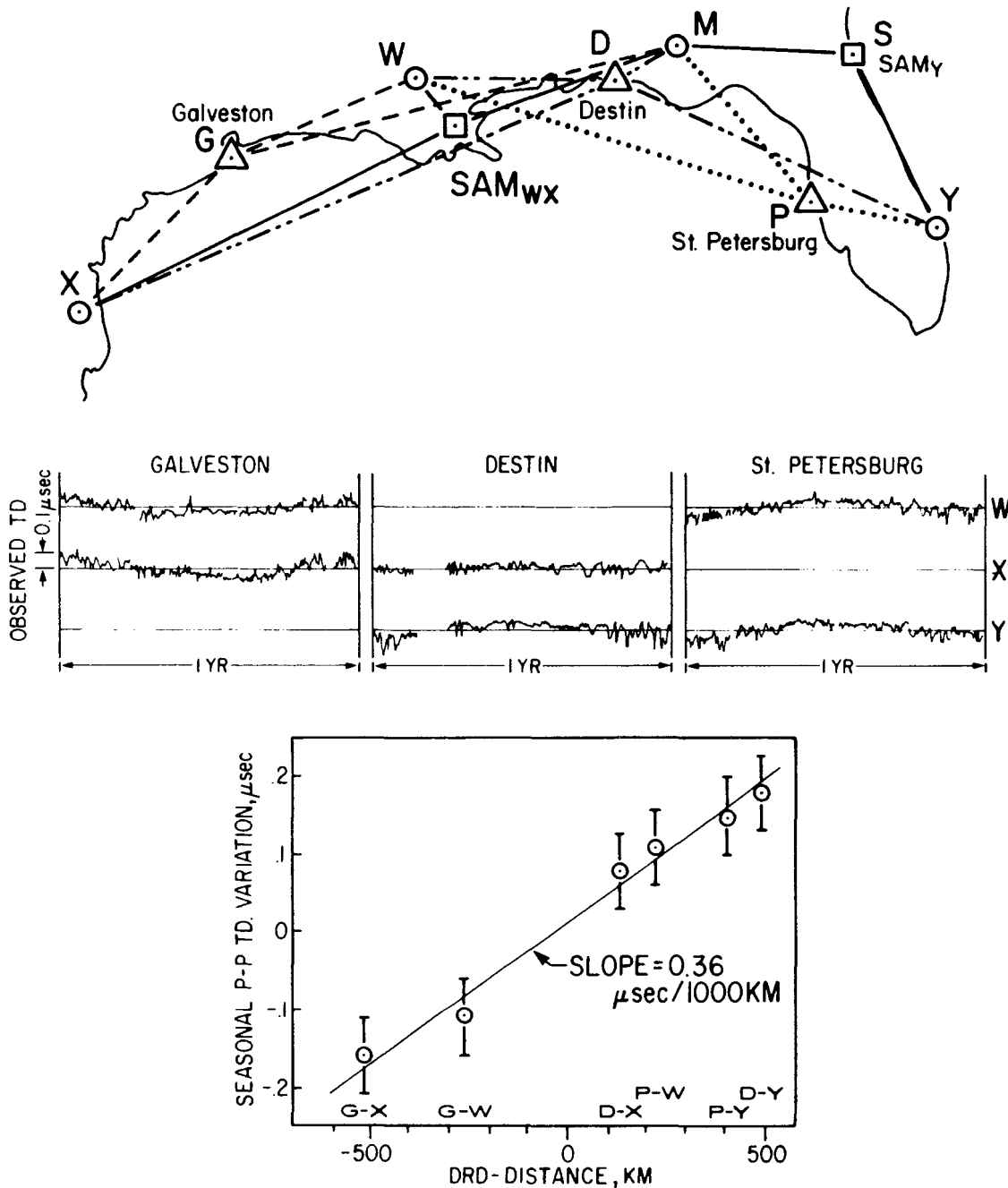


Figure 6. Observed seasonal TD variations at three monitors - Galveston, Destin, and St. Petersburg (top) - show peak-to-peak yearly variations (center) of about 0.2 microseconds for stations W-X-Y. Monitor variations are influenced by the land portions of the four signal paths connecting the SAM and monitor to the transmitters. For example, consider the quadrilateral, MSYPM, for monitor P, SAM S, and transmitters M and Y (top right). By alternately adding and subtracting the land lengths around the quadrilateral (in the order MSYPM), the double-range-difference (DRD) is found.

The signed peak-to-peak yearly variation (bottom) is correlated with such DRD distances. The 0.36 microsec/1000 km sensitivity estimated is about one-third that observed in New England. DRD model predictions indicate seasonal variations throughout the Gulf similar to those of the monitors shown.

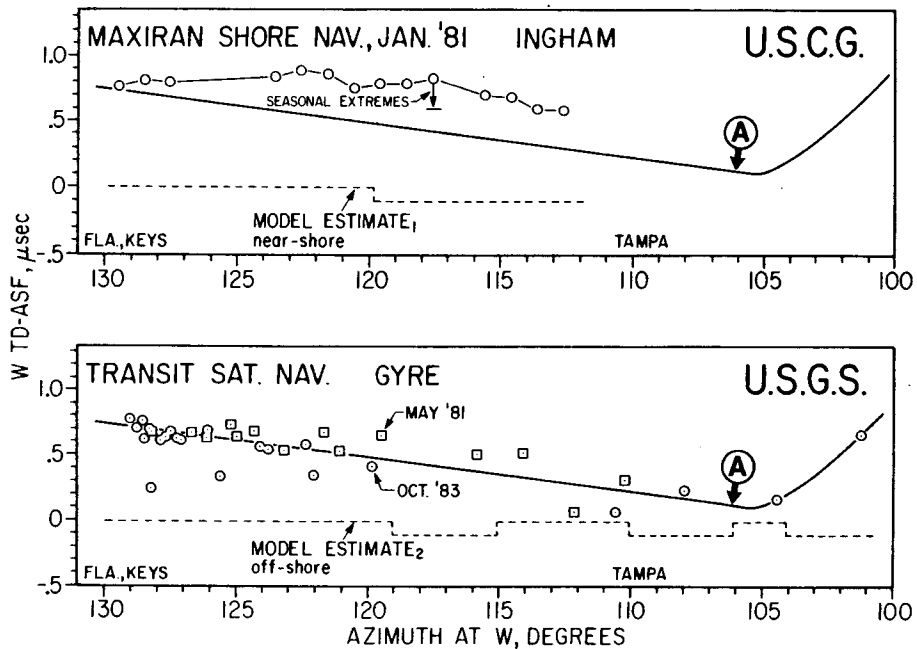
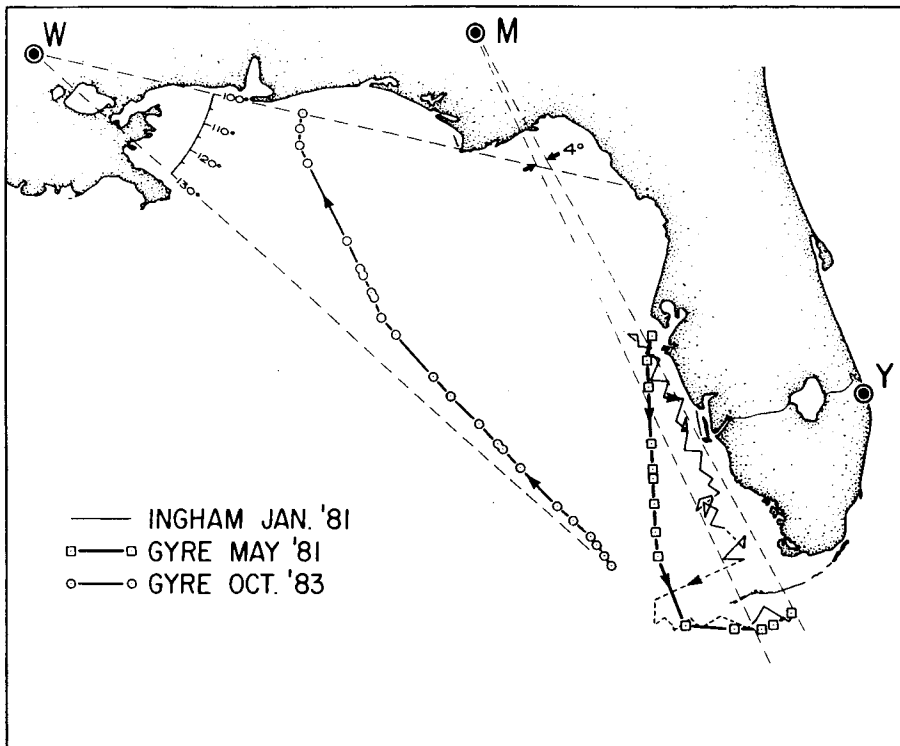


Figure 7. Observed TD-ASF's for Secondary W in the eastern Gulf as a function of azimuth at W (top left). Data from three cruises (top) show a trend as indicated by solid lines A (center and bottom). Systematic differences between the observations and model estimates (dashed lines) can be reduced by changing the nominal emission delay (NED) of Secondary W. Smaller systematic differences between the USCG and USGS observations are apparently due to reference navigation and seasonal effects. Consistency of the observations suggests an upper bound for the accuracy obtainable with calibrated LORAN in this region.

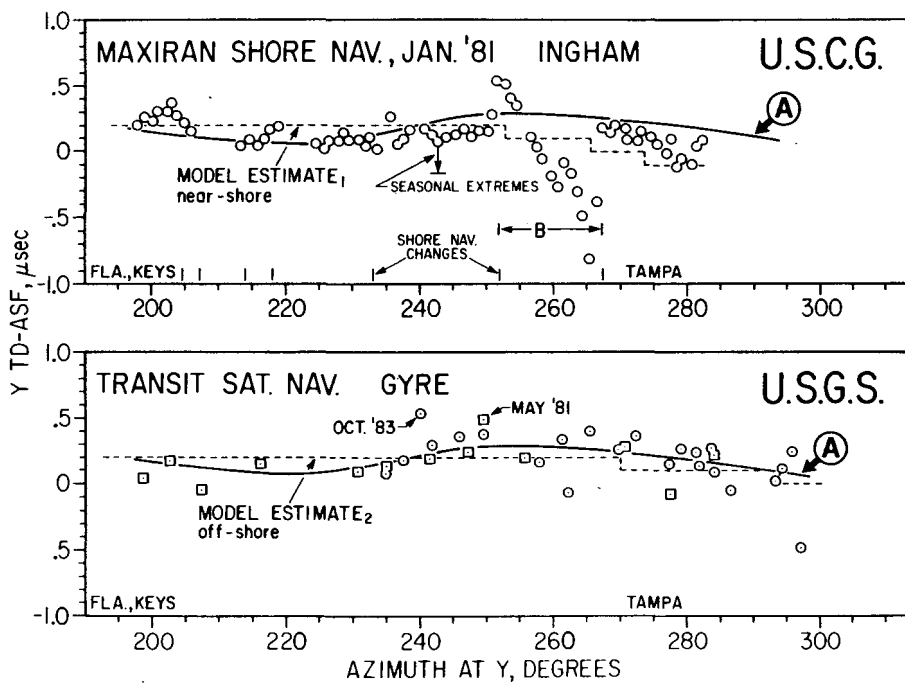
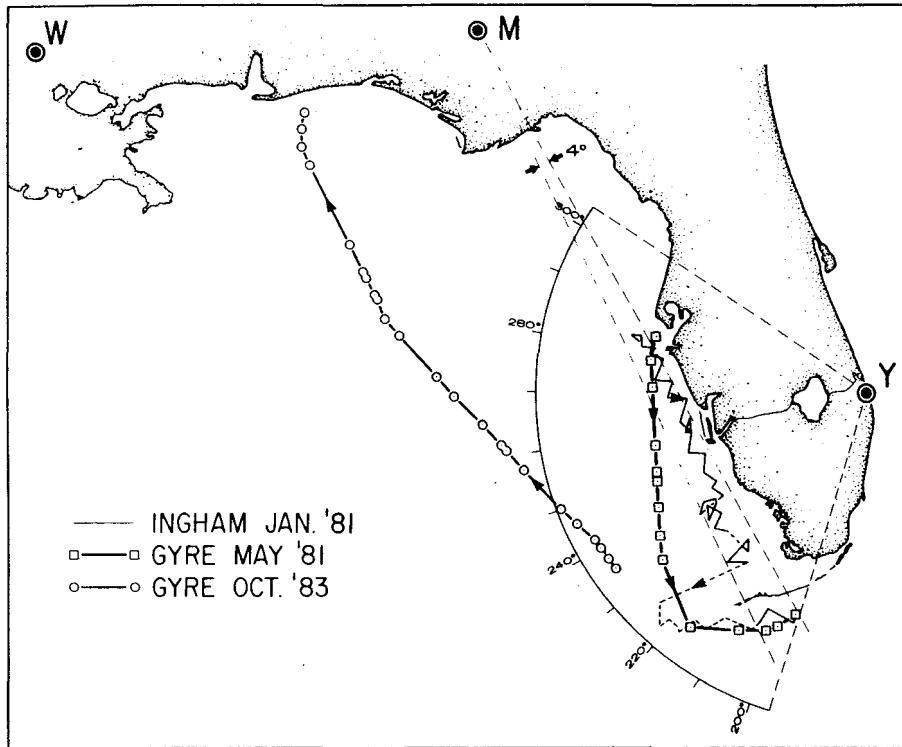


Figure 8. Observed TD-ASF's for Secondary Y in the eastern Gulf, as a function of the azimuth at Y (top). The observations and model estimates are in close agreement (below). The INGHAM data (center) show small trends between shore navigation zones, particularly noted in the zone labeled B. The USCG observations lie in a 4 degree azimuthal arc at M, and thus represent variations primarily due to Y and observational error.

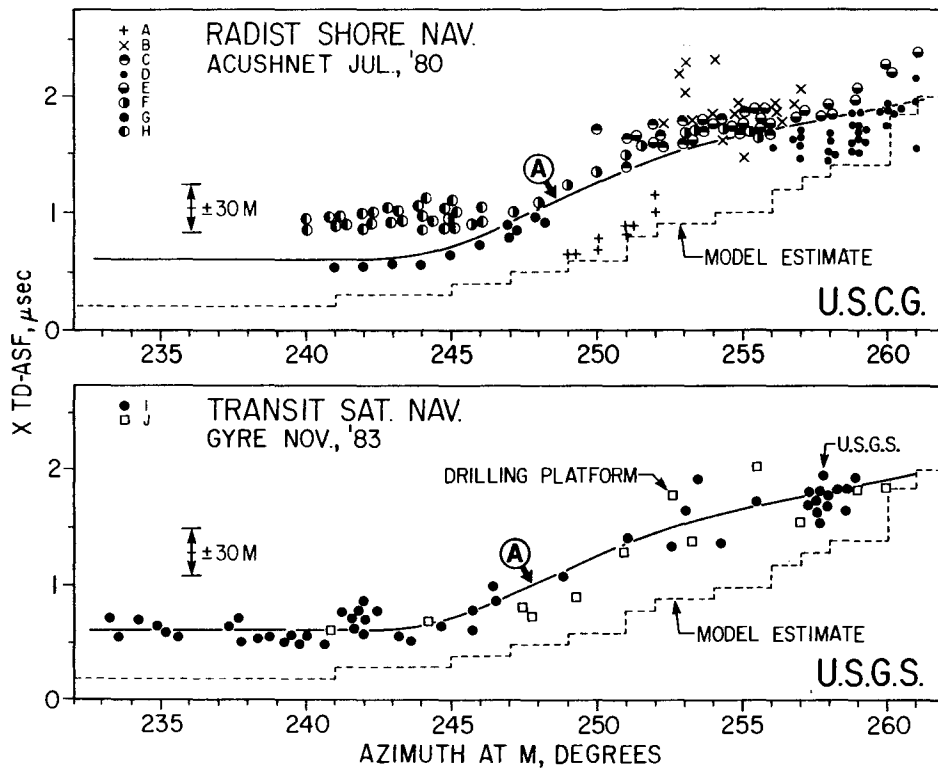
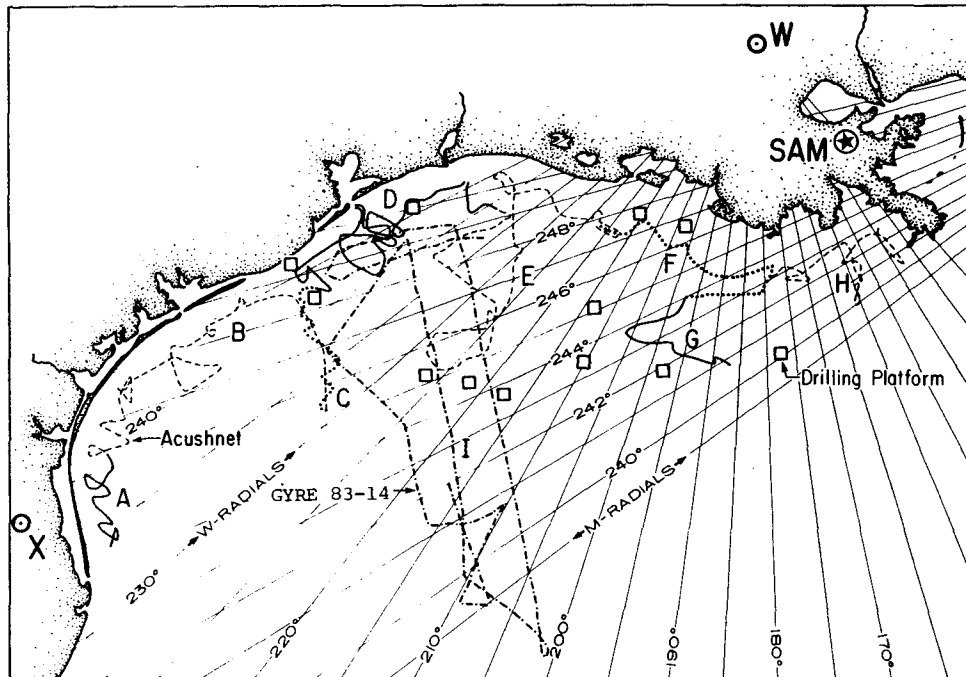


Figure 9. Observed TD-ASF's for Secondary X in the western Gulf as a function of the azimuth at M. The ACUSHNET cruise segments A through H (top) show systematic ASF differences (center). Again, the model bias (dashed lines) can be adjusted as a NED bias. The ± 30 m arrows provide an approximate distance scale for the observations.

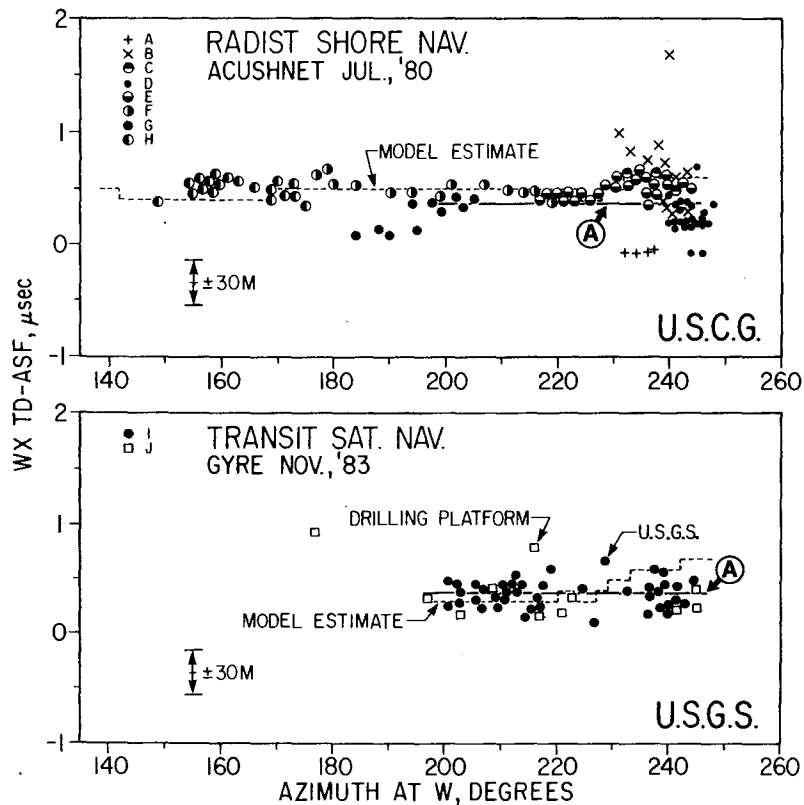
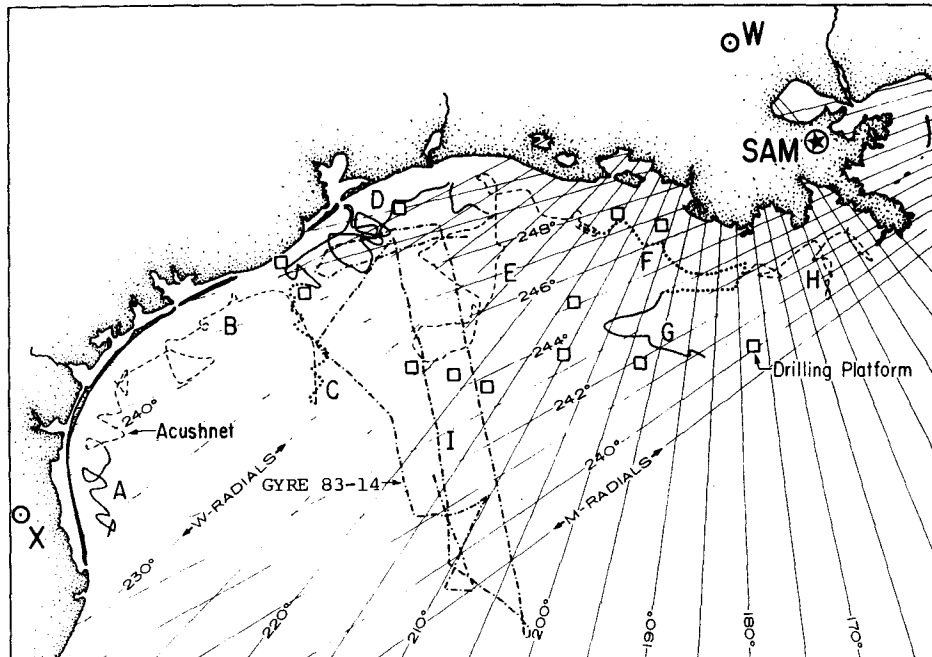


Figure 10. Observed TD-ASF's for Secondary W in the western Gulf (relative to Secondary X) as a function of the azimuth at W. The observations and model estimates are in close agreement except for azimuths near 240 degrees where model conductivity adjustments may be needed. The $\pm 30\text{ m}$ arrows provide an approximate distance scale.

navigation biases, and observational scatter. The USCG data (center frame) were selected to lie within a 4-degree arc of relatively uniform land at M. The observed W-TD variations must, therefore, be due largely to land length and conductivity variations between W and the sea. Little variation is predicted (dashed line) or observed (circles, center frame).

At St. Petersburg (fig. 6), the W-TD's are observed to be smaller in winter than in summer. Thus winter ASF's will be larger than summer ASF's by perhaps as much as 0.2 microsec. The TD calibrations given in this paper are intended to represent the more stable summer conditions. We therefore take line A as our best estimate for all observations of the W-ASF's of the eastern Gulf.

The four northernmost USGS GYRE-83 (fig. 7) observations must be considered separately because they involve large M-land azimuthal variations and offshore recoveries for both M and W. The directly comparable and well-observed portion of line A is thus limited to the linear portion on the left (i.e., azimuth at W greater than 120°) which reduces the apparent difference in slope noted between the USGS and USCG data sets.

The DMA model predictions lie about 0.7 microsec below the USCG observations (about 0.6 microsec after correction for seasonal offset). Unfortunately, the seasonal component cannot be determined directly because fixed-monitor data were not taken. The bias could result from any combination of three model assumptions:

- o NED too large.
- o M path conductivity too high.
- o W path conductivity too low.

Circumstantial evidence (Appendix C) suggests the Rate-7980 NED's are uncertain by about 0.5 microsec. Considering the observational scatter and sparsity of data, only a NED bias adjustment (0.6 microsec) seems justifiable from the present observations. Bias adjustments could be implemented as changes in the published NED's or as offsets in the DMA model. Adjustments via the conductivity assumptions also seem reasonable and are being studied by DMA (see appendix B). We strongly recommend, however, that the controlling standard time differences (CSTD's) be held constant for long-term continuity.

Y-TD-ASF's, Eastern Gulf

Figure 8 summarizes the Y-TD-ASF observations in the eastern Gulf as a

function of the azimuth at the Y (Jupiter) transmitter. The trend of the USGS data (bottom frame) is indicated by the arbitrary line labeled A in both data frames. The 4-degree azimuth arc at M can, again, be used to separate the ASF effects due primarily to the Secondary. The USCG INGHAM data (center) are locally consistent at less than 100 nanosec, but show small abrupt jumps during shore-navigation transponder changes (indicated by the short vertical lines above the azimuth axis). The effect is particularly pronounced at B, but we were unable to independently establish whether this change is due primarily to shore-navigation changes or to propagation effects over fresh-water Lake Okeechobee. Because observations farther seaward on the GYRE 1983 cruise do not show the feature at B, we assume that shore-navigation changes are responsible.

As seen in Figure 6, the seasonal effects at St. Petersburg for W and Y are similar. In this case (fig. 8), however, inclusion of the seasonal effects increases the difference between the USCG and USGS observations by 0.1 to 0.2 microsec. The systematic discrepancy remains unexplained.

As before, model predictions depend on the combined effects of three assumptions: the NED bias, the conductivity of ground along the Master and Secondary paths. Model results are in good agreement with the observations, but if the 0.25 microsec NED offset determined in Appendix B is considered, a conductivity adjustment is required. Some iterative adjustment of this sort might be considered after atomic clock (Hot-clock) observations have been made for Rate-7980. Additional insights might be found in the 1980-TINO records. We conclude that model conductivity adjustments are not presently justified by these rather limited, noisy, and somewhat conflicting observations.

X-TD-ASF's, Western Gulf

The over-land path from the X-transmitter at Raymondville, Tex., is relatively short and uniform over the azimuth arc of interest. Accordingly, we have used X as the reference and assumed that the MX and WX TD-ASF variations are primarily correlated with azimuth angles at the M and W transmitters. Figure 9 summarizes the X-TD-ASF observations in the western Gulf as a function of azimuth at the M transmitter at Malone, Fla. The USGS and platform data (bottom frame) are in general agreement. An arbitrary trend line, A, has again been matched to the data in the lower frame and repeated for reference in the middle frame. Distance

scales of ± 30 m are shown at the left. Each of the various USCG cruise segments (center frame) show ASF scatter generally within the ± 30 m specification of the Maxiran and Raydist Shore-based Navigation, but larger segment-to-segment biases are again obvious. The navigation logs for this cruise were unavailable, so it was not possible to match the data steps with changes in shore navigation. There is no reason to suspect that LORAN changes in this stepwise fashion.

Therefore, even though the data volume and cruise coverage are extensive in the western Gulf of Mexico (fig. 9), the results are difficult to interpret. The data from each ACUSHNET cruise segment must be treated as independent observations of questionable bias and slope. The larger data sets (middle frame) should carry no more weight than the smaller ones (middle frame). The earlier TD-ASF's of the 1978 BIBB cruise were also examined and were found to be unusable for the western Gulf area. The eastern Gulf BIBB data show some promise in spot checks, but are not yet fully available in computer-readable form.

The platform location data (Maynard, 1983) were determined from fixed-position, multiple-pass, Transit Satellite surveys, and are thought to be accurate to within ± 5 meters in World Geodetic Standard of 1972 (WGS-72) coordinates. The associated LORAN TD estimates were made from ships of opportunity working near the platforms. These observations, unlike the others, are limited primarily by the ship offset and receiver-tracking loop delays and not by the reference navigation. The TD's of the platforms are probably well known to helicopter pilots in the area, but that information was not available. A program of instrumented helicopter flights to selected offshore platforms would greatly increase our knowledge of western Gulf ASF's.

Model observations are in general agreement except for an offset of about 0.5 microsec, suggesting that the X-NED is 0.5 microsec too large.

WX-TD-ASF's, Western Gulf

Figure 10 summarizes the WX-TD-ASF observations in the western Gulf as a function of the azimuth at W. The observed WX-TD-ASF is defined here as,

$$WX.TD.ASF = X.TD.ASF - W.TD.ASF \quad (1)$$

by definition (see Appendix D, Eq. D-5)

$$X.TD.ASF = M.Range.ASF - X.Range.ASF - (X.BED - X.NED) \quad (2)$$

$$W.TD.ASF = M.Range.ASF - W.Range.ASF - (W.BED - W.NED) \quad (3)$$

or

$$WX.TD.ASF = W.Range.ASF - X.Range.ASF + (W.BED - W.NED) - (X.BED - X.NED) \quad (4)$$

Where M, W, and X are the transmitters, and the (BED-NED) terms are the emission delay anomalies. The USGS and platform data are again in general agreement. As before, the clustering of the USCG observations suggests systematic errors.

In summary, the observational data in Figures 7-10 are in first-order agreement with the predictions if corrections of reasonable magnitude are made to the published NED's. These changes are shown in Table 3.

Table 3

TD	Area	NED Corr.	Ref.	Cond. Change
W	E. Gulf	-0.6	Figure 7	Hold
Y	E. Gulf	-0.25	Apx-B, Fig-8	Adjust
X	W. Gulf	-0.5	Figure 9	Hold
WX	W. Gulf	0.0	Figure 10	Hold
W	W. Gulf	-0.5	Eq. 4	Hold

Thus subtract:
0.6 microsec from the present W-NED,
0.5 microsec from the present X-NED, and
0.25 microsec from the present Y-NED.

Although providing a simple solution, these NED corrections are unlikely to give an optimum adjustment of the combined NED and conductivity assumptions (Eq. D-9). They are proposed as a first iteration.

In all, good agreement (order 0.2 microsec peak to peak) is suggested by many of the independent observations that span thousands of kilometers of ocean, the full extremes of seasonal variation, and several years of observation in the Gulf of Mexico. If calibrated for ASF and seasonal variation, LORAN could provide geodetic accuracy of typically 0.1 microsec rms for each TD or roughly 30 to 100 m 1D-rms (see Table 2, bottom) in contrast to the present conventional "quarter-mile 2D-rms" (250 m, 1D-rms) accuracy tolerance generally given for TD and chart navigation. This represents a potential improvement of about 2 to 10 in accuracy utilizing existing equipment. Real-time differential LORAN could further improve the accuracy to perhaps 30 nanosec rms per TD or about 10 to 30 m 1D-rms in Gulf areas with good LORAN coverage.

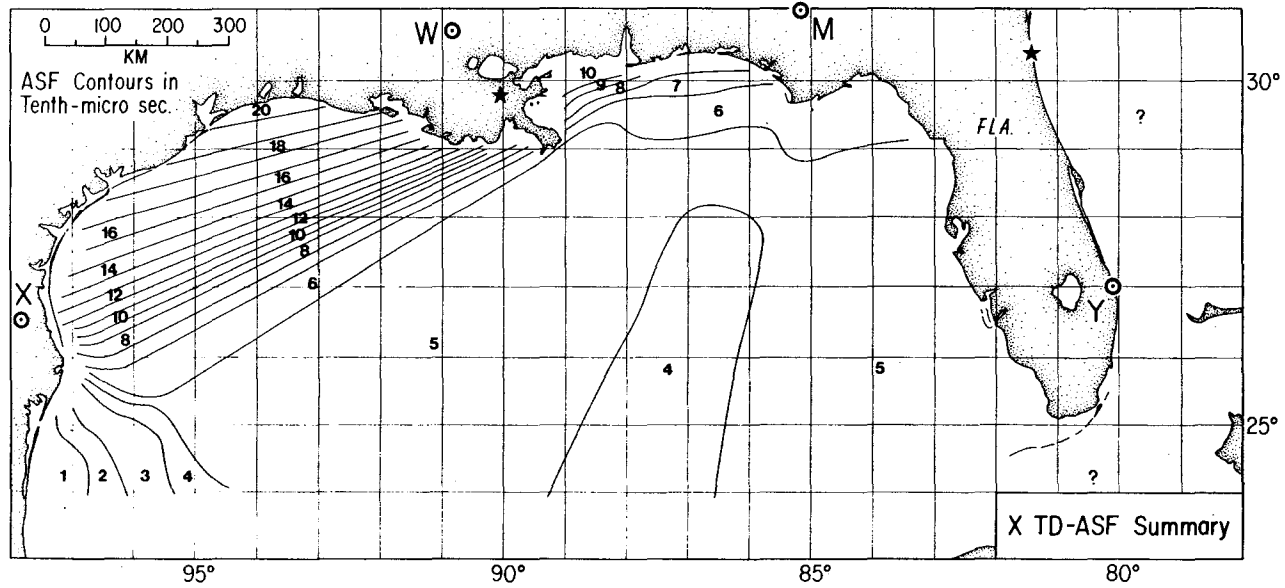
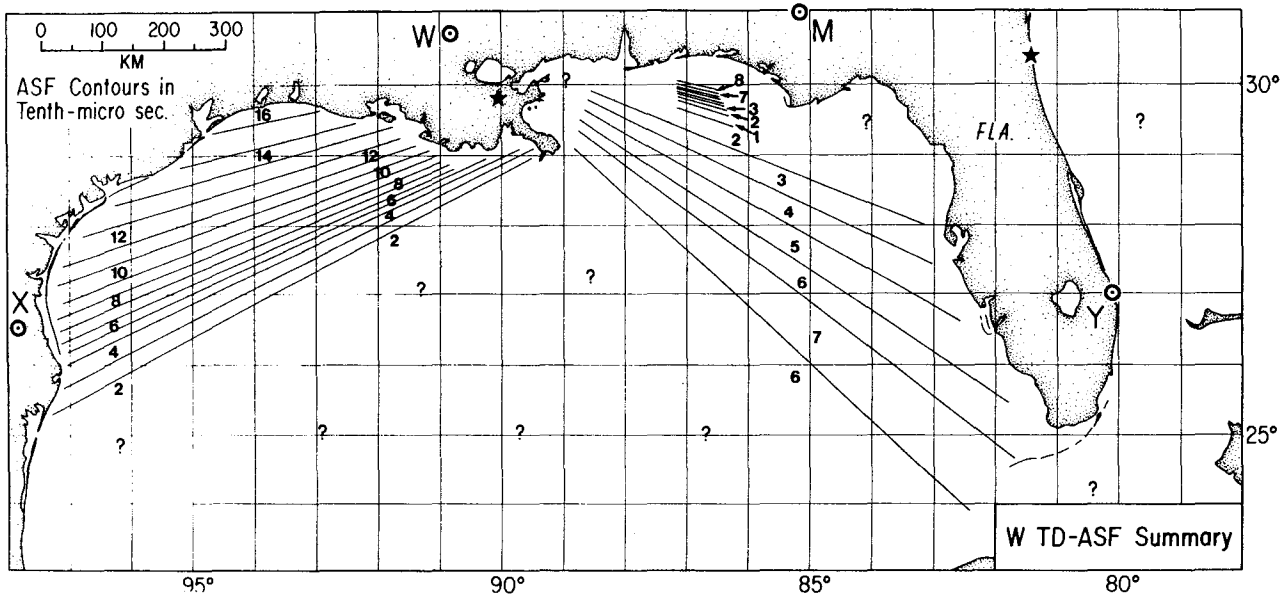


Figure 11. (Continued on next page.)

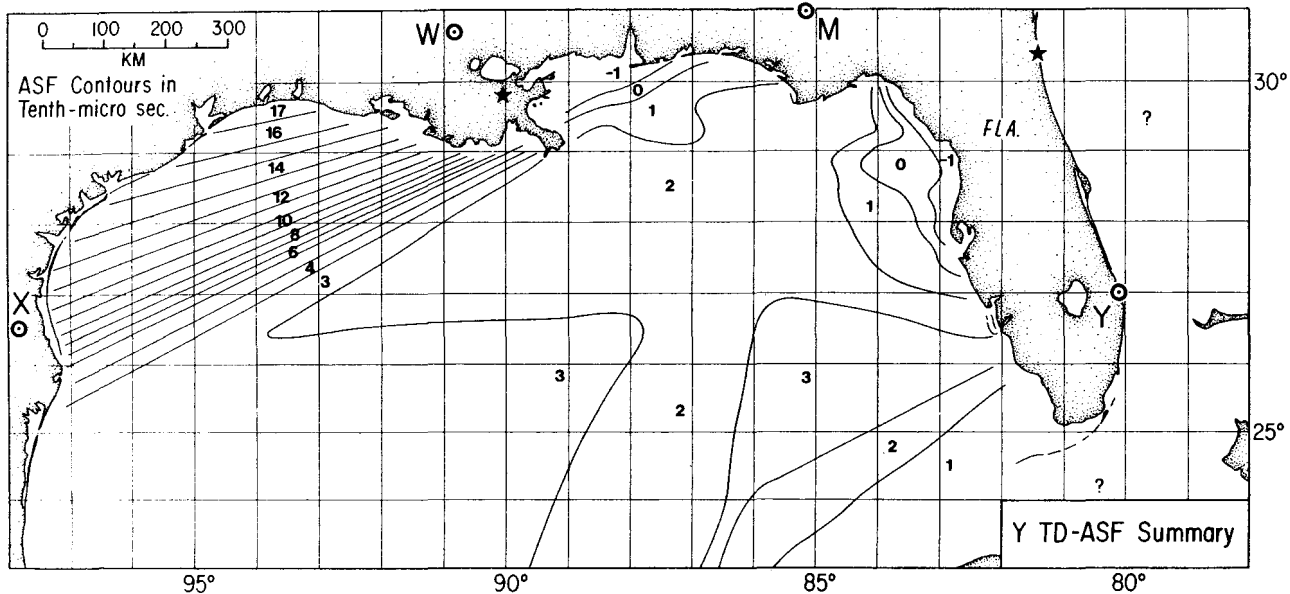


Figure 11. Provisional Gulf TD-ASF's for Rate-7980 W-X-Y in the summer. The three frames summarize all available model and observational data. Question marks show areas where adequate observational data is presently unavailable and areas east of Florida not treated here. Contour values (TENTHS of microseconds) are ADDED to the receiver TD's before converting to latitude and longitude with the SALT-model. To improve the visibility of the ASF gradients, contours are shown to 0.1 microseconds, but they may be in error by as much as a few tenths due to seasonal effects and NED bias.

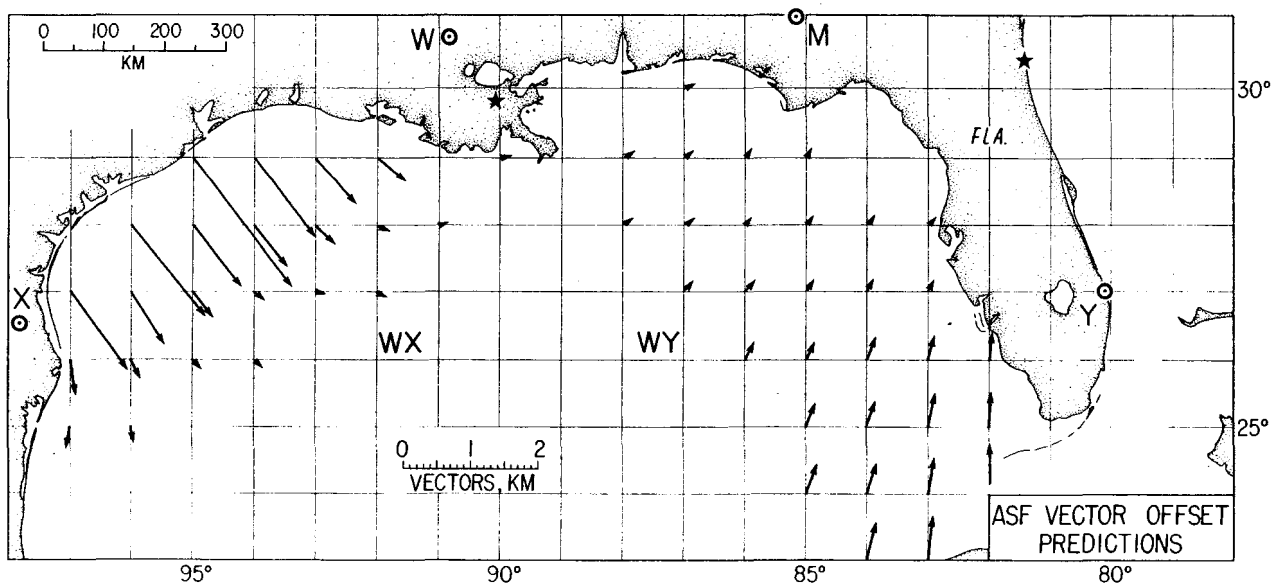


Figure 12. Gulf ASF displacement vectors for one-degree squares (calculated from Figure 11). Arrow tails represent uncorrected SALT-model fixes; arrow tips represent ASF corrected fixes. Arrow and chart scales are different. The largest offset vector (at 29 N, 95 W) is 2.47 km southeast. Large values in the western Gulf are primarily due to long overland paths from M and poor local LORAN geometry.

DATA SUMMARIES

Figure 11 summarizes the land anomaly data of the W, X, and Y TD-ASF's relative to the SALT-model (McCullough and others, 1982) and published NED's. The contours are hand-smoothed versions of the DMA contours of Figure 5; the contour separation and values were set by the observational data (figs, 7-10) for summer conditions. These contours are quite arbitrary, however, for there are few cross checks and several unresolved inconsistencies. The adjustment procedure used was to:

- o Adjust the Eastern W-TD-ASF's to fit the Figure 7 trend line.
- o Do the same for Y from Figure 8.
- o Do the same for X from Figure 9.
- o Assume Western Y-TD-ASF has the same shaped contours as Western X-TD-ASF. (The Y path over Florida subtends a small arc of known uniformity.)
- o Use the uniform WX-ASF's (fig. 10) in conjunction with the W-azimuth observations to set the numeric value of western W-ASF contours.

This arbitrary procedure leaves an unexplained 0.4-microsec difference between the eastern and western W-ASF's. Additional data along the XY baseline would be particularly useful in tying together the regional observations reviewed. Over some areas, the W ASF's could not be estimated at all from the observations. In only a few areas are the W, X, or Y ASF's established at the ± 0.1 -microsec level. Note that although the contours are shown at 0.1 precision throughout, they may be in error by as much as a few tenths microsec.

Figure 12 provides the same ASF information represented as offset position vectors for each one-degree-square for which at least two ASF's are known. The tail of each arrow represents the predicted location with no ASF correction; the tip of the arrow gives the local offset (km) after ASF corrections are applied. Thus, for example, the largest ASF corrections at 29 N., 95 W. will cause a fix offset of some 2.47 km at 144-degrees relative to the fix predicted using just the SALT-model (McCullough and others, 1982) and present NED's. This spatial vector presentation gives a general first impression of the ASF vector field in the Gulf. A more detailed and accurate picture could rapidly evolve if GPS positioning were applied to LORAN calibration.

COMMENTS ON: FUTURE LORAN CALIBRATION PROGRAMS

Smart Receivers: The Future of LORAN

It may be possible to extend the useful life of LORAN by continuing to evolve receivers that include ASF and seasonal corrections in their latitude/longitude converters. Such "smart" receivers can improve LORAN navigation with performance exceeding that now projected for civilian GPS (50 m D-rms = 100 m 2D-rms).

Smart receivers are opening potentially large new markets in aviation and pleasure boating. To build smart receivers, however, each manufacturer is currently burdened with the redundant task of independently determining the LORAN corrections for all chains. For the industry to progress rapidly and economically, a consolidated effort is needed to collectively obtain and distribute the basic calibration data needed for full utilization of LORAN via smart receivers. By drawing attention to the problem and by publishing corrections for the Gulf of Mexico, we hope to contribute to progress in this area.

GPS Applications

GPS provides a significant new tool for ASF calibration and LORAN seasonal/weather anomaly studies. For the first time, we have an independent location system with coverage, response time, and geodetic accuracy comparable to that of LORAN. GPS provides a single, uniform, traceable datum available in all LORAN chains.

An aircraft equipped with differential GPS and differential LORAN would allow continuous land-sea ASF calibration surveys along critical routes such as the transmitter baselines and sea radials. It could rapidly survey all required chains in a uniform manner. LORAN calibrations would then be traceable to a single system; results could be made available rapidly. The on-going program of LORAN airport surveys alone could provide extensive ASF data if conducted and published in a uniform manner. The uses of GPS for LORAN ASF calibration should continue to be encouraged.

LORAN Calibration Program

We propose a LORAN calibration program to keep pace with the evolution of GPS navigational capabilities. LORAN can stay competitive with GPS by continuing to provide cost/performance benefits in regions of high user interest. To

maintain this advantage, existing LORAN signals should be calibrated and new transmitters should be provided particularly in the central U.S.A. for aircraft. (The official role of LORAN should be expanded to include aircraft.) But until that happens, calibration of the existing transmitters seems to be our least expensive, fastest response option for performance improvement.

LORAN is in place, operationally sound, and relatively inexpensive to use. User acceptance is growing. Intercomparisons of LORAN and GPS should help both systems evolve. Extending the LORAN/GPS overlap period will benefit LORAN users by providing the option of converting to GPS at lower projected costs. As long as both systems are maintained, users can benefit from navigational redundancy. For these and other reasons, it seems worthwhile to explore ways of extending the useful life of LORAN.

If LORAN is to keep pace with GPS, there is no longer a choice between plotting TD's or plotting latitude/longitude. LORAN charts cannot provide automatic navigation with sufficient speed, accuracy, consistency, convenience, and coverage. Current chart coverage and production practices are severely hampering progress toward full use of LORAN signals. If the LORAN community is to break the limited coverage dilemma and provide correction data in a timely manner, new methods and policies are needed. The community as a whole should gather and share calibration knowledge in the same way that other information about the radiated signal is now shared. To have accuracy comparable to the 50m 1D-rms of degraded GPS, LORAN must have at least a 0.1 microsec rms accuracy in the Gulf (see Table 2, bottom section).

The technical approach of separating the TD predictions into a standard term (the SALT-model) and a local bias (the AFS) has considerable merit. It allows compression of diverse theoretical and observational data in a user-friendly format. The results are easily carried onboard ships and planes for manual or automatic use. As shown above (fig. 11), a few pages can adequately represent all the available theoretical and observational correction information for an area the size of the Gulf of Mexico. Figure 11 illustrates the considerable data compression (approximately 1000:1) possible.

Future TD-anomaly diagrams should include both land and sea to the limits of LORAN ground-wave reception. Seasonal

variations should be published in a similar fashion. Efforts to check end-product validity and improve coverage should be on-going. Critical observations made with dedicated equipment are needed (see Appendix F). Because useful LORAN ground wave accuracy varies over at least two orders of magnitude, D-rms accuracy diagrams or the like showing the local tolerances should be published.

Anomaly chart updates could be made in weeks instead of years. Research to find better corrections would not be stifled by the long turn-around time now required from the time of a verification cruise to the final publication of TD charts. (For the Gulf, the turn-around time extends from the BIBB cruise of 1978 to the anticipated publication of corrected charts of limited coverage some time in the next few years -- a total duration of 5 to 10 years.)

In addition to user-friendly charts, we need computer-friendly algorithms. Here industry might take the lead if official correction estimates were available in some compact form. If standard algorithms were adopted, charts could be switched or revised by simply changing the algorithm coefficients. Calibration data could be published as tables of coefficients.

Publication of anomaly charts for each entire LORAN coverage area (including land and sea as well as seas beyond the 100 fathom line) should be a major goal of the LORAN community.

The Next Steps

Near term. We should:

- o Start a LORAN calibration program.
- o Extend anomaly coverage to the land and beyond the CCZ.
- o Promote industry participation.

In the Gulf we should:

- o Apply the provisional NED corrections to the DMA model.
- o Perform atomic clock (Hot-clock) measurement of 7980 in the summer.
- o Re-determine the residuals and charts.
- o Model and observe 7980 seasonal variations.

Within the next few years. We should:

- o Conduct ASF observations along baselines and sea radials.
- o Instrument and conduct LORAN calibration flights using differential GPS and differential LORAN.

- o Couple ASF land and sea methods and observations.
- o Promote work on standards.
- o Publish updated conductivity charts.
- o Publish a continuing series of ASF and seasonal anomaly charts
- o Develop computer-friendly anomaly algorithms.
- o Promote international cooperation, especially with Canada.

DISCLAIMER

Any use of trade names is for descriptive purposes only and does not imply endorsement by the U.S. Geological Survey, the Woods Hole Oceanographic Institution, or any of the cooperative agencies who contributed data to this report.

ACKNOWLEDGMENTS

It is a pleasure to thank L. Gazlay, R. Kirkman, J. Ligon, M. Letts, J. McKeever, W. Schorr, D. Slagle, D. Taggart, W. Thrall, and R. Wenzel of the U.S. Coast Guard for their numerous contributions, observational data, and general help; also, E. Danford, M. Iacona, and L. Funakoshi of DMA for data and valuable discussions; and M. Eaton and D. Gray of the Canadian Hydrographic Service for general encouragement and advice. We wish also to thank K. Maynard of John E. Chance and Associates and W. O'Halloran, Jr., of Jaycor for the drilling platform and Eglin AFB data, respectively. Of the numerous others who have contributed to this paper we wish particularly to thank C. Daly, W. Dean, L. Fehlner, P. Forrestel, J. Illgen and R. Till, as well as T. Aldrich, W. Dillon, T. O'Brien, W. Green and E. Winget for their reviews of the manuscript.

REFERENCES

- Arcone, S.A., and Delaney, A.J., 1978, Electrical ground impedance measurements in the United States between 200 and 415 kHz: FAA Report, FAA-RD-78-103, NTIS Doc. AD-A068088.
- Bowditch, N., 1977, American practical navigator: Defense Mapping Agency Hydrographic Center, v. 1, 1386 p.
- Creamer, P.M., and DePalma, L.M., 1981, Literature review of LORAN-C grid stability and warpage tests: The Wild Goose Association, Annual Technical Symposium, 10th, Proceedings, p. 103-127.
- DMA, 1982, Defense Mapping Agency, and National Ocean Survey, Proceedings of the Third International Geodetic Symposium on Satellite and Doppler Positioning: No. 1 and 2, New Mexico State University, Las Cruces, 1336 p.
- Fehlner, L.F., and Jerardi, T.W., 1983, Observations of the performance of the Southeast U.S. LORAN-C chain: The Wild Goose Association, Annual Technical Symposium, 12th, Proceedings, 64 p., preprint.
- Fehlner, L.F., Merritt, B.D., Jerardi, T.W., McCarty, T.A., Cohick, W.D., and Criss, T.B., 1980, LONARS launch area calibration report: The Johns Hopkins University, Applied Physics Laboratory, APL/JHU, POR-2791, 113 p.
- Fine, H., 1954, An effective ground conductivity map for continental United States: Proceedings of the IRE, Septmeber 1954, p. 1405-1408.
- Frank, R.L., 1983, Current developments in LORAN-C: Proceedings of the IEEE, v. 71, no. 10, p. 1127-1139.
- Frank, R.L., 1974, Real-time compensation of LORAN-C/D temporal variations: The Wild Goose Association, Annual Technical Symposium, 3rd, Proceedings, 26 p.
- Gray, D.H., 1983, Notes on the use of LORAN-C charts: Radionavigation Journal, The Wild Goose Association, p. 49-63.
- Maynard, K.L., 1983, Private communication.
- McCullough, J.R., Irwin, B.J., and Bowles, R.M., 1982, LORAN-C latitude-longitude conversion at sea: programming considerations: The Wild Goose Association, Annual Technical Symposium, 11th, Proceedings, p. 42-75.
- Miller, R., Illgen, J., Weseman, J., and Falconer, R., 1981, LORAN-C calibration Gulf Coast and Eastern Seaboard: The Wild Goose Association, Annual Technical Symposium, 10th, Proceedings, p. 19-38.
- Munk, W., and Wunsch, C., 1979, Ocean acoustic tomography: a scheme for large scale monitoring: Deep-Sea Research, v. 26A, p. 123-161.

O'Halloran, W.F., and Natarajan, K., 1982, A semi-empirical method for LORAN grid calibration/prediction: The Wild Goose Association, Annual Technical Symposium, 11th Proceedings, p. 145-154.

Pearce, D.C., and Walker, J.W., 1975, The behaviour of LORAN-C ground waves in mountainous terrain: in Electromagnetic wave propagation involving irregular surfaces and inhomogenous media, A.N. INCE, Ed., NATO-AGARD-CP-144, The Hague Netherlands, AD-A008-583.

Piplin, F.M., and Ritter, R.C., 1983, Precision measurements and fundamental constants: Science, v. 219, no. 4587, p. 913-921.

Slagle, D.C., and Wenzel, R.J., 1982, LORAN-C signal stability study: St. Lawrence seaway: Department of Transportation, U.S. Coast Guard, G-DST-1, Report No. CG-D-39-82, 213 p.

Taggart, D.S., and Slagle, D.C., 1984, Tangible effects of LORAN-C phase modulation: U.S. Coast Guard Research and Development Center, Groton, Conn., Project Area, 742110, 48 p.

U.S. Coast Guard, Department of Transportation, 1983, Harbor monitor system, first quarter review for October 1982 through December 1982: U.S. Coast Guard Research and Development Center, Groton, Connecticut, p. Q-1.

U.S. Coast Guard, Department of Transportation, 1980, LORAN-C user handbook: Washington, D.C., G-WAN-2, COMDTINST M16562.3, 82 p.

U.S. Coast Guard, Department of Transportation, 1981, Specification of the transmitted LORAN-C signal: Washington, D.C., G-NRN-1, COMDTINST M16562.4, 65 p.

Voigt, R.E., and Wester, R.S., 1982, A comparison of methodologies for airborne LORAN grid data gathering: The Wild Goose Association, Annual Technical Symposium, 11th, Proceedings, p. 27-31.

Wenzel, R.J., and Slagle, D.C., 1983, LORAN-C signal stability study: NEUS/SEUS: Department of Transportation, U.S. Coast Guard, G-DST-1, Report No. CG-D-28-83, 264 p.

TABLE OF CONTENTS OF APPENDICES

- A. Conductivities from baseline TD's.
- B. Conductivities from scattered TD's.
- C. NED's from baseline extension data.
- D. ASF's, BED's, and NED's.
- E. Contours of lowland ASF's.
- F. Gulf ASF error sources.
- G. Plots of raw varification cruise data.
- H. Glossary of LORAN terms.

Appendix A

A New Strategy for Determining LORAN Ground Conductivities

INTRODUCTION

The magnitude of the LORAN ASF depends on the conductivity of the land, its roughness, and other surface properties (see McCullough and others, 1982). To measure ASF's, pulse travel times from single transmitters are needed, but these are considerably more difficult to measure than are the arrival time differences (TD's). In this appendix we propose a new systematic method for determining the travel times and, hence, the Range-ASF's directly from TD observations made along the great ellipse path or baseline between transmitters.

The travel times from each of two transmitters cannot be determined directly from a single TD observation but they can be inferred from a series of baseline TD observations. As a receiver is moved from one TD observation point to the next on the baseline, the land lost to the transmission path of one transmitter is gained by the other, so that each pair of baseline TD observations determines the delay due to the enclosed land segment. The total delay along a baseline can be constructed from a series of such observations. Using these data, the total delays from all the other transmitters of the chain to the baseline observation points can be calculated within the uncertainty of the individual emission delays of each Secondary. The broadcast emission delays (BED's) can be determined: (1) By traveling atomic clock, (2) By GPS time transfer, or (3) Indirectly as free parameters in the baseline solution.

If this process is carried out along two or more baselines, we can estimate the conductivities not only along the baselines, but also in the unobserved zones bounded by them. This appendix outlines the proposed method. Two less data-efficient techniques for estimating ground conductivities from randomly distributed TD observations are discussed in Appendix B.

MODEL

Figure A-1 (top, right) models the two-way Range-ASF anomalies along the Seneca-Nantucket baseline of LORAN Rate-9960. The curve labeled M Range-ASF shows the cumulative time delay (in excess of the predicted all-saltwater path and emission delay) as a function of range from Seneca. In like manner, the X Range-ASF curve shows the cumulative land-delay anomaly in the reverse direction, from Nantucket to Seneca. The total delay between the two transmitters must be the same in both directions (Fermat's principle), but the distribution of the delays will vary if the conductivities are not uniform. The difference (M minus X) of the two Range-ASF curves, labeled Delta-Range-ASF, represent the model prediction of the delay anomalies that would be observed with a TD receiver on the baseline, assuming that the Secondary's broadcast emission delay (BED) is known and removed.

The delays shown (fig. A-1, top right) were calculated by Millington's method (see McCullough and others, 1982) using the conductivities shown along the bottom of the graph. The simplified model conductivities selected are: 0.5 mmho/m in the Catskill Mountains and west, 5.0 for the Connecticut and Rhode Island farmlands, and 5000 for the sea path. Sensitivity of the predictions to the conductivity assumptions is suggested by the short segment, Sigma = 0.4, shown in the mountain zone.

The inverse-problem of finding the two Range-ASF curves from an observed Delta-Range-ASF curve appears convergent for practical values of conductivity. That is, given a set of Delta-Range-ASF observations along a baseline, it is possible to converge on one or more sets of model conductivity zones that satisfy the observations. The total number of conductivity zones and emission delays that can be determined will necessarily be fewer than the number of independent baseline observations, and should in practice be considerably less. Typically, a few conductivity zones have been sufficient for modeling offshore ASF's; more may be required for precise land navigation, particularly in rough terrain.

Having determined the Range-ASF from the Master to each of the observation stations along one baseline, the Range-ASF to the other Secondaries can be determined directly from the observed TD's and the assumed (or observed) emission delays of the Secondaries. Panel A (fig. A-1, bottom left) shows the radial paths from W

Figure A-1. A new method of estimating LORAN ground conductivities from baseline TD observation. The technique is illustrated with model data. Using the Seneca and Nantucket transmitters (top left), the TD observable (top right) is represented by the solid line labeled Delta-Range-ASF. By symmetry and iteration this function can be decomposed into the M and X Range-ASF's (dashed lines) and the X broadcast emission delay (BED) not shown. Knowing the M Range-ASF and BED's, the Range-ASF's from all Secondaries observed along the baseline can be calculated. Some typical paths for which delay sums could be determined are shown in panel A (lower left).

Measurements along a second baseline MY, panel B, create crossing delay sum integrals which can be resolved by tomography to determine regional delays and land conductivities enclosed by the baselines. Because LORAN propagation at sea is highly predictable, ocean observations can be extended to the baseline XY as in panel C (lower right).

Thus from a few dozen TD observations along baselines and at sea, it should be possible to independently determine the enclosed conductivities, the baseline Range-ASF's, and the Secondary BED's - basic parameters needed for navigation. Measurements on all baselines (six in this case) would improve the resolution and confidence levels.

and Y along which the delay-sums are determined for each of the ten observation stations shown along the MX baseline. Recall that the model conductivity profile along the observed baseline is determined as well.

In the same way, observations along a second baseline can provide additional delay-sums, illustrated in Panel B (fig. A-1, bottom) for the MY baseline. In the large area south of the MX baseline

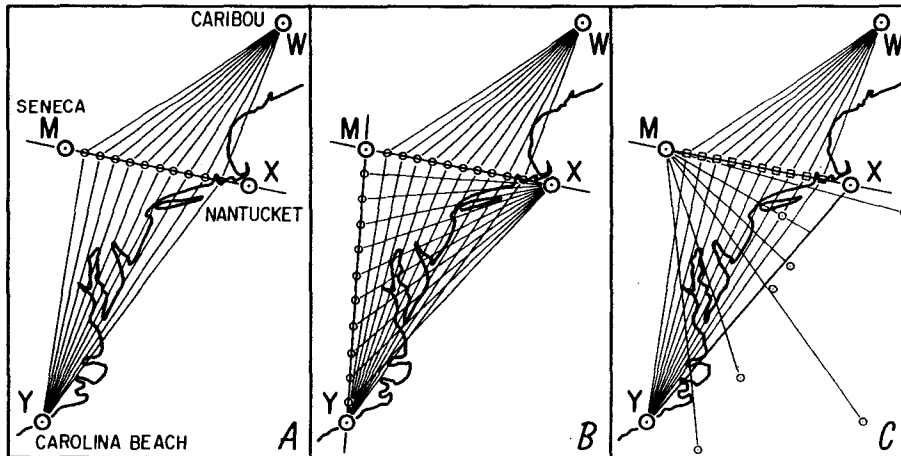
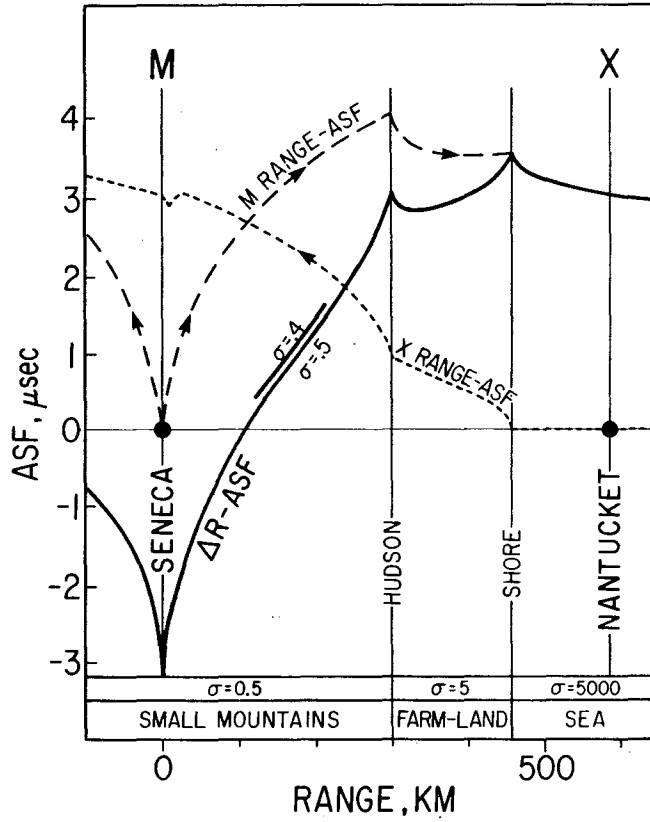
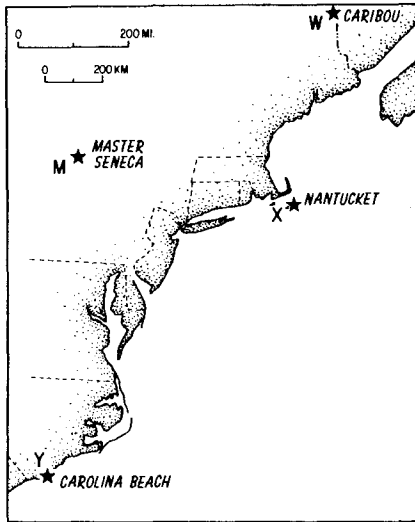


Figure A-1.

Appendix B

and east of the MY baseline where the delay-sum lines cross (panel B), conductivities can be estimated by tomographic techniques (i.e., Munk and Wunsch, 1979) or by a prior iterative modeling of the conductivities -- aided by soil, terrain, and geological information in the usual way.

Baseline observations might be made on land using local or satellite geodesy, or from GPS-instrumented calibration flights. Even a car equipped with differential-LORAN and differential-GPS receivers could make efficient land surveys.

Because propagation over sea water is quite predictable, arbitrarily positioned offshore observations, such as those in Panel C (fig. A-1, bottom, from McCullough and others, 1982) can be accurately extrapolated along transmitter radials to the sea portions of baseline segments, as shown for the XY baseline. Observations on several or all baselines (six in this case) would allow detailed modeling of the land conductivities within the baselines.

To review, TD's are observed at surveyed locations along two or more baselines. These are used to determine the propagation delay from the Master (fig. A-1, top). From the Master transmission delays and broadcast emission delays, the Range-ASF's from all of the Secondaries to these baseline stations can be found from their TD's. At this stage, the delay-sums along transmitter radials as illustrated in Panel A are known. In like manner, other baseline observations can provide additional overlapping delay-sums as in Panel B. Where the radials intersect, estimates of the off-baseline conductivities can be made. Arbitrarily positioned ocean observations (Panel C) can be used as well.

Thus, from a few dozen TD observations made along the baselines, conductivities in large remote areas can be determined. The process is similar to the Computer-Aided Tomography (CAT) SCAN method used to generate computer-reconstructed images through internal planes of the body from conventional X-ray observations made at various angles outside the body. In LORAN, conductivities within the baselines can be determined from TD's observed along the baselines. Results can be checked directly with off-baseline TD calibration stations.

Comparison of Two ASF Models Using Distributed TD Observations

The previous appendix discusses a new method for estimating LORAN conductivities from baseline TD observations. This appendix treats the same problem using arbitrarily distributed TD observations. Two models are discussed using 7980 Y-TD observations taken at fifteen Florida area stations (fig. B-1).

MODEL ONE

The first model (fig. B-2) assumes a linear relation between ASF's and Net-M-Land. The Y-TD-ASF's were calculated from USCG and LONARS TD observations, using the SALT-model (McCullough and others, 1982). The Net-M-Land was estimated by measuring the land length from the station to the Master transmitter at Malone and subtracting from it the land-length from the station to the Y Secondary at Jupiter. The general positive correlation observed (fig. B-2) is apparent for all stations except the two numbered 375 and 377. The ASF's of these stations, however, are consistent with each other and with independent observations taken in the Elgin Air Force Base series (Appendix E). Because the overland path from the Y-transmitter is very nearly the same for all four stations west of M, the reciprocal of the slope of the line shown, 2.75 microsec/1000 km, apparently is not representative of the land between the M-transmitter and stations 375 and 377. An offset of 0.35 microsec in the nominal Y-emission delay is indicated by the arbitrary linear trend shown (fig. B-2). The simplicity of the linear model is attractive, but the approach has three major difficulties: It assumes constant velocity with range; it does not account for known land/sea phase recoveries; and it does not easily accommodate zones with different propagation speeds. The next model addresses these problems.

MODEL TWO

The second propagation prediction model (figs. B-3 and B-4) is based on assumed conductivities and Millington's method. The Millington model technique predicts the Range-ASF as a function of ground conductivity and range from the transmitters. Figure B-3 illustrates the ASF model results for two observation stations with two conductivities, 3.1 and 7.9 mmho/m. Station locations and transmission paths are shown in the inset. Using the assumed conductivities, the upward-curving values of Range-ASF versus range from M (fig B-3 left) and on

Table B-1
Land and Sea Observations.

#	Station	Latitude		Longitude		TDY	Obs. ASF	Net M-Land km	Model 2 ASF's Microsec
		Deg	Min	Deg	Min				
1	375	30 ^o	13.7437	88 ^o	01.2227	47083.38	1.33	- 28	0.95
2	377	30	28.5758	87	11.1951	47162.00	1.18	- 89	0.78
3	378	30	03.5005	85	35.7831	44941.55	-0.09	-194	-0.31
4	379	29	08.0581	83	03.0692	43471.89	-0.36	-185	-0.42
5	380	27	23.8015	82	33.2451	44441.37	0.07	-100	-0.52
6	382	28	25.0310	80	37.3907	41988.26	2.05	537	1.53
7	Destin	30	23.5131	86	32.2578	47146.26	-0.21	-165	-0.37
8	Mayport	30	22.9808	81	25.2185	45290.72	1.54	300	1.25
9	L-5060	28	58.9829	79	22.8901	43953.42	1.80	650	1.20
10	L-5012	28	59.0658	80	21.0504	44205.16	1.90	560	1.31
11	L-1060	28	10.7798	79	24.0340	43548.67	2.00	690	1.38
12	L-1010	28	11.0330	80	24.0090	43775.82	2.22	640	1.50
13	I-10	27	37.39	83	04.58	44784.26	0.05	- 72	-0.45
14	I-1450	25	28.4514	79	55.9764	43113.58	1.46	483	1.12
15	I-1800	27	39.6688	80	03.9577	43369.38	2.11	574	1.83

a reversed range scale from Y (right) were constructed. Offshore recoveries (fig B-3, solid lines curving down toward the horizontal) were calculated for signals moving from land to sea. Note that in this model the ASF's versus range are nonlinear, especially for land/sea paths. The net or Delta-Range-ASF's are indicated by three vertical arrows near the graph center. The graphic approach is helpful for illustrating the various model parameters.

Unfortunately, arbitrary criteria are needed to select the conductivity zones. To do so, we first assumed a single provisional conductivity zone for all land paths and determined by inspection if more conductivity zones were needed. From a figure like Figure B-4, stations 375 and 377 were considered offset from the trend of the other data and were assigned to a separate group. Using all other stations, the provisional conductivity was adjusted (to 7.9 mmho/m) to produce unity slope. A linear fit to these data was then used to determine the emission-delay offset (0.25 microsec) shown in Figure B-4. Finally, the conductivity for the separate group, 375 and 377, was adjusted to fit the other observations.

Due to the offshore-recovery feature of the second model, the LONARS observations (fig. B-4, squares) have somewhat less scatter than seen in the Net-M-Land model of Figure B-2. The free-conductivity

parameter allows adjustment of stations 375 and 377, but further observations would be required to determine if such ad hoc adjustment is justified. The conductivity trend modeled in western Florida is consistent with Elgin observations discussed in Appendix E. The Destin station (fig. B-4, triangles) might be expected to have a conductivity somewhere between that of the adjacent stations, 378 and the pair 375-377. This would be consistent with the general scatter shown below the x-axis in Figure B-4, in which two extremes of assumed conductivity are shown for Destin.

Thus from the 15 independent observations we: assigned two arbitrary conductivity zones, determined the conductivity of the zone with the greatest distribution of ASF's, found the emission delay anomaly, and adjusted the conductivity of the remaining zone. Convergence is rapid, but the selection of the conductivity zones is arbitrary.

DISCUSSION

Because many observations per zone are required for stable estimates, both methods are less observationally efficient than the baseline approach of Appendix A. Estimation of the emission-delay anomaly requires a distribution of observed ASF's in at least one zone of constant conductivity...a significant constraint for general use.

To overcome these limitations, at-sea observations are needed along station radials so that changes in only one land path per TD at a time are observed. In like manner, TD observations along the baselines involve only one land path at a time.

The emission-delay offset is essentially the same in both models. The model residuals, of order of 0.1 microsec, seem small for a two-zone, three-free-parameter model applied to 15 diverse observations taken over a three-year span in all seasons of the year. Clearly, the chain is well controlled; the land has nearly uniform propagation properties; and the seasonal variations are relatively small. Such highly favorable conditions are not to be expected everywhere.

The data used in the figures are summarized in Table B-1. Observations 1-6 were made in the fall of 1978 when a different Y-CSTD was in use (Appendix C) and have been adjusted accordingly. One-hour to four-hour time averages were made on two separate days at each station. Adjustment for LPA's were made. The station positions were surveyed with a JMR-1 Transit Satellite receiver and are given in WGS-72 coordinates. Observations 7-8 for Destin and Mayport were provided by the USCG from control station data. The LONARS observations, table items 9-12, were interpolated from manually contoured TD data from Fehlner et al (1980). The INGHAM observations, table items 13-15, were averaged from the January 1981 USCG calibration cruise. Austron-5000 and LONARS type receivers were used.

This appendix illustrates some of the difficulties inherent in estimating LORAN conductivities from arbitrarily distributed TD observations. Specifically, it is difficult to establish the conductivity zones and their boundaries. The data shown provide some insight into the capabilities and limitations of the Net-M-Land model and, hence, the Double-Range-Difference model of Wenzel and Slagle (1983). Model 2 (figs. B-3 and B-4) shows a convenient graphical presentation for visualizing the relative contributions of various Millington-model parameters, including nonlinear range dependency, conductivity sensitivity, conductivity zone adjustment, offshore recovery, and Delta-Range-ASF polarity. The Millington-model scatter suggests that a model with two conductivity zones can predict LORAN TD's to within about 0.1 microsec in the Florida areas observed. There is evidence of a conductivity gradient to the south and west of M.

Figure B-1. Locations of fifteen sites used to illustrate two methods of estimating conductivities from arbitrarily distributed TD observations discussed in Figures B-2, B-3, and B-4.

Figure B-2. Model 1. Measured Net-M-land and observed TD-ASF's at fifteen stations. Data suggest a strong correlation with a 364 km/microsec slope and a 0.3 microsec emission delay offset. The two western most stations, 375 and 377, however, do not fit the general trend.

Figure B-3. Model 2. Range-ASF's for stations #1 (379) and #2 (377) as shown in the inset. The three upward curving solid lines give the predicted Millington model Range ASF's versus range from the M and Y transmitter. Transmitter M is shown for two uniform conductivities, 3.1 and 7.9 mmho/m; Y is shown for 7.9 mmho/m. The downward curving solid lines represent offshore recoveries. The predicted Delta-Range-ASF's are represented by the three vertical arrows. Using similar graphs, a single, uniform land conductivity was adjusted iteratively to bring the model ASF's into agreement with those observed. Conductivities for stations 375, 377, and Destin were adjusted separately. Results are shown in Figure B-4.

Figure B-4. Model 2 continued. Millington model conductivity assumptions were adjusted as in the previous figure to reach agreement between the model and observed TD-ASF's. The emission delay offset determined from the observations remains about the same as in model 1 (fig. B-2).

Conductivities of land to the south and west of M are found to be lower, agreeing with other independent estimates. The LONARS observations show a more nearly linear trend than in model 1 where offshore recoveries were not modeled.

The emission-delay anomaly between the published value and that derived from observation emerges as an independent parameter in both models provided a sufficient numeric range of ASF's are available in at least one propagation velocity zone. The emission-delay anomaly is not particularly model-sensitive in this example, but could be elsewhere.

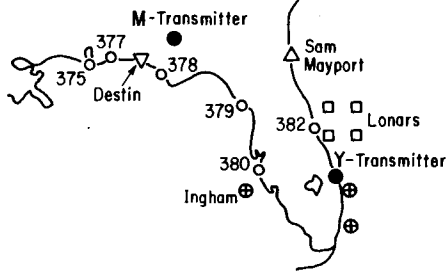


FIGURE B-1

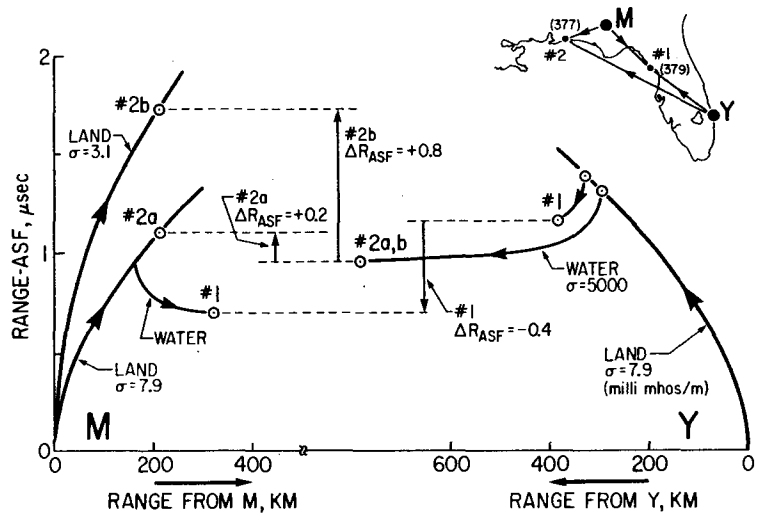


FIGURE B-2

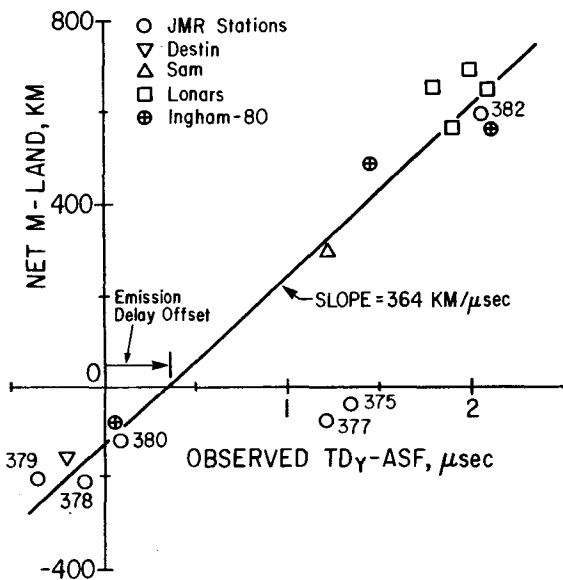


FIGURE B-3

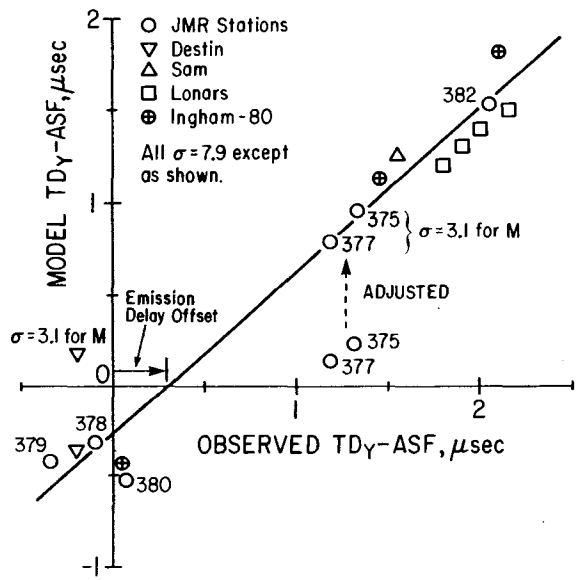


FIGURE B-4

Appendix C

Determining Emission Delays from Baseline Extension Data

INTRODUCTION

Figures C1-C3 summarize the USCG Rate-7980 baseline-extension crossing observations for all six baseline extensions labeled A through F in Figure C-1. The data were taken on August 2 and September 26-29, 1978, at altitudes of 1800-2400 feet and air speeds of 160 to 212 knots. Observed TD's on the baseline extension at ranges between 45 and 160 km from the transmitters are shown in Figure C-2. Crossings near the Master are shown as plus signs, those near the Secondaries as dots. Arbitrary dash lines have been added for clarity. Numeric estimates of the TD's at 111 km (the vertical dash line) are listed along the Y-axis for each baseline extension.

Three groups of model Range-ASF curves are sketched in Figure C-3. They show the predicted cumulative Range-ASF delays as a function of range from the Master and Secondary transmitters. In the top graph for Secondary W, for example, the vertical distance between the two arrows at A represents the model Delta-Range-ASF. Note at A, the model predicts slowly decreasing Delta-Range-ASF with increasing range to the left of W, i.e., the rising curved lines get somewhat closer together toward the left of W. The same situation exists at B and, in like manner, for the X and Y Secondaries discussed below. The modeled Delta-Range-ASF's monotonically decrease with distance from the transmitter.

The observed TD's should show the same slope as the Delta-Range-ASF's since by definition they differ by only the emission delay anomaly (see Appendix D, Eq. D-4). The rate of ASF decrease with range over water is expected to be about equal to that observed in Rate-9960 (McCullough and others, 1982) and shown by the solid line (the "observed offshore slope" above the observations of fig. C-2).

In Figure C-2, the observations are in general agreement with the model, except for baseline extensions A and F. The discrepancy at A can be resolved by assuming reasonable conductivity variations in the land west of W. The offshore recovery expected at F, however, is not observed and cannot be explained as changes in ocean conductivity. The discrepancy between the model predictions and observations is puzzling. A possible explanation may be inappropriate modeling

Figure C-1. Map of six Rate 7980 baseline extensions labelled A through F.

Figure C-2. Repeated aircraft crossing of the baseline extensions provided TD estimates as a function of range (dots and crosses). These observations were used in 1978-1979 to determine the nominal emission delays (NED's) for Rate-7980. They are reexamined here, and in Figure C-3, to show the sensitivity of such estimates to model assumptions.

Figure C-3. Millington model Range-ASF's are used to model the TD-ASF's observed in Figure C-2. The distance between the vertical arrows at A, for example, represents the modeled TD-ASF near transmitter W. Note that the modeled and observed TD-ASF's decrease slowly with range from the transmitter. The predicted ASF gradients with range and those observed are in general agreement except for baseline extensions A and F. The discrepancy at A can be resolved by reasonable adjustments of the assumed conductivities west of W. The discrepancy at F, however, cannot be adjusted in this way because the conductivity over water is uniform and known at this scale. The interesting possibility that the model predictions are not representative at altitude should be investigated, for such sensitivity with altitude might be used to remotely determine horizontal ASF's from observations made in the vertical.

OBSERVED TD's at BASELINE EXTENSIONS Baseline-Extension Crossings LORAN 7980

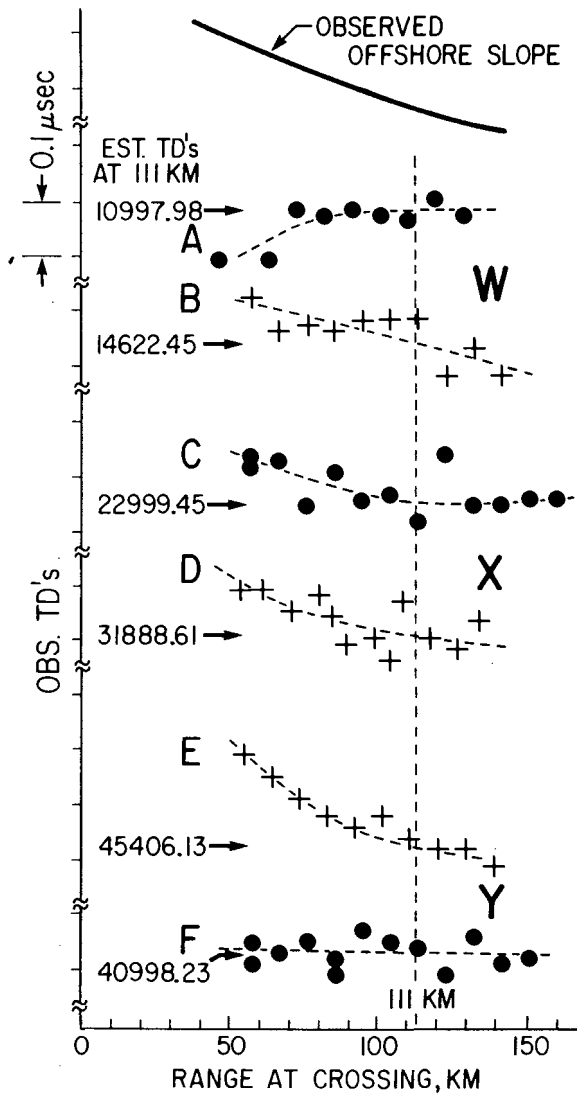


FIGURE C-2

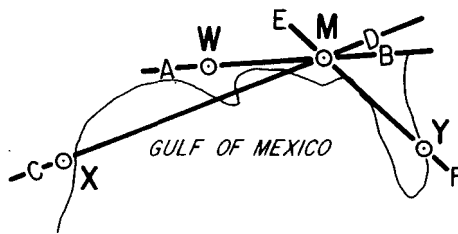


FIGURE C-1

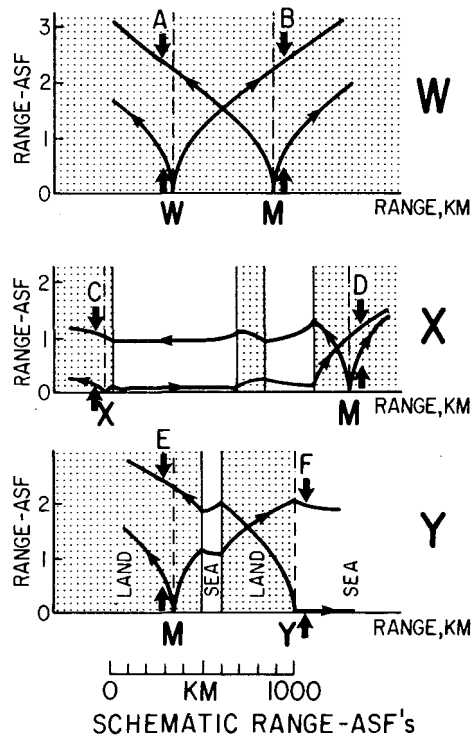


FIGURE C-3

of the nearshore Y transmitter at Jupiter, Florida, at altitude. It would be interesting to look more carefully at this clue, for it has been suggested (McCullough and others, 1982) that the vertical dimension may provide a fruitful, unexplored, means of observing and modeling surface ASF's.

In hindsight, the observations might have been more easily interpreted if they had been spaced farther apart and had included the baseline as well as its extension. The unexplained differences between model predictions and observations at A and F (fig. C-2) suggest caution in extrapolating the observation via the model to the TD's at the transmitters. We will use the ASF's at 111 km for illustration and show the same analysis with the more appropriate, but less accurate, ASF's extrapolated to the transmitters.

MODEL

Consider a Master M and a single Secondary S. Assuming reciprocity, the pulse travel time from M to S is the same as from S to M. The ASF, as used here, is the additional travel time in excess of that computed from the McCullough and others (1982) SALT-model.

$$T_{MS} = T_{SM} = T_{SALT} + ASF \quad (C-1)$$

The TD at the Master is the baseline travel time from the Secondary plus the broadcast emission delay, BED.

$$TD_M = T_{SM} + BED \quad (C-2)$$

In like manner, the TD at the secondary is the emission delay less the baseline travel time.

$$TD_S = - T_{MS} + BED \quad (C-3)$$

Subtracting equation C-3 from C-2 and substituting from C-1, we have

$$TD_M - TD_S = 2T_{MS} = 2(T_{SALT} + ASF)$$

or

$$ASF = 0.5(TD_M - TD_S) - T_{SALT} \quad (C-4)$$

Adding equation C-2 and C-3 gives

$$TD_M + TD_S = 2 BED$$

or

$$BED = 0.5(TD_M + TD_S) \quad (C-5)$$

From equations C-4 and C-5 and the observed TD's extrapolated to the

transmitters, we can compute the baseline ASF, the broadcast emission delay (BED), and the difference between the broadcast and nominal emission delay (BED-NED).

NUMERIC EXAMPLES

Numeric results are shown in Table C-1 for the MW, MX, and MY baselines. From Figure C-2, the observed TD's of the Master and Secondaries at 111 km are repeated in lines 1 and 2 of the table. The McCullough and others (1982) SALT-model travel times are shown in line 3. (All values are in microseconds.) From equations C-4 and C-5, we compute the ASF and BED of the observations and show the results in lines 4 and 5.

In 1979, the controlling standard TD's (CSTD's) were changed as follows:

	Pre-Dec. 1978	Dec. 1978 to present	Diff.
W	11613.30	11612.46	-.84
X	28657.65	28656.71	-.94
Y	45291.21	45290.72	-.49

Because the CSTD's were changed after the baseline extension flights, the emission delays needed to be corrected by the amounts of these differences, resulting in the table values on line 7. The published nominal emission delays are shown on line 8 and the residuals, on line 9. The residuals are somewhat larger than suggested by the observational scatter seen in Figure C-2. The systematic bias is undoubtedly the result of assuming a different distance (111 km) than that assumed for the published values. The -2000 microsec offset in MY was caused by a logistic problem that was later corrected.

Line 10 lists our manually-extrapolated TD's at the transmitters, and line 11 shows their emission delay residuals. The residual magnitudes are even larger than before, illustrating the difficulty of estimating nominal emission delays from such data. Line 12 shows the emission-delay anomalies discussed in this paper (Table 3) relative to the USGS nominal emission delay (Publ. NED, line 8). As expected, the anomalies at 111 km (line 9) are larger than those observed in the far field (line 12). There is, of course, no reason to assume that the published emission delays represent the broadcast emission delays at the time of the calibration flights; they are only used here as an independent estimate made from the same flight data. Rate-7980 has not been hot-clocked.

Table C-1
Emission delays computed from
baseline extension observations.

Item	MW Microsec	MX Microsec	MY Microsec
1. Obs. M-TD	14622.45	31888.61	45406.13
2. Obs. S-TD	10997.98	22999.45	40998.23
3. Cal. T-SALT	1809.54	4443.38	2201.88
4. Cal. ASF	2.70	1.20	2.07
5. Obs. BED	12810.22	27444.03	43202.18
6. Delta CSTD	-0.84	-0.94	-0.49
7. Corr. BED	12809.38	27443.09	43201.69
8. Publ. NED	12809.54	27443.38	45201.88
9. ED' (Obs.- Publ)	-0.16	-0.29	-2000.19
10. Extrap. ED	12810.20	27444.30	43202.49
11. Extrap.- Publ.	+0.66	-0.92	-1999.39
12. Tbl.3 - Publ.	-0.55	-0.50	-0.25

In this method of estimating emission delays from good quality baseline-extension data, the limiting factor is the uncertainty in extrapolation of the TD observations from the baseline-extension observations to the hypothetical TD at the transmitter. A better method would include observations along the baseline as well as along its extension. Direct methods for determining emission delays with portable clocks provide greater resolution and repeatability, and are less expensive and easier to conduct. For those chains, such as 7980, that have not been hot-clocked, one should recognize the uncertainty inherent in estimating emission delays from baseline-extension data, i.e., the published emission delays are not necessarily very accurate estimates of the true, time varying, broadcast emission delay. This suggests a fundamental way of improving LORAN navigation, i.e., provide better estimates of the broadcast emission delays (BED's).

Appendix D

ASF's and Emission Delays

ASF's

The acronym ASF, or additional secondary (phase) factor, has been used in a variety of ways (see discussion in McCullough and others, 1982) The USCG definition of ASF is:

"The amount, in microseconds, by which the time difference of an actual LORAN signal that has traveled over varied terrain differs from that of an ideal signal which has been predicted on the basis of travel over an all-

seawater path. (LORAN signals travel slower over ground.)"

In this paper, we further define Range-ASF, Delta-Range-ASF, and TD-ASF, and call the standard model used to calculate the predicted travel time over seawater, the SALT-model (McCullough and others, 1982).

Range-ASF

We restrict the term Range-ASF to mean the LORAN propagation travel time anomaly of pulses from a single transmitter relative to the SALT-model. Because LORAN signals travel slower over land, and we choose to ignore smaller signal variations over seawater, the Range-ASF's used here are always positive.

$$T_R = T_{SALT} + R.ASF$$

or

$$R.ASF = T_R - T_{SALT}$$

Where T_R is the one-way travel time for the transmitted pulse to reach the receiver, T_{SALT} is the travel time predicted from the SALT-model, and R.ASF is the travel time anomaly relative to the model, i.e., the number of microseconds to be added to the SALT-model prediction to best represent the actual propagation travel time. The propagation travel time may be an estimate or a measurement.

Delta-Range-ASF

A Delta-Range-ASF is the difference between two Range-ASF's. It can be positive or negative.

$$\text{Delta-Range-ASF} = R.ASF_2 - R.ASF_1$$

TD-ASF

In like manner, the TD-ASF is the time anomaly needed to bring the calculated TD into agreement with the observed TD, i.e.,

$$TD.obs = TD.salt + TD.ASF' \quad (D-1)$$

Where TD.obs is the observed TD, TD.salt is the SALT-model predicted TD, and TD.ASF' is the anomaly. Neglecting receiver bias, the observed TD is the difference of the observed travel time from the Secondary, X, less the observed travel time from the Master, plus the broadcast emission delay (BED) for X

$$X.TD.obs = T.xobs - T.mobs + BED \quad (D-2)$$

The SALT-model TD is calculated from the difference of the SALT-model travel times from the two transmitters, plus the nominal emission delay (NED),

$$X.TD.salt = T.xsalt - T.msalt + NED \quad (D-3)$$

Where T.xsalt is the predicted SALT-model propagation time from the Secondary transmitter, T.msalt is the predicted time from the Master, and NED is the nominal emission delay published by the USCG.

From the above for X we have,

$$\begin{aligned} X.TD.ASF' &= X.TD.obs - X.TD.salt \\ &= (T.xobs - T.mobs + BED) \\ &\quad - (T.xsalt - T.msalt + NED) \\ &= (T.xobs - T.xsalt) \\ &\quad - (T.mobs - T.msalt) \\ &\quad + (BED - NED) \\ &= X.R.ASF - M.R.ASF + ED' \quad (D-4) \end{aligned}$$

That is, the TD.ASF' is the difference of the Secondary Range-ASF less the Master Range-ASF, plus the emission delay anomaly (ED' = BED - NED).

The negative of the above symmetrical definition is used for the operational definition,

$$\begin{aligned} X.TD.ASF &= - X.TD.ASF' \\ &= X.TD.salt - X.TD.obs \\ &= M.R.ASF - X.R.ASF \\ &\quad - (BED - NED) \quad (D-5) \end{aligned}$$

The sign convention arises from older procedures used for manual ASF corrections with LORAN charts. The TD.ASF is the number of microseconds added to the observed TD before using an uncorrected SALT-model chart for latitude-longitude conversion. However, many charts are now corrected for model ASF's, further adding to the complexity (see also McCullough and others, 1982).

The observed ASF (figs. 7-10) are of the form

$$\begin{aligned} X.TD.ASF.obs &= X.TD.salt - X.TD.obs \\ &= (T.xsalt - T.msalt + NED) \\ &\quad - X.TD.obs \quad (D-6) \end{aligned}$$

The "model estimates" (figs. 7-10) are

$$\begin{aligned} X.TD.ASF.model &= M.R.ASF.model \\ &\quad - X.R.ASF.model \\ &= (T.mmodel - T.msalt) \\ &\quad - (T.xmodel - T.xsalt) \quad (D-7) \end{aligned}$$

The ASF.Bias, observed less model, (Eq. D-6 less Eq. D-7) is

$$\begin{aligned} ASF.Bias &= (T.xsalt - T.msalt + NED) \\ &\quad - X.TD.obs \\ &\quad - (T.mmodel - T.msalt) \\ &\quad + (T.xmodel - T.xsalt) \\ &= (T.xmodel - T.mmodel + NED) \\ &\quad - X.TD.obs \quad (D-9) \\ &= X.TD.model - X.TD.obs \quad (D-10) \end{aligned}$$

The bias is thus reduced by smaller NED, larger M-model-delay, or smaller X-model-delay.

EMISSION DELAYS

The Broadcast Emission Delay (BED)

The USCG (1981, p. 4-1) specification defines emission delay as:

"the time interval between the master station's transmission and the secondary station's transmission in the same GRI (both stations using a common reference)."

The broadcast emission delay (BED) of the Secondary transmitter is controlled to maintain a nearly constant TD at the system area monitor (SAM). The nominal value of the TD at the SAM is called the controlling standard time difference (CSTD). Because LORAN propagation velocities vary with changing atmospheric and ground conditions, especially over land, significant changes in the BED are required to maintain constant CSTD at the SAM.

While TD propagation variation is compensated locally by the SAM control, these same control procedures cause large navigational errors in some other parts of the chain. Navigators operating beyond the long, thin SAM-controlled zone will therefore favor receivers that automatically compensate for BED and propagation variations.

Thus, the BED is a variable parameter of fundamental importance to LORAN navigation. It is the emission delay defined by the USCG above, but is not the same as the nominal emission delay (NED) discussed next.

The Nominal Emission Delay (NED)

The nominal emission delay (NED) is a constant defined by the USCG and published with the transmitter specification data (USCG, 1981). It is estimated from theory, from field surveys such as those discussed in Appendix C for Rate-7980, or by direct traveling-atomic-clock time transfer (Hot-Clock) as for Rate-9960.

The traveling-clock procedure is referred to as "chain calibration," a misnomer inasmuch as "calibration" generally implies more than a spot-check of one variable parameter (the BED). We suggest, therefore, that the traveling-clock timing process be renamed "hot clocked" to avoid confusion and fruitless discussion. The method and date of the nominal emission delays (NED's) for each chain should be published along with the numeric values and should be related to typical seasonal variations of the BED's.

The older concepts of coding delay and baseline delay, associated with the NED, should be retired. They presently serve no useful purpose, and add unnecessary confusion and difficulty to the LORAN learning process. The distinction between NED's and BED's should be included in LORAN handbooks.

Appendix E. CONTOURS OF LOWLAND ASF's.

THE EGLIN SURVEY

Voight and Webster (1982) and O'Halloran and Natarajan (1982) discuss LORAN TD observations made by the U.S. Air Force (Eglin Air Force Base) in a 85 by 370 km rectangular area between the Mississippi River and Pensacola, Fla. Figure E-1 shows the 7980 W-TD-ASF's contoured from an array of 10 by 41 TD observations taken on ten east-west flights spaced on a nominal 9-km-square grid in the area bounded by 30°23'N, to 31°10'N; and 86°45'W, to 90°38'W. Reference navigation control was provided by nine ground-based transponders having an estimated accuracy of 4 m in each of three axes. The geodetic tie to WGS-72 is not known to us.

The three-dimensional view (fig. E-2) shows a noise-like surface superimposed on the expected east-west ASF trend. The contour map (fig. E-1) shows considerable local detail relative to this trend. Additional observations would be required, however, to separate the relative contributions of terrain and observational noise. Discontinuities between successive flights suggest caution in interpreting the detail. No cross-grid north-south control lines were flown; there are few internal consistency checks in the existing data. It would be interesting to extend the analysis east to the M transmitter at Malone and south well out to sea. Full baseline coverage would allow the methods discussed in Appendix A to be applied; sea coverage would tie the observations to cruise data, and help establish noise levels.

Figure E-3 shows the ASF section interpolated along 370 km (68%) of the 542 km MW baseline. As seen, the slope of the observed ASF's with range from W is nearly constant from 140 to 390 km. The estimated slope of -1.03 microsec/100 km corresponds to a model conductivity of 1.4 mmho/m. The inset graph gives the conductivity versus ASF slope relation used. This particular estimate was derived by assuming uniform conductivity from M to W and calculating the ASF slope with a Millington model for various conductivities.

The ASF level shows a general offset below the linear trend starting at ranges less than about 140 km in the Pearl River basin. A similar change is seen at ranges smaller than about 50 km in the Mississippi River basin. Additional flights (not included here) extend the coverage eastward toward Malone. At the baseline geometric mid-point, the ASF is 0.12 microsec, and from Table 3, the W NED is about 0.5 to 0.6 too large. These values require that the ASF curve fall off less rapidly eastward of the observations shown, i.e., the conductivity increases as suggested by other data discussed below.

The Eglin LORAN-C data document an upper bound for the degree of ASF complexity that might be expected over relatively smooth lowlands such as those encountered between the Mississippi basin and Choctawhatchee Bay, Fla. Pearce and Walker (1975) show much larger variations in the mountains near State College, Pa., but have reservations about the quality of their observations. Creamer and DePalma's (1981) review includes extreme ASF's observed in Death Valley, Calif.

THE FINE SURVEY

Figure E-4 (from Fine, 1954), shows estimated ground conductivities (mmho/m) for the contiguous U.S.A. Fine based his estimates on approximately 7000 standard AM field strength measurements and 144 electrically distinct soil types. Most of the AM transmission paths were less than 40 km in length. Conductivities measured over the same terrain varied by more than a factor of two depending on propagation direction, frequency, and interpretation equipment. Consequently, Fine adapted the logarithmic conductivity classes of 0.5, 1, 2, 4, 8, 15, 30 and 5000 as shown on the map. The map was drawn from overlay maps of the signal attenuation observations and soil types. Fine estimated the overall standard error to be 0.23 mmho/m. Arcone and Delaney (1978) provide similar data for the 200 to 415 kHz band.

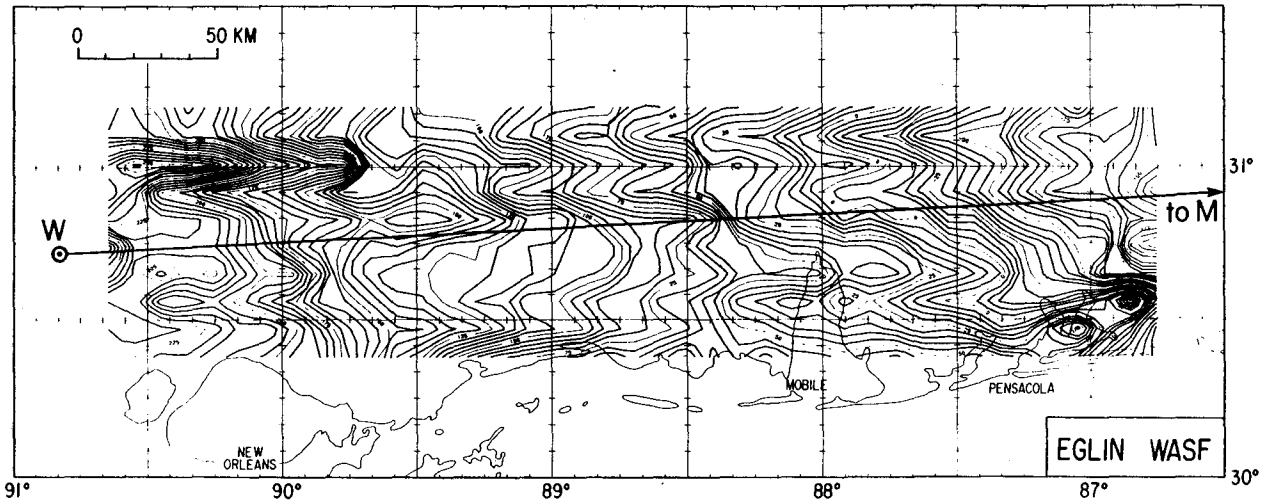


FIGURE E-1

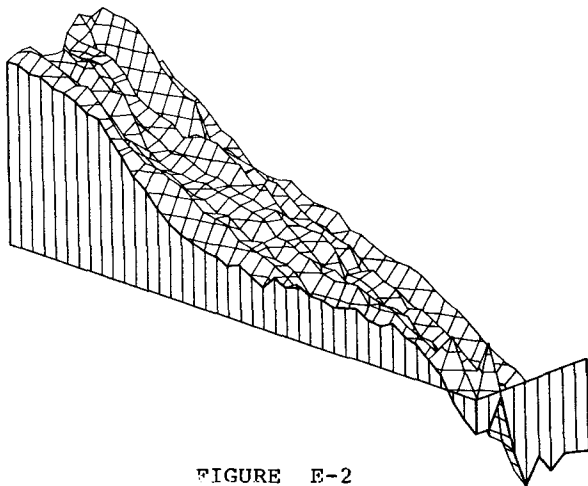


FIGURE E-2

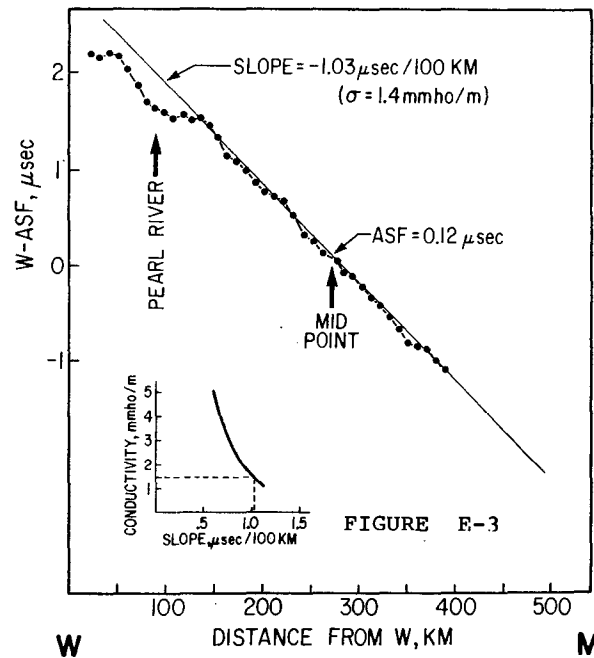


FIGURE E-3

Figure E-1. ASF contour map of aerial W-TD observations taken north and east of New Orleans. Observations were made on a 5-mile grid from an aircraft navigated with ground transponders.

Figure E-2. A three-dimensional sketch of the Eglin Air Force Base ASF data shown in Figure E-1. The noise-like surface contains observational noise and topographically induced ASF variations, and thus sets only an upper bound to the LORAN ASF variability for such low lands.

Figure E-3. Eglin W TD-ASF's along the WM baseline. Propagation changes in the Pearl River Valley are apparent. From there eastward, the ASF slope is nearly uniform with an equivalent conductivity of 1.4 mmho/m as indicated in the inset. If continued to M, such data would allow application of the methods of Appendix 1.

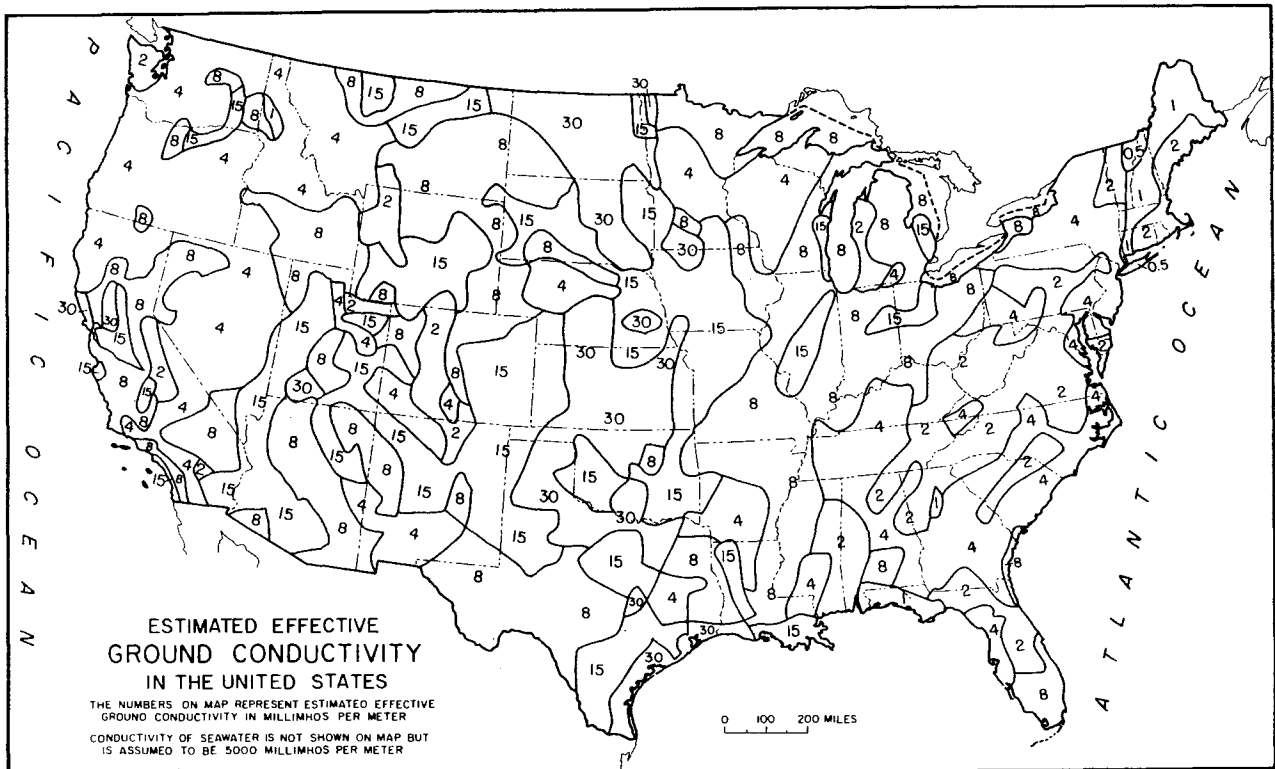


Figure E-4. Conductivity estimates derived from AM radio amplitude observations and soil types (after Fine, 1954). Values and gradients in the Florida area are similar to those estimated at lower LORAN frequencies.

CONDUCTIVITY ESTIMATES

We calculated the LORAN conductivity in Eastern Florida as 7.9 mmho/m; that near Pensacola as 3.1 (see Appendix B), and that along the western MW baseline as 1.4. These are in general agreement with the Fine (1954) observations. The MW baseline agrees within observational uncertainties, while the 7.9 and 3.1 LORAN estimates, based largely on central and northern Florida propagation paths, are somewhat higher than Fine's AM values. DMA assumes a conductivity of 5 interspersed with zones of 30 as shown in Figure 3. Thus, there is considerable variation in the conductivity estimates and their boundaries, but some useful first approximations at 100 kHz may be possible from the Fine (1954) AM map (fig. E-4). Estimates of LORAN conductivity could be significantly improved with differential GPS/LORAN observations along the baselines, along transmitter radials at sea, and in critical areas of rapidly changing land conductivity.

WHAT TO CONTOUR; TD's, RANGE-ASF's, OR CONDUCTIVITIES?

TD anomaly charts can be derived (1) from observed TD's at known locations in the area of interest, (2) from Range-ASF's and ED's based on observations and theory, and (3) from conductivity maps. Which is the best way?

An example of the first approach is the Eglin data (fig. E-1), wherein TD anomaly maps were generated directly from a grid of TD observations reduced to TD-ASF's via the SALT-model and W-NED. No other constraints were applied, and hence the data could be used to derive land conductivities (fig. E-3), compare observed and theoretical shapes, etc. An example of the second method is given in Figure 11. There, observed TD's are first used to derive the Range-ASF's for each transmitter and to set the Secondary ED's. These in turn are used to generate the TD anomaly maps. Finally, land conductivities could be established and used with a Millington model (or other model) to calculate the ASF's.

TD Anomalies Directly from TD's.

The advantage of directly contoured TD anomalies is that they are easier to compute. Disadvantages include:

- o They require a dense grid of TD observations.
- o They assume a quasi-linear local TD-ASF field.
- o They ignore outside constraints.
- o They lump all variations into one parameter.
- o They give no insight into seasonal variations.

Because the observations must stand alone, greater data densities in both space and time are needed. Directly contoured TD anomalies have generally been used in small area surveys such as harbors, airports, and calibration studies where the local linearity assumption is justified and a dense observational grid is practical.

TD Anomalies from ASF's and ED's.

TD anomalies derived from Range-ASF contours for each transmitter, on the other hand, more nearly model the underlying physics of the individual pulse anomalies and facilitate separation of various effects. They can be used individually or collectively for extrapolation, interpolation, smoothing, editing, and observational planning over large areas. More importantly, they can incorporate detailed specific information from geography, propagation theory, control theory, and remote observations. Abrupt anomaly gradient changes, such as offshore recovery effects, can often be identified with known causes. ASF surveys can be planned to provide a more uniform distribution of observations in anomaly space. In ASF charting, the Master ASF, the Secondary ASF, and the emission delay anomaly, must be derived from the TD observations, so additional computation is involved. But where large areas with low data density such as the Gulf of Mexico are studied, a nonlinear interpolation approach is mandatory. Even in smaller, well observed areas there may be advantages if seasonal and weather effects are important.

TD Anomalies from Conductivities.

DMA computes ASF's from estimated land conductivities via the Millington model. The basic information is stored as conductivity charts from which the ASF and LORAN charts are derived. It appears, however, that this approach is marginally adequate (0.1 microsec offsets) in typical near shore regions (McCullough and others,

1982), and may be inadequate (1.0 microsec offsets) in near shore regions with large conductivity changes such as those observed in Nova Scotia (Gray, 1983). Because the conductivity method is model dependent, each poorly modeled condition must be treated as a special case. Receiver storage of the conductivity field is somewhat easier than storage of the ASF field, but with low-cost memories, there is no clear advantage.

In summary, although each method discussed has accepted areas of application, we recommend that a single industry-wide standard be adapted. Present technology appears to favor storing the ASF field as a standard algorithm with variable coefficients, but however the data are stored, a standard approach is needed to help expedite ASF development in smart receivers.

Appendix F

GULF OF MEXICO ASF ERROR SOURCES AND FUTURE TESTING

Determination of ASF's requires knowledge of the receiver's location, the observed TD, and the broadcast emission delay (BED) at the time of observation. This appendix reviews error sources in each of these terms in this Gulf of Mexico study and provides suggestions for future work.

ERROR SOURCES

Reference Navigation

The largest error source in this Gulf ASF study is thought to be uncertainty of the reference positioning. No independent check of the reference navigation was made for any of the Gulf of Mexico ASF data presented. Shore-based navigation was specified as ± 30 m and apparently was worse at times. As discussed in Appendix G, all of the western Gulf of Mexico BIBB cruise data are unusable due apparently to problems with shore-based reference navigation. Observations from the ACUSHNET cruise (figs. 8, 9, G-1, and G-2) are limited by uncertainty in the reference navigation. The INGHAM cruise (figs. 7 and 8) had at least one questionable shore-navigation segment and the data include detectable ASF steps at other shore navigation changes. The GYRE data are limited by Transit Satellite underway navigation errors. The Eglin geodetic datum and control are unknown and show steps at boundaries of different flights. Thus, with the exception of the USCG land station data, LONARS data, and drilling platform data, the accuracy of

this Gulf of Mexico ASF study is primarily limited not by LORAN, but by the geodetic positioning. We are in effect using LORAN to check the reference navigation. More accurate geodetic reference positioning methods are needed to adequately calibrate LORAN in the Gulf.

No uniform or traceable convention was used in converting NAD-27 to WGS-72 coordinates in the USCG cruises.

Transit satellite broadcast ephemeris (BE) and precise ephemeris (PE) have been used interchangeably and both have been assumed to be WGS-72 coordinates, which they are not. These assumptions cause known longitude biases and larger seasonal biases (DMA, 1982).

No corrections were made for the difference in location of the reference and LORAN antennas. For the GYRE cruises, the reference location antenna leads the LORAN antenna by 7 m. The offset for the USCG cruises is not known.

Receivers, Transmitters, and Propagation

Broad-band and narrow-band receivers were used interchangeably. Austron 5000, North Star 6000, LONARS type receivers, and a Trimble Model 200 receiver were used for the USCG, USGS, APL, and platform data sets, respectively. No corrections for receiver tracking-loop delays were made for moving receivers. Only the Austron-5000 receivers were calibrated. No field control of receiver performance was made. No systematic allowance for SNR or interference related errors were made. Interference from intermittent ship's equipment, manmade transmissions, and lightning may have contributed significant errors in the Gulf of Mexico.

Broad-band and narrow-band receivers can detect transmitter changes of order 20 nanosec (Taggart and Slagle, 1984). Short term transmitter variations are seen in Rate-7980 (Fehlner and Jerardi, 1983). Large diurnal signal-to-noise related TD variations are observed, especially at long range.

Model Assumptions

The published nominal emission delays (NED's) were applied uniformly for all ASF computations in this paper. This assumes that the emission delay anomaly (BED-NED) is zero. Figure 6 suggests this may cause seasonal biases as large as 0.2 microsec. (An error in the NED will appear as a bias in the ASF's relative to the prediction, but will not effect ASF corrections based on the same NED. The NED simply sets the zero-point of the ASF's.)

Local phase adjustment (LPA) corrections were not applied except for observations taken at the six USCG land stations 375-382 listed in Table B-1.

No attempt was made to test the SALT-model assumptions (McCullough and others, 1982). Although these assumptions do not enter directly as a bias error, they may introduce range dependency in the ASF's and cause extrapolation errors in the predictions. It can be argued that because ASF's are anomalies relative to an arbitrary model, it doesn't matter what model is used so long as everyone uses the same model. On the other hand, the ability to interpolate and extrapolate observations accurately relies on good modeling of local conditions. It may be desirable at some stage to separate reference and prediction functions into two models: one fixed model for reference, and a second model for local interpolation and extrapolation.

SUGGESTIONS FOR FUTURE ASF CALIBRATION SURVEYS

The largest sources of error in this study are thought to be the reference positioning, NED bias, seasonal BED related variations, and receiver differences. For future surveys we recommend:

- o Data oriented survey strategies.
- o More uniformly distributed observations.
- o At least two (redundant) reference navigation systems.
- o At least one satellite reference navigation system.
- o Differential GPS.
- o Fixed local LORAN monitors (for BED and NED observations).
- o At least two LORAN receivers of different band width.
- o Calibrated receivers.
- o Analysis of LORAN signal quality and noise levels.
- o Independently calibrated LORAN control standards.
- o Baseline TD observations.
- o Transmitter radial TD's at sea.

Selected stations should be revisited. Receiver motion induced errors, should be determined. Uniform signal-quality rejection criteria should be used. Independent surveys of the same area should be made for quality control. Publication of provisional results should be encouraged to facilitate evolution of ASF charts. (Discrepancies seen in the observations of this paper emphasize the need for repetition and comparison.)

It is not sufficient to survey along the coasts where offshore phase-recovery gradients are largest and TD effects cannot be unambiguously decoupled. ASF observations should be distributed throughout the coverage area. Not all areas need the same density of ASF observations.

Appendix G

USCG VERIFICATION CRUISE RAW DATA

Figures G-1 and G-2 show the raw USCG ACUSHNET verification cruise data in the western Gulf of Mexico before data editing or averaging. The USCG frames of Figures 9 and 10 show the same data after editing and averaging. The raw plots emphasize extreme values and, as such, give some feeling for the range of variations in the data. A point-by-point study shows that the various clusters of data correspond to the cruise segments shown in Figure 9. The scatter of the clusters is greater than the local LORAN scatter. Because there is no reason to expect local LORAN discontinuities at sea, much of the observed scatter we assume is caused by shore-based reference navigation errors. The raw data from the Western Gulf USCG BIBB cruise were plotted in the same way, but show no usable segments.

Appendix H

GLOSSARY

This appendix defines some of the LORAN terminology used in the paper. Additional background is provided in Frank (1983), McCullough and others, (1982), and USCG (1980). The primary source of LORAN definitions is USCG (1981).

LORAN terminology has evolved over the years, so a term and its units occasionally are inconsistent. For example additional secondary phase factors (ASF's) are now commonly measured in microseconds, which is not a unit of phase. It would be useful to retire some older terms, such as baseline delay and coding delay.

Our definitions are intended to unburden the main text and suggest general concepts to readers with LORAN background. They are not formal definitions.

ASF. Additional secondary (phase) factor microsecond. A generic term used to describe land-induced propagation delays. (LORAN pulses go slower over land than over salt water.) Usually expressed as a time (microseconds), but occasionally as a phase angle (radians) or as a length (meters). Also used to represent the propagation-time anomaly relative to the SALT-model. Both sign conventions are used. (See McCullough and others, 1982 and Appendix D.)

BED. Broadcast emission delay, microsecond. The ED at a specific epoch. An operational variable adjusted over a range of a few microseconds to maintain a constant TD at the SAM. (See Appendix D.)

Calibrate. Mixed meanings. Generally the process of establishing the relationship between the indicated value of a measuring device and the value determined from a standard. For example, we calibrate LORAN for geodetic surveying with measured TD's at known geodetic locations and times. The implied standards in this case are the LORAN WGS-72 coordinates, the receiver characteristics, and the method of extrapolating the observations to other locations and times. (A two-dimensional problem similar to the one-dimensional problem of calibrating a precision lead screw by tabulating its turns count at carriage positions established from a standard.)

Unfortunately LORAN terminology has restricted the term to mean the hot-clock measurement of the NED. We propose eliminating this confusing restriction and have attempted to do so in this paper.

CCZ. Coastal confluence zone, a near shore ocean region. The ocean zone shoreward of the 100-fathom contour and 50 nautical miles from the nearest land. The present limit of the published DMA ASF tables.

Crossing angle. The smaller angle between two LOP's, degrees. Also called the cut.

CSTD. Controlling standard time difference, microsecond. The nominal value of the TD at the SAM, a defined numeric constant. The Secondary BED is continuously adjusted to keep the observed TD at the SAM as close as possible to the desired CSTD.

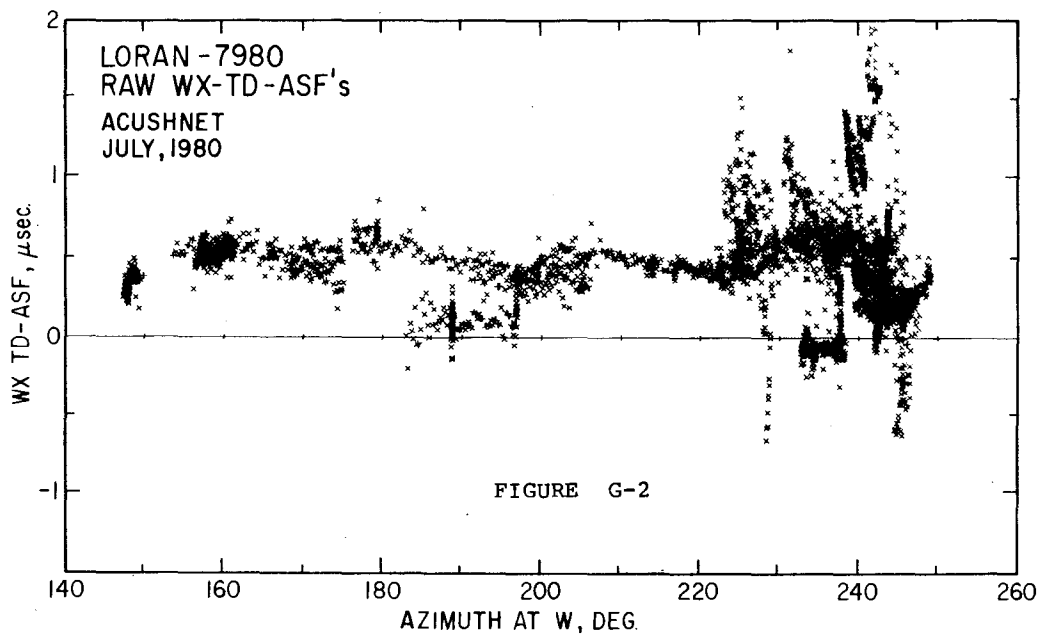
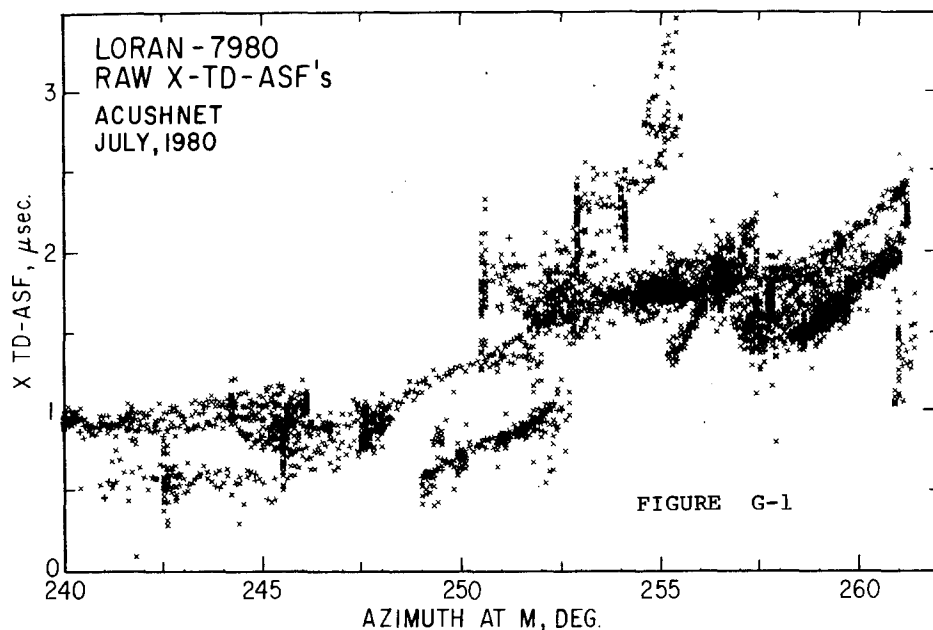


Figure G-1. Unedited, unaveraged X TD-ASF from the ACUSHNET western Gulf verification cruise of 1980, shown as a function of the ship's azimuth at the M transmitter. Data grouping is related to the cruise segments shown in Figure 9. General scatter emphasizes the extreme observations encountered, but does not necessarily represent scatter due entirely to LORAN.

Figure G-2. Same as Figure G-1, but for Transmitter W with Transmitter X as reference, shown as a function of azimuth at W. Data grouping is associated with the same cruise segments as before (fig. G-1). Note in both figures that the groups associated with cruise segments show greater scatter than the LORAN variations within groups, i.e., LORAN is being used to detect changes in the shore navigation when, of course, the opposite calibration is desired.

- Delta-Range ASF. Delta-Range-ASF, microsecond. The numeric difference of two Range-ASF's. Similar to the TD-ASF, but without the ED anomaly. (See Appendix D.)
- DRD. Double range difference, km. The difference between the Net-M-Land of the SAM controlling the Secondary and the Net-M-land at the observed TD (see Appendix B). DRD's are correlated with seasonal variations. Also used to describe models based on DRD's.
- D-rms. The distance rms (root mean square), same units as the data. A measure of navigation precision which accounts for the crossing angles of the lines of position (LOP's) as well as the standard deviation of the each LOP. (See Bowditch, 1977, p. 1129 for a mathematical formulation.) The "2D-rms" is twice the D-rms.
- ED. Emission delay, microsecond. A general term denoting the absolute time interval between the Master and Secondary transmissions in the same GRI. (The ED is the interval between Master and Secondary transmission; the TD is the time interval between Master and Secondary reception. See also BED and NED.)
- ED'. Emission Delay anomaly, microsecond. The BED - NED of a Secondary. See Appendix D, Eq. D4-D5.
- GRI. Group repetition interval, microsecond. The time interval from one group of nine Master pulses to the next. The GRI in microseconds is numerically equal to ten times the chain rate designation, i.e., LORAN Rate-7980 has a GRI of 79800 microsec (0.0798 sec) or repeats somewhat more than 12.5 times per second. (Actually alternate GRI's have different phase coding, so the full pattern repeats after two GRI's -- See Frank, 1983.)
- Ground wave. That portion of the LORAN signal which propagates near the ground. The LORAN signal component used for precise navigation at ranges of up to about 800 nautical miles, after which the ionospheric or "sky-wave" component begins to dominate. Because of large ionospheric delay variations, ASF's, etc., only have practical significance for LORAN ground wave positioning.
- Hot-clock. A traveling atomic clock used to determine NED's. A traveling atomic clock, called a "hot-clock," is carried from the Master to the Secondaries and back to the Master to measure the broadcast emission delay (BED) and thus establish the nominal emission delay (NED) at that epoch. Measurements are made relative to the base currents of the antennas, not to the electric vector seen by whip antenna receivers in the far field.
- Hot-clocked. The process of determining the NED's of a LORAN chain via a hot-clock. The process is called calibration by the USCG.
- Lane. Hyperbolic LOP separation, meters per microsec. For one Secondary, the local minimum distance (meters) between two hyperbolic lines whose TD's differ by one microsec.
- LOP. Line of position.
- LPA. Local phase adjustment, nanosecond. The discrete time increment used to make small (20 nanosec) changes in the BED in order to maintain a constant TD at the SAM. Called a phase, but used as a time. Called an adjustment, but used as time increment.
- Millington model. A numeric procedure for finding LORAN propagation times over ground of mixed conductivity. (See McCullough and others, 1982.)
- NAD-27. North American Datum of 1927. The standard of horizontal position control in the U.S.A., Canada, and Mexico used until recently for most maps and charts. NAD-27 will be replaced by WGS-84 during the next decade or so. NAD-27 may differ from the WGS-72 LORAN standard by many tens of meters. Therefore, most maps and most charts are now based on a different geodetic system than LORAN.
- In this paper, all positions were converted to approximate WGS-72 coordinates, but not always in a consistent or traceable way. (See error discussion in Appendix F.)
- NED. Nominal emission delay, microsecond. The standard value of the ED assigned to each Secondary and published by the USCG with the transmitter specification data. A NED value is determined from baseline-extension crossing data (see example in Appendix C) or, more recently, by traveling clock (hot-clock) measurements. Because the BED changes with season and weather, the NED should include the date of observation. Used in navigation to represent the desired BED.

Net-M-land. Net Master land length, km. The difference between the distance traveled by the Master pulse over land and the distance traveled by the Secondary pulse over land. Used as a rough estimate of the ASF. (See Appendix B.)

Offshore phase recovery. A reduction of the cumulative ASF seaward beyond the shore, microsecond. The decrease (recovery) in cumulative ASF of a LORAN pulse as it travels from land to sea. (fig. 1). A general term for the effect of offshore ASF reduction; also the size of the effect in microseconds. Called a phase, but usually expressed as a time.

Phase recovery. A reduction of the cumulative ASF, microsecond. The decrease (recovery) in the cumulative ASF of a pulse as it travels to a zone with higher conductivity. Called a phase, but usually expressed as a time.

Range-ASF. The ASF of a single path or range, microsecond. The propagation time anomaly relative to the SALT-model of the observed or predicted one-way travel time of a LORAN pulse. Generally, a small positive number of microseconds representing the land-induced delay of a pulse. (See Appendix D.)

SALT-model. The ASF reference standard. A numeric, fixed coefficient model used to:
(1) Calculate the great ellipse distance between two points of known latitude and longitude and (2) Convert this distance to a unique LORAN propagation time. The SALT-model reference accounts for some 99.98% of the actual LORAN travel time and is easily reproducible in small computers.

The SALT-model is based on two other models: (1) An earth model used to find the great ellipse distance and (2) A model to convert the distance to a LORAN travel time. The times derived with the SALT-model approximate LORAN propagation times over ocean salt water, hence the name. Not all ocean conditions match those of the SALT-model, thus ASF's are not necessarily zero over the ocean. ASF's also change over the ocean due to offshore phase recovery effects.

Because a standard LORAN SALT-model has not been established, we elected in this paper to use the code in Appendix B. of McCullough and others

(1982), as a provisional working definition. Recognized difficulties with this definition exist and ways to resolve them are being discussed with DMA.

SAM. System area monitor. A remote LORAN receiving station used to monitor far-field TD's. SAM observations are used to control the BED of the Secondary in order to maintain, as nearly as possible, a constant TD at the SAM. (See also CSTD.)

TD. Time difference, microsecond. Time interval between the reception of the Master pulses and the reception of the pulses of a Secondary in the same GRI. The basic LORAN observable. (See Frank, 1983.)

TD-ASF. Time difference ASF, microsecond. The time difference (TD) anomaly of an observed or predicted TD relative to that calculated by the SALT-model and NED. The sign of the TD-ASF is such that the sum of the receiver TD and TD-ASF gives the SALT-model propagation time. TD-ASF's and Net-M-land are positively correlated (fig. B-2), i.e., increasing the Master land delay will increase the TD-ASF. (See also Appendix D.)

TINO. Time interval number, microsecond. The time interval between the start of the GRI of the local transmitter timer and the arrival of a pulse from a remote transmitter of the same LORAN-rate. Timer, propagation, receiver, and antenna coupler delay variations cause the TINO to change. Differences of TINO's from the the same transmitter are used with other TINO's to monitor chain performance. Differences of TINO's taken at separate transmitters can be used to monitor propagation changes. (See fig. 2.)

Tomography. A technique allowing reconstruction of a mathematical field from knowledge of linear path integrals through the field.

WGS-72. World geodetic system of 1972. A satellite geodetic position standard widely used in geodesy and LORAN. It differs by generally less than a meter or so from the new standard, WGS-84. WGS-72 is not the same as the North American chart and map standard, NAD-27, which may differ from WGS-72 by many tens of meters. (See DMA, 1981 for extensive discussion.)

"VIEWNAV"

PRECISION NAVIGATION, PLANNING, AND TACTICAL CONTROL

MORTIMER ROGOFF
NAVIGATION SCIENCES, INC.
BETHESDA, MD 20815

Navigation Sciences, Inc. has developed a marine navigation system, with vessel positioning based upon differential Loran C, which displays own-ship vessel position against the background of a multi-color electronic chart, and which includes radar targets of nearby vessels.

Position accuracy of five to ten yards is routinely available, made possible by a combination of prior surveys, and by the use of continuously operating monitors in covered areas.

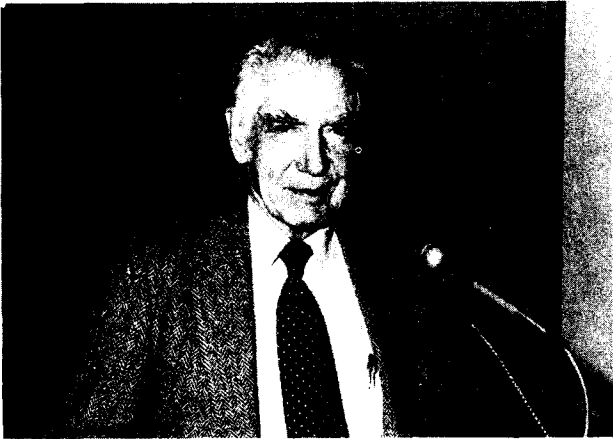
The high level of accuracy in determining own-ship position allows the

overlapping display of electronic chart and radar, with total suppression of the radar shoreline. This results in a uniquely clean display that is unambiguous as to land vs. water, with aids to navigation and channel boundaries clearly evident.

The computerized system automatically displays the appropriate electronic chart, and allows the user to measure courses and distances to any place or object of interest.

Mr. Rogoff narrated a film presentation demonstrating operation of the VIEWNAV system in the area of Baltimore Harbor.

SESSION ONE SPEAKERS



Walt Dean



LT Doug Taggart



Jim McCullough



Mort Rogoff



Larry Sartin

SESSION TWO

CHAIRMAN

A.W. Marchal
Offshore Navigation

CONTROL ALGORITHM FOR A RHO RHO LORAN-C SYSTEM

Marty Poppe
 Cambridge, Engineering
 P.O. Box 66
 Cambridge, Vermont 05444

Per Enge
 Megapulse, Inc.
 8 Preston Ct.
 Bedford, MA 01730

Abstract

In this paper, we describe the chain control algorithm that Megapulse has developed for range/range LORAN-C chains and plans to implement in the French Systeme National de Radionavigation. This control algorithm is unique and interesting for the following reasons. Even though many hyperbolic chains and controllers have been realized, the SNR is the first LORAN chain designed to operate in the range/range mode. Secondly, the SNR controls the time of pulse transmission in an absolute sense, where absolute time is defined by a remotely located master clock. Finally, the SNR controls time of transmission as measured at the transmitter rather than at a remote location.

chains since it will operate in the range/range mode, as opposed to the time difference mode. For a conventional LORAN-C chain, the time differences between the Master and the Secondary transmissions are controlled through measurement made at a monitor site. The monitor site is typically located near the coastline in the area of coverage. The control system for the SNR differs from those of conventional chain in two major ways:

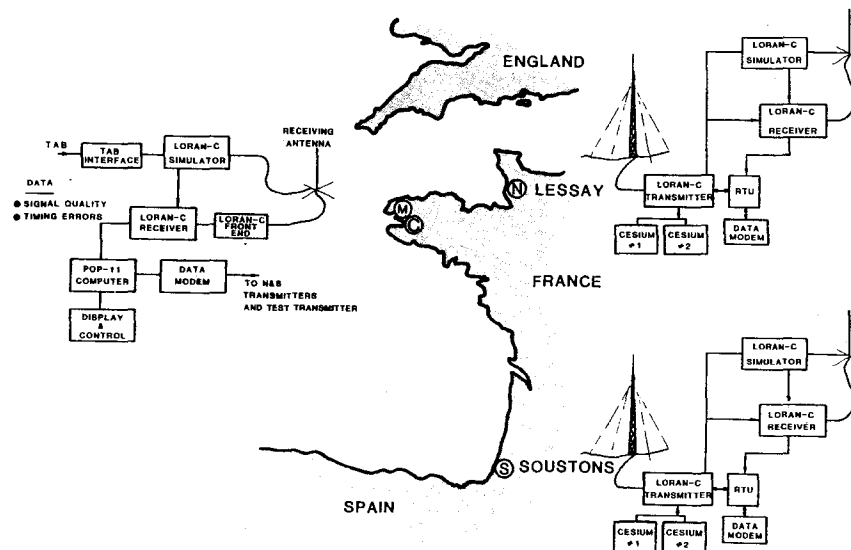
- First, the SNR controls the time of transmission of the LORAN-C pulses in an absolute, rather than in a time difference sense. In this case, absolute time is defined by a remotely located master clock.
- Second, the SNR system controls the time of transmission as measured at the transmitter, rather than at a remote location.

INTRODUCTION

Megapulse, Inc. is under contract to the French Navy to supply a LORAN-C navigation system which is designed to provide coverage in the Bay of Biscay. This paper describes the control of that chain known as the Systeme National de Radionavigation (SNR). The control of LORAN-C transmitters is not a new topic, however, the SNR is different from most

AN OVERVIEW OF THE SYSTEM

Figure 1 is an overview of the SNR which shows the major elements of the chain. These elements are located at four physically separate locations. The two transmitters are located at extreme



ELEMENTS OF THE CHAIN CONTROL SYSTEM

northern and southern sites which provides maximum baseline separation given the geometry of the coastline. The chain control center and system master clock are located approximately 350 Km west of the northerly station. A maintenance center which contains duplications of the major system elements for the purposes of training and maintenance is located near the chain control center.

Each transmitting site consists of a transmitter and a co-located monitor receiver. The transmitting equipment at each site is fully redundant, consequently there are two identical timers, each controlled by a separate cesium beam standard. For purposes of describing the control algorithm, these timers are distinguished as the on-line and the off-line timer. The LORAN-C monitoring equipment consists of a LORAN-C receiver and an associated LORAN-C simulator. The LORAN-C simulator is time synchronized to the transmitter and injects a low level signal into the monitor receiver antenna and therefore calibrates receiver delays in real time. This technique measures remote signal time of arrival with respect to the local timer, while avoiding receiver overload. At the chain control center, a third monitor receives signals transmitted by both transmitters, and here to a LORAN-C simulator is used to calibrate the LORAN-C receiver. At the control center, the LORAN-C simulator and the LORAN-C monitor receiver are referenced to the system master clock. Locating the system master clock remote from both transmitters increases the complexity of the control problem, however it has the advantage of ease of interface with the user. Indeed, it permits the user's frequency standards (required for range/ range navigation) to be compared directly to the system standard.

CHAIN CONTROL

The objectives of chain control are:

- to maintain the times of pulse transmissions in close synchronization with the system master clock
- to obtain remote control of the transmitters through the use of a remote control unit
- to manage unexpected events
- to keep system records.

This paper addresses only the first of these requirements, the synchronization to the master clock.

Synchronization is essentially a time transfer problem. That is, we must accurately transfer our notion of time at the master clock to both the Master and Secondary transmitters. The principal difficulties involved in time transfer are caused by:

- offset between the cesium time standards at the transmitters and the master clock. (Offset between two cesium clocks will cause two clocks which have been precisely aligned at one time to drift apart over a period of time.)
- temporal variations in the LORAN-C propagation delay. (Temporal variations in propagation delay decrease the observability of the transmitter emission times. That is, we cannot accurately measure time of transmission but must view it through a propagation path which adds uncertain and variable delays.)

The time standards selected for the transmitter sites are the Oscilloquartz OSA 3216 cesium beam frequency standard. These standards frequently exhibit time drifts of approximately 25 nsec/day when installed in a well controlled environment. This implies that we cannot simply set the time and forget it, rather we must provide for daily corrections of transmitter timing.

To correct the time of the transmitter with respect to the master clock, we must transfer time from the master clock to the station. This may be accomplished by either using a portable clock (that is, physically carrying the time from the master clock to the transmitter) or by propagating a signal through a medium.

While it is anticipated that portable clock trips will be used to assure system calibration, the use of portable clocks to control the operational system is impractical due to the low update rates obtainable (i.e. one/trip) and the cost of physically transporting the clock.

The use of signal propagation to transfer time is common, because good update rates can be achieved and a wealth of techniques exist. The techniques available include using television synchronization pulses, microwave signals, satellite signals, radio waves propagated

on the surface of the earth (groundwaves) and the transmission of time signals through cables. To make the SNR system self-contained, we have selected the use of the LF LORAN-C pulses as the time transfer medium.

Having selected the LORAN-C pulse to transfer time from the master clock to the LORAN-C transmitters, we next had to consider the temporal variations in the propagation delay of the LORAN-C signal, that is, variations in the time of arrival due to external causes. The time of arrival of a LORAN-C pulse varies because weather and climatic changes cause changes in the ground's surface impedance, the air's index of refraction and the vertical gradient of the air's index of refraction (vertical lapse rate). Using assumptions felt to be reasonable in the SNR environment, we predict the following variations due to temporal propagation effects:

1) On the path from the southern transmitter to the master clock, which is approximately 600 km long and mainly over seawater, we predicted negligible variation due to the surface impedance changes and index of refraction. Thus, in this case, the majority of change will come from changes in the vertical gradient of index of refraction. Assuming a nominal 15% change, the time variations of the southern transmitter signal as received at the master clock are expected to be between 150 and 200 nsec.

2) The path from the northern transmitter to the master clock is approximately 240 km in length, half seawater and half land. The errors due to the seawater portion are anticipated to be very small. However, the 120 km land portion will introduce variations due to the climatic effect on vertical gradient of index of refraction and changes in ground surface impedance due to, for example, the wet and dry seasons of the year.

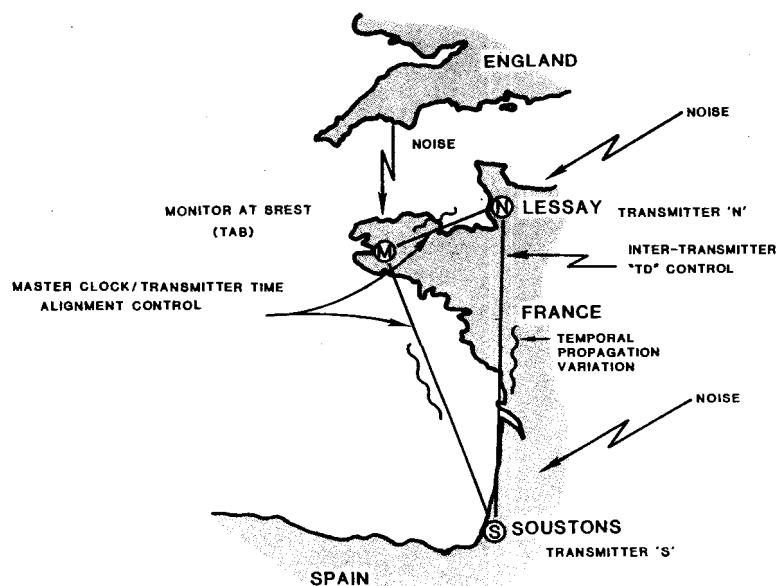
These changes are anticipated to yield a total variation of approximately 250 nsec.

On both paths, steep weather fronts or storms might result in additional variations of up to 200 nsec.

The implications of these temporal propagation effects are twofold:

- First, we may not simply control the chain by maintaining a constant time of arrival of the transmitted signal at the master clock. This is because propagation delay variations are indistinguishable from true transmitter time errors.
- Second, we must learn to interpret or measure the effects of weather on the signal delay.

As shown in Figure 2, the selected approach to the control problem employs two control loops. The first loop links



the two transmitters together, and the second loop links the individual transmitters back to the master clock. The first loop measures the error of the southern transmitter with respect to the northern transmitter, the error between the northern on-line and standby timers and the error between the southern on-line and standby timers. This provides us with a total of four cesium standards from which we determine our estimate of transmission times for the transmitter/transmitter control loop.

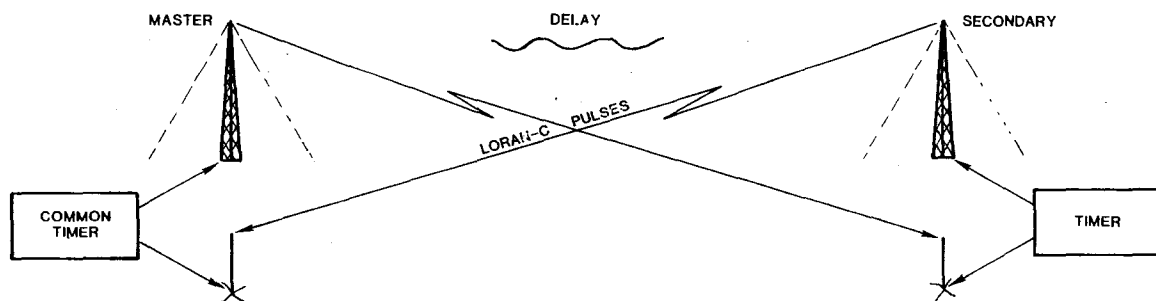
The inter-transmitter loop takes advantage of a technique which cancels the effect of the propagation delay, and hence propagation delay variations, on the path between the two transmitters, while providing a measure of time of transmission errors between the two transmitters. This technique is shown briefly in Figure 3. As shown, the time of arrival (TOA) of the northern station is measured at the southern site with respect to the southern timer; while the southern signal TOA is measured at the northern site with respect to the northern timer. Adding these two TOA measurements, we see that the delay term cancels, leaving us with an expression for the error in the difference between the time of transmission of the two stations. Thus, using the transmitter/transmitter loop, it is possible to tightly control the time difference of emission from these two transmitters.

Additionally, by subtracting the TOA measurements, we obtain an estimate of the propagation delay and we will discuss the use of this estimate later.

The control loop between the transmitter and the master clock is used to correct the absolute time of transmission of both the northern and the southern transmitters with respect to the master clock. This loop measures the time of arrival of both transmitters at the monitor site, and the error between the transmitter cesiums. Although the inter-transmitter loop controls the time difference, it is possible for the average drift of the four cesium standards to cause the absolute time of transmission of both transmitters to drift either earlier or later in time. Through the use of the monitor at the master clock, and bearing in mind the uncertainty introduced by propagation delays, it is possible to maintain a good degree of time alignment between both transmitters and the master clock.

In summary, we have broken the control problem down into two separate problems:

- The control of the time difference of emission between the two transmitters
- The control of the overall time error between the two transmitters and the master clock.



$$\begin{aligned}
 TOA_M &= TOT + ERROR + DELAY \\
 TOA_S &= TOT - ERROR + DELAY \\
 TOA_M + TOA_S &= TOT + TOT + 2(DELAY)
 \end{aligned}$$

$$\text{ERROR} = (TOA_M - TOA_S)/2$$

A summary of the quantities is measured in each control loop is shown in TABLE I.

TABLE I also shows the point at which we gain control over the system. These control points are:

- The application of local phase adjustments (LPAs) to the northern transmitter
- The application of LPAs to the southern transmitter
- The application of pseudo, or mathematical, LPAs to both the northern and southern off line timers.

The LPAs applied to the off-line timers are called "pseudo" because the transmitter control system always keeps the on-line and off-line timers in close time synchronization. This allows the timers to be interchanged without a system time jump. The time difference which would exist between these two timers without synchronization is therefore accumulated in the control computer software, and when an LPA is applied, it is applied by adjusting the accumulated time error between the two-timers, rather than by physically stepping the off-line timer.

TABLE I

Intertransmitter Loop

Measured

- North-South transmitter timer difference
- Northern on-line vs. off-line time difference
- Southern on-line vs. off-line time difference

Control Points

- Northern on-line timer LPA
- Southern on-line timer LPA

Master Clock/Transmitter - Loop

Measured

- Northern transmitters signal time-of-arrival at master clock
- Southern transmitter signal time-of-arrival at master clock
- Northern on-line vs. off-line timer error
- Southern on-line vs. off-line timer error.

Control Points

- Northern and Southern on-line timers, equal LPAs applied to both
- Northern off-line timer 'pseudo' LPA
- Southern off-line timer 'pseudo' LPA

THE CONTROL ALGORITHM

Based on the measurement and prediction of time errors, the SNR uses control metrics to anticipate the effect of applying LPAs on future system errors. The selected control metrics are:

- The predicted time error
- The predicted integrated or accumulated time error
- The total number and size of the applied LPAs.

With each of these metrics, we associate a cost. That is, we penalize the system with varying costs for differing types or errors. An analogy may be helpful here: Consider the requirement of driving an automobile from your home to a given destination. Included in this problem are the concerns of automobile operating costs and the desire to arrive at a specific time. If the reason for driving to the destination is to take a young lady to the theatre, then the penalty for arriving late is relatively high, and by comparison, the cost of gasoline is less important. In this case, the costs are adjusted such that speed will be increased, wasting gas, but assuring a timely arrival. Note here also, there is perhaps a third constraint, as too much speed will mean a delay by a police officer. A second example with the same control metrics, but with cost selected for a different goal, might be driving to work. In this case, arriving on time is not perhaps as important and, due to its daily cost, the expense of the gasoline and especially the cost of being stopped for speeding become much more important. In this case, speed is reduced for increased fuel efficiency. (Hopefully, your manager is using a similar criteria!) The consideration of the various cost elements for the LORAN-C problem are not quite as interesting, but are the key to the control algorithm.

The calculation of costs are considered separately for the transmitter/transmitter loop and the master clock/transmitter control loop. For the intertransmitter loop, we calculate costs by trial application (mathematically) of local phase adjustments to both the northern and southern transmitters, in all combinations ranging from -20 to +20 nsec, in 10 nsec steps. For each combination of north and south

LPAs, we estimate the cost at the northern transmitter on future north/north timer errors. Secondly we estimate the cost at the southern transmitter on future south/south time errors. Finally, we estimate the cost on future north/south time difference errors.

After computing the cost for all possible combinations of LPAs, we select the north and south on-line timer LPAs which yield the lowest cost. By considering the time error between the on-line and off-line timers, as well as the time difference errors between the two transmitters, we force the adjustment of the time difference in such a way that the system absolute time will be influenced by the consensus of the four cesium beam standards.

The correction of the absolute time of transmission of both the north and south transmitters with respect to the master clock must consider the reduced accuracy available on the 'one-way' transmissions to the chain control center. We do this by calculating costs under a constraint which requires that equal LPAs be applied to both the northern and southern transmitters. That is, we apply the LPA in a manner which will not disturb the relatively precise control of the time difference between the two transmitters. Also, we consider the effect of applying a pseudo phase adjustment to both the north and south off-line timers. Through the application of both the on-line and off-line LPAs, based on the signals monitored at the chain control station, we can both reduce the divergence between the on-line and off-line timers and move the entire chain either earlier or later in time. By associating a cost with the application of LPAs, both real and mathematical, we still give weight to the estimate of time obtained from the four transmitter cesiums. For example, if, based on the monitoring, we determine that all four cesium standards must be moved to produce better time alignment, we will incur a fairly large cost, due to the number of LPAs required, and therefore tend to move in this direction rather slowly. On the other hand, if the monitoring indicates that three of the four timers do not require adjustment, then the system will allot its entire cost budget to the adjustment of one timer, aligning it with the remaining three rather quickly.

The ability to control the SNR system is ultimately dependent upon the errors involved in measuring the time errors at the various control points. Table II shows the inter-transmitter error budget. We have listed here both precision and stability. The main difference appears in the value for receiver bias error. This entry acknowledges that there will be a larger difference between two randomly selected receivers than will be experienced with a given receiver as a function of time. A non-reciprocity term for the inter-transmitter loop has been included in the error budget, but it is listed in the rms value table as zero, because non-reciprocal groundwave propagation has not yet been measured. Computing

the rms sum for the inter-transmitter loop yields time uncertainty of 23 nsec, to which we add a time transfer error of 20 nsec. For stability, we anticipate 18 nsec rms error.

Table III shows the "uncorrected" error budget for the master clock/transmitter loop. By uncorrected, we mean that no estimates of the propagation delay variation are being used by the control algorithm. As shown, this omission results in an error which is dominated by the propagation delay errors. The effect of severe weather is ignored in the computation, because such storms can readily be monitored and the data can be correspondingly edited.

TABLE II
THE INTER-TRANSMITTER BUDGET

PARAMETER	RMS ERROR (NSEC)	
	PRECISION	STABILITY
Transmitter N Quantization	2.9	2.9
Transmitter S Quantization	2.9	2.9
Receiver N Quantization	2.9	2.9
Receiver S Quantization	2.9	2.9
Receiver N Bias	15	10
Receiver S Bias	15	10
Background Noise at N (15db SNR)	0.46	0.46
Background Noise at S (15db SNR)	0.46	0.46
Non-reciprocity (10 maximum)	0	0
Cesium Noise	4.9	4.9

These values yield an rms total time uncertainty of 23 nsec plus a time transfer error of 20 nsec.

rms stability = 18 nsec

TABLE III

THE UNCORRECTED ERROR BUDGET FOR THE MASTER CLOCK/TRANSMITTER LOOP

PARAMETER	RMS ERROR (NSEC)	
	NORTHERN PATH	SOUTHERN PATH
Transmitter Quantization Error	2.9	2.9
Receiver Quantization Error	2.9	2.9
Receiver Bias Error	15	15
Background Noise (+15db SNR)	0.46	0.46
Cesium Noise	4.9	4.9
Propagation Delay Error	250	250
Severe Weather Effect	200	200

Total Error (less severe weather)

Northern Path 250 nsec rms.

Southern Path 200 nsec rms.

A master clock/transmitter loop employing "corrected" propagation estimates is under development at Megapulse. These corrections are based on the:

- spatial correlation of propagation delay
- correlation of propagation delay with observable weather parameters.

The first of these techniques is based on the assumption that propagation velocity is uniform over the area including the transmitters and the master clock. In this case, the propagation velocity can be measured between the northern and southern transmitters, (by applying the two way measurement technique described earlier) and then used to calculate either transmitter to master clock delay. The possible drawback of this approach is the questionable validity of the uniform propagation velocity assumption over a geography which includes seawater, land and mixed signal paths. (It may be possible to mitigate this drawback by using a computer model of the various paths.)

The second technique for providing corrected propagation delay is based on the well established dependence of propagation delay on vertical lapse rate,

index of refraction and ground conductivity. These "weather" parameters can be measured and corresponding propagation delay estimates can be made.

Currently, Megapulse is performing an extensive field measurement program to determine the error budget for a "corrected" master clock/transmitter control loop.

SUMMARY

The SNR system being developed for the French Navy by Megapulse is being designed from the outset to be a rho/rho system, consisting of two transmitters and a remotely located master clock. Through the use of co-located transmitters/monitor pairs and a monitor at the remotely located master clock, the system will be kept in very close time difference alignment and good absolute time alignment with respect to the master clock.

Noting that the largest errors are associated with propagation uncertainties between the transmitters and the master clock monitor site, we anticipate improvement in the time accuracy obtained from this system as experience teaches us the best way to react to observed weather and propagation conditions.

DIFFERENTIAL LORAN-C FOR
BUOY POSITION CHECKING

David E. Wells
Bradford G. Nickerson
Department of Surveying Engineering
University of New Brunswick
P.O. Box 4400
Fredericton, N.B.
Canada
E3B 5A3

James C. Rennie
Telecommunications & Electronics Branch
Canadian Coast Guard
Tower A, Place de Ville
Ottawa, Ontario
Canada
K1A 0N7

ABSTRACT

We have investigated the feasibility of using LORAN-C in a differential mode to determine whether or not a floating aid to navigation has been moved off its correct position (due to storm action, for example). Time difference (TD) measurements on the Canadian East Coast LORAN-C chain (GRI 5930) were made along the coast of Nova Scotia during August, September, and October 1982. Measurements were made at a differential monitor site, and at 23 remote sites up to 180 kilometres from the monitor. A receiver-equipped van visited 10 of the remote sites and a receiver-equipped helicopter landed at 8 remote sites, and hovered over 5 actual buoys. Each remote site was visited 4 or 5 times to establish the repeatability of the differential technique. The total of 32,858 TD measurements, and the (remote-monitor) TD differences, were statistically analysed and plotted. The variations in TDs and TD differences from visit to visit were converted to (remote-monitor) position difference variations. These results indicate that in a region of reasonable chain geometry, the differential LORAN-C technique can detect buoy position movements of 15 metres, at the 95% confidence level, although some recommended improvements to the technique need to be developed and tested before it can be put into routine practice.

INTRODUCTION

Determining whether or not a floating aid to navigation (buoy) has been moved off its correct position (due to storm action, for example) is a difficult and expensive procedure. In order to find a more cost-effective solution to this problem, the Telecommunications and Electronics Branch of the Canadian Coast Guard is investigating the feasibility of using LORAN-C in a differential mode. The criterion of acceptable performance is that this (or any other technique) must be capable of detecting buoy position shifts as small as 15 metres, at the 95% confidence level.

A first experiment to evaluate the usefulness of differential LORAN-C for buoy position checking was held along the Nova

Scotia south shore between August and October 1982 [1]. Reduction and analysis of the data obtained during this experiment are described in [2]. This paper presents the results of this experiment.

FIELD PROGRAM

The experiment was designed to test the repeatability of differential LORAN-C positioning of fixed sites. Rather than addressing the basic question of whether differential LORAN-C can detect a 15 metre change in position, a slightly different question was addressed: Given repeated visits to the same site (no change in coordinates), will the positions computed from the differential LORAN-C measurements be repeatable within 15 metres? The assumption is made that if the resolution and repeatability of differential LORAN-C is satisfactory, as judged from this experiment, then it will also be capable of detecting whether a position shift has occurred.

In fact (unknown to us at the time) part of the experiment became a blind test of movement detection, since the buoys at sites 14 and 15 (see Table 1 below) were actually serviced and removed on 2 October 1982 in the midst of the experiment.

The area selected for the experiment was along the south shore of Nova Scotia. Figure 1 shows that this test area lies near the centre of the coverage area for the Canadian East Coast LORAN-C chain (Group Repetition Interval 59300 microseconds).

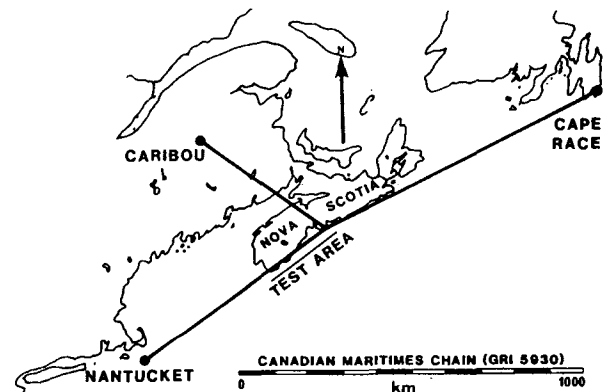


FIGURE 1. TEST AREA

A monitor station was established at Ketch Harbour, near Halifax, Nova Scotia (shown as a triangle on Figures 2 and 3). The twenty-three sites listed in Table 1 were visited repeatedly over a 75-day period from August to October, 1982. Ten of these sites (shown in Figure 2) were visited four times by a LORAN-C receiver, mounted in a van, which acquired about two hours of observations per site per visit. Thirteen sites (shown on Figure 3) were visited up to five times each by the same receiver mounted in a helicopter. At eight of the helicopter sites (denoted by circles in Figure 3), the helicopter landed to make approximately five minutes of observations. The other five of the helicopter sites (denoted by squares in

TABLE 1
Test Sites.

Site	Type	Name	Distance From Monitor (km)
1	van	Lower Prospect	15
2	van	Peggy's Cove	30
3	van	Blandford	46
4	van	Battery Point	62
5	van	Dublin Shore	70
6	van	Medway Head	91
7	van	Western Head (Liverpool)	102
8	van	Port Joli Harbour	128
9	van	Western Head (Lockeport)	157
10	van	Ingomar Cemetary	178
11	light	Devils Island	11
12	light	Sambro Island	6
13	light	Betty Island	19
14	buoy	Peggy's Point	30
15	buoy	Horseshoe Ledge	36
16	light	Pearl Island	43
17	light	Mosher Island	68
18	light	Coffin Island	100
19	buoy	White Point Rock	115
20	light	Little Hope Island	125
21	light	Gull Rock Island	155
22	buoy	Jig Rock	163
23	buoy	Budget Rock	183

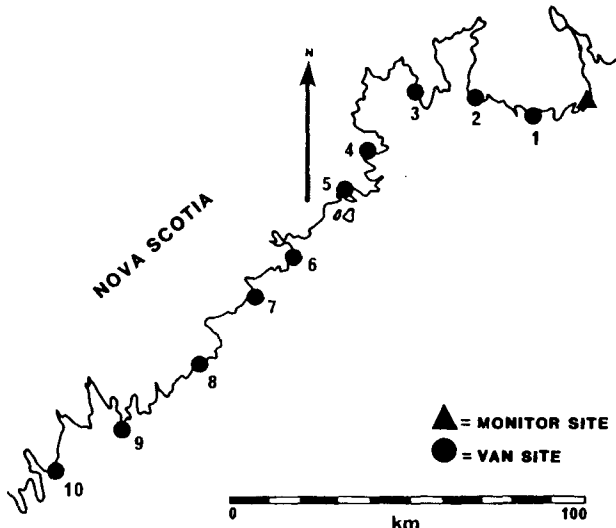


FIGURE 2. VAN SITES

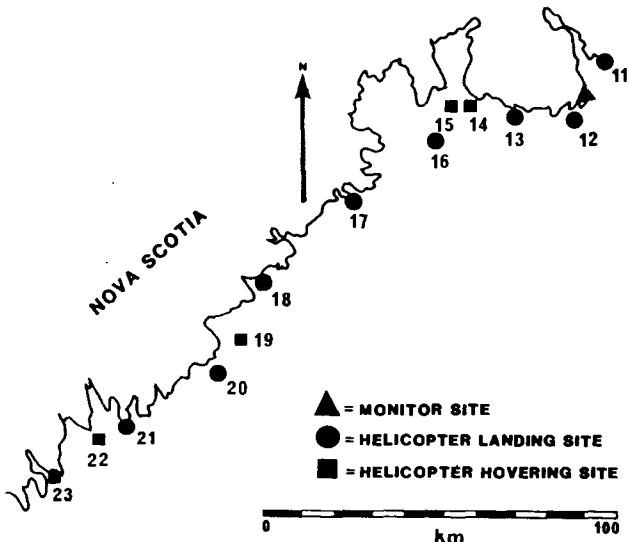
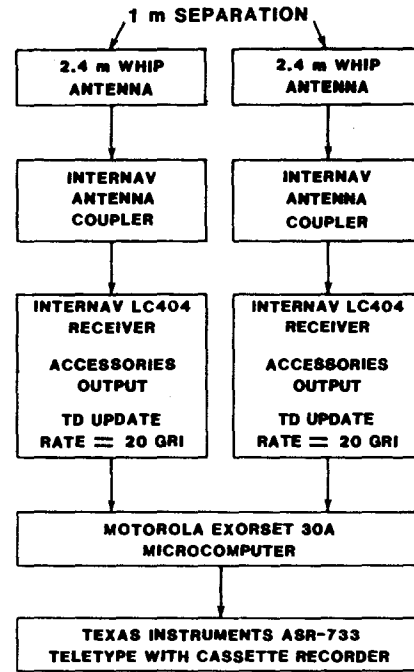


FIGURE 3. HELICOPTER SITES

Figure 3), were actual buoys, over which the helicopter hovered for two or three minutes while the observations were being made, after first hovering for an initial two to five minutes to allow the receiver tracking loops to settle.

The monitor station was operated simultaneously with the van/helicopter receiver, in order to permit differential LORAN-C corrections to be made. Three Internav LC404 receivers were used: two at the monitor station (serial numbers 1017 and 2220) and one in the van/helicopter (serial number 1053). A microcomputer was interfaced to the two receivers at the monitor to acquire and record the data (see Figure 4).



MONITOR SYSTEM

FIGURE 4.

Two receivers were used to study receiver-to-receiver differences in recorded data, when both receivers operated in an identical environment. The time constant for both receivers was set to 40 seconds (i.e., step response of tracking loop at 90% after 5 seconds). Due to operational constraints, it was necessary to use a different type of microcomputer (running different software) with the van/helicopter receiver (see Figure 5). The van and helicopter installations for this equipment were kept as similar as possible. Both installations used the same avionics-type antenna, same system grounding technique, and operated on a 28 volt DC power supply (except for the ASR-733 which required 115 volt AC power). The time constant of this receiver, both for van and helicopter use, was set to 8 seconds (step response of tracking loop at 90% after 1 second). Every 20 GRIs (1.186 seconds) one pair of TD readings was acquired from each receiver. The two microcomputers then accumulated a preset number (called the sample size) of these readings, computed the mean and standard deviation, and recorded these, together with a time tag (in Universal Time). The sample size for these

records was changed during the experiment, as was the resolution with which the mean

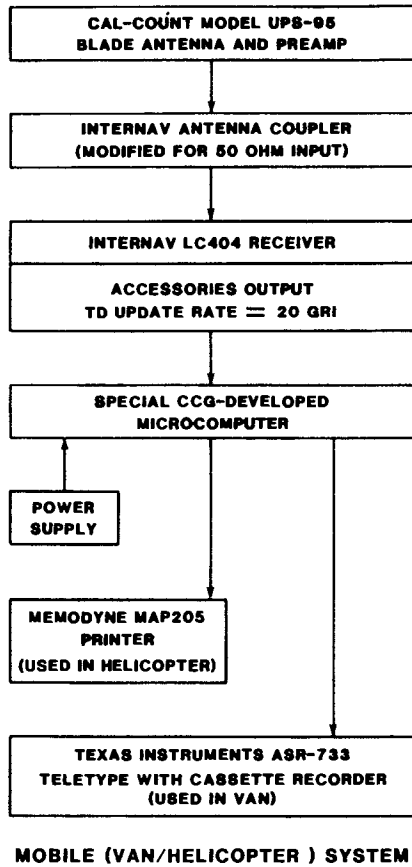


FIGURE 5.

TABLE 2
Changes in data recording interval and resolution during the experiment.

Visit	Sample Size (readings per record)	Recorded Data Interval (sec)	Resolution (nsec)	Record Standard Deviation
MONITOR				
Van				
#1	150	186	10	yes
#2	150	186	10	yes
#3	150	186	10	yes
#4	30	44	1	yes
Helicopter				
#1	75	98	10	yes
#2	75	98	10	yes
#3	150	186	1	yes
#4	30	44	1	yes
#5	30	44	1	yes
REMOTE				
Van				
#1	30	38	10	no
#2	30	38	10	no
#3	30	38	10	no
#4	30	38	1	yes
Helicopter				
#1	20	27	10	no
#2	20	27	10	no
#3	20	27	1	yes
#4	20	27	1	yes
#5	20	27	1	yes

and standard deviation was recorded. Table 2 shows these changes. As the experiment progressed, it was found that smaller sample sizes and higher resolution were both desirable. A total of 24,062 records were obtained at the monitor station, 8193 at the van sites, and 603 at the helicopter sites. Figures 6, 7, and 8 show plots of typical TD data from the monitor, the van, and the helicopter, respectively. Plots of the complete data set were made [2].

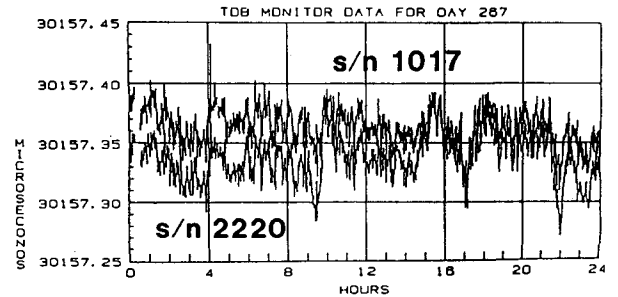


FIGURE 6. TYPICAL MONITOR RECORD

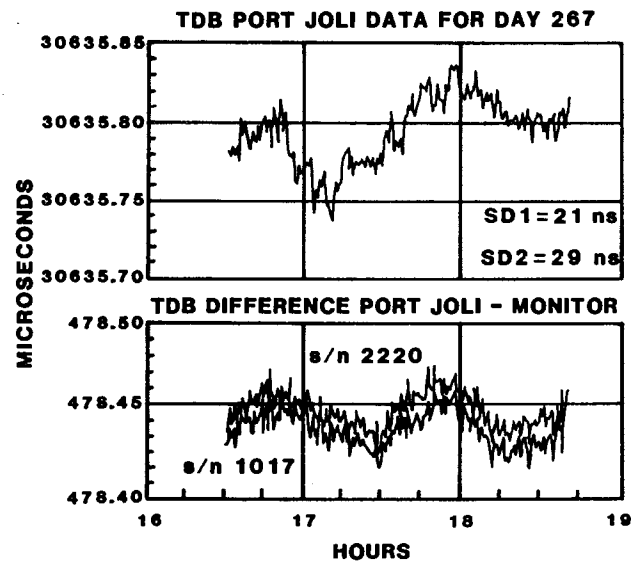


FIGURE 7. TYPICAL VAN RECORD

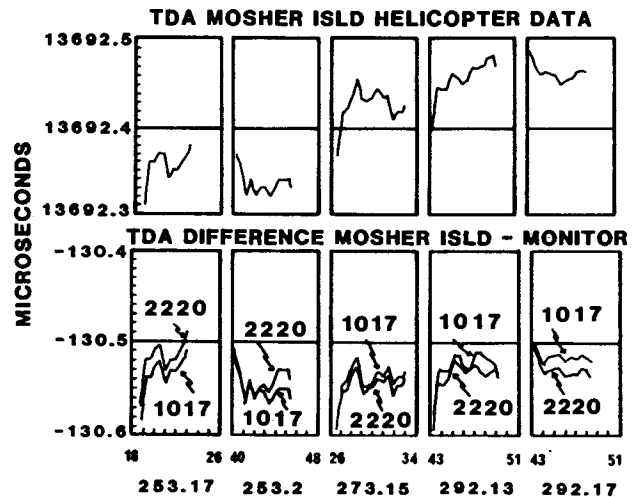


FIGURE 8. TYPICAL HELICOPTER RECORD

DATA ANALYSIS

The data were analysed for stability of the TD and differential TD measurements from visit to visit. The corresponding stability in position was also analysed.

The monitor and remote site data recording epochs were not synchronized (nor were the data intervals equal, as seen from Table 2). In order to obtain a differential TD value, the monitor data was linearly interpolated to extract a TD value referred to the same time as the recorded remote site TD value. Once data values referred to the same epoch of time were obtained, they were differenced (in the sense remote-monitor). Since there were two receivers at the monitor, two sets of differential TD values (remote-monitor serial number 1017, and remote-monitor serial number 2220) were obtained. Figures 7 and 8 show plots of typical differential TD values, for van and helicopter respectively.

The basic observable can be considered either to be each recorded value, or to be the individual readings which are accumulated to obtain the recorded values (see Table 2). The second choice requires that the sample standard deviation be recorded, as well as the sample mean, and this was not done at the remote sites for the early visits. Both options were considered in this analysis.

Reference values for the raw (undifferenced) and differential TD data at each site were computed as the mean of all readings (and differential TD readings) from all visits to that site. Subsequent to the initial analysis, it was learned that the buoys at sites 14 and 15 had actually been moved between visits 3 and 4. Hence these two sites were re-analysed, using new reference values which were the mean of all readings up to the end of visit 3. The results of this re-analysis are shown as footnotes in Tables 3 to 8, and in Figure 12.

For each visit, "visit mean" values for the raw and differential TD values were computed, also as the mean of all readings. Discrepancies between these "visit mean" values and the above reference values (overall "site mean" values) were computed. These TD and differential TD discrepancies are shown in Tables 3, 4 and 5. They represent the long term (from visit to visit) inconsistencies in the data, and form the information from which the technique must be judged.

"Visit mean" standard deviations for the raw and differential TD values were computed in three ways: treating the recorded values as the basic observable; treating the individual readings as the basic observable (used when both monitor and remote site recordings included the sample standard deviation); and a hybrid, where the recorded standard deviations at the monitor were taken into account, but the remote site recorded standard deviation was taken as zero (used when the remote site recordings did not include the sample standard deviation). These standard deviations

TABLE 3
Discrepancies between "visit mean" and "site mean" raw (undifferenced) TD readings (in nanoseconds).

Site	Visit1		Visit2		Visit3		Visit4		Visit5	
	TDX	TDY								
1 V	21	-17	-6	-19	-29	38	-8	17		
2 V	18	-10	8	-23	-28	22	2	11		
3 V	-16	-31	26	0	-11	19	1	12		
4 V	-38	-55	28	4	-10	-12	19	63		
5 V	-43	-17	28	-10	-9	-7	25	34		
6 V	-46	-4	30	-33	-9	18	-4	53		
7 V	-47	31	7	-39	-6	-22	46	30		
8 V	-57	24	48	-39	-18	-3	27	18		
9 V	-43	33	32	-34	-10	-11	21	12		
10V	-52	13	31	-33	-13	2				
11L	-27	26	-14	-24			30	-29	20	-14
12L	-117	-30	-75	-19			98	20	9	-4
13L	-83	-17	15	-45	13	70	41	-3	15	-5
14B	-93	-71	-1	-239	-90	101	184	209*		
15B	-189	-178	-120	-218	36	-157	274	552*		
16L	1	-28	-70	52	22	59	38	-35	9	-48
17L	-51	43	-72	7	18	61	49	-47	55	-65
18L	-60	27	-71	55	2	22	74	-53	56	-51
19B	-93	57	-155	89			67	-52	182	-95
20L	-68	68	-55	70			62	-58	60	-80
21L	-50	67	-40	76			55	-69	36	-75
22B	-134	106	-153	81			96	-74	191	-112
23B	-129	122	-94	118			101	-111	121	-130
*Results of original analysis, assuming no actual buoy motion. Buoys at sites 14 and 15 were serviced and removed between visits 3 and 4. Recomputing the "site mean" from only visits 1, 2, and 3, we obtain:										
14B	-32	-1	-60	-169	-29	170	246	279		
15B	-97	6	-29	-34	127	27	365	736		

TABLE 4
Discrepancies between "visit mean" and "site mean" differential TD readings using monitor s/n 1017 (in nanoseconds).

Site	Visit1		Visit2		Visit3		Visit4		Visit5	
	TDX	TDY								
1 V	13	-11	5	-19	-21	21	-9	18		
2 V	22	-10	11	-16	-20	14	-12	12		
3 V	6	2	18	-10	-10	-4	-13	12		
4 V	-3	-19	27	7	-1	-10	-23	23		
5 V	-9	-13	22	-15	-5	-5	-8	33		
6 V	-25	3	32	-19	-17	2	-21	33		
7 V	-16	33	33	-29	-14	-28	-3	23		
8 V	-10	24	29	-22	-13	-17	-6	14		
9 V	-11	21	24	-21	-15	-17	2	17		
10V	-8	10	23	-12	-15	2				
11L	22	22	8	-1			-18	-12	-12	-10
12L	-29	-10	-28	-4			57	17	0	-3
13L	-9	4	27	-39	1	51	3	7	-22	-23
14B	-44	-69	8	-235	-109	90	145	213*		
15B	-124	-179	-104	-224	-4	-158	231	561*		
16L	30	-4	-10	44	0	48	-12	-47	-8	-41
17L	0	32	-18	15	-7	40	7	-36	19	-51
18L	-6	32	-23	57	-5	26	7	-58	26	-56
19B	-46	53	-105	76			2	-60	149	-69
20L	-9	67	7	56			-7	-59	9	-64
21L	10	72	15	62			-13	-66	-11	-67
22B	-81	94	-97	78			35	-60	143	-112
23B	-76	121	-38	114			40	-109	74	-126
*Results of original analysis, assuming no actual buoy motion. Buoys at sites 14 and 15 were serviced and removed between visits 3 and 4. Recomputing the "site mean" from only visits 1, 2, and 3, we obtain:										
14B	4	2	56	-164	-60	162	193	285		
15B	-46	8	-26	-37	73	29	308	749		

TABLE 5
Discrepancies between "visit mean" and "site mean" differential readings, using monitor s/n 2220 (in nanoseconds).

Site	Visit1		Visit2		Visit3		Visit4		Visit5	
	TDX	TDY								
1 V	1	5	10	7	7	27	-17	-44		
2 V	8	12	9	0	7	29	-24	-41		
3 V	21	47	7	15	6	-7	-34	-54		
4 V	22	30	15	29	11	-9	-48	-51		
5 V	12	27	12	5	11	3	-35	-35		
6 V	5	34	20	-3	-2	4	-44	-32		
7 V	8	62	18	5	5	-25	-31	-43		
8 V	7	54	19	8	6	-8	-33	-54		
9 V	12	58	12	5	1	-19	-25	-44		
10V	8	23	4	-7	-12	-17				
11L	27	25	17	-2			-31	-12	-13	-11
12L	-23	-11	-16	-4			44	19	-5	-4
13L	5	2	20	-32	-2	36	-8	13	-14	-20
14B	-32	-71	3	-231	-110	83	138	219*		
15B	-117	-175	-110	-221	-1	-168	228	564*		
16L	22	5	9	27	-4	38	-19	-37	-8	-33
17L	16	26	-6	13	-13	27	-3	-26	6	-41
18L	9	29	-6	52	-14	13	-4	-50	14	-44
19B	-34	45	-92	69			-11	-54	137	-60
20L	3	60	22	54			-23	-56	-3	-57
21L	19	64	29	53			-26	-58	-22	-59
22B	-63	88	-88	69			19	-52	131	-105
23B	-61	110	-28	106			27	-100	63	-116

*Results of original analysis, assuming no actual buoy motion. Buoys at sites 14 and 15 were serviced and removed between visits 3 and 4. Recomputing the "site mean" from only visits 1, 2, and 3, we obtain:

14B	15	2	49	-158	-63	156	185	292
15B	-41	13	-34	-33	76	19	305	751

represent the short term (during the time span of each visit) inconsistencies in the data. A linear regression was performed to test the degree to which these short term inconsistencies can be used to predict the long term inconsistencies of interest to us. The results were negative, that is short term (minutes or hours) noise does not predict long term (weeks or months) noise.

To evaluate the stability in position corresponding to the TD discrepancies of Tables 3, 4, and 5, a simple procedure was developed: For each site, coefficients were computed of the linear relationship between shifts in TD patterns and shifts in coordinates (see Appendix). The TD discrepancies of Tables 3, 4, and 5 were converted to coordinate discrepancies using this linear model. Radial position discrepancies were computed from the coordinate discrepancies and are shown in Tables 6, 7 and 8. These apparent position shifts were divided into three sets: van sites, helicopter landing sites, and helicopter hovering sites. Each set was ranked in magnitude and deciles of the resulting cumulative distributions plotted in Figures 9, 10, and 11. The two-hour "visit means" of the van data met the 15 metre specification, even without the differential technique. However, for the five-minute "visit means" of the helicopter landing site data, the raw data did not meet the specification, but the differential data did.

TABLE 6
Apparent position shifts from raw (undifferenced) data (in metres).

Site	Visit 1	Visit 2	Visit 3	Visit 4	Visit 5
1 V	5.9	3.8	9.6	3.4	
2 V	4.6	4.3	7.5	2.1	
3 V	7.1	6.2	4.0	2.2	
4 V	14.1	6.8	3.4	12.8	
5 V	10.7	6.4	2.6	8.8	
6 V	10.5	9.5	3.7	9.9	
7 V	11.5	7.6	4.6	12.1	
8 V	13.0	12.5	3.9	7.1	
9 V	10.7	9.3	3.2	5.2	
10V	10.9	9.1	2.6		
11L	7.7	5.7		7.3	8.7
12L	30.4	19.7		22.9	25.3
13L	21.8	8.6	13.0	10.4	3.8
14B	27.2	42.4	26.9	61.6*	
15B	58.8	51.1	28.2	124.6*	
16L	5.1	18.3	12.4	10.5	8.6
17L	13.4	16.4	12.4	13.5	16.5
18L	13.9	18.3	4.2	18.5	15.2
19B	22.6	37.3		17.2	42.9
20L	19.1	17.5		16.9	19.8
21L	16.6	17.1		17.4	16.5
22B	34.3	34.8		24.3	44.6
23B	35.8	30.6		30.3	35.9

*Results of original analysis, assuming no actual buoy motion. Buoys at sites 14 and 15 were serviced and removed between visits 3 and 4. Recomputing the "site mean" from only visits 1, 2, and 3, we obtain:

14B	7.9	34.8	30.1	82.1
15B	23.7	9.8	32.0	166.1

TABLE 7
Apparent position shifts from differential data, using monitor s/n 1017 (in metres).

Site	Visit 1	Visit 2	Visit 3	Visit 4	Visit 5
1 V	5.3	3.4	6.3	3.9	
2 V	5.4	3.7	5.3	3.4	
3 V	1.5	4.4	2.6	3.6	
4 V	3.6	6.6	1.9	6.4	
5 V	3.4	5.5	1.6	6.2	
6 V	5.7	7.5	3.9	7.4	
7 V	7.0	8.7	6.4	4.5	
8 V	5.1	7.3	4.4	3.0	
9 V	4.7	6.3	4.8	3.5	
10V	2.6	5.3	3.1		
11L	7.1	2.1		5.2	3.7
12L	7.8	7.1		14.9	0.5
13L	2.4	9.4	9.1	1.5	7.3
14B	17.2	41.4	29.5	54.7*	
15B	46.3	49.5	28.1	119.9*	
16L	7.2	8.0	8.7	9.2	7.9
17L	5.9	4.8	7.4	6.7	9.9
18L	6.1	11.7	5.0	11.1	11.9
19B	13.9	26.5		11.6	34.5
20L	13.2	11.2		11.9	12.5
21L	14.9	13.2		14.0	14.1
22B	24.7	25.0		13.8	36.5
23B	29.1	24.8		23.9	29.9

*Results of original analysis, assuming no actual buoy motion. Buoys at sites 14 and 15 were serviced and removed between visits 3 and 4. Recomputing the "site mean" from only visits 1, 2, and 3, we obtain:

14B	1.1	30.7	30.7	72.9
15B	11.2	9.6	19.2	159.8

These results indicate the stability of differential LORAN-C is adequate to meet the 15 metre specification. The helicopter hovering results shown in Figures 11 and 12 obviously do not meet this specification.

TABLE 8
Apparent position shifts from differential data, using monitor s/n 2220 (in metres).

Site	Visit 1	Visit 2	Visit 3	Visit 4	Visit 5
1 V	1.7	2.9	5.2	9.2	
2 V	2.9	2.3	5.5	9.7	
3 V	10.2	3.2	1.7	13.3	
4 V	7.9	6.7	2.9	15.2	
5 V	5.9	3.1	2.6	10.8	
6 V	6.5	4.6	0.9	12.0	
7 V	12.2	4.1	4.8	11.0	
8 V	10.8	4.6	2.0	13.1	
9 V	12.2	2.8	3.9	10.6	
10V	5.3	1.6	4.4		
11L	8.5	4.3		8.4	4.0
12L	6.3	4.1		12.0	1.6
13L	1.3	7.2	6.3	2.9	5.3
14B	15.5	40.8	29.1	54.4*	
15B	44.6	50.0	29.8	119.9*	
16L	5.5	5.5	6.9	8.6	6.4
17L	6.4	2.7	5.6	4.8	7.6
18L	6.2	10.0	3.7	9.7	8.8
19B	11.2	23.5		10.9	31.5
20L	11.8	11.9		12.4	11.3
21L	13.9	12.8		13.4	13.1
22B	21.6	22.4		11.3	33.6
23B	25.6	22.7		21.4	26.9

*Results of original analysis, assuming no actual buoy motion. Buoys at sites 14 and 15 were serviced and removed between visits 3 and 4. Recomputing the "site mean" from only visits 1, 2, and 3, we obtain:

14B	3.7	29.2	30.1	72.5
15B	10.0	10.7	19.3	159.7

HELICOPTER HOVERING TESTS (18 DATA POINTS)
(WITH REMOVED BUOYS OMITTED)

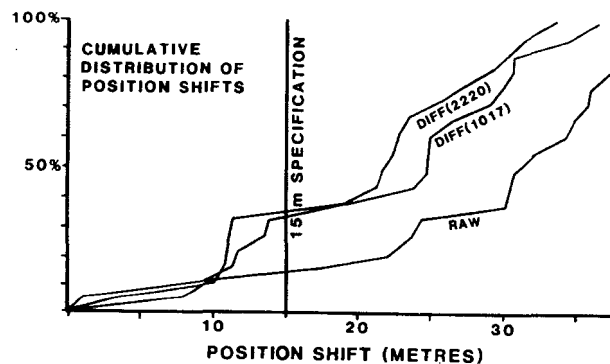


FIGURE 12.

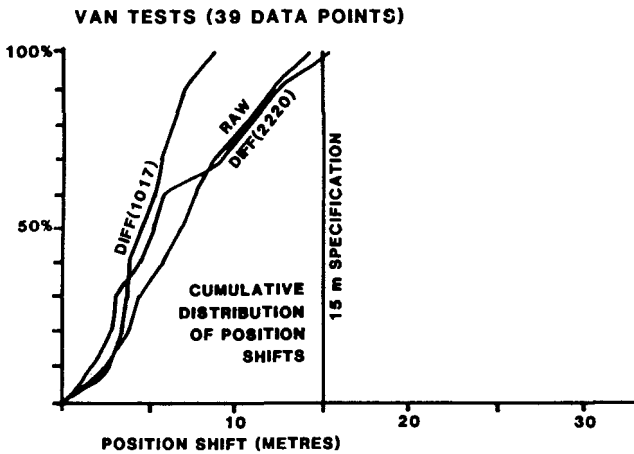


FIGURE 9.

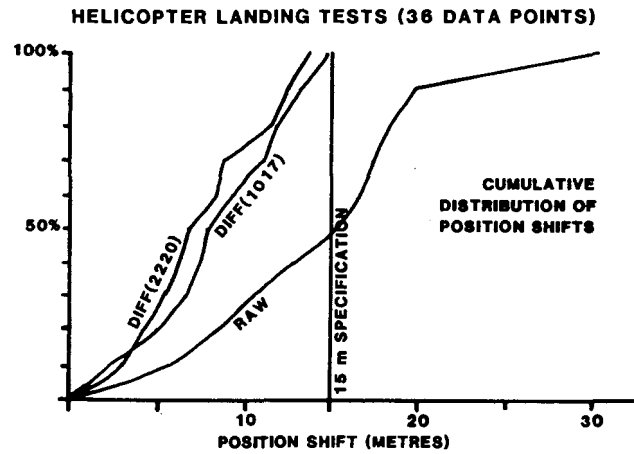


FIGURE 10.

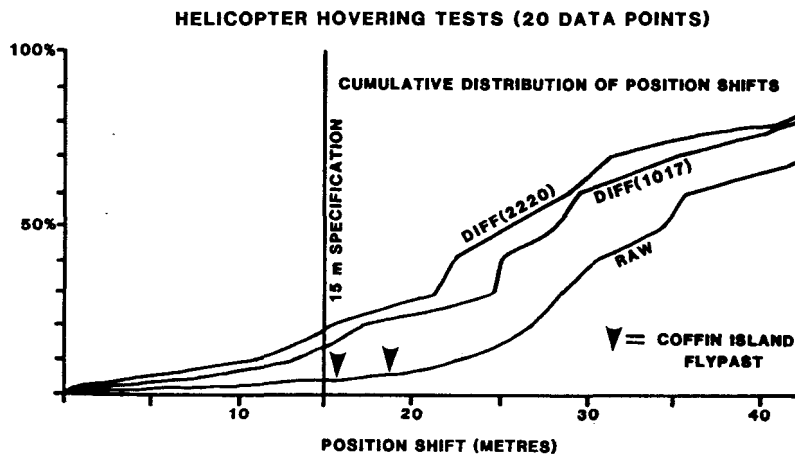


FIGURE 11.

There are three probable reasons for this. (1) Two of the buoys were intentionally moved (for servicing) during the experiment. Figure 11 does not take this fact into account, but Figure 12 does. From Tables 7 and 8 it would appear that buoy 14 was removed approximately 73 m, and buoy 15 approximately 160 m from their initial positions. (2) The maximum watch circle radius for each buoy in Table 9 is generally twice the maximum apparent position shift for that buoy during the experiment. This indicates that actual buoy motion, rather than deficiencies in the differential LORAN-C technique, may be the cause of the unsatisfactory results in Figure 12. (3) The hovering stability of the helicopter over the buoys is questionable, due to inability of the pilot to see a buoy directly below the helicopter. An alternative to hovering was tested during two visits to Coffin Island (one of the landing sites): the helicopter flew over the remote site marker, flying along two or more straight lines. Analysing this flypast data to estimate the common intersection point appears to be superior to hovering as a method of positioning the marker. From these two flypast visits, one set of differential TD shifts can be formed, in the sense (visit 2 - visit 1), for each of the two monitor receivers. These lead to corresponding position shifts of 19 metres (using monitor serial number 1017) and 16 metres (using monitor serial number 2220).

TABLE 9
Watch circle radius
for helicopter hovering buoys.

Site	Name	Water Depth (m)	Mooring Length (m)	Maximum Watch Circle radius (m) **	Maximum Apparent Position shift (m)
14	Peggy Pt	35	91	84	31
		24	91	88	73*
15	Horseshoe Ledge	38	82	73	19
		33	82	75	160*
19	White Pt Rock	31	82	76	35
		26	55	48	37
23	Budget Rock	18	55	52	30

*After buoys serviced and removed on 2 October 1982. These apparent shifts are probably actual shifts.

**Calculated assuming mooring chain is tight with no sag. Actual radius will be less.

These are also shown on Figure 11. Refinement of the flypast technique (more lines, provision for radar range and bearing measurements from the helicopter to the buoy to be recorded along with LORAN-C readings, optimization of sampling interval, etc.) are likely to improve this performance.

RESULTS

The results of this initial experiment are encouraging. Of the total of 150 van

and helicopter landing differential comparisons in this experiment, all but one indicated repeatability to better than the 15 metre criterion, and the exception was 15.2 metres. Only 35% of the helicopter hovering differential comparisons met the criterion, but this seems likely to be due to actual movement of the buoy within its watch circle, and possibly to helicopter hovering stability, rather than a deficiency in the LORAN-C technique itself.

Several specific questions were involved in this experiment. We will deal with them in turn.

Is the LORAN-C signal stable enough (differentially) to meet the 15 metre repeatability criterion? These results, over 75 days, indicate the answer is yes. However, this may not be true over longer periods, particularly when seasonal effects (freezing ground, etc.) occur. One puzzling instability event which occurred during the experiment is shown in Figure 13. TDY dipped about 0.05 microseconds (10 metres) at the monitor, then about 20 minutes later dipped about 0.15 microseconds (30 metres) at the remote site (150 km away). There is nothing unusual in the weather patterns for that period that might account for this event. A possible explanation may be the effect of in-band synchronous noise on the LORAN signal, which has been known to cause such instability events [3].

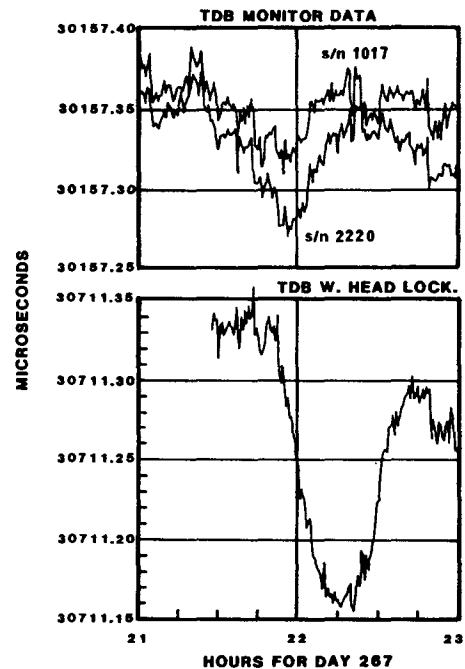


FIGURE 13. ANOMALOUS EVENT

Are LORAN-C receivers stable enough to effectively use the apparent stability of the differential LORAN-C signal? Notch filter adjustment appears to adversely affect repeatability. During the experiment the receivers were notched prior to the fourth van visits, which were the worst (in terms of repeatability) for monitor serial number 2220. This resulted in the poorer

performance of this monitor for the differential results shown in Figure 9. Two methods of overcoming this problem are being considered. It may be possible to design a stable narrow band prefilter, designed to pass the LORAN-C pulse, which would reduce or eliminate the need for notching. An alternative is to use a double differential technique. A set of fixed points (say, lighthouses) would be visited by the helicopter during each buoy position checking run. The variations in the differential TDs at these fixed points from run to run would be used to calibrate the differential TDs at the buoys.

Can the helicopter be positioned relative to the buoy sufficiently accurately on each visit to meet the 15 metre criterion? Hovering (at least as performed during this experiment, with no special vertical sighting modifications to the helicopter) may not be good enough. Further hovering tests over stationary sites should be conducted. The flypast technique shows promise, but requires further development.

Does the differential technique improve LORAN-C repeatability? For short period sampling (five minutes or less) as would be practical for buoy position checking, the answer is yes, as shown by Figure 10. Careful synchronization of the monitor and remote data record timing, and use of identical data intervals may further enhance this improvement. The differential TD data does not appear to be distance dependent (at least to 150 kilometres from the monitor) for the van sites, or for the helicopter landing TDX data. However, the helicopter landing TDY data repeatability degraded with distance (see Tables 4 and 5). This may be due to some kind of coastal "edge" effect, since the Cape Race signal "grazes" the Nova Scotia coastline.

In conclusion, differential LORAN-C appears to be capable of checking for buoy movements at the 15 metre level. However, further testing for possible seasonal effects, work on the receiver notching problem, and a helicopter flypast technique are required before it can be put into routine practice.

ACKNOWLEDGEMENTS

Support for work on this project at the University of New Brunswick was provided in part by a contract with the Telecommunications and Electronics Branch of the Canadian Coast Guard, and in part by a strategic research grant from the Natural Sciences and Engineering Research Council of Canada, entitled "Marine Geodesy".

REFERENCES

- [1] Canadian Coast Guard (1982). Test plan-differential LORAN-C for buoy position checking.
- [2] Wells, D.E., B.G. Nickerson and D. Davidson (1983). Differential LORAN-C for buoy position checking. Department of Surveying Engineering Technical Report 99, University of New Brunswick, Fredericton, Canada, 189 pages.

- [3] Burke, R. (1983). Personal communication. CDR, U.S. Coast Guard.

APPENDIX

A simple linear transformation from TD shifts to position shifts was developed [2] in the form

$$\begin{bmatrix} \Delta N \\ \Delta E \end{bmatrix} = \underline{M} \begin{bmatrix} \Delta TDX \\ \Delta TDY \end{bmatrix}$$

where ΔTDX , ΔTDY are TD shifts in microseconds, and ΔN , ΔE are the resulting shifts in northing and easting in metres. The matrix \underline{M} is given by

$$\underline{M} = \frac{1}{\sin(\alpha_x - \alpha_y)} \begin{bmatrix} H_x \cos \alpha_y & H_y \cos \alpha_x \\ H_x \sin \alpha_y & H_y \sin \alpha_x \end{bmatrix}$$

where H_x , H_y are the conversion factors of TD shifts from microseconds to metres, and α_x, α_y are azimuths of the TD lines of

position. All four of these will vary from point to point within the pattern. They can be determined by scaling from a large scale latticed chart, or by using the relationships

$$H_x = 150 \operatorname{cosec} \left(\frac{a_{\text{mpx}}}{2} \right)$$

$$H_y = 150 \operatorname{cosec} \left(\frac{a_{\text{mpy}}}{2} \right)$$

$$\alpha_x = \alpha_{\text{mp}} - \left(\frac{a_{\text{mpx}}}{2} \right)$$

$$\alpha_y = \alpha_{\text{mp}} + \left(\frac{a_{\text{mpy}}}{2} \right) - 180^\circ$$

where α_{mp} is the azimuth from LORAN-C master to the point, a_{mpx} is the angle subtended at the point by the master/slave x baseline, and a_{mpy} is the angle subtended at the point by the master/slave y baseline. These three quantities can be measured on a small scale regional chart showing the entire LORAN-C chain coverage area.

Observations of the Performance of the Southeast
U.S. Loran-C Chain

by
Leo F. Fehlner and Thomas W. Jerardi

Introduction

The Southeast U.S. Loran-C Chain began operating on 1 October 1979. The services of this chain are used to establish the positions of vessels at sea off the coast of Cape Canaveral with great geodetic accuracy. See Reference 1. The Loran receiving system being used was developed and supplied to the Navy by The Johns Hopkins University Applied Physics Laboratory. The receiving system is known by the name LONARS and was described at the 7th and 8th Annual Conventions of the WGA in 1978 and 79. See References 2, 3, 4, and 5.

While vessels are at sea, Loran data are recorded at a fixed site known as the Signal Pattern Monitor. The purpose of these recordings is to establish the magnitude of signal deviations from fixed standard values so that these deviations can be removed from the data taken at sea, thus contributing to the means of maximizing ship position accuracy. It is the statistics of these monitor data that will be shown as a measure of chain performance.

Discussion

The statistics shown in the exhibits characterize the time differences used in establishing ship position. These time differences are Malone minus Jupiter (M-J) and Carolina Beach minus Jupiter (C-J). The statistical parameters shown for each period during which data were recorded are the means, standard deviations, and 2-sigma limits on the means for both M-J and C-J. The data used for the statistics are the difference between the observed time differences and the reference values established for the Pattern Monitor antenna, namely -43981.765 for M-J and 18061.522 for C-J. These values are the averages of a very large number of samples taken on five different days during the LONARS calibration described in Reference 1.

LONARS records data every 1.0374 seconds. The time constant of the phase tracking loops of LONARS is such that these data are essentially uncorrelated at a lag of six data points, or approximately 6 seconds. To avoid the effect of tracking-loop correlation on the signal statistics, every sixth recorded data point was read, and 145 of these were used to obtain the statistics over a period of approximately 15 minutes (more nearly 15 minutes, 24 seconds). The values of the 15-minute means and means ± 2 standard deviations were then plotted in terms of nanoseconds versus time in seconds from midnight UTC. The scale for nanoseconds is ± 100 , which is the tolerance for time difference prescribed by the United States Coast Guard in Reference 6 for the Southeast U.S. Loran-C Chain. The exhibits are labeled with the dates of the observations.

The plotted statistical data are shown in Exhibits 1 through 50. The calibration data that were used to establish reference values for M-J and C-J are shown in the first 13 exhibits. Gaps in the data will be noticed in some 12-hour periods. These gaps are not the fault of either the receiver or the transmitters but are the result of operational considerations.

One of the continuing concerns regarding the use of Loran for high accuracy or consistent repeatability is the impact of seasonal and diurnal effects. We have not found a pattern of seasonal changes in either the means or standard deviations. Also, we have not found any diurnal changes in the means; however, noticeable diurnal changes occur in the standard deviations, with the larger values occurring at night. Sunrise is shown by the symbol \blacktriangle , and sunset by \blacktriangledown . The absence of seasonal changes is reinforced by the daily averages shown in Exhibit 51. These averages are arranged in chronological order, and a seasonal pattern is not obvious. The column headings of Exhibit 51 are defined as follows: MEAN is the average of the 15-minute averages, ST.DEV is the standard deviation of the 15-minute averages, CORR is the correlation coefficient between M-J and C-J, and COUNT is the number of 15-minute averages in the day's sample. Means and standard deviations are in nanoseconds.

As with any extrapolation, readers are cautioned not to extrapolate these seasonal observations too far, especially to areas that experience extended periods of time with below-freezing tem-

peratures. Significant effects on the electrical properties of the ground are attributable to the frozen state.

It will be noted in paging through the exhibits that occasionally the standard deviation for one 15-minute period suddenly becomes larger, then returns for the next 15-minute period to a value consistent with the local history. The pattern produced looks something like this:



Exhibit 52 shows that this behavior is due to the presence during the period of one of the large signal anomalies that occur intermittently. See the large deviation about 15 minutes before 64800 seconds. This typical large anomaly is shown in Exhibit 53. Smaller anomalies also occur, one of which is shown in Exhibit 54. It occurred at about 60120 seconds. Possible causes of these anomalies include the transmitter and the receiver. To isolate the cause, two experiments were run that involved simultaneous recording of Loran data observed both at the LONARS Pattern Monitor at Cape Canaveral and at the USCG Monitor at Mayport, FL. Exhibits 55 and 56 show that both receivers recover the signal with the same fidelity and Exhibits 57 and 58 show that both receivers recover the same signal anomaly.* We concluded that the transmitters are responsible for the anomalous behavior of the system.

An attempt was made to determine the nature of the disturbance that causes large signal anomalies of the type shown in Exhibit 53. The first speculation on the cause was an impulse disturbance. Exhibit 59 shows the response of the LONARS tracking loops to an impulse. Although the rise time on the output is close to that of the observed anomaly, it decays much too fast. After some experimentation, it was found that a sudden rise followed by a gradual stair-step decline as in Exhibit 60 produces an output that closely approximates the observed anomalous output. This disturbance was fitted to the actual observations, and the match is shown in Exhibit 61.

Concluding Remarks

The significance of the performance observations shown by the exhibits is left to the observer since assessment of signal quality is strongly determined by one's view or vantage point. However, it can be concluded that the tolerance placed by the U.S. Coast Guard on the chain's time differences is realistic.

* The Mayport data were provided by the USCG as magnetic tape copies of the data transmitted by the Mayport Monitor to Malone. We appreciate the cooperation of the USCG in establishing the source of the signal anomalies.

References

1. "The Calibration of Loran-C at Sea," *Radionavigation Journal, 1980-81*, The Wild Goose Association, Acton, MA.
2. Peters, W. J. "Loran Navigation Receiving System (LONARS)," *Proceedings of the Seventh Annual Technical Symposium, 1978*, The Wild Goose Association, Acton, MA.
3. Boyd, J. E., "LONARS: Thirty Foot Geodetic Positioning from Loran-C," *Proceedings of the Eighth Annual Technical Symposium, 1979*, The Wild Goose Association, Acton, MA.
4. Jerardi, T. W., "LONARS: An Example of Robust Real Time Filtering," *Proceedings of the Eighth Annual Technical Symposium, 1979*, The Wild Goose Association, Acton, MA.
5. Perschy, J. A., "The Design of the LONARS Sensor," *Proceedings of the Eighth Annual Technical Symposium, 1979*, The Wild Goose Association, Acton, MA.
6. *Specification of the Transmitted Loran-C Signal*, Department of Transportation, United States Coast Guard COMDTINST M16562.4, July 1981.

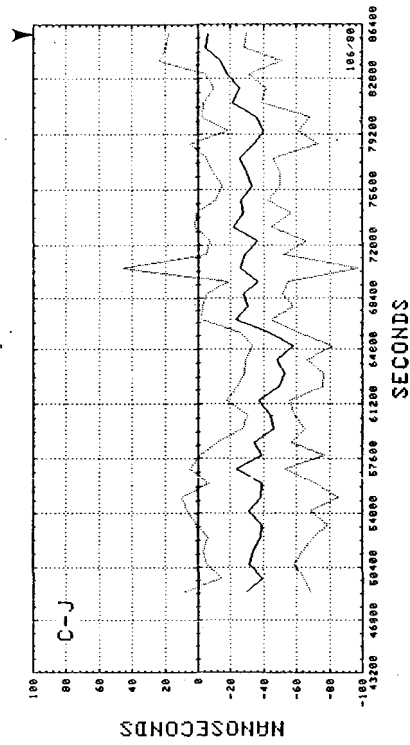
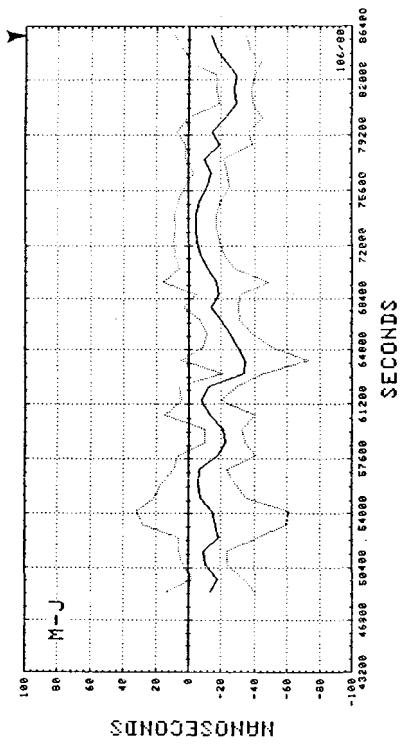


Exhibit 1 16 April 1980.

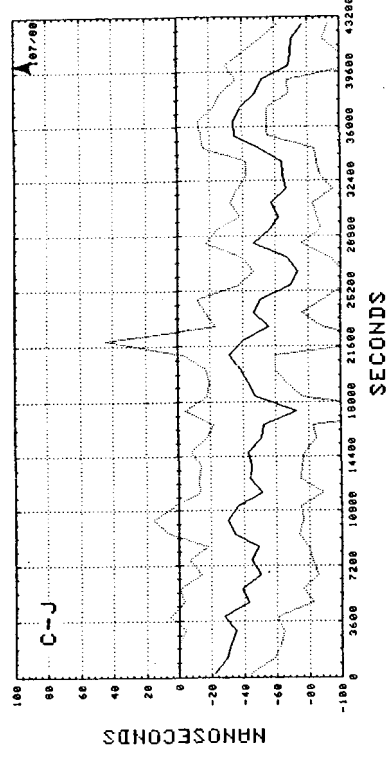
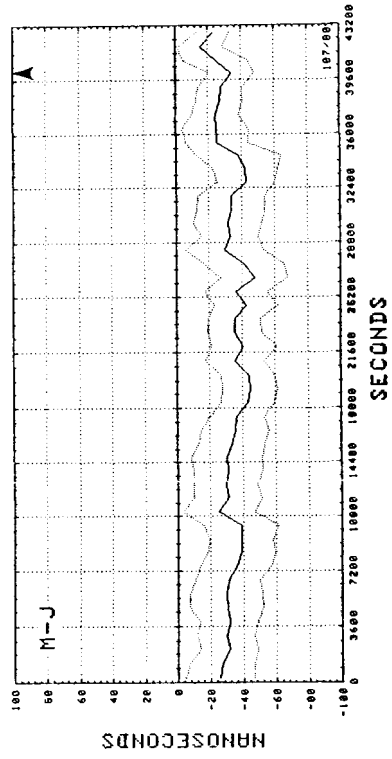


Exhibit 2 16 April 1980.

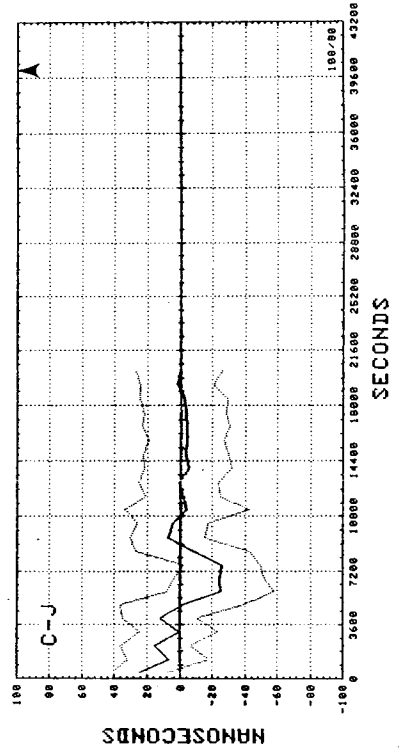
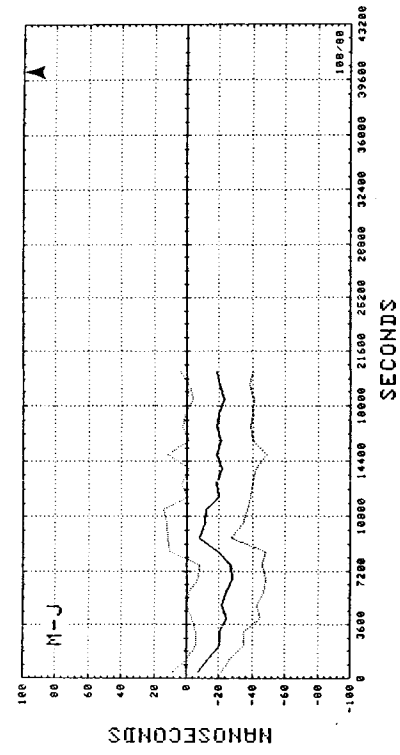


Exhibit 4 17 April 1980.

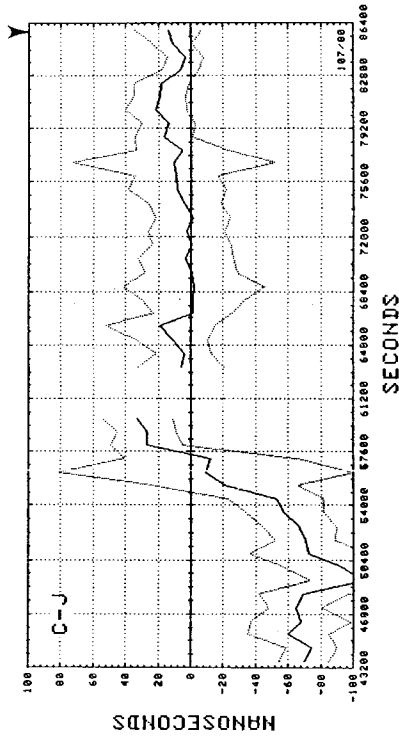
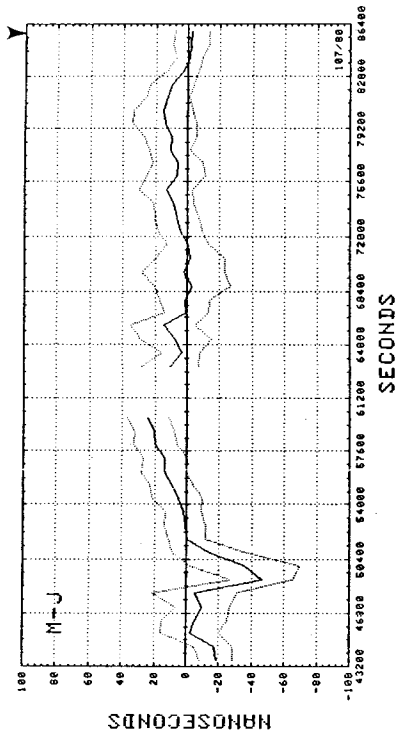


Exhibit 3 16 April 1980.

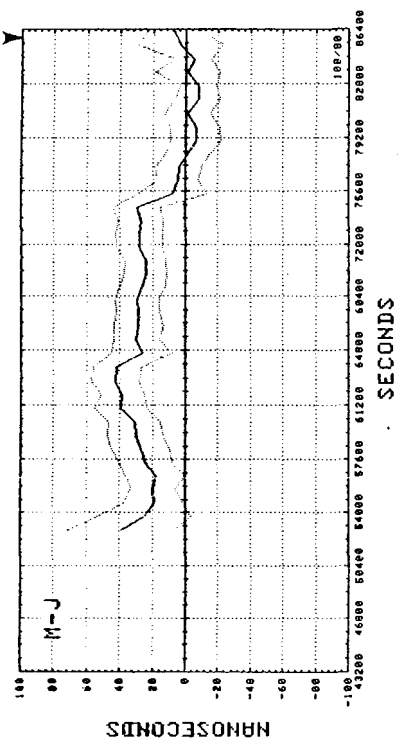


Exhibit 5 17 April 1980.

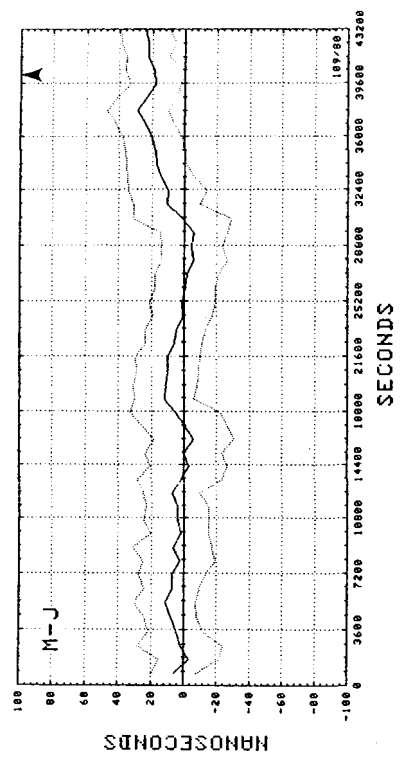
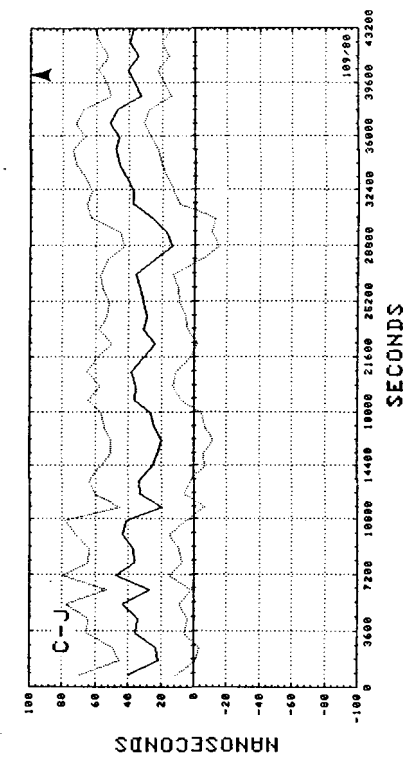
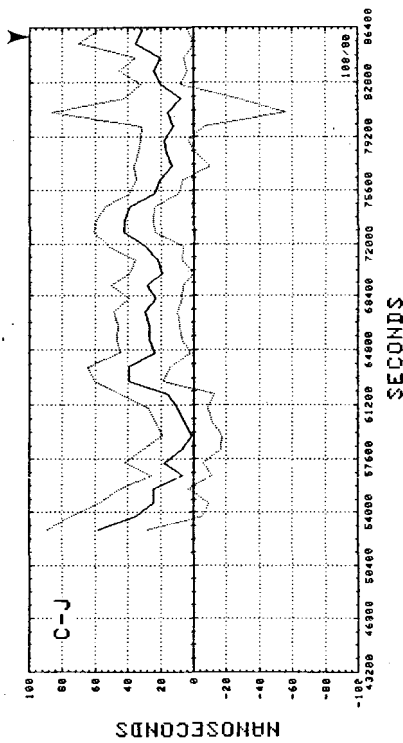


Exhibit 6 18 April 1980.



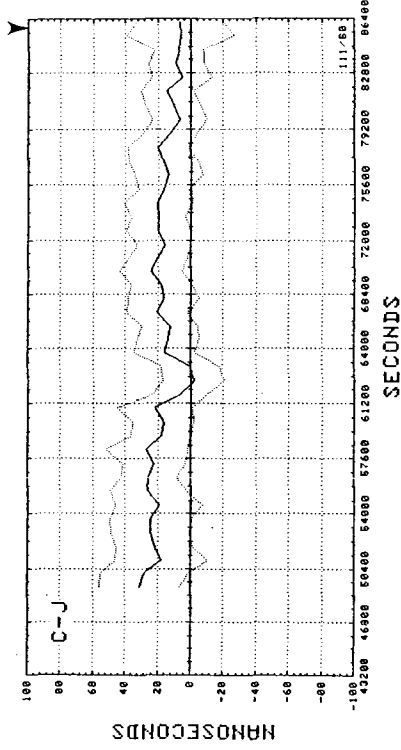
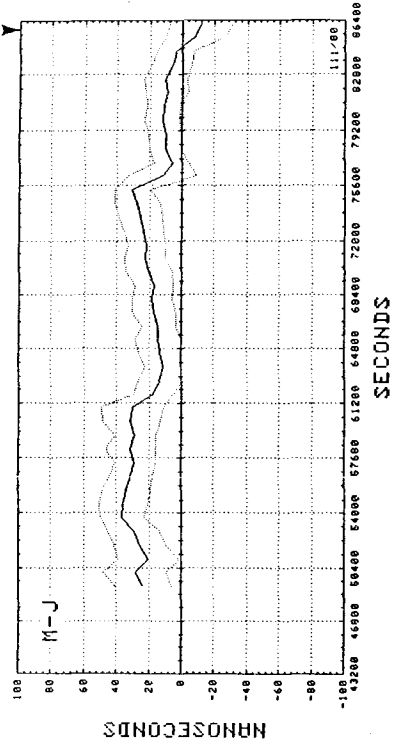


Exhibit 8 20 April 1980.

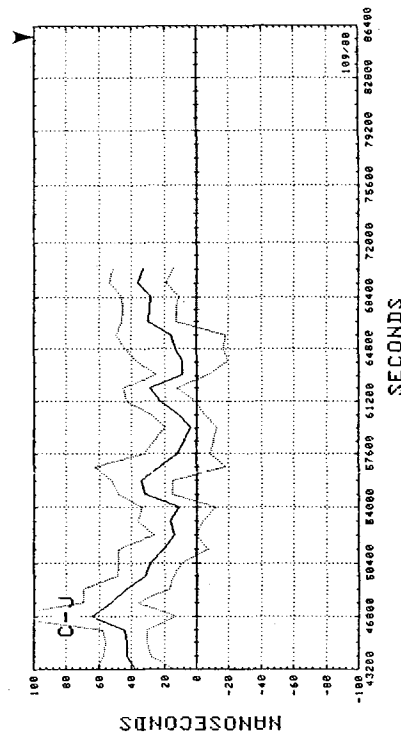
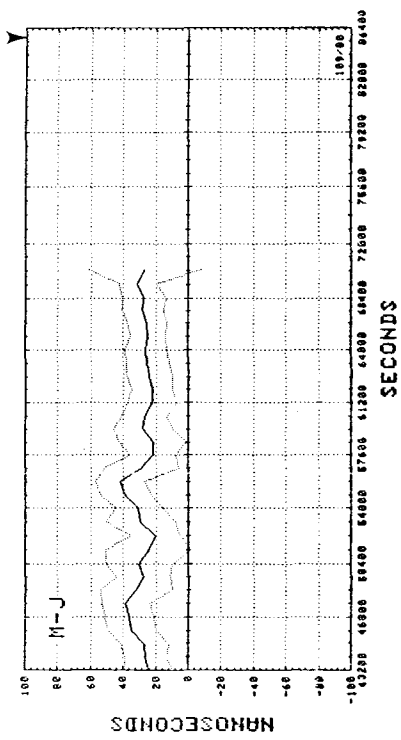


Exhibit 7 18 April 1980.

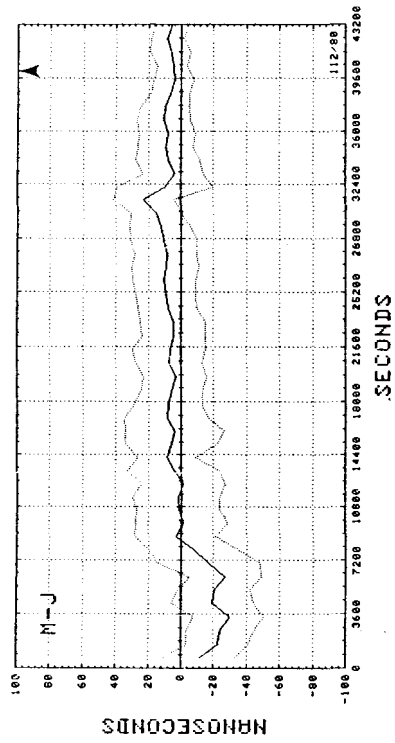


Exhibit 9 21 April 1980.

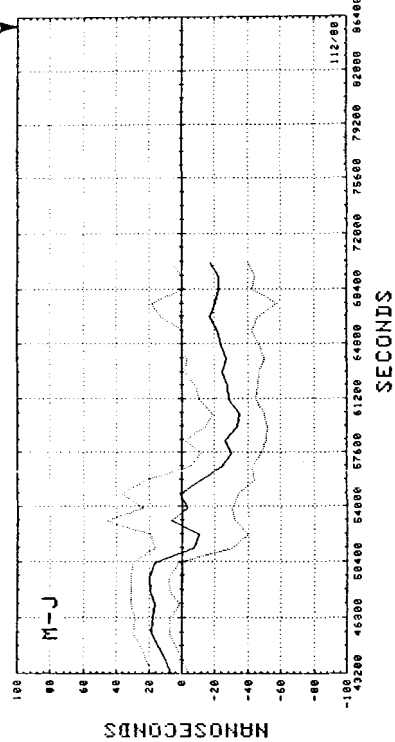


Exhibit 10 21 April 1980.

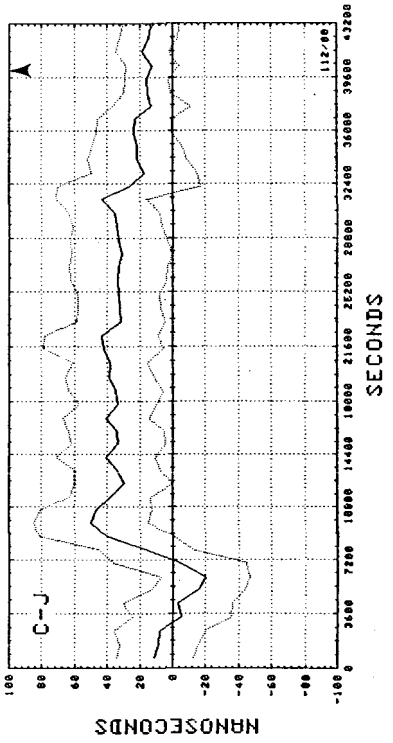


Exhibit 9 21 April 1980.

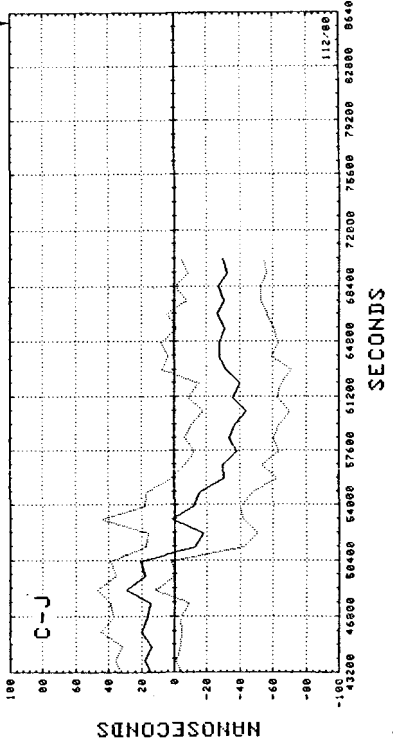


Exhibit 10 21 April 1980.

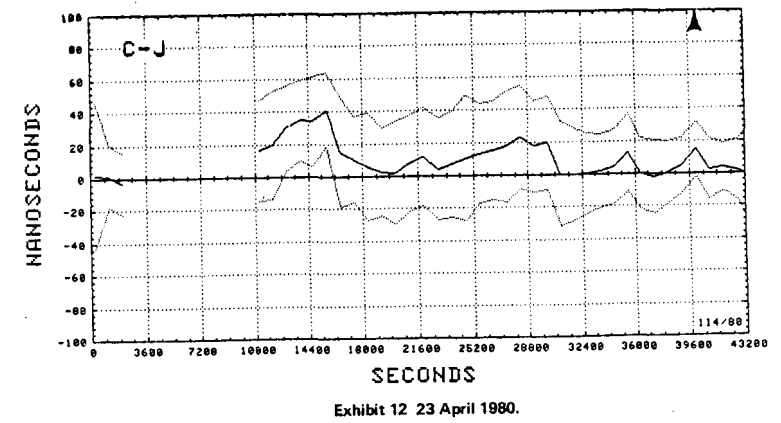
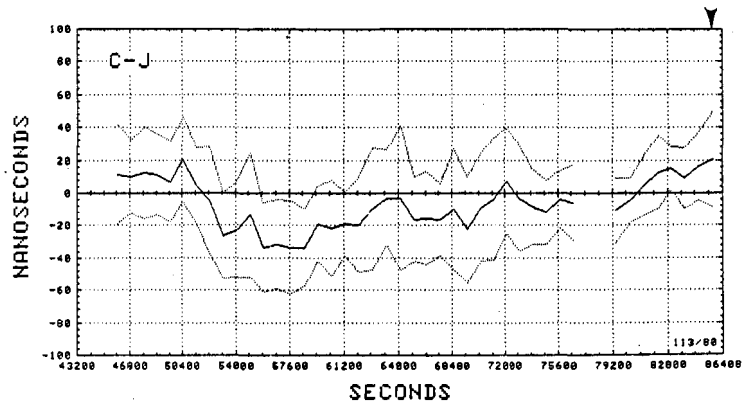
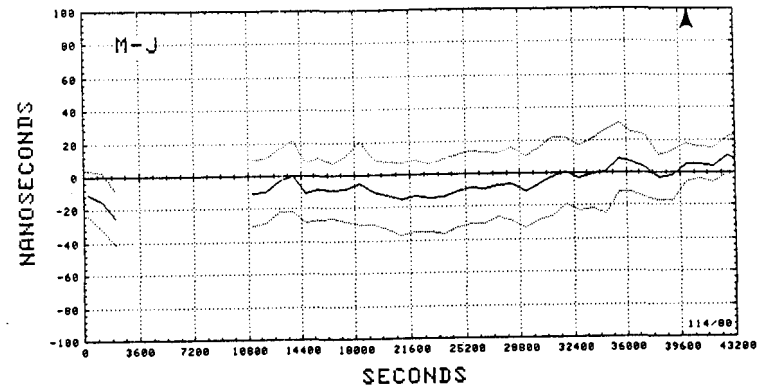
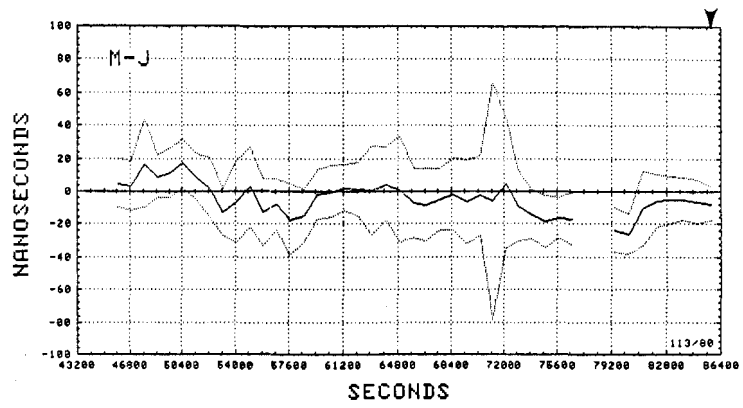


Exhibit 11 22 April 1980.

Exhibit 12 23 April 1980.

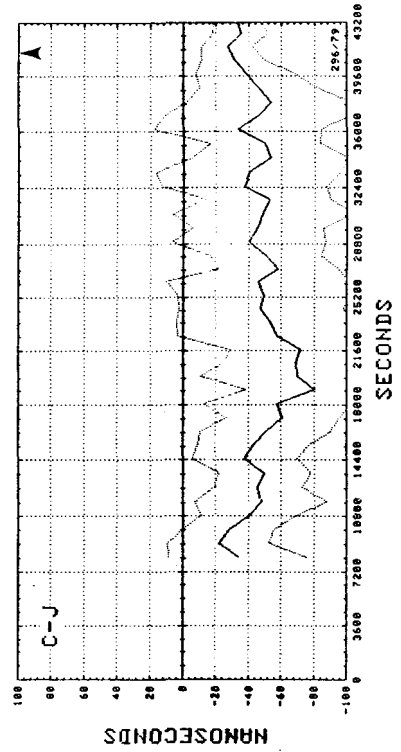
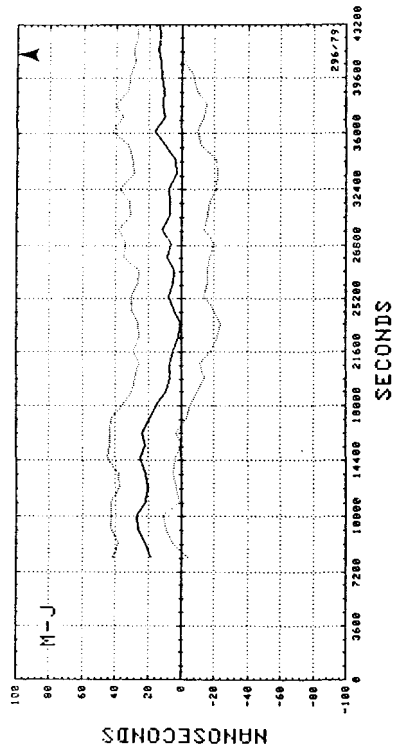


Exhibit 14 6 October 1979.

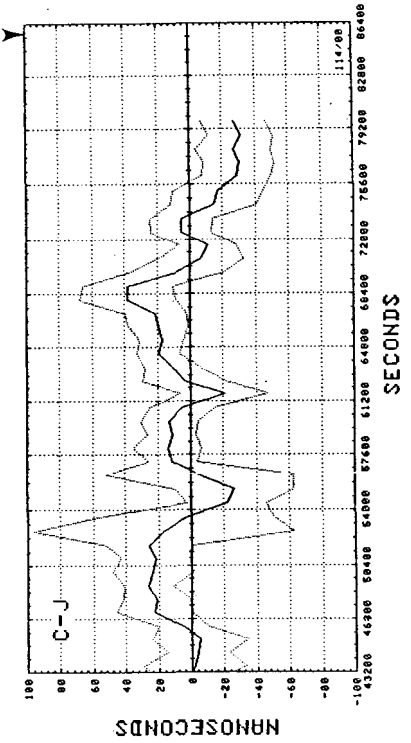
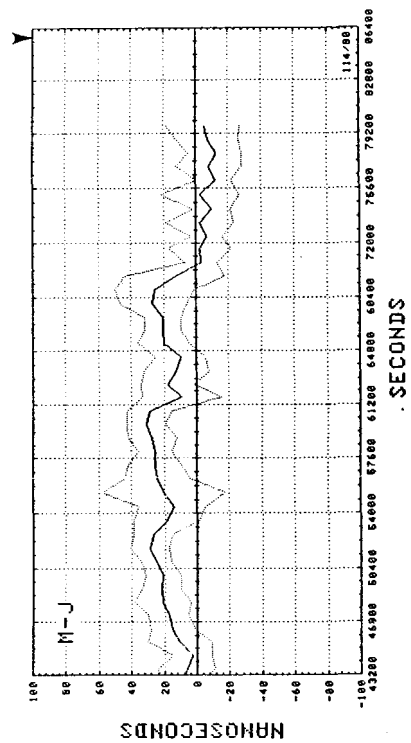
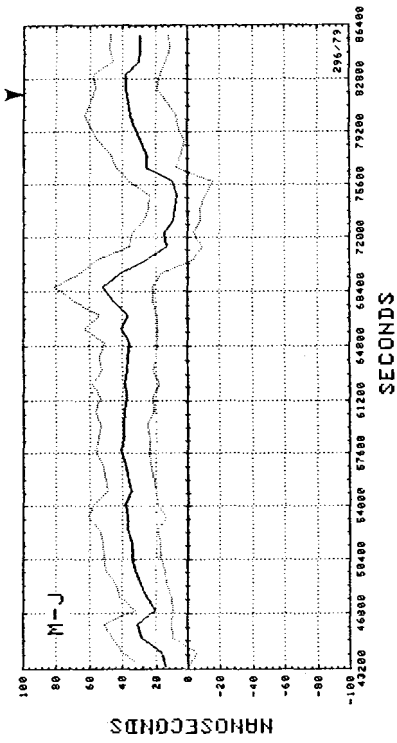
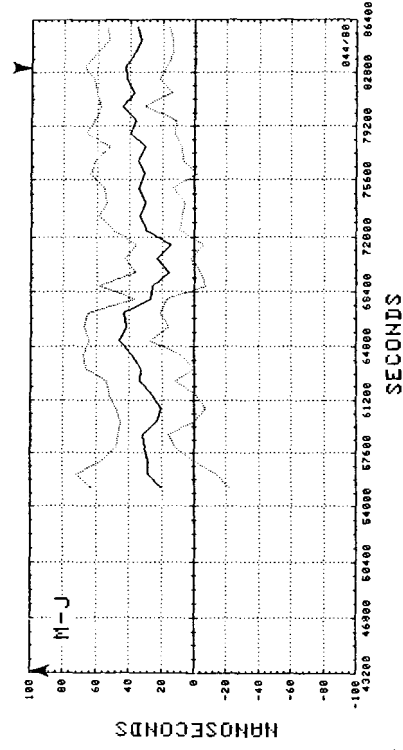


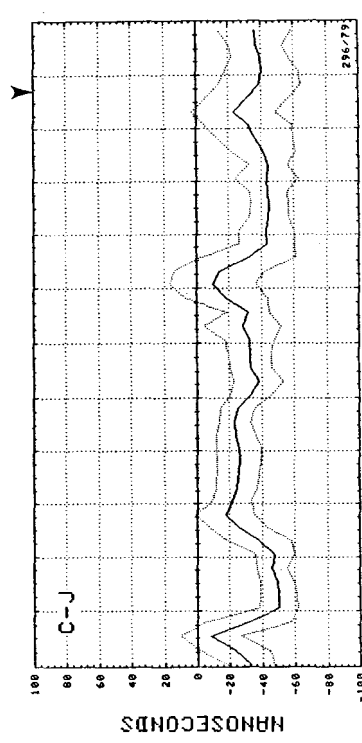
Exhibit 13 23 April 1980.



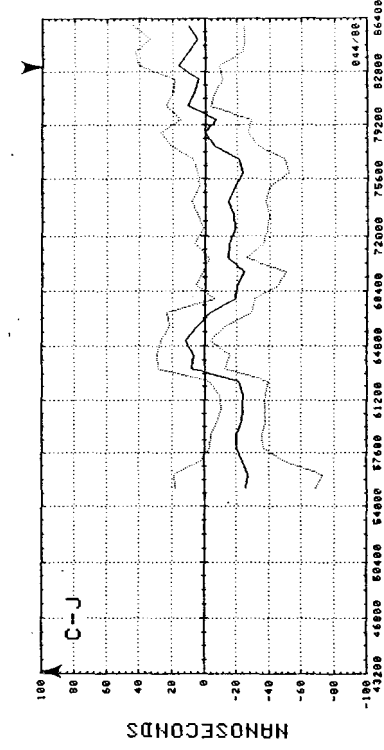
SECONDS



SECONDS



SECONDS



SECONDS

Exhibit 15 6 October 1979.

Exhibit 16 13 February 1980.

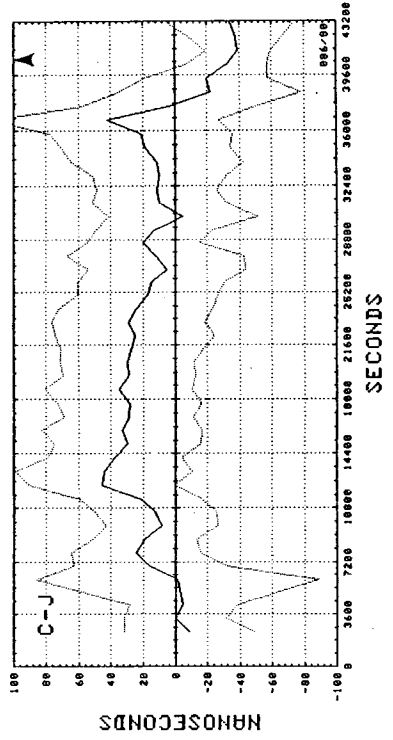
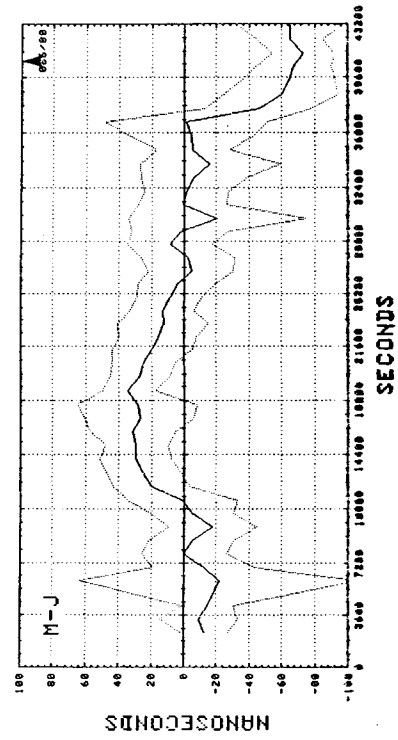


Exhibit 17 26 March 1980.

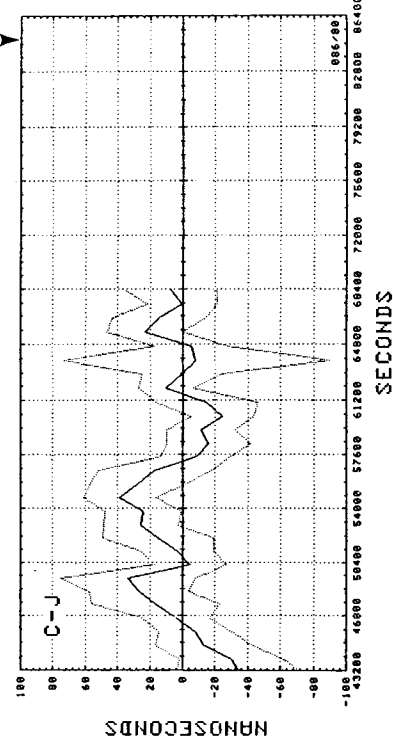
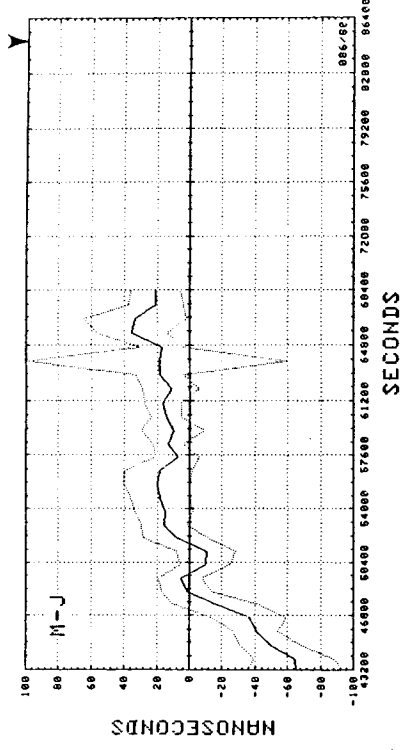


Exhibit 18 26 March 1980.

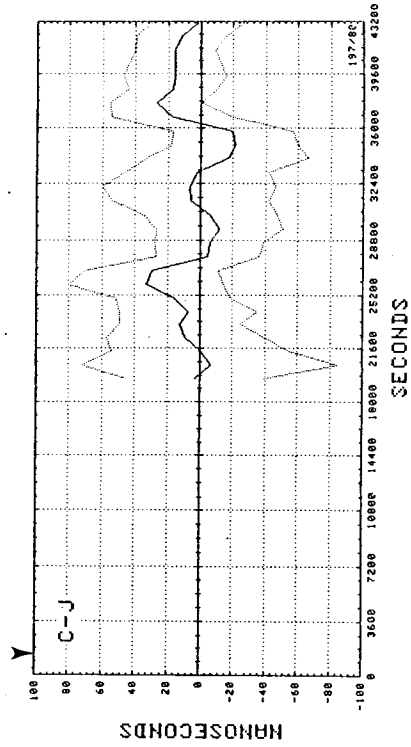
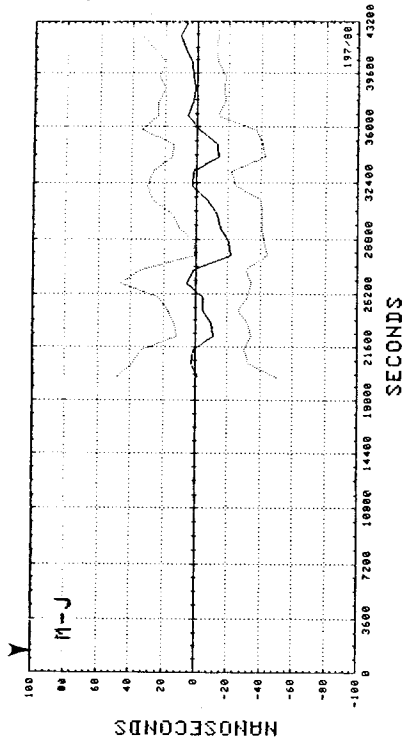


Exhibit 20 15 July 1980.

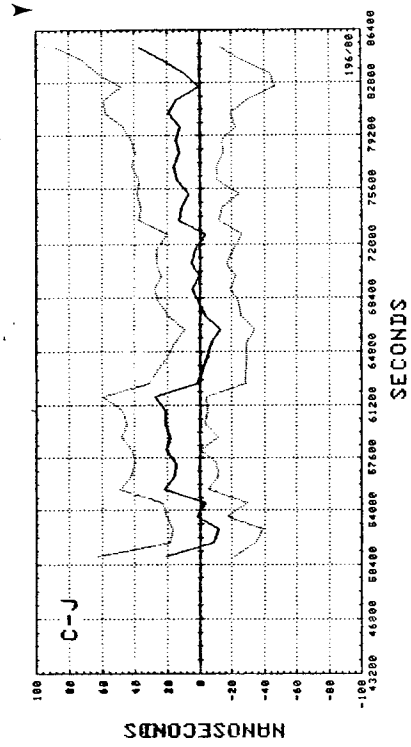
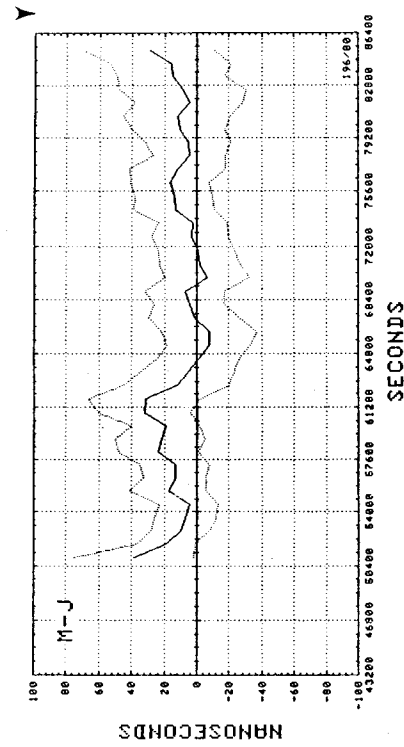


Exhibit 19 14 July 1980.

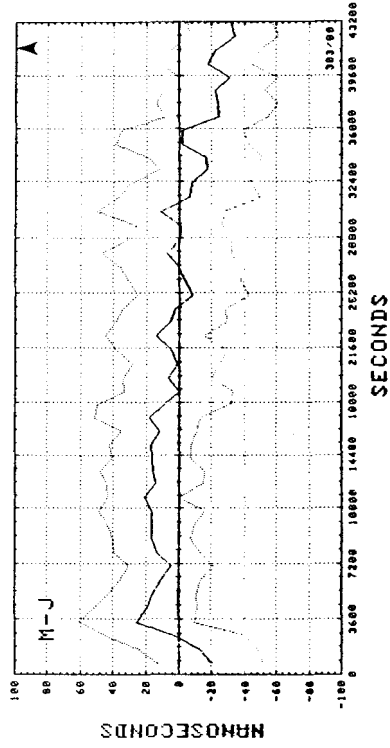


Exhibit 22 29 October 1980.

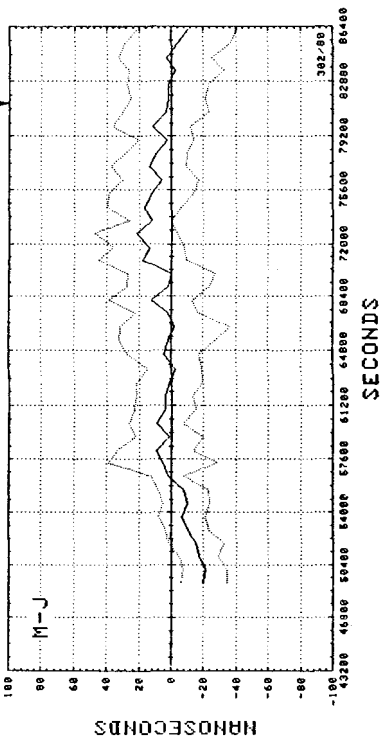
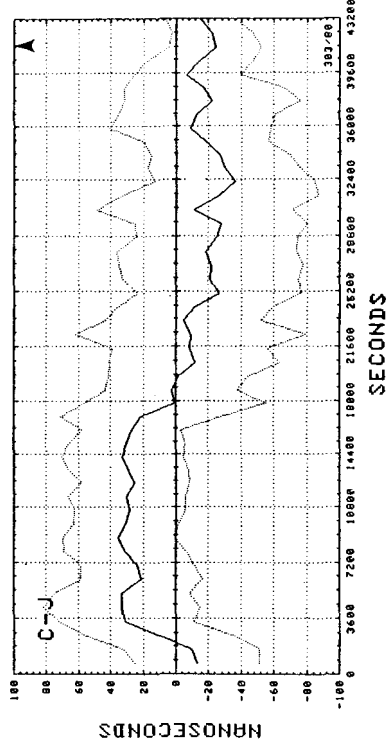
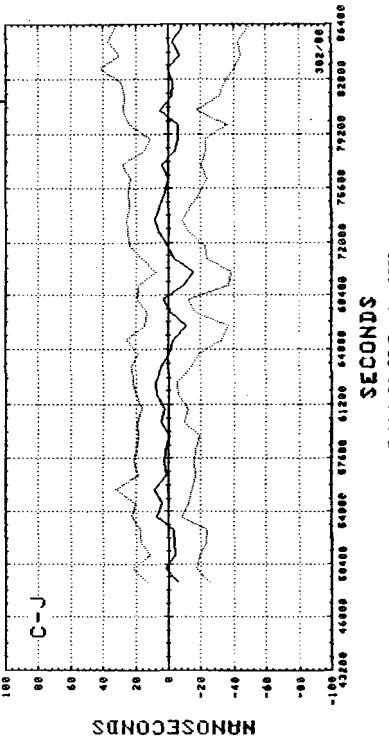


Exhibit 21 28 October 1980.



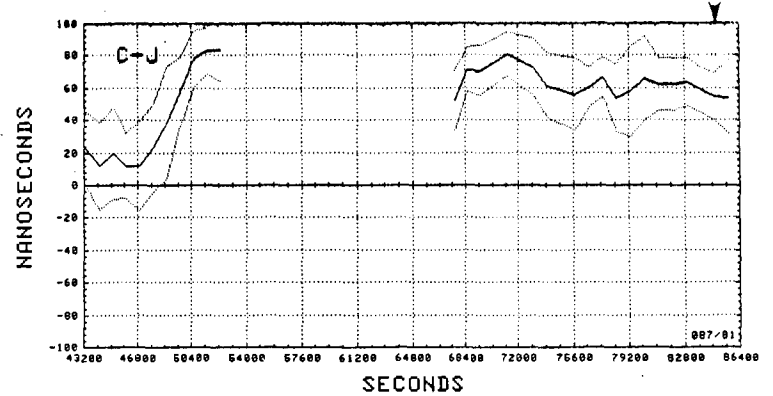
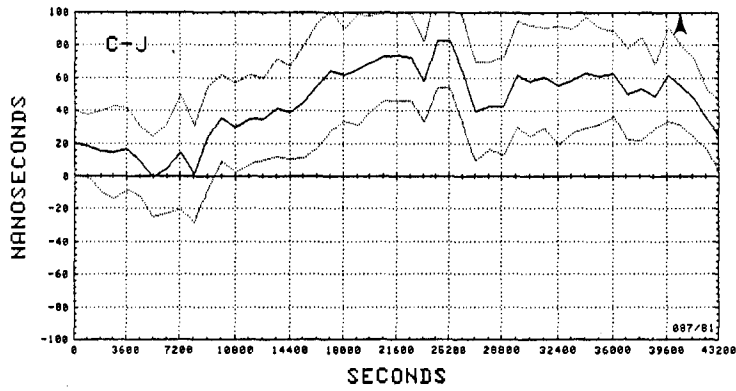
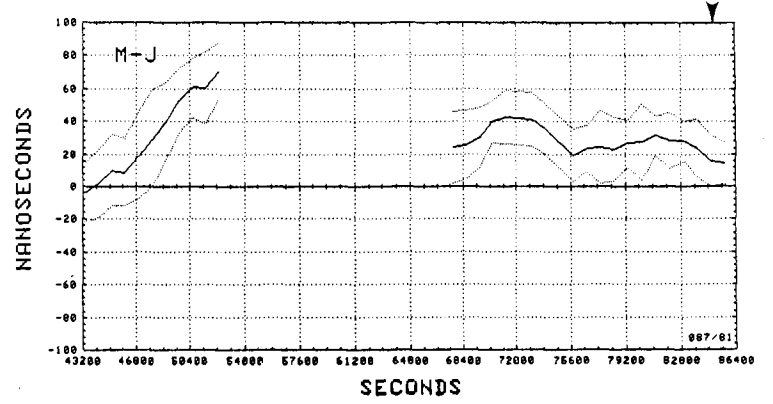
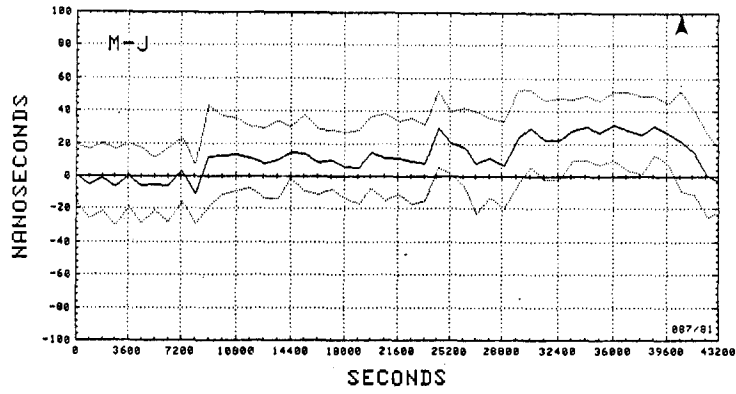


Exhibit 23 22 March 1981.

Exhibit 24 22 March 1981.

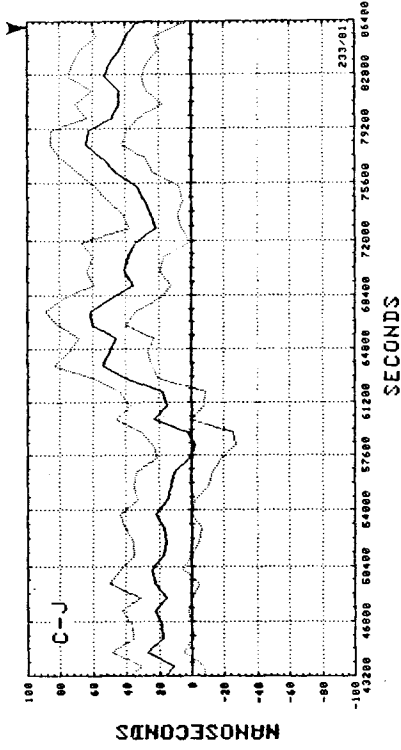
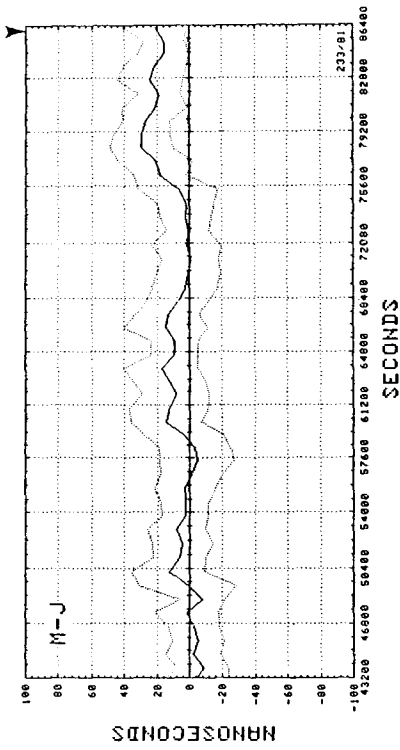


Exhibit 26 21 August 1981.

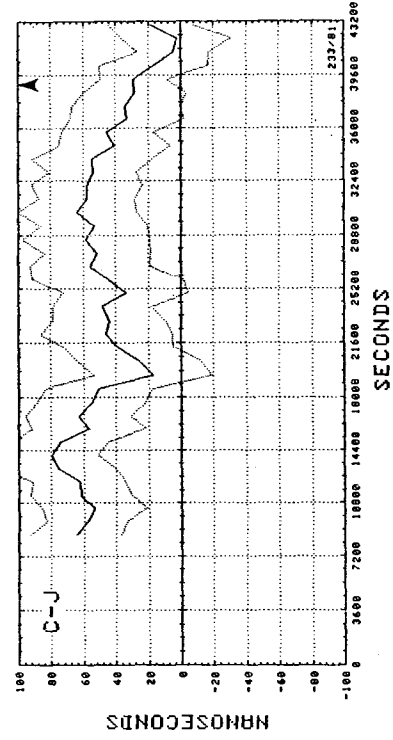
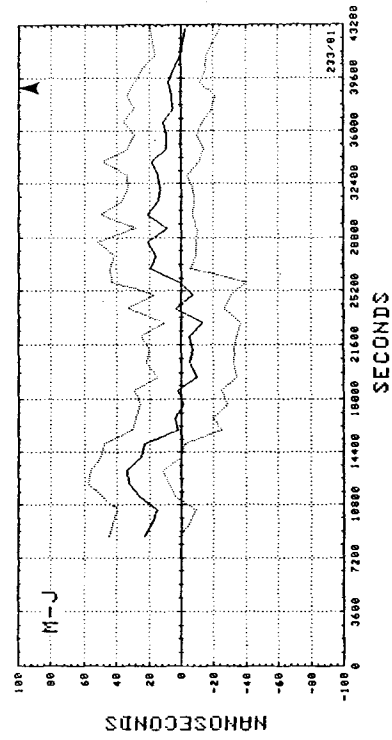


Exhibit 25 21 August 1981.

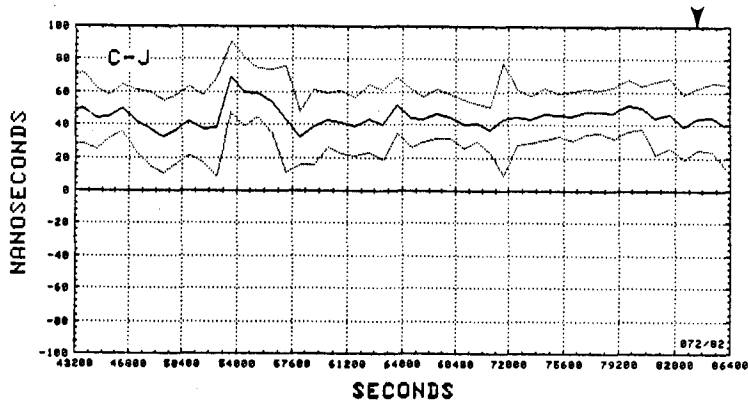
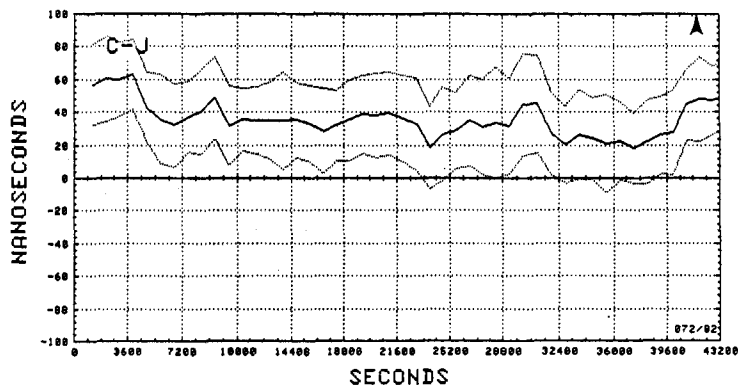
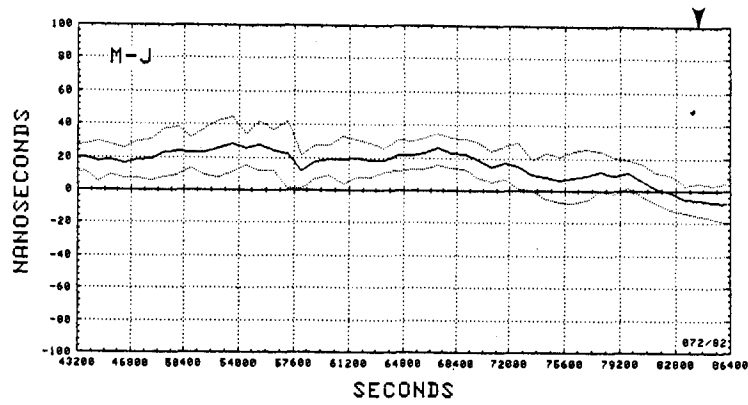
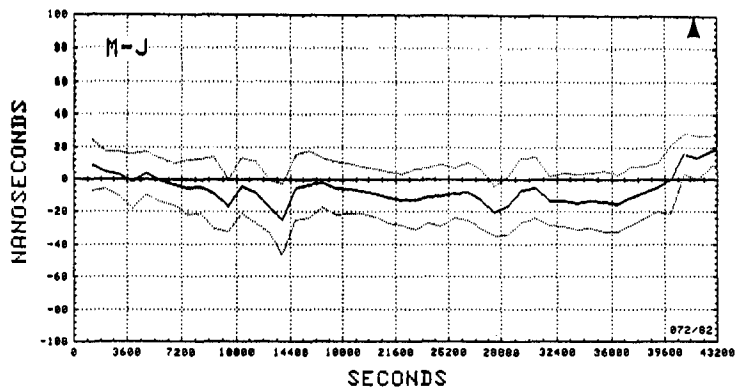


Exhibit 27 13 March 1982.

Exhibit 28 13 March 1982.

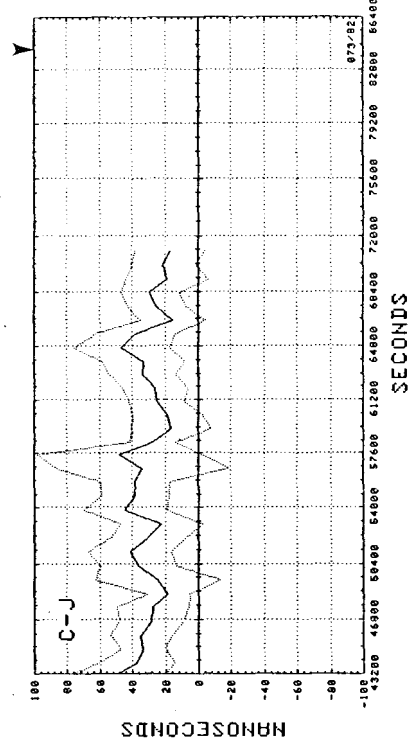
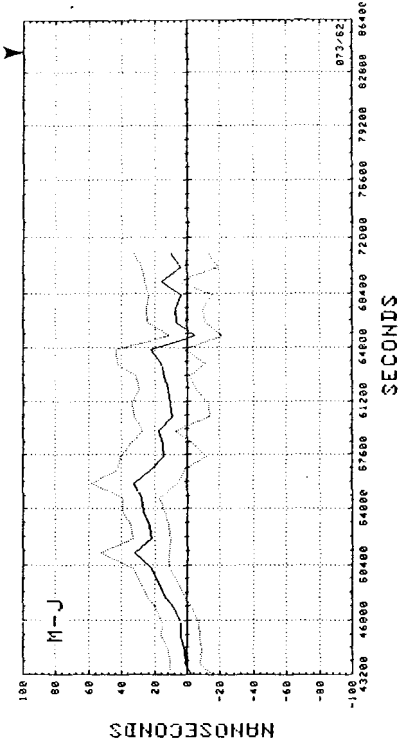


Exhibit 30 14 March 1982.

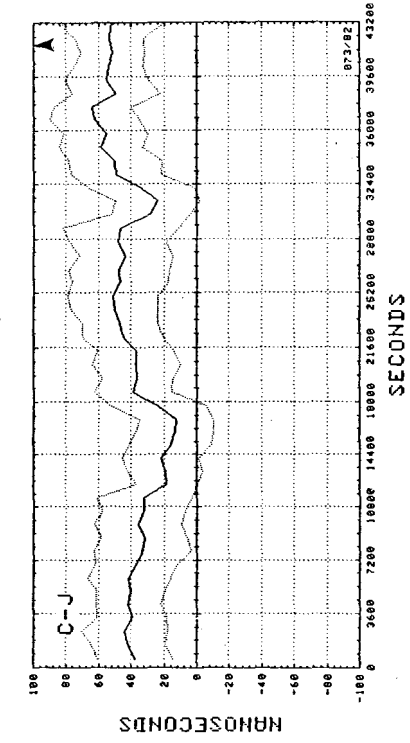
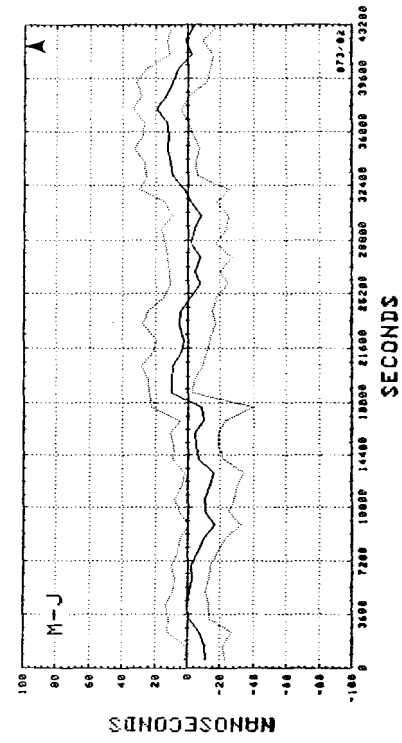


Exhibit 29 14 March 1982.

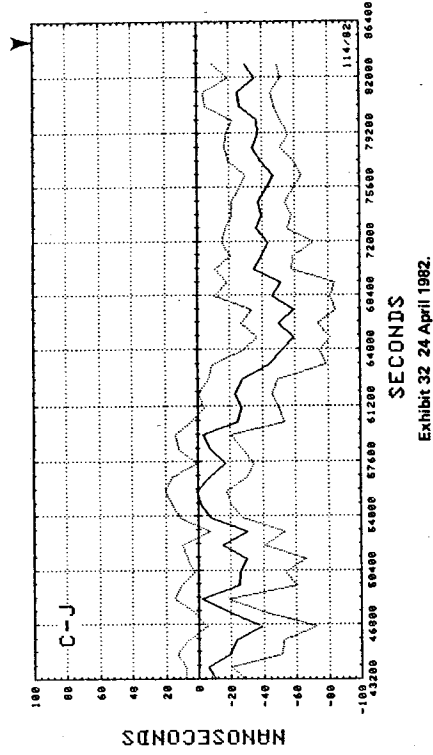
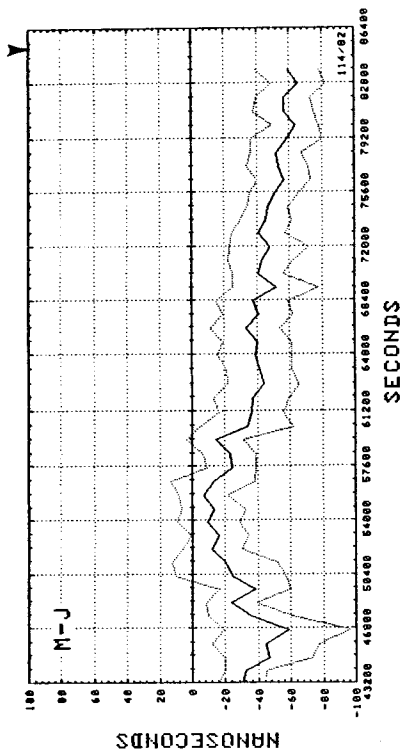


Exhibit 32 24 April 1982.

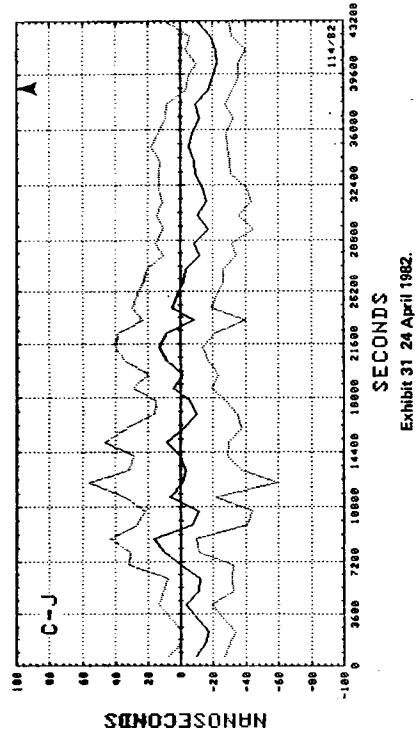
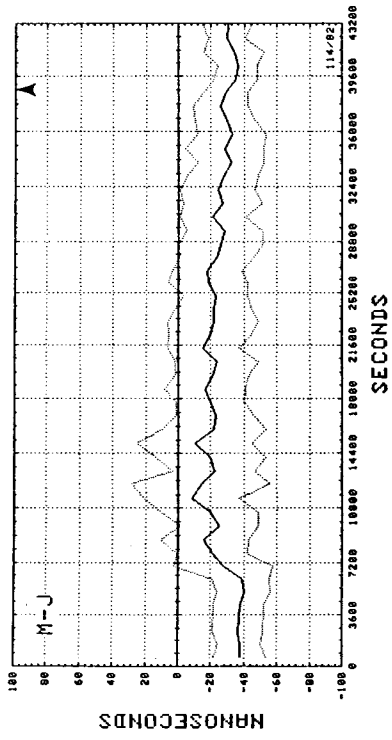


Exhibit 31 24 April 1982.

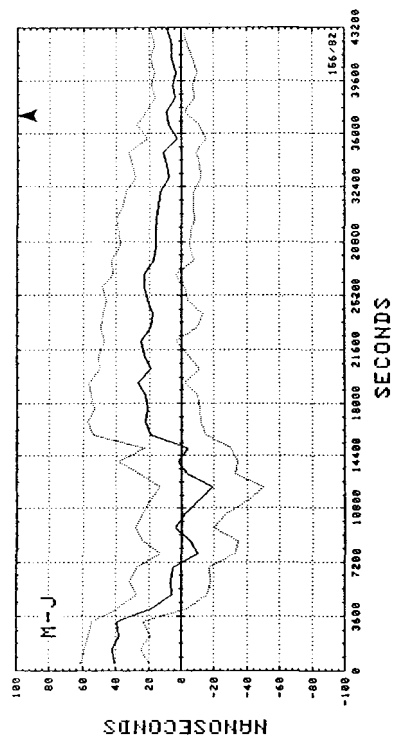


Exhibit 33 5 June 1982.

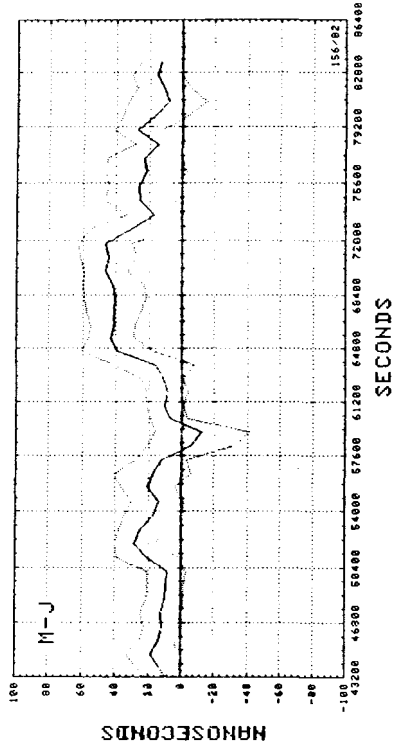
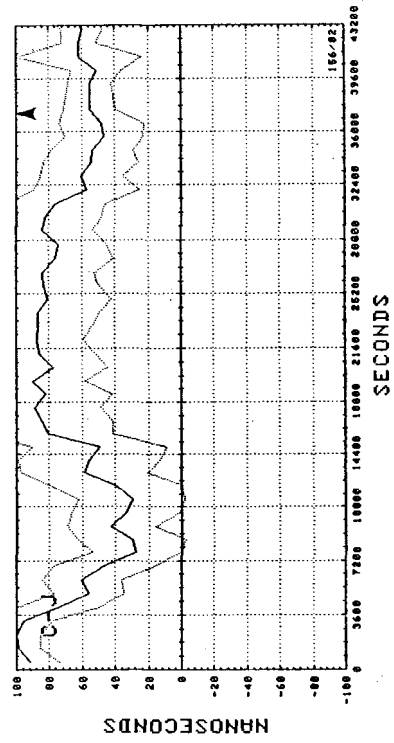
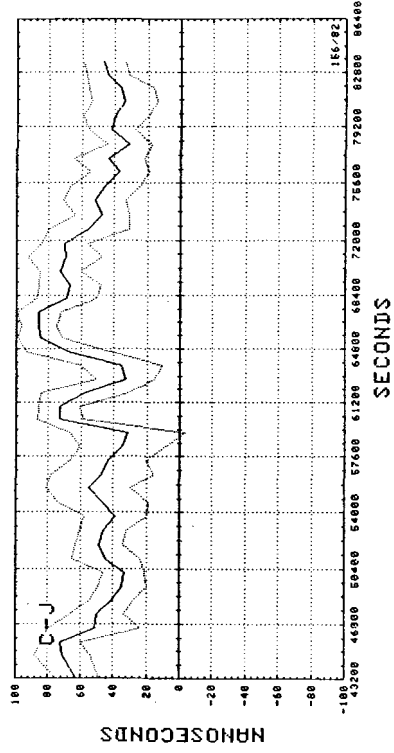


Exhibit 34 5 June 1982.



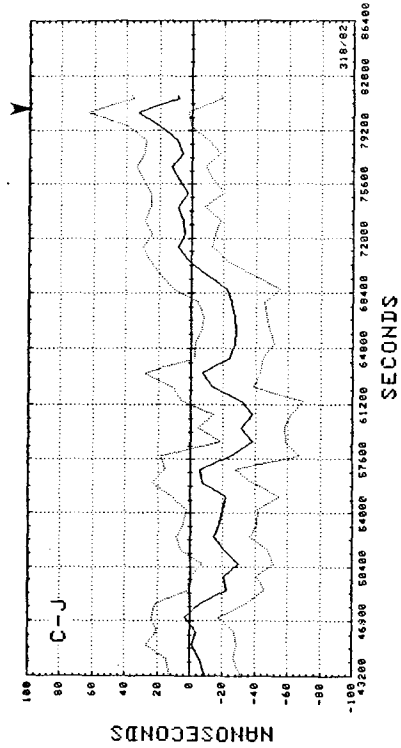
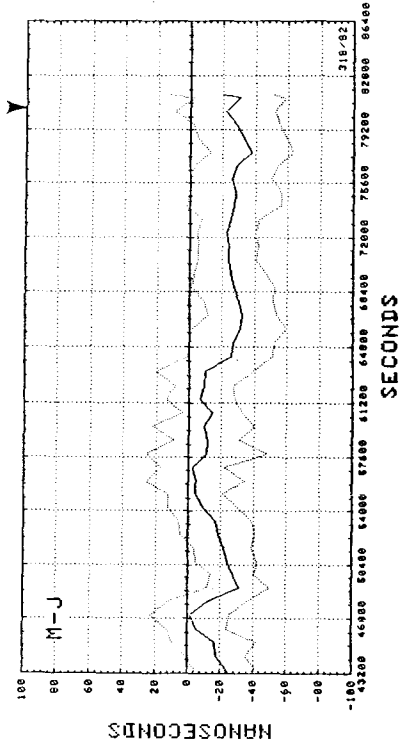


Exhibit 36 14 November 1982.

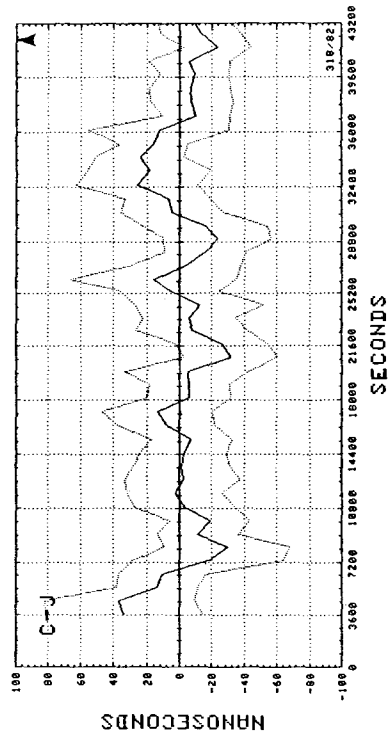
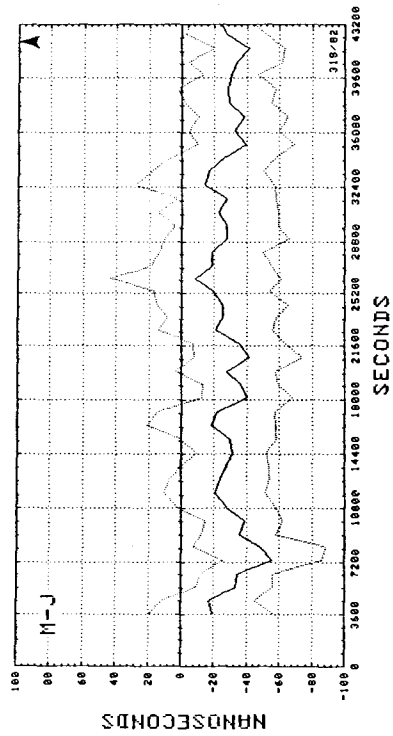


Exhibit 36 14 November 1982.

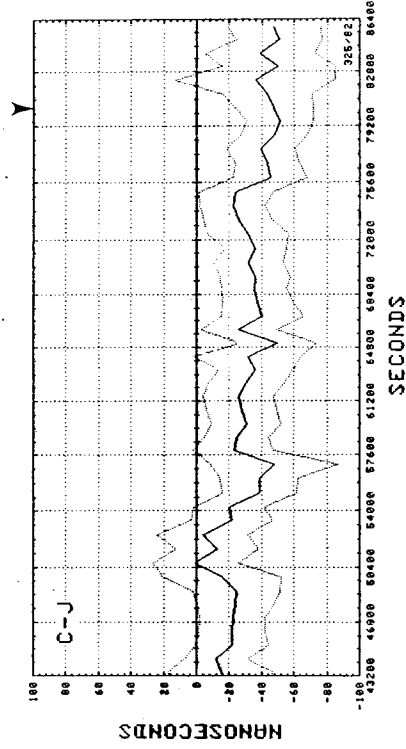
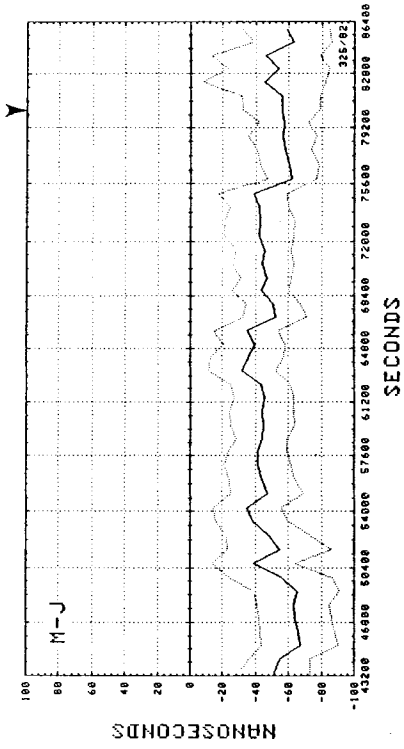


Exhibit 38 21 November 1982.

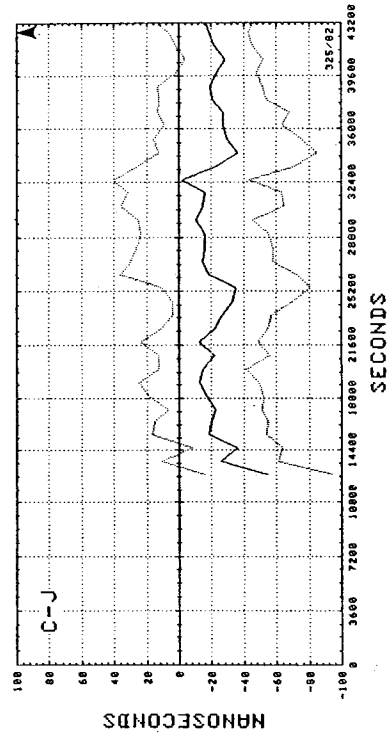
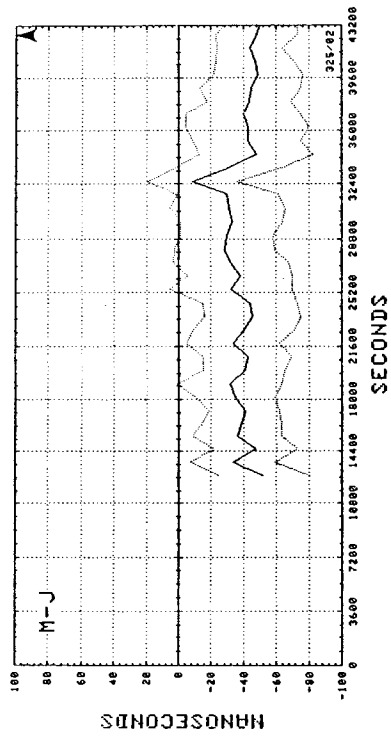


Exhibit 37 21 November 1982.

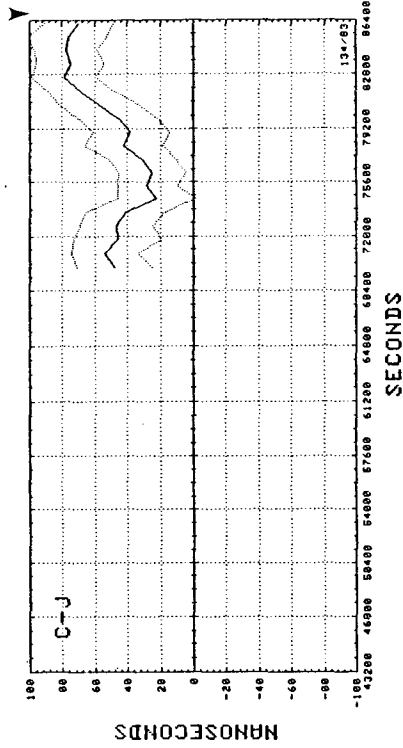
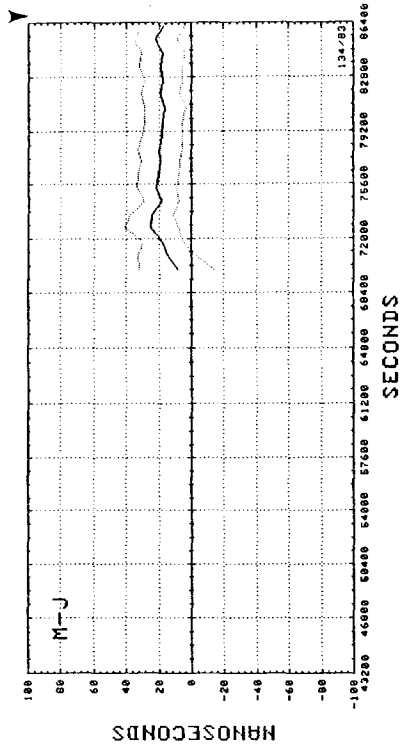


Exhibit 40 14 May 1983.

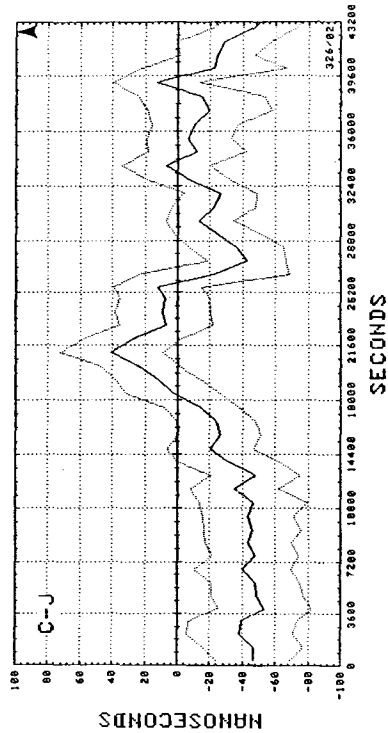
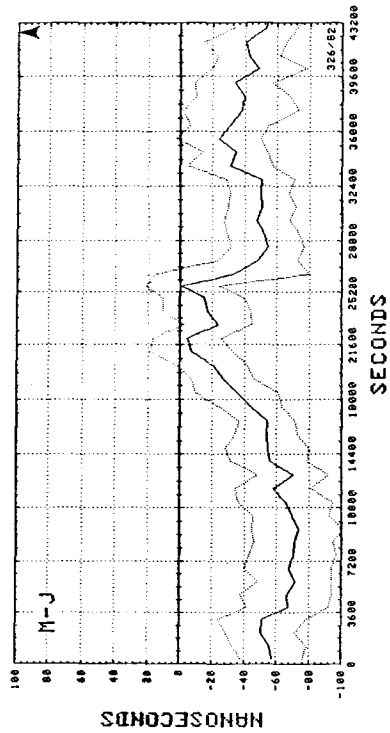


Exhibit 39 22 November 1982.

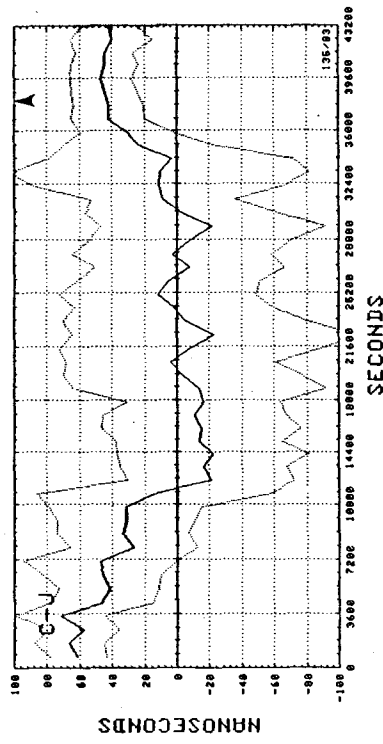
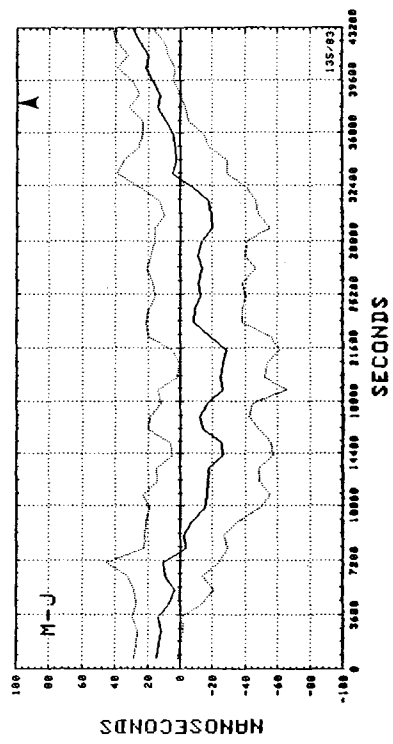


Exhibit 41 15 May 1983.

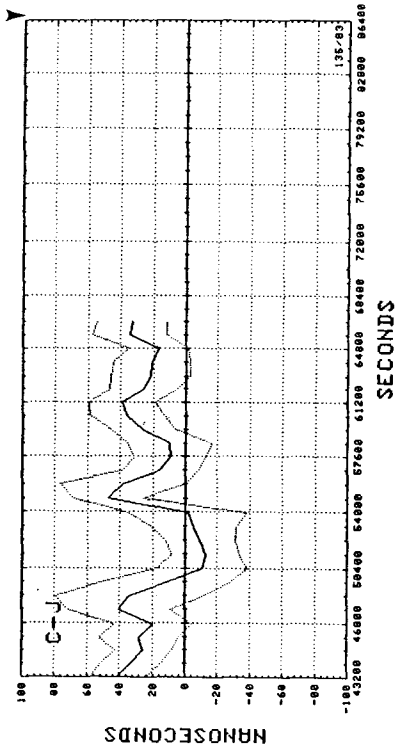
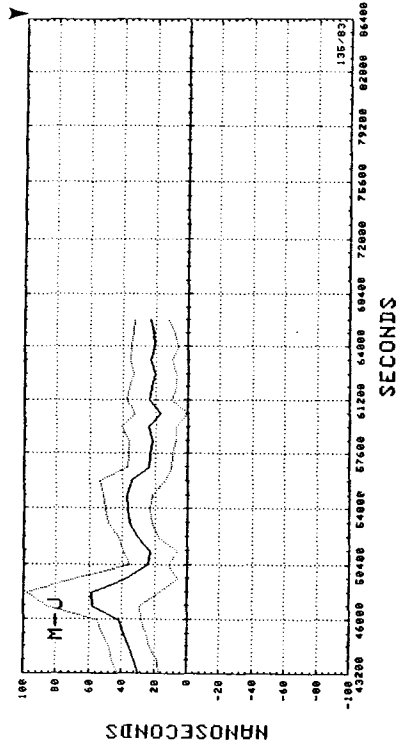


Exhibit 42 15 May 1983.

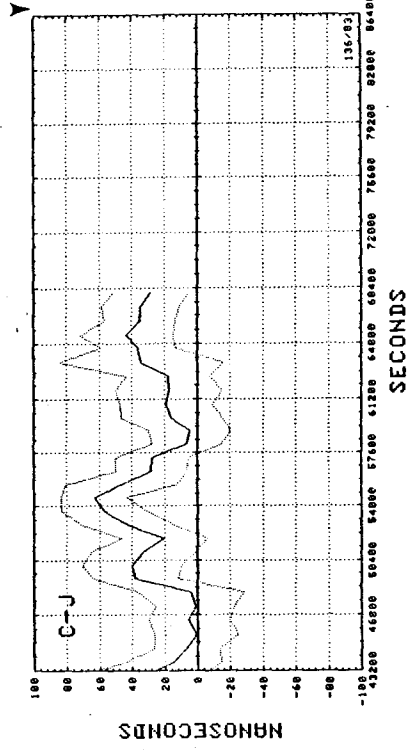
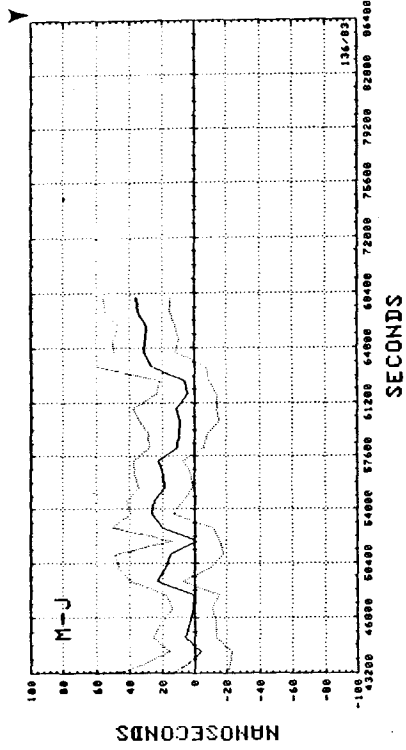


Exhibit 44 16 May 1983.

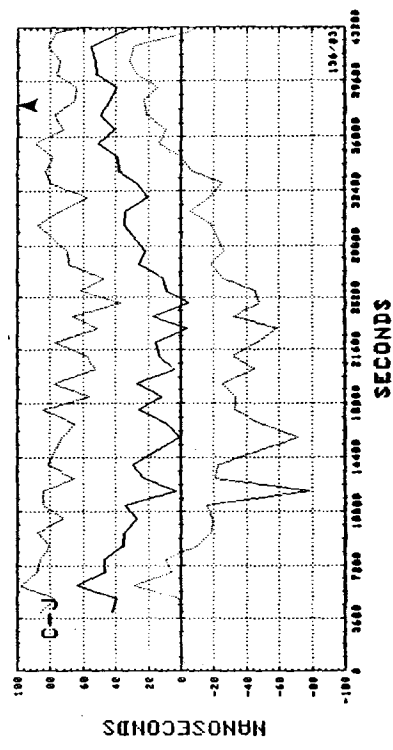
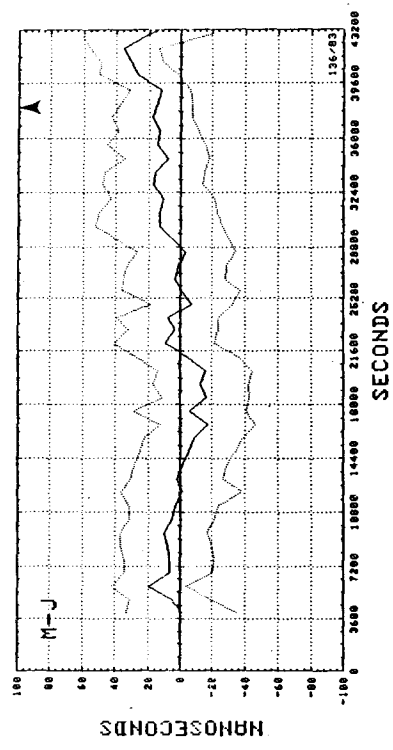


Exhibit 43 16 May 1983.

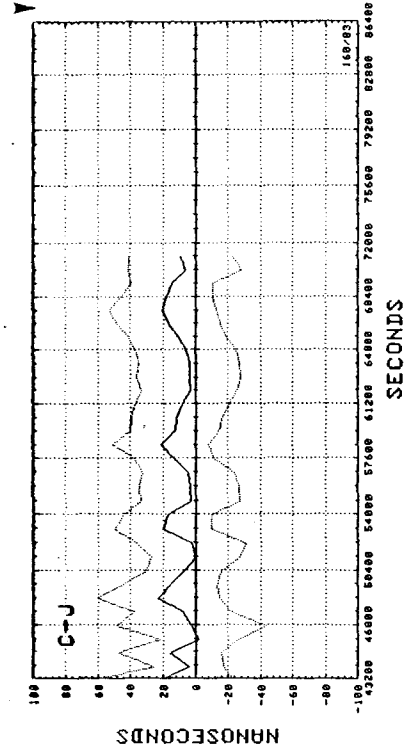
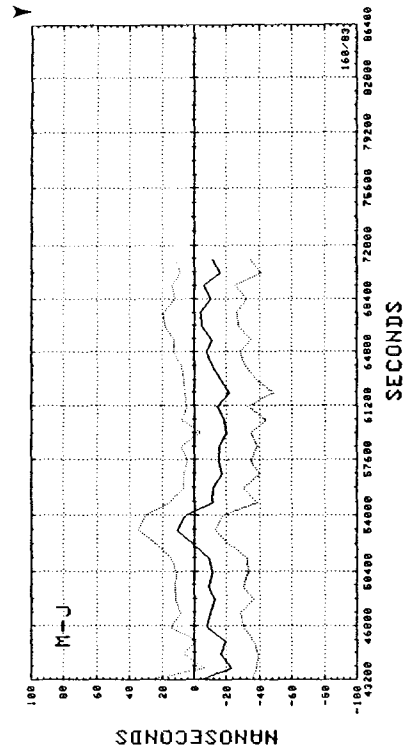


Exhibit 46 9 June 1983.

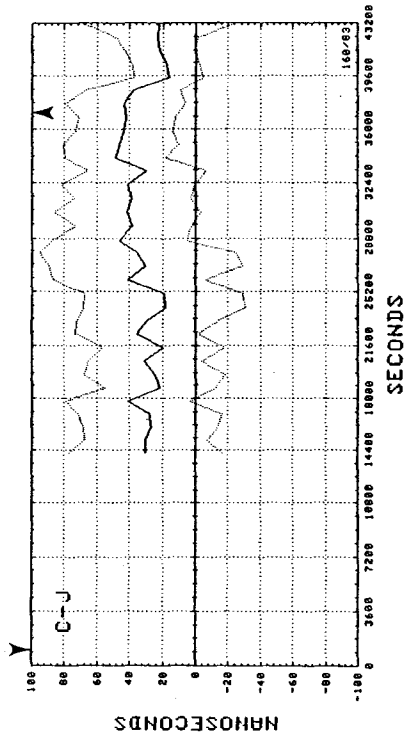
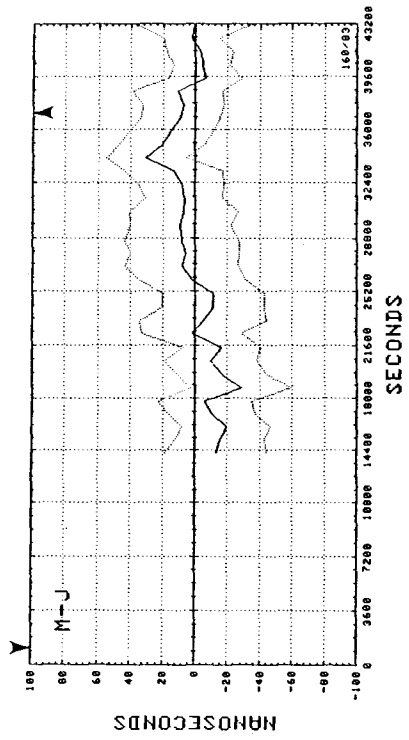


Exhibit 45 9 June 1983.

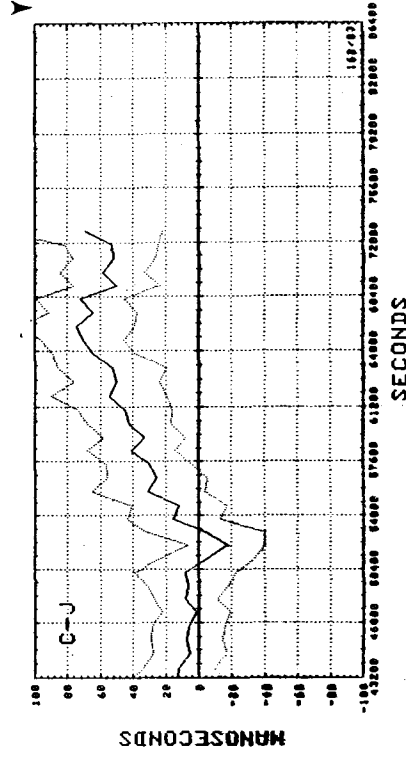
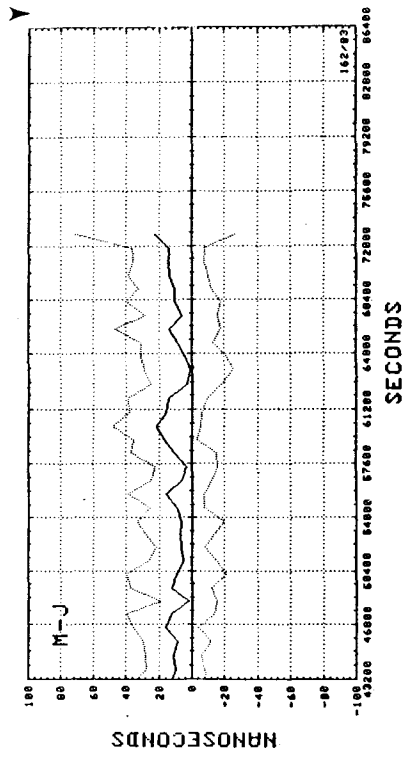


Exhibit 48 11 June 1983.

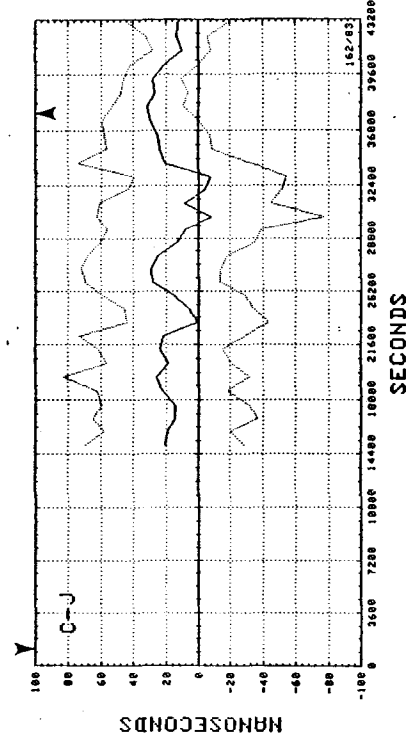
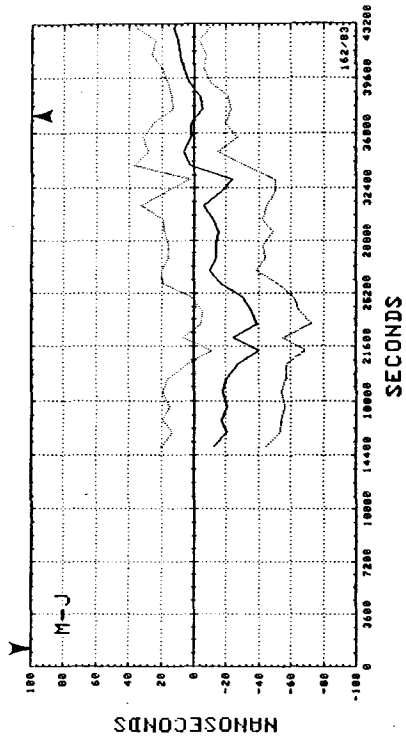


Exhibit 47 11 June 1983.

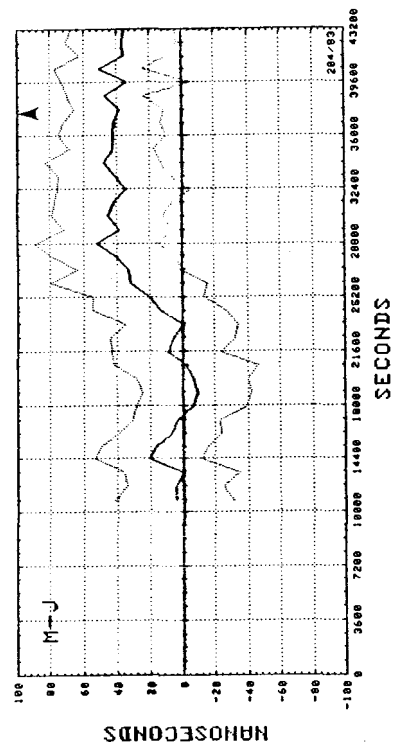


Exhibit 49 23 July 1983.

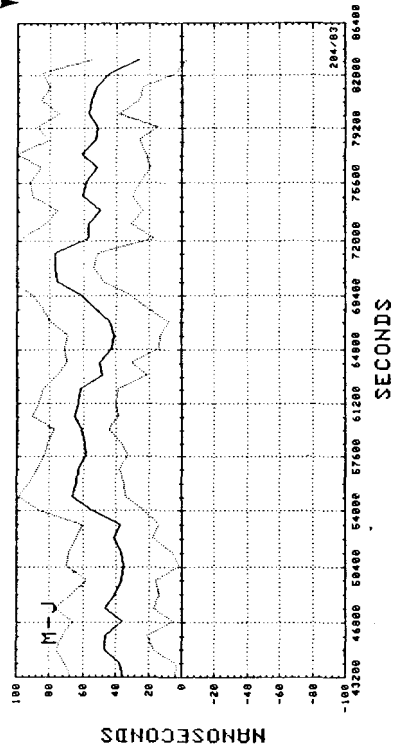


Exhibit 50 23 July 1983.

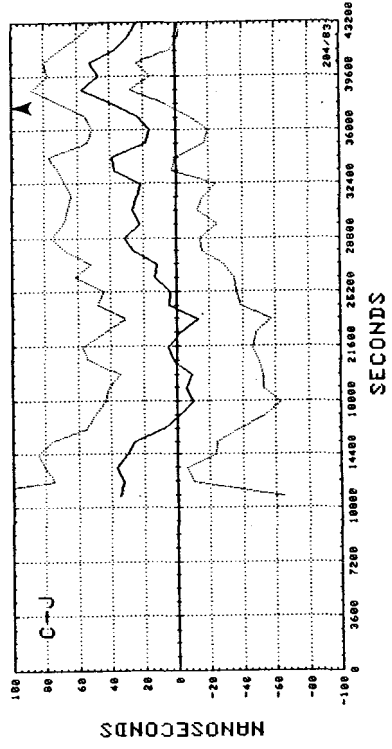
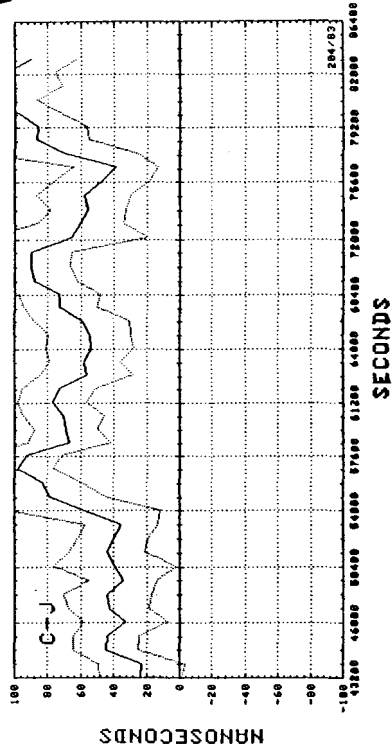


Exhibit 49 23 July 1983.



AVERAGE DEVIATIONS OF TIME DIFFERENCE
AT LONARS PATTERN MONITOR

M-J		C-J		CORR	COUNT	DATES
MEAN	ST. DEV	MEAN	ST. DEV			
22.8	12.2	-42.1	14.3	.564	99	22 23 OCT 79
32.2	7.7	-6.0	14.1	.658	46	13 14 FEB 80
-1.7	27.9	9.5	20.4	.718	73	26 MAR 80
-21.3	15.5	-42.1	21.8	.498	109	15 16 APR 80
-5.9	13.6	3.3	10.7	.633	49	16 17 APR 80
16.8	13.8	28.4	12.5	.153	116	17 18 APR 80
5.0	17.6	11.8	22.6	.716	120	20 21 APR 80
.8	13.4	2.1	17.0	.372	123	22 23 APR 80
5.3	12.0	7.4	12.4	.598	70	14 15 JUL 80
-1.4	16.2	-1.3	17.1	.647	96	28 29 OCT 80
16.2	16.0	42.0	22.8	.617	69	27 28 MAR 81
26.7	8.2	62.1	8.5	.821	21	28 29 MAR 81
10.9	12.3	39.8	19.5	.688	113	21 22 AUG 81
4.7	13.1	38.3	11.4	.354	174	13 14 MAR 82
-32.2	14.2	-17.6	16.6	.714	112	23 24 APR 82
18.2	15.3	56.9	21.3	.629	125	4 6 JUN 82
-24.4	10.3	-5.6	16.7	.054	88	14 15 NOV 82
-45.2	13.9	-26.1	18.4	.721	134	21 22 NOV 82
10.1	19.9	25.0	26.7	.516	93	14 15 MAY 83
10.0	12.7	27.7	17.2	.648	70	16 MAY 83
-5.6	11.7	21.3	13.8	.691	64	9 JUN 83
-.7	15.6	25.0	21.8	.378	65	11 JUN 83
40.4	20.8	45.7	30.7	.781	81	23 JUL 83

Exhibit 51 Daily average deviations and the standard deviations of the 15-minute means.

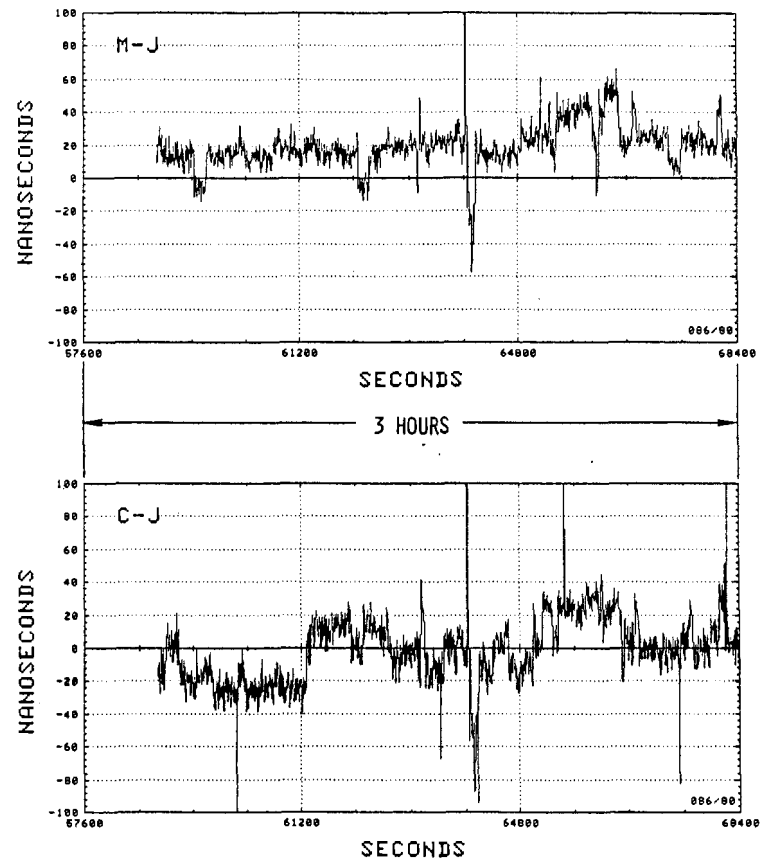


Exhibit 52 Details of signal variation in the vicinity of the anomaly of Exhibit 18.

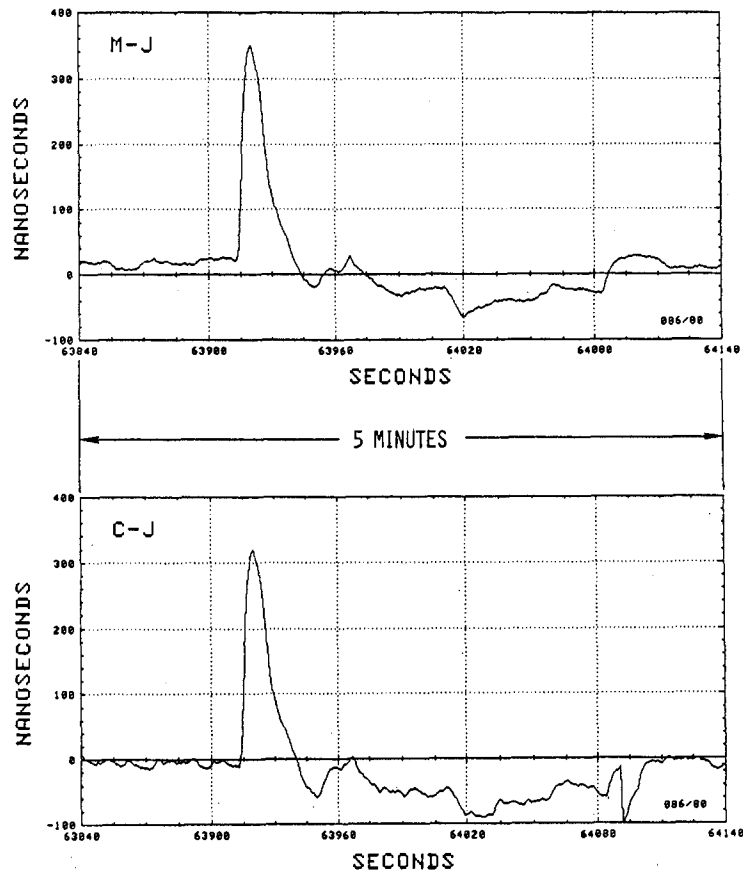


Exhibit 53 Expanded view of the anomaly occurring shortly after 63900 seconds in Exhibit 53.

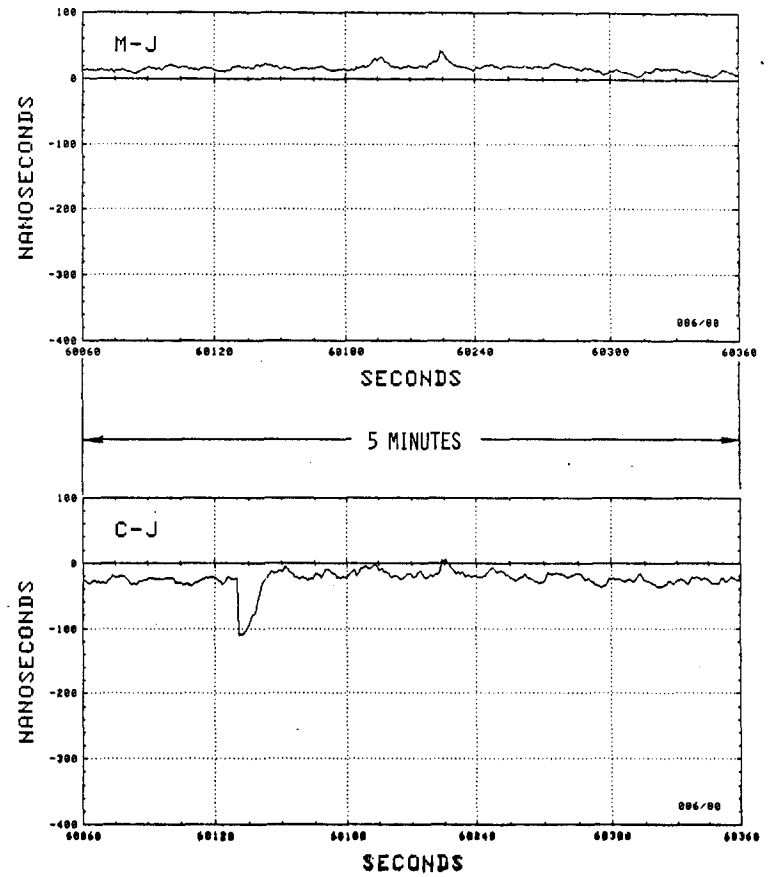
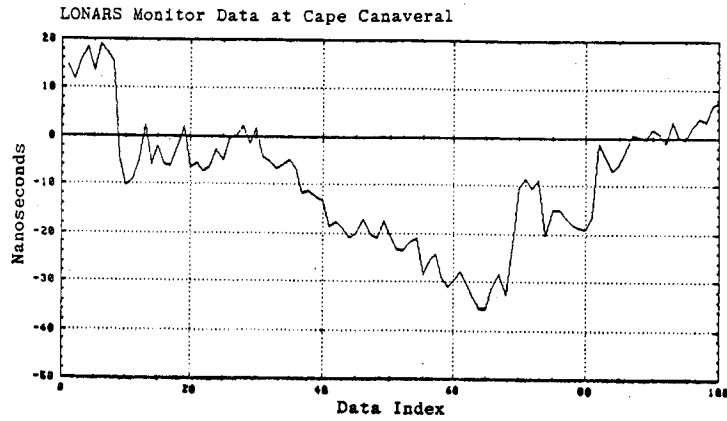
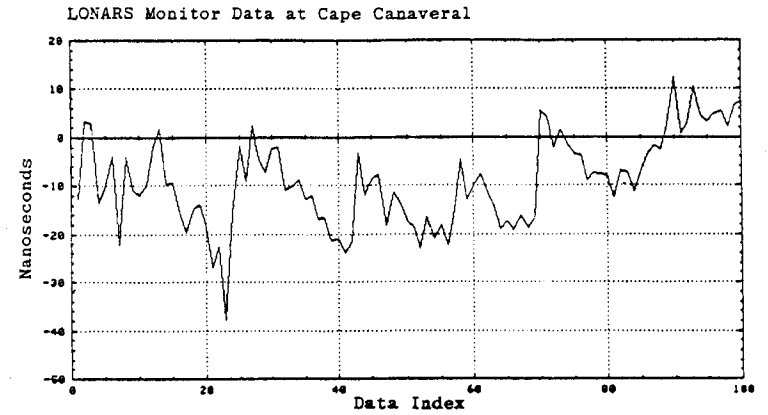


Exhibit 54 Expanded view of the anomaly occurring shortly after 60120 seconds in Exhibit 53.

JUPITER MINUS MALONE
7 February 1982



CAROLINA BEACH MINUS MALONE
7 February 1982



USCG Monitor Data at Mayport

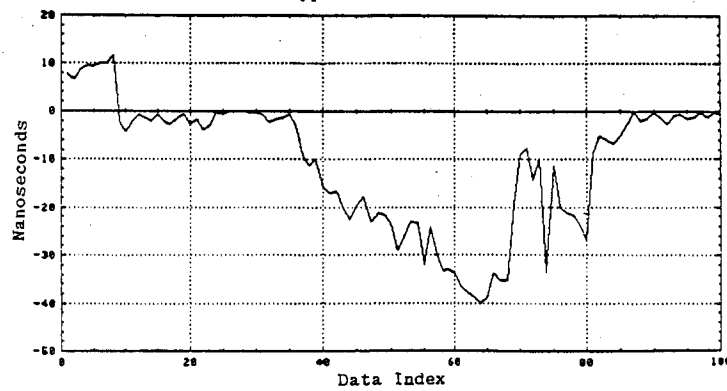


Exhibit 55 Data showing the similarity of the responses of two different widely separated receivers.

USCG Monitor Data at Mayport

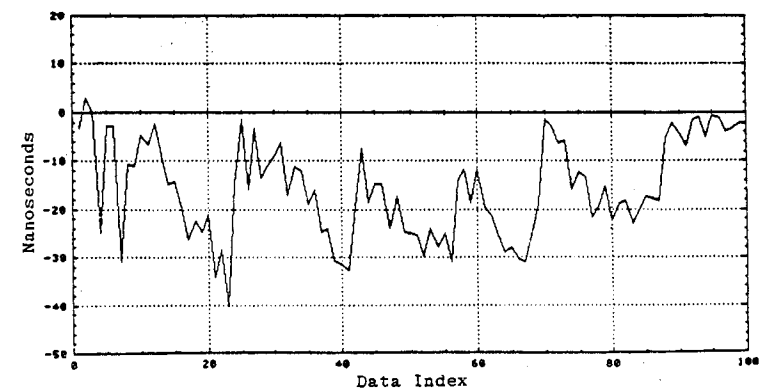


Exhibit 56 Data showing the similarity of the responses of two different widely separated receivers.

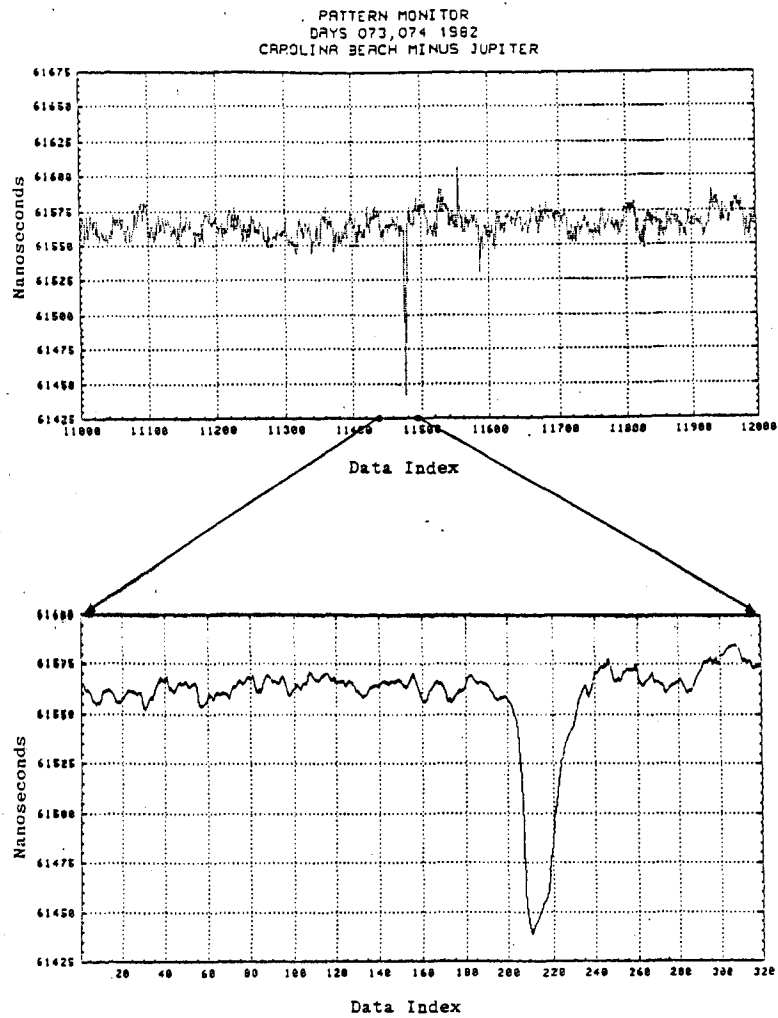
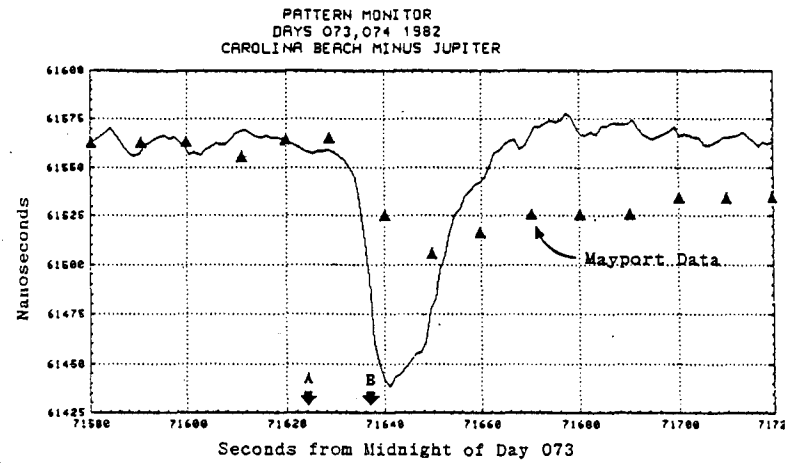


Exhibit 57 Loran signal anomaly on day 073 as seen at the LONARS pattern monitor.



LONARS Pattern Monitor Data
Compared to USCG Mayport Data

- Note: 1. At time A, USCG reported "GAIN ERROR BGN"
2. At time B, USCG reported "GAIN ERROR END"

Exhibit 58 Comparison of receiver responses to the anomaly shown in Exhibit 57.

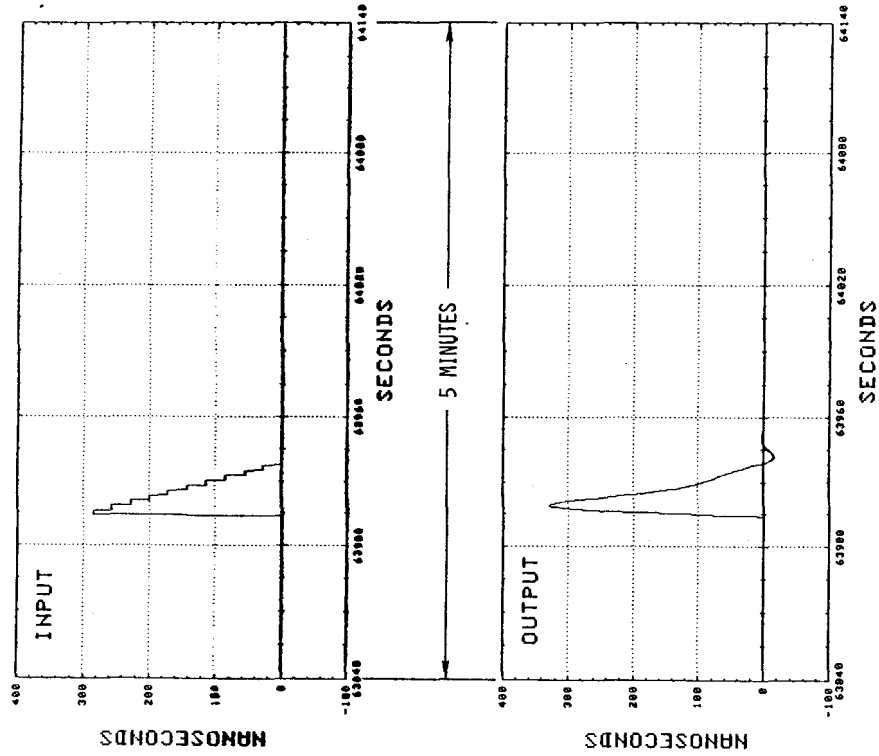


Exhibit 60 Simulated response of LONARS phase tracking loop to a step followed by gradual step decreases.

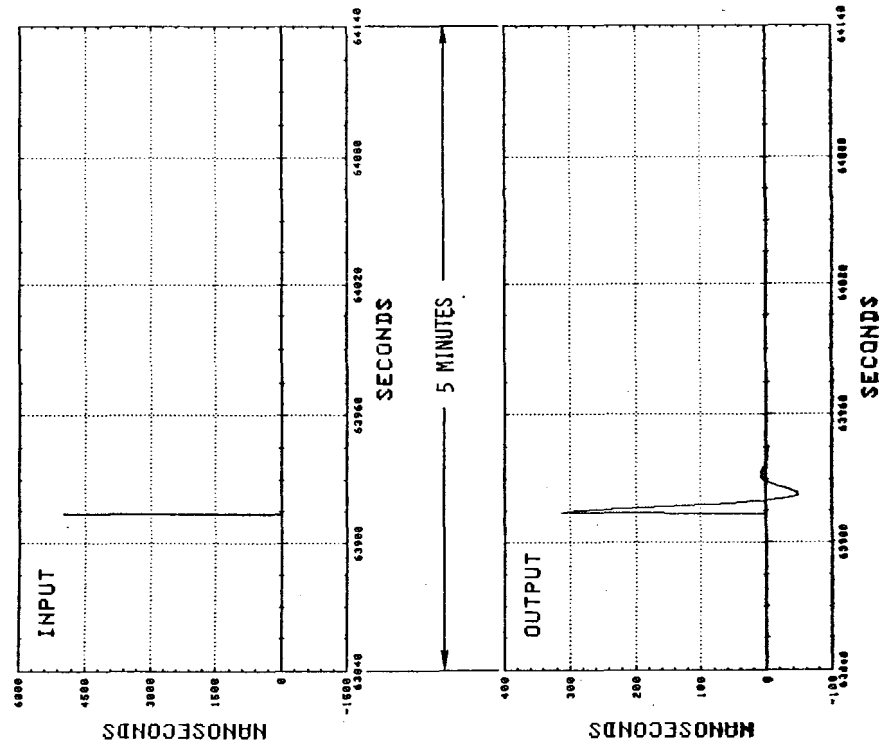


Exhibit 60 Simulated response of LONARS phase tracking loop to an impulse.

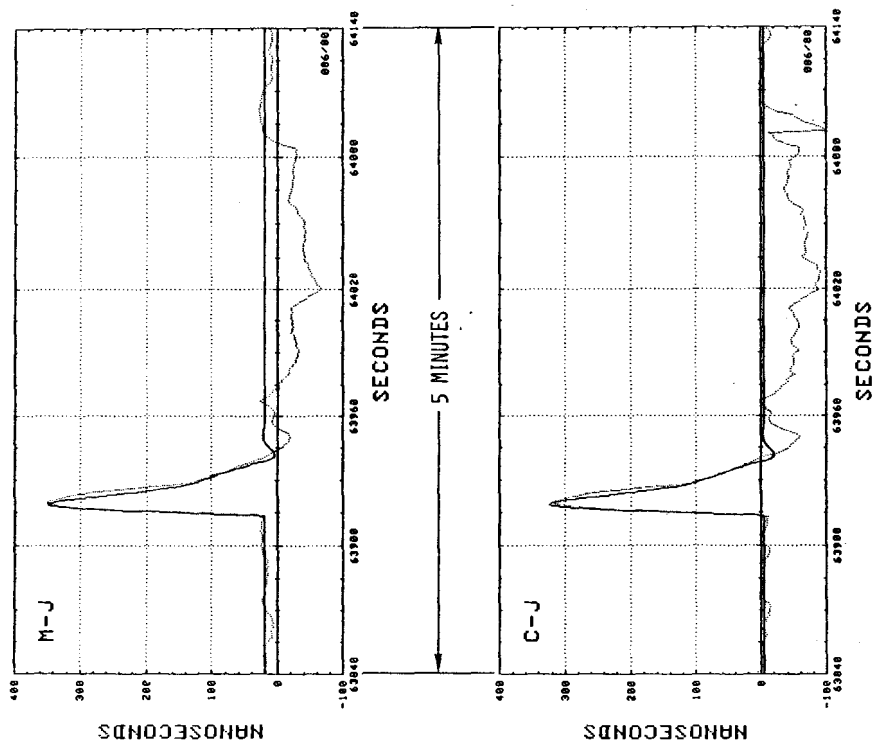


Exhibit 61 Fit of response shown in Exhibit 60 to the response data shown in Exhibit 53.

SAUDI ARABIA LORAN-C CHAINS

VERNON L. JOHNSON
ITT AVIONICS DIVISION
NUTLEY, NEW JERSEY 07110

ABSTRACT

Two new Loran-C chains are being implemented in Saudi Arabia by Standard Electric Alireza Ltd. under turnkey contract with the Saudi Ports Authority. Loran-C service will be provided in the Red Sea, Arabian Gulf, and other waters around the Arabian Peninsula as shown by the coverage diagram presented.

The system is comprised of seven high-power Loran-C transmitter stations and three area monitor station configured into two chains with the chain control station co-located with one of the transmitter stations. Functional diagrams and photographs are presented to define the elements of the system together with typical station layouts and description of the various Loran-C equipments. It is expected that chain calibration will be started in early 1984 with operational status planned later in 1984.

INTRODUCTION

A major expansion of Loran-C navigation service is in process by Standard Electric Alireza Ltd. (an ITT/Alireza Saudi company) under turn-key contract with the Saudi Ports Authority to provide Loran-C coverage of the Red Sea, Arabian Gulf, and other waters around the Arabian Peninsula. The systems engineering and Loran-C equipments are provided by ITT Avionics. The civil engineering, construction, installation, operation, and maintenance are provided by ITT Federal Electric International. This program is the first turn-key implementation of general use Loran-C service on a commercial basis with no U.S. government agency involved.

The Red Sea and Arabian Gulf are waterways of significant marine transportation. The increase in traffic through the Suez Canal together with rapid growth in the size and number of operational ports on both coasts of Saudi Arabia lead to further increase in the already heavy traffic in these areas. Much of the coastline is almost totally devoid of natural or man-made features and has many reefs far off-shore, thus making navigation difficult. The increasing use of off-shore mining rigs and platforms also gives rise to the need for accurate all-weather navigation to prevent collision and environmental damage as well as for supporting these off-shore operations. Saudi Arabia has recognized the growing need to provide accurate and wide-area radio-location and navigation services to these waterways, as well as other waters around the Arabian Peninsula, to improve the safety and efficiency of the extensive marine transportation. The decision to install Loran-C is in keeping with the growing

world-wide trend toward expansion of this accurate, reliable, and cost effective hyperbolic navigation aid.

SYSTEM CONFIGURATION

Two new Loran-C chains are being implemented in Saudi Arabia, comprised of seven high-power transmitter stations and three area monitor stations. The chain control station is co-located with one of the transmitter stations. The principal requirements governing configuration of the system are to provide good Loran-C coverage throughout the Saudi Arabian waters of the Red Sea and Arabian Gulf and to site all stations within Saudi Arabia. The system layout and the predicted limits of coverage to be provided are shown by Figure 1. Although not specifically shown by the coverage diagram, the repeatable fix accuracy of 0.1 nautical miles (2 drms) or better is projected in the Saudi waters of the Red Sea and Arabian Gulf, which include the principal ports of Jeddah, Yanbu, Jubail, and Dammam.

The system configuration has been expanded since the start of the program in 1981. The South chain was added in order to extend coverage into the waters around the Arabian Peninsula, thus allowing circumnavigation of the peninsula with use of Loran-C. Figure 1 shows the predicted coverage for both the North and South chains. The use of modular solid-state transmitters allows the radiated power from each station to be tailored to the coverage requirements and varies from 200KW to 800KW. It will be noted that 800KW radiated power was selected for the four stations that are most important to coverage to the south over long overland transmission paths, where signal attenuation is much greater than over sea water. Four of the seven transmitter stations are operated on two rates (double rated) and thus function in both the North and South chains.

SYSTEM ELEMENTS

The precisely timed Loran-C pulses required for accurate navigation are provided by radiating signals from the seven transmitter stations and making timing corrections from a chain control station where tracking data from three monitor stations are received and analyzed. The stations are all interconnected by dedicated data communication channels provided by microwave links and dedicated telephone lines in the Saudi Post Telephone and Telegraph (PTT) system as shown by Figure 2. Multichannel carrier-telegraph units at all stations serve to multiplex thirteen data channels on one four-wire voice-frequency multipoint communications network.

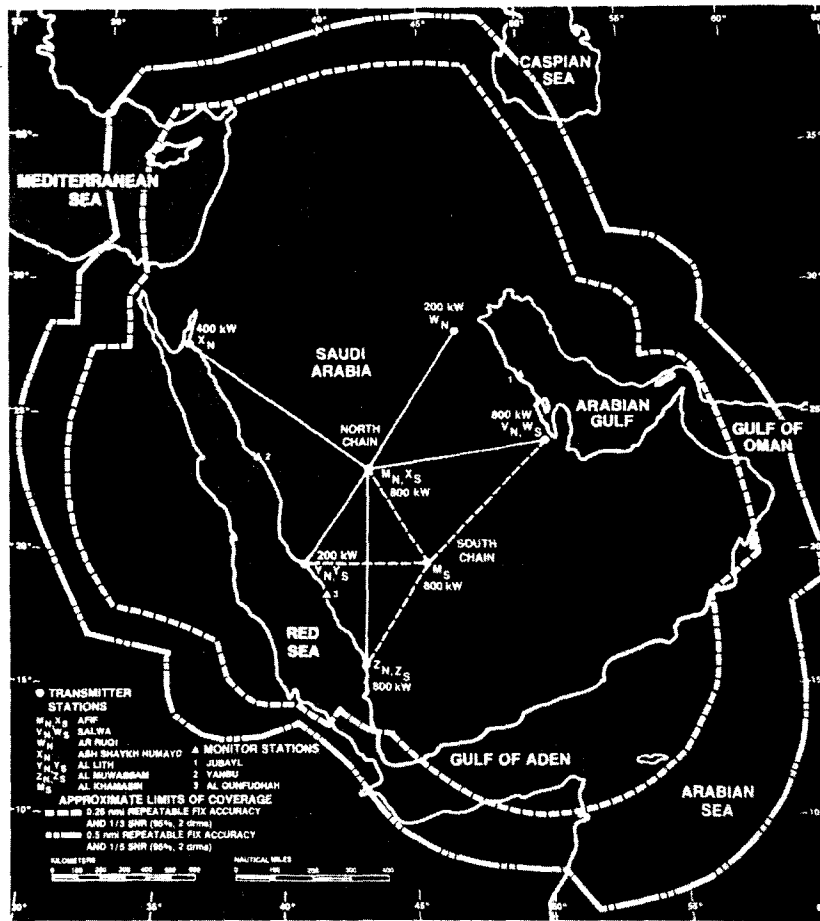


Figure 1. Loran-C System of Saudi Arabia

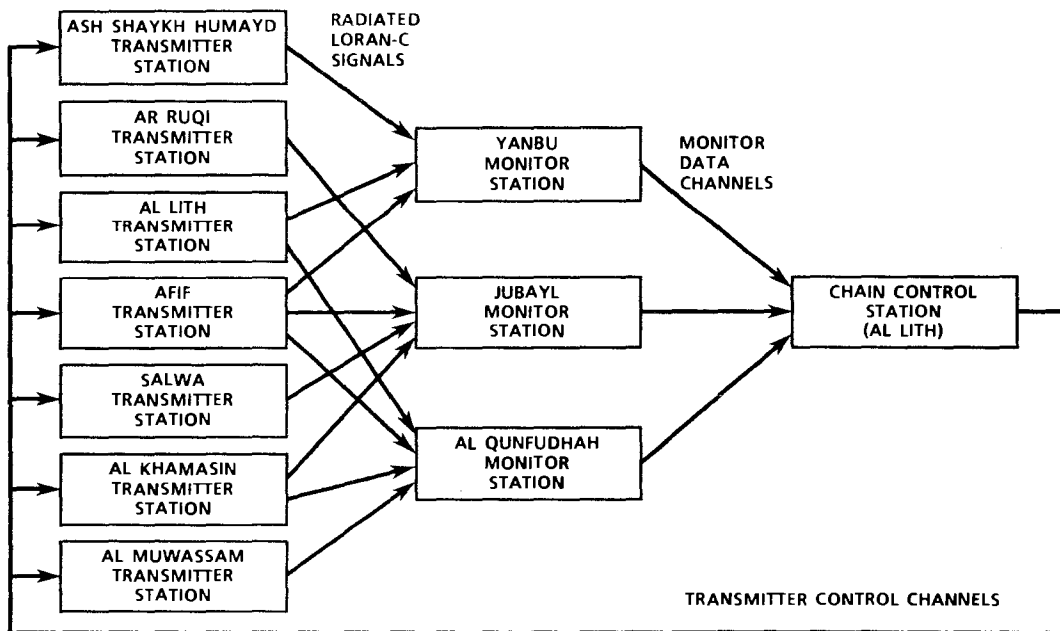


Figure 2. Loran-C System Elements

Computer-controlled receivers and the associated signal processors at the monitor stations measure, digitize, format and store the data on the radiated Loran-C signals and transmit regular reports to the chain control station. The data from the monitor stations are recorded and continuously subjected to computer and operator analysis to determine the need for adjustment of transmitter timing or signal characteristics. Remote control facilities allow making timing adjustments and operational changes to any of the seven transmitters from the chain control station.

The chain control station is co-located with the Al Lith transmitter station and provides central monitoring and control for both the North and South chains, with continuous watchstanding. The transmitter stations are all manned, but do not require watchstanding. The monitor stations are unmanned.

The system has been designed to provide repeatable accuracy of 0.05 to 0.1 nmi (2 drms) in the areas of principal coverage with fix availability of 99.5%.

TRANSMITTER STATIONS

Each Loran-C transmitter station is a complete self-supporting facility having its own living quarters and prime AC power generating capability. The key functional elements of each transmitter station are shown in Figure 3.

Transmitter Set

The Loran-C signals are generated by solid-state transmitters having a modular

design which allows the r.f. power level to be determined by the number of modules (half-cycle generators) used. The lower-power stations incorporate 16 half-cycle generators (HCG), medium power stations have 32 HCGs, and the higher-power stations use 64 HCGs. The HCGs are combined and timed such as to drive the output network and antenna to radiate properly shaped Loran-C pulses. Adjustment of the pulse envelope-to-cycle difference is provided by varying the number of HCGs used in each of the drive half cycles. The multiple HCG configuration provides a fail-soft capability to maintain the transmitter on-air with acceptable output signals when several HCGs are off-line from failure or servicing.

The Transmitter Equipment Set, manufactured by Megapulse, Inc., Bedford, MA., is comprised of two major equipment groups: the transmitter, Figure 4, and the control console. The three-cabinet control console group is shown on the left side of the operations room photo, Figure 5.

The control console incorporates all basic timing and control functions in an operate-standby redundant configuration with automatic switchover if the operate timing signals are lost. The transmitter consists of multiple identical HCGs along with redundant coupling and output networks with automatic switchover to provide high operating reliability. The high stability timing signals are derived from a cesium beam frequency standard together with a phase microstepper which provides a means of correcting for small frequency-standard offsets.

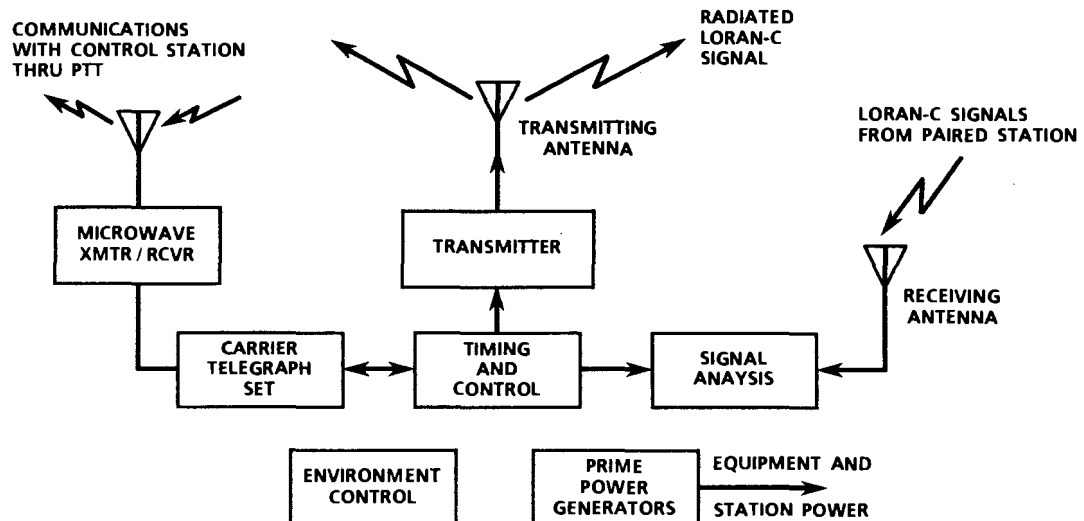


Figure 3. Transmitter Station Functional Elements

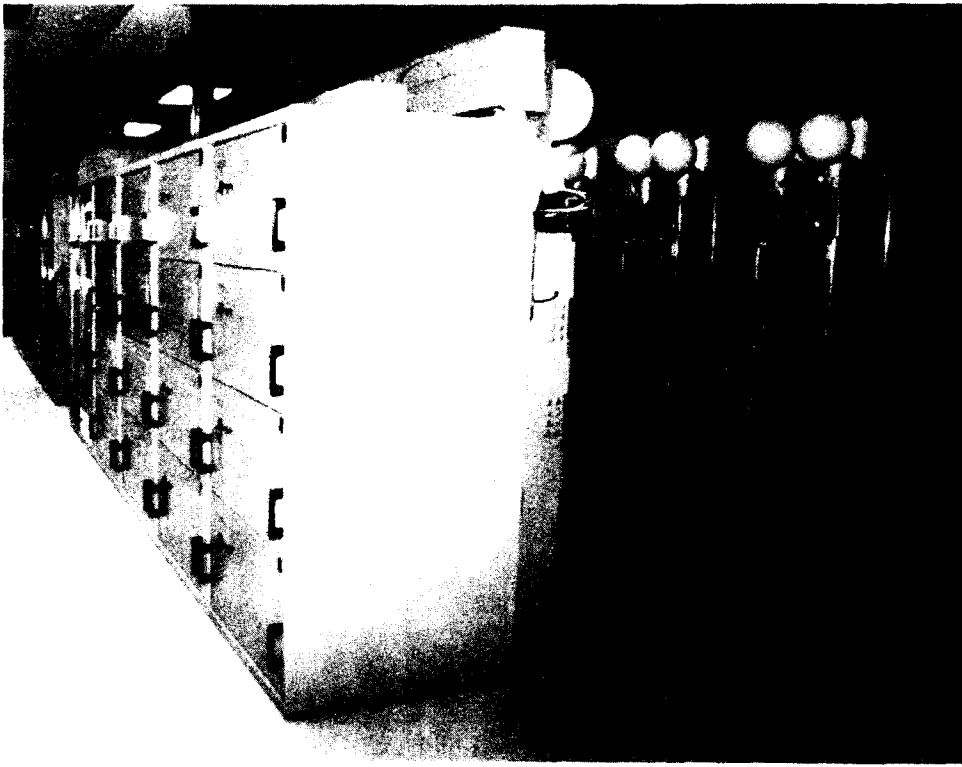


Figure 4. Loran-C Transmitter at AFIF

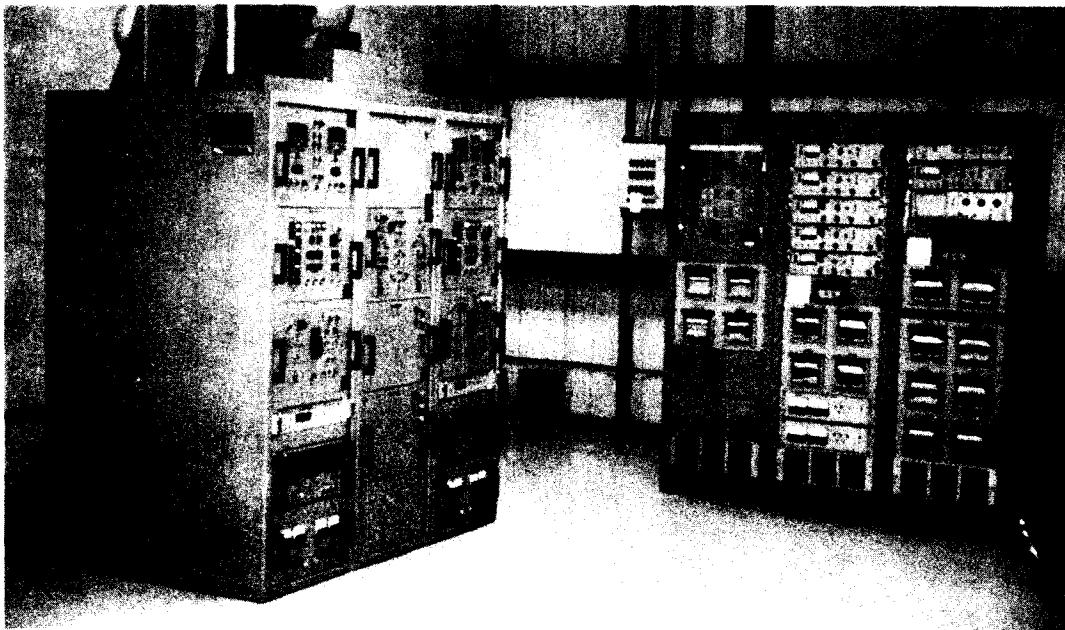


Figure 5. Operations Room at AFIF

Antenna

The Loran-C signals are radiated from a top-loaded monopole antenna constructed with a guyed steel tower 220 meters (720 feet) high. The uppermost guy level consists of 18 top-loading elements each 200 meters (656 feet) long. The antenna counterpoise consists of 120 radials each approximately 325 meters (1066 feet) long.

Signal Analysis Set

The Signal Analysis Set, shown on the right side of the operations room photo, Figure 5, is used to monitor and verify proper pulse shape and timing of the transmitted Loran-C pulses. It also provides a back-up capability for maintaining correct station timing in the event that the capabilities of the chain control station are interrupted. Timing receivers operating in conjunction with time interval counters establish a time relationship between the transmitter timers and signals received from the other paired station on each baseline. Stripchart recordings provide a continuous record of pulse amplitude and phase. The frequency of the standby cesium standard is compared to the operate cesium standard and continuously recorded to assure that the standby frequency standard is stable. A recording of the transmitter cycle-compensation performance provides verification that transmitter time delay is being maintained constant. A pulse analyzer measures the pulse amplitude and envelope shape of the transmitter antenna current waveform. The relationship between the pulse leading edge and the pulse standard RF zero crossing, designated envelope-to-cycle difference (ECD) and which must be maintained within specific limits, is continuously recorded and also monitored by an alarm system. The ECD alarm, alarms from the transmitter, and a lost-carrier alarm from the carrier telegraph unit are among inputs to an alarm repeater unit which initiates both audible and visible alarms to alert station personnel in the operations building or living quarters to any abnormal operating condition. The carrier telegraph unit includes modems for remote control of the transmitter and for administrative teleprinter communications.

Communications

Each transmitter station is connected into the Saudi PTT at the nearest access point via a dedicated one-hop microwave link. One dedicated duplex data channel is provided at each station which serves for chain control and for administrative teletype communications. The standard dial-up telephone circuits are also provided for voice communications between all stations and into the PTT network.

Power Generators

None of the stations at present use commercial power, but are equipped with triple diesel generators, any one being able to carry the full station load. Provisions are incorporated for automatic switchover

from an on-line generator to a standby generator within 20 seconds, with the third unit allowed to be down for scheduled maintenance. Size of the generators range from 225 to 450 KW. The prime power system is 208 V, 3 phase, 60 cps and is thus compatible to the use of commercial power now being rapidly developed in Saudi Arabia if it becomes available to any station.

Environmental Control

Controlled temperature and humidity conditions are maintained by an air conditioning system in the living quarters and the Loran-C equipment areas. Construction of the buildings is such that filters and air pressure differentials are provided to resist the entry of dust during the sand storms that occur frequently in Saudi Arabia.

MONITOR STATIONS

Each of the three Loran-C monitor stations is a complete self-supporting facility having its own prime AC power generating capability, but is unmanned and thus does not need living quarters. A monitor set, as shown in Figure 6, is located at each of the three monitor stations. The signals are received on a 35-foot (11 meters) fiberglass whip antenna and a ground system of buried radials and driven rods. The monitor receiver, under processor control, filters, amplifies, and samples Loran-C signals from the transmitters in both chains. Time differences are measured to an accuracy of 15 nanoseconds. Each Red Sea monitor includes a spare processor. The Jubayl monitor set on the Arabian Gulf has two receivers and processors to provide redundant monitoring capability for that area.

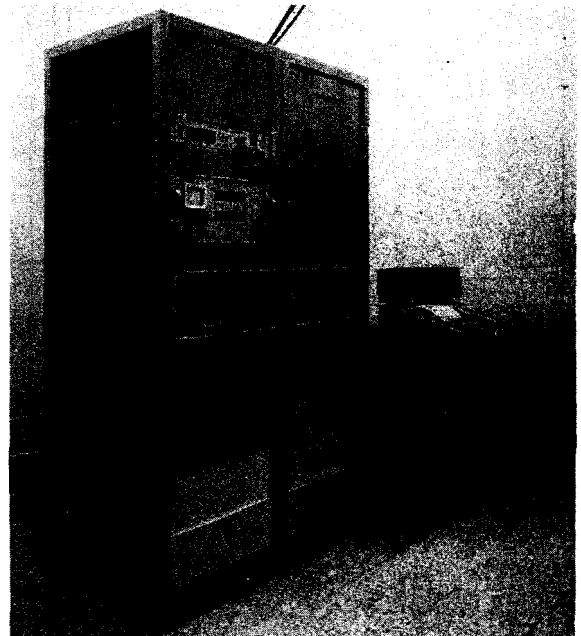


Figure 6. Red Sea Monitor Set

Each receiver tracks stations and prepares reports according to instructions received from the chain control station. These reports include data on time differences, signal levels, ECD, noise levels, and lost signals. The reports on all stations being tracked are encoded, multiplexed, and transmitted on one dedicated data channel. Full duplex communications to and from the processor is provided by a carrier telegraph modem with separate receive and send channels.

The operating receiver and processor are supported by an uninterruptible power source. AC power from a battery-operated inverter protects the equipment from line transients and from power failures during generator switching.

CHAIN CONTROL STATION

The monitor station reports are transmitted to the Data Analysis set, Figure 7, in the chain control station, which is co-located with the Al Lith transmitter station. Time difference data for each master-secondary pair are received from two monitor receivers and recorded on strip charts. The envelope-to-cycle relationship for each transmitted signal is also recorded.

Three desktop computers analyze the data from the South chain, the Red Sea section of the North chain, and the Arabian Gulf section of the North chain. Each computer receives data from two or more monitor receivers and drives a printer, a plotter, and an alarm unit. Each computer makes a statistical analysis of the time-difference data from the monitor receivers and presents transmitter timing adjustment recommendations.

These recommendations, typically ± 20 nanoseconds, are based on both the long-term cumulative time-difference error and the current time-difference data. The watchstander evaluates the recommendation and inserts adjustments in the transmitter through the remote control set when necessary.

An alarm is sounded and abnormality information is printed whenever an analysis of the monitor data indicates that transmitted signals are not within specified tolerances. A printed log of chain activities is provided as they occur together with a daily summary of time-difference averages and other data. The plotter provides daily graphs of time-differences averages and cumulative time-difference errors for each selected master-secondary pair.

A multi-channel carrier telegraph unit is included at this station to provide thirteen 110-baud channels multiplexed on one four-wire line for communications with all monitor and transmitter stations.

A Remote Control set (central cabinet in Figure 7) is used by the watchstander to monitor and control the Loran transmitters at all stations. Reports on abnormal conditions are sent automatically by each transmitter to the chain control RCU. These conditions include equipment failures, over temperature, and antenna current changes. The watchstander can use the RCU to send a variety of commands to any selected transmitter, such as:

- Insert a timing adjustment
- Switch to a standby timing channel
- Turn the transmitter output on or off
- Send a status summary report.

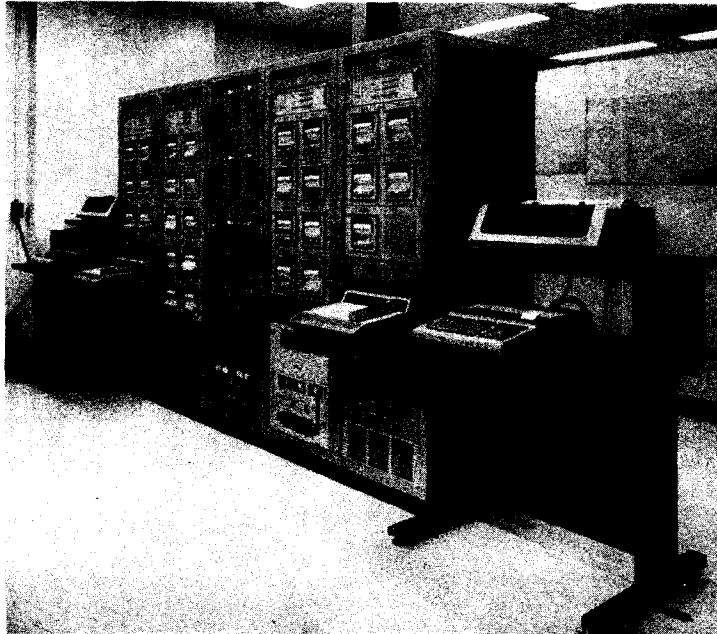


Figure 7. Chain-Control Subsystem

Each outgoing message has an address code so only the selected transmitter will respond.

An uninterruptible power source is provided so that computer programs, constants, and data will not be lost in the event of a local power failure.

IMPLEMENTATION STATUS

The civil works construction is well along with installation of the Loran-C equipment and communication facilities for the North chain proceeding close behind. The master transmitter station at Afif (Figure 8) has been checked out and is transmitting test signals. Field measure-

ments show the radiated peak power to be 1 megawatt with the radiation resistance of the 720 foot transmitting antenna as 3.3 ohms.

It is expected that chain calibration will be started in early 1984 and that the North chain will be operational at mid 1984. The South chain, which is comprised of a master transmitter station at Al Khamasin and shares four dual-rate secondaries with the North chain, will follow with operational status expected later in 1984. SEAL has responsibility for operation and maintenance (O&M) of the Loran-C system for two years. Training will be conducted during the O&M period to allow hand-over of the system to the Saudi Ports Authority at the end of this period.



Figure 8. Transmitter Station at AFIF

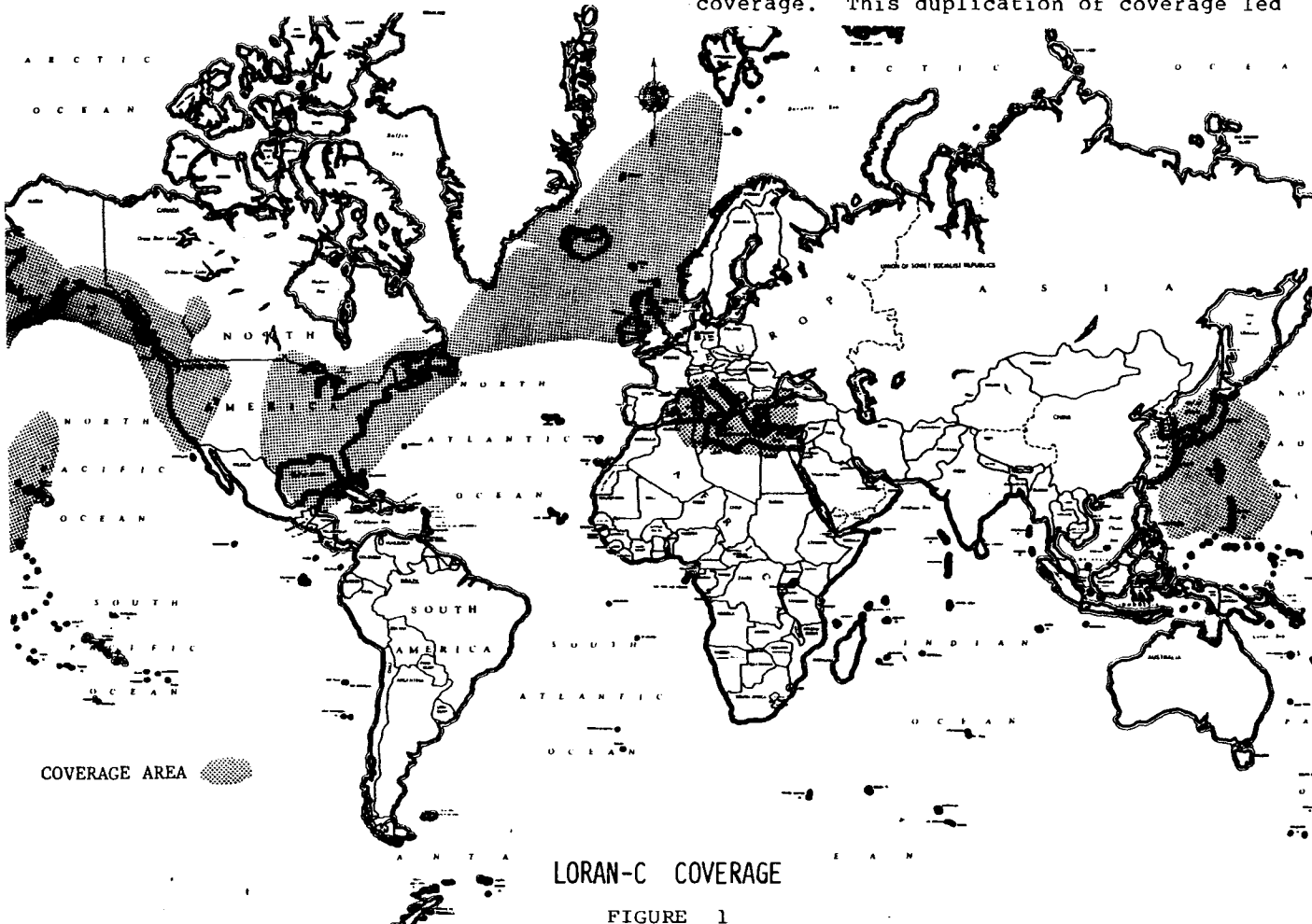
LORAN-C
 The Present and The Future
 by
 Nevin A. Pealer
 Radionavigation Advisor
 Department of Transportation
 Research and Special Programs Administration

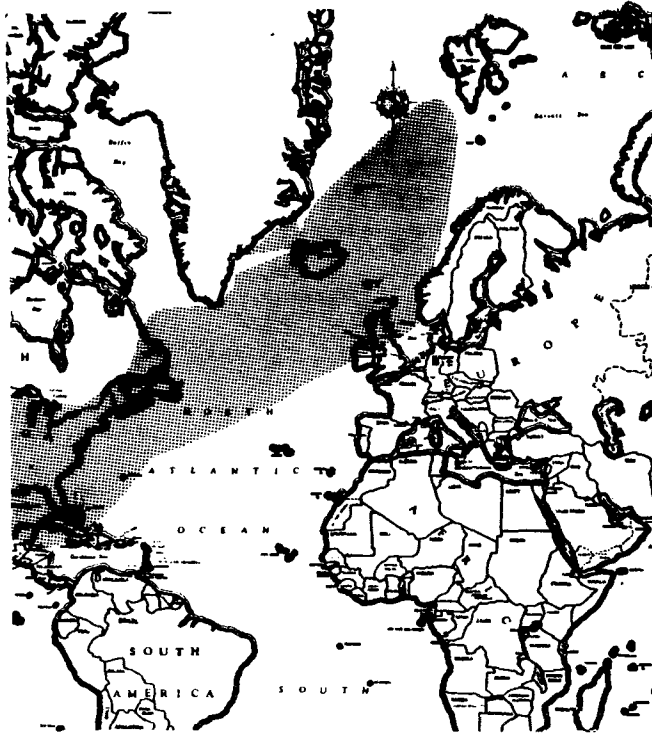
From the time that the LORAN-C system was designated as the primary radionavigation system for the coastal confluence zone of the United States, it was destined to become the most extensive high accuracy radionavigation system serving the United States maritime community. The high accuracy and reliability of the LORAN-C system has also gained it many users outside the maritime community. It is a time standard used by laboratories and industry throughout the world and it has found extensive applications in exploration for resources. In addition it has found use as a land vehicle monitor system and has recently been approved by the Federal Aviation Administration for certain enroute and terminal aircraft operations. Today aviation, especially general aviation, is the fastest growing LORAN-C user community.

Today's LORAN-C system covers the total coastal confluence zone of the

United States, except for the Caribbean Islands, and two thirds of the land area of the United States. In addition to providing coverage in the United States LORAN-C provides coverage of the Canadian coastal confluence zone and parts of the North Atlantic Ocean, Norwegian Sea, Mediterranean Sea and Western Pacific Ocean. The LORAN-C coverage is shown in figure (1). The LORAN-C system is also expanding. The Canadian Coast Guard will commission a new LORAN-C station at Fox Harbor Labrador on December 31, 1983. The Fox Harbor station will operate as master for the newly formed Labrador Sea Chain. The Labrador Sea Chain will add LORAN-C coverage as indicated in figure (2). The Saudi Arabians are adding LORAN-C coverage along their entire coast and the French are adding coverage along their Atlantic coast.

An examination of coverage charts for existing and proposed radionavigation systems (ref 1) reveals much duplicate coverage. This duplication of coverage led





LORAN-C COVERAGE AFTER 1 JANUARY 1984
 COVERAGE CHANGE IN ICELANDIC AND IN
 LABRADOR SEA CHAINS

FIGURE 2

to charges of government waste due to unnecessary proliferation and overlap of radionavigation systems. The U.S. Government radionavigation planning process is designed to preclude proliferation and overlap of radionavigation systems. The planning will have an impact on the future of the LORAN-C system. We must examine this planning process to assess the future of the LORAN-C system.

Prior to 1978 all radionavigation planning for civil users was conducted by the Department of Transportation and the specific agency concerned with each user group i.e. the FAA for air users and the Coast Guard for marine users. The planning documentation was contained in the National Plan for Navigation. In this same time period all radionavigation planning for military users was conducted by the Department of Defense. This planning documentation was contained in the JCS Master Navigation Plan.

In March of 1978 the United States General Accounting Office published a report titled "Navigation Planning -- Need for a New Direction". This report criticized the various agencies and departments of the federal government, specifically the Departments of Defense and Transportation, for building and operating radionavigation systems that were potentially unnecessary due to what the General Accounting Office considered proliferation of systems and overlap of system capabilities. The General Accounting Office report recommended that a government wide plan be developed to reduce the unnecessary proliferation and overlap of federally operated radionavigation systems. The report also stated that a strong central management focus was needed to plan and direct government wide radionavigation matters.

The General Accounting Office report prompted Congress to legislate a degree of control over the proliferation of federally operated radionavigation systems. The legislation was contained in section 507 of the International Maritime Satellite Communications (INMARSAT) Act (Public Law 95-564 November 1978). Section 507 of the INMARSAT act directed that:

"(a) The President, in conjunction with government agencies which will or may be affected by the development of a government wide radionavigation plan, shall conduct a study of all government radionavigation systems to determine the most effective manner of reducing the proliferation and overlap of such systems. the objective of such a study shall be the development of such a plan."

"(b) The President shall transmit a report to the congress no later than 12 months after the date of the enactment of this title relating to the study conducted under subsection (a) of this section. Such report shall contain a detailed statement of the findings and conclusions of such study, any action taken by the President related to such findings and conclusions, and any recommendations of the President for such legislation or other action as the President considers necessary or appropriate for implementation of a government wide radionavigation plan."

These events of 1978, particularly the INMARSAT act, resulted in the formation of an interagency study group to provide the required study of federal radionavigation planning. This study group was co-chaired by the Office of Management and Budget and the National Telecommunications and Information Agency. The study group was composed of the Department of Defense, the Department of Transportation, the National Aeronautics and Space Administration, the Department of State, the Department of Commerce and the Central Intelligence Agency. The study resulted in coordinated Department of Transportation and Department of Defense radionavigation

planning and the publication of the document known today as the Federal Radionavigation Plan. The study also recommended that the Departments of Transportation and Defense revise the Federal Radionavigation Plan periodically. This recommendation was accepted.

The Federal Radionavigation Plan thus prepared is periodically revised thru joint efforts of the Departments of Transportation and of Defense. The Department of Transportation looks after the interests of the civil user for civil and joint civil/military radionavigation systems. The Department of Defense looks after the military user for military and joint civil/military radionavigation systems. The purpose of the Federal Radionavigation Plan is to:

- Present an intergrated federal military and civil policy and plan for all common civil/military radionavigation systems.
- Provide a comparison of civil and military radionavigation systems on a common basis.
- Present an approach for achieving the maximum consolidation of civil and military radionavigation systems.
- Provide a multi-year plan for federally operated radionavigation systems.
- Provide government radionavigation planning information for users and manufacturers.

The planning process established by the Federal Radionavigation Plan cites two key decision points for selecting the post 1995 mix of federally operated radionavigation systems. The first is a 1983 preliminary recommendation. This preliminary recommendation will be included in a 1984 revision of the Federal Radionavigation Plan and will be open for public comment. The second event is a 1986 national decision.

The Secretaries of Defense and Transportation will consider all radionavigation systems, for both surface and air users, in determining the preliminary recommendation for the future radionavigation systems mix. The preliminary recommendation has not been published as of the writing of this paper, however, an examination of the capabilities of each radionavigation system, the needs of each navigation user group and the economics of various combinations of radionavigation systems will give us a good idea of the future of existing radionavigation systems and some insight as to what role planned radionavigation systems, such as the NAVSTAR GPS satellite system, will play in the future mix. This analysis will also allow us to make some predictions about the future of LORAN-C.

As previously mentioned the preliminary radionavigation systems mix will consider all existing systems and all

planned systems. The systems considered are LORAN-C, OMEGA, VOR, VOR/DME, VORTAC, TACAN, ILS, TRANSIT, Radiobeacons, MLS and NAVSTAR GPS. It will also consider the marine, air and land user. To start our analysis we must first look at the requirements of the users.

The requirements of the marine user can be categorized under the ocean, coastal and the harbor and harbor approach phases of navigation (ref 2). The ocean phase of marine navigation is that phase of navigation that occurs more than 50 nautical miles from land and beyond the continental shelf. The continental shelf is generally defined as waters within the 200 meter curve. The oceanic phase of marine radionavigation can be satisfied by a system that has a predictable 2 to 4 nautical mile 2 drms accuracy, however a 1 to 2 nautical mile 2 drms accuracy is preferred. The maximum interval between fixes must be 2 hours or less, however, 15 minutes or less is desirable. The signal should be available at least 95% of the time.

The coastal phase of marine navigation is navigation conducted within 50 nautical miles of land or on the continental shelf when the safe water path is 1 nautical mile or more for one way traffic and 2 nautical miles or more for two way traffic. The coastal phase of marine navigation requires a higher degree of radionavigation accuracy than does the ocean phase. The requirements for safety of navigation for large vessels can be satisfied by a system that provides an accuracy of 0.25 nautical mile 2 drms and a position fix at least every 15 minutes. The requirements for safety of navigation for small vessels and pleasure boats can be satisfied by a system providing 2 nautical mile 2 drms accuracy and a fix at least every 15 minutes. The radionavigation system serving these users must have a signal availability greater than 95%. There is an additional requirement placed on mariners in the coastal phase of navigation when in U.S. waters. U.S. regulations (33 CFR part 164) requires vessels of 1600 gross tons or more to have a LORAN-C or satellite navigation receiver installed.

The harbor and harbor approach phase of marine navigation is navigation in any inland waters, harbors or waterways more restricted than defined by the coastal phase. The accuracy requirements for safety of navigation in the harbor and harbor approach phase vary from 8 to 20 meters 2 drms. Safety of navigation in the harbor and harbor approach phase also requires a fix frequency of 10 seconds and a radionavigation signal availability of 99%. These requirements stem from the need to navigate very large vessels through congested harbors and in channels with a precision measured in tens of feet.

The maritime user of the radionavigation systems has some needs that can be classified as economic rather than safety of navigation. These economic needs tend to relegate a particular radionavigation

system to a particular user nearly as much as the safety of navigation requirements do. The large ocean going vessels may derive an economic benefit from a long range radionavigation system in spite of moderate accuracy or infrequent fixes, the commercial fisherman and coastal trade vessel is frequently at an economic disadvantage with these same characteristics. In the oceanic phase of navigation economic benefits are most often derived from a system that provides from 10 to 460 meters 2 drms accuracy and a maximum fix interval of from 1 to 5 minutes. In the coastal phase of navigation accuracy requirements, to obtain economic benefits, vary from 1 meter 2 drms for science, hydrography and resource exploration to 460 meters 2 drms for most other users. Other maritime operations, such as commercial fishing, derive economic benefits from a radionavigation system that provides a very high, 20 to 90 meter, repeatable accuracy thus permitting return to a particular location without regard to its precise geographic coordinates. (ref 3)

The requirements of the air user of radionavigation can generally be categorized under two distinct phases; the approach and landing phase and the enroute and terminal phase. These phases of air navigation are further broken down into many sub-phases, each of which has its own unique requirements. The approach and landing phase is broken down into precision and non-precision approaches. The enroute and terminal phase is broken down into oceanic, domestic, terminal, remote and helicopter operations.

The requirements for safety of navigation in the air are defined much differently than are the requirements for marine navigation. They are defined based on the capabilities of the existing systems (ref 4). At first this seems like an unusual way to define user requirements, but it has merit when one looks at the system of airways and the need for a term of reference that will make safe maximum use of the airways. The airways are created and marked, in accordance with international standards, by radionavigation signals such as VOR. User needs are defined in terms of radionavigation necessary to use these airways. In the oceanic sub-phase of air navigation there is not a universally accepted navigation system and there is not the capability for radar assistance. In this area aircraft tracking is accomplished primarily through position reports and navigation conducted through use of long range or internal systems. In the oceanic sub-phase of air navigation accuracy of 12.6 nautical miles is acceptable. This figure could change in the future if systems are available to allow closer control of aircraft and more efficient use of the airways. In the domestic, terminal, remote and helicopter sub-phases of air navigation the accuracy requirements can vary from 1,800 meters to 14,400 meters depending upon specifics of operation in the sub-phase. The specific requirements for the enroute and terminal phase of air navigation are tabulated in

figure 3.

The safety of navigation requirements for the approach and landing phase are much more precise than are those for the enroute and terminal phase. The non-precision approach sub-phase requires a system accuracy in the order of 100 meters 2 drms. This accuracy can usually be met by general purpose radionavigation systems. The precision sub-phase requires an accuracy of from plus or minus 0.5 to 3 meters 2 drms. This accuracy usually requires a dedicated radionavigation aid. The specific requirements for the approach and landing phase of air navigation are tabulated in figure 3.

The economic benefits that an aviator derives from specific levels of radionavigation accuracy are difficult to quantify. The existing systems, whose accuracy define the system, provide the user with entry to the airway system and all of the benefits of the system. Any change to system requirements would create an economic burden to the user as the user would be required to update his equipment to continue to derive the benefits of the airway system.

The land use of radionavigation can also be divided into phases. These phases are automatic vehicle monitoring and site registration. There is a very small number of land radionavigation users, therefore the requirements for this user group are defined more in theory than in actual practice (ref 5). The accuracy requirements for land use radionavigation will vary between 100 feet and 10,000 feet. These accuracy requirements are defined in figure 4.

With the foregoing requirements of the various radionavigation user groups in mind we can look at the capabilities of LORAN-C and other radionavigation systems to determine how the systems meet user needs and identify the overlap cited in the GAO report. This type of a determination is also the first step in the selection of the future mix of radionavigation systems.

The United States participates in the operation of fourteen LORAN-C chains. These chains provide navigational signals with a 500 meter 2 drms geographical and 18 to 90 meter 2 drms repeatable accuracy throughout the coverage area shown in figure 1. LORAN-C chains provide navigational availability exceeding 99.7%. The LORAN-C fix rate is 10 to 20 fixes per second depending upon the group repetition interval of the particular chain.

The OMEGA system is operated as a cooperative effort of seven nations. The U.S. has paid all construction costs. The U.S. operates two of the eight OMEGA stations and funds the operation of two others. OMEGA provides 2 to 4 nautical mile 2 drms radionavigation accuracy worldwide. It provides the three signals necessary for a fix 95% of the time. The fix rate is one independent fix every 10 seconds. OMEGA is also used in the dif-

ferential mode to increase accuracy. Differential OMEGA has been shown to provide accuracies of 500 meters 2 drms in an area of up to 50 nautical miles from the differential station (ref 6). This accuracy decreases to 1 nautical mile 2 drms at 500 nautical miles from the differential station.

Aeronautical and marine radiobeacons operating in the low and medium frequency band provide angular bearing information. Two or more of these bearing lines can be combined for a fix. There are 600 federal, 1,200 private and 200 military aeronautical radiobeacons. There are 200 federal marine radiobeacons. The accuracy of radiobeacons is a function of the angular characteristics of the signal therefore it is not normally expressed in a precise distance as is other systems. The radiobeacon accuracy is generally considered as plus or minus 3 to 10 degrees and signal availability is 99%. The fix rate is continuous unless a beacon is sequenced. For a sequenced beacon the fix rate is dependent upon the sequence time duration.

TRANSIT is a military satellite based radionavigation system that provides worldwide navigation coverage with a fix accuracy of 25 to 500 meters depending upon the receiver and the vehicle dynamics. The TRANSIT satellites provide availability of 99%, however fixes are only available when a satellite is in view. Since the fix rate is dependent upon the period that a satellite is in view it normally varies from about 30 to 110 minutes.

The very high frequency omni-directional range (VOR) is the primary directional navigation system for civilian aviation use. It is an angular system and therefore its accuracy is expressed in angular measure rather than a precise position. The VOR station has an accuracy of plus or minus 1.4 degrees. The VOR station provides continuous fixes with a signal availability approaching 100%. The distance measuring equipment (DME) is a companion to the VOR system. With a single DME and VOR signal a pilot can determine his actual fix. A pilot is also able to determine his fix with two VOR bearings or two DME distances. Determining a fix with two DME distances is rarely done. DME provides nearly continuous distance information accurate to 0.1 nautical mile. DME equipment availability also approaches 100%. The VORTAC and TACAN systems operational characteristics are similar to those of the VOR and DME system.

The aircraft landing systems, ILS and MLS, are very specialized systems. They provide precise navigation for aircraft in the approach and landing phase of air navigation. These systems cannot be replaced by a general purpose navigation system. They will not be discussed further in this paper as they can not be considered as duplicating LORAN-C coverage and their future will not have any impact on the future of LORAN-C.

There is one radionavigation system whose capabilities we have not yet looked at, that is the NAVSTAR GPS satellite navigation system. NAVSTAR GPS is a new system being implemented for national security. It will have an ability; however, to provide highly accurate radionavigation to civil users anywhere in the world. Civil users will experience some degradation of NAVSTAR GPS navigation signal accuracy to protect the national interests of the United States and NATO. The NAVSTAR GPS system will consist of 18 operational and 3 operating spare satellites in six coplanar orbits. NAVSTAR GPS will provide civil users with 100 meter 2 drms navigational accuracy anywhere in the world. The NAVSTAR GPS fix rate will be nearly continuous; anything less than continuous will be due to user equipment parameters. NAVSTAR GPS availability will approach 100%. If present schedules are met the NAVSTAR GPS system will be on air in 1989.

Now that we have defined radionavigation user requirements and the capabilities of U.S. Federally operated radionavigation systems a picture starts to emerge indicating why the General Accounting Office made the original allegations of radionavigation proliferation and overlap. As a recap we can summarize the various radionavigation users and the systems that are in place or planned that will fulfill their needs.

There are many radionavigation systems available to the mariner. In the ocean phase of navigation he has OMEGA, TRANSIT and LORAN-C (limited coverage areas) available. When it becomes operational NAVSTAR GPS will also meet his needs. When the mariner enters the coastal phase of navigation he has TRANSIT, LORAN-C, Marine Radiobeacons and Differential OMEGA (limited coverage areas) available. Again NAVSTAR GPS will meet the mariners needs in this phase of radionavigation. In the harbor and harbor approach phase of marine navigation there is no existing or planned radionavigation system that will meet the mariners needs. There are studies to evaluate the effectiveness of differential LORAN-C and differential NAVSTAR GPS to determine if sufficient accuracy and signal availability can be achieved.

The aviation user of radionavigation also has more than one radionavigation system to serve his needs. The enroute and terminal phase of air navigation is served by VOR, VOR/DME, VORTAC, TACAN, LORAN-C, OMEGA and Aeronautical Radiobeacons. VORTAC and TACAN are used primarily by the military. The LORAN-C and OMEGA systems are limited to specific areas due to their characteristics. LORAN-C is also limited in that it does not cover the mid section of the North American continent. OMEGA accuracy limits its use to oceanic, high altitude or remote operations. In the non-precision approach sub-phase of navigation the aviator has all of the previous systems, except LORAN-C and OMEGA available. When making a precision approach the aviator is served by the ILS

and MLS system. When it becomes operational, NAVSTAR GPS has the potential to serve all of the aviator's needs except for those associated with the precision approach sub-phase. The Department of Transportation and Department of Defense are working together to resolve coverage, availability and integrity questions that could limit NAVSTAR GPS's use in civil aviation.

The land user of radionavigation is served by LORAN-C and TRANSIT. This user group will also be served by NAVSTAR GPS when it becomes operational.

The foregoing discussion indicates a level of redundancy in the federally operated radionavigation systems. It appears that a straight forward economic analysis would allow the Departments of Transportation and Defense to prepare their 1983 recommendation for the future mix of federally operated radionavigation systems. This is not the case however as there are a number of issues that are institutional in nature that must be resolved prior to making the recommendation.

The first of these institutional issues is cost recovery. There are various tax systems in effect today that recover some of the federal cost for navigation and air traffic control services. Fuel taxes and passenger ticket taxes are examples of these cost recovery techniques. These methods, however do not impose a direct charge for a safety service such as navigation. With the development of NAVSTAR GPS Congress has directed a comprehensive plan be developed to recoup as much of the development, acquisition and operational NAVSTAR GPS costs as feasible.

Another major institutional issue is international acceptance of a radionavigation system. The VOR, DME and Radiobeacon systems are international standard systems. LORAN-C and OMEGA, although not officially standardized, are widely used and accepted. The TRANSIT system, also not officially standardized, is widely used and accepted by the maritime community. The NAVSTAR GPS system is not internationally standardized or accepted and may have great difficulty gaining international standardization and acceptance. This is due to the fact that it will be operated and controlled by the U.S. military. This military control factor is emphasized by the wide publicity given to the accuracy denial and the fact that NAVSTAR GPS service may be denied in the event of a national emergency.

In preparing their 1983 recommendation for the post 1995 mix of federally operated radionavigation systems the Secretaries of Transportation and Defense are looking at all of the preceding factors. They are also examining the economics of each radionavigation system or combination of systems and national security needs. They are expected to make their recommendation in late 1983.

Some general conclusions regarding the post 1995 mix of U.S. federally operated radionavigation systems can be made prior to the official policy statement by examining the available facts. The first and most obvious conclusion is that NAVSTAR GPS, with its 100 meter 2 drms accuracy and worldwide coverage, will duplicate and in most cases exceed the capability of existing radionavigation services. The government's stated policy to reduce the proliferation and overlap of radionavigation systems and the national support for NAVSTAR GPS will mandate that some of the existing radionavigation systems be phased out. The government has already announced a 1992-1996 phaseout for overseas LORAN-C stations (ref 7). That is U.S. operation or funding of these stations. The U.S. Government has also announced a 1992 phase out for the TRANSIT and TACAN systems (ref 8). That leaves domestic LORAN-C, OMEGA, VOR, DME and radiobeacons open for discussion.

The radiobeacon service is a relatively low cost high benefit service. A radiobeacon station costs the government less than \$50,000 a year to operate compared to the approximately \$500,000 for a LORAN-C station. The marine radiobeacon user equipment costs \$100 to \$500 compared to \$1,000 to \$23,900 for LORAN-C equipment and a projected \$4,200 to \$26,300 for NAVSTAR GPS equipment (ref 9). These economic factors will favor continued use of radiobeacons for general purpose navigation. The U.S. Government has previously stated (ref 8) an intent to continue marine radiobeacons indefinitely.

The LORAN-C, OMEGA and VOR/DME systems are higher cost systems for the government to operate. Their service will be, in many cases, duplicated by the NAVSTAR GPS system. It is logical to assume some reduction in these systems. Major considerations will be international obligations and phase out costs to users. The phase out of these would be after a suitable overlap or transition period. If a system is phased out, a 15 year overlap with the replacement system could be expected.

In summary, for the LORAN-C system's future we can expect to see overseas LORAN-C, that is operated by the U.S. Government phased out in the early 1990's. We eventually expect to see some reduction or a phase out of domestic LORAN-C in favor of NAVSTAR GPS. The domestic reduction or phase out, if it occurs, will not be before the year 2000.

Phase	Sub-Phase	Altitude (Flight Level)	Traffic Density	Route Width (NM)	Source Accuracy 2 drms (meter)	System Use Accuracy 2 drms (meters)
EnRoute/ Terminal	Oceanic	FL 275 to 400	Normal	less than 60		better than 12.6nm
	Domestic	FL 180 to 600	Normal	8	1000	3,600
			High	8	1000	3,600
		500 ft to FL 180	Normal	8	1000	3,600
	Terminal	500 ft to FL 180	High	4	500	1,800
	Remote	500 ft to FL 600	Normal	8 to 20	1000 to 4000	3,600 to 14,400
	Helicopter Operations	500 ft to 5000 ft	Low (Off-Shore)	8	1000	3,600
500 ft to 3000 ft		High (Land)	4	500	1,800	
Approach and Landing	Non-Precision	250 to 3000 ft. above surface	Normal	1 to 2	100	150
	Precision	Cat I	100 to 3000 ft. above surface	Normal	± 9.1 meters*	± 3 meters**
					at 100 ft. above Surface	
	Cat II	50 to 3000 ft. above surface	Normal	± 4.6 meters	± 1.4 meters	
				at 50 ft. above Surface		
Cat III	0 to 3000 ft. above surface	Normal	± 4.1 meters	± 0.5 meters		
			at Surface			

- * This column is the 2 sigma lateral accuracy in meters
- ** This column is the 2 sigma vertical accuracy in meters

AIR NAVIGATION REQUIREMENTS FIGURE 3

APPLICATION	REPEATABLE ACCURACY (2 drms) *	COVERAGE	AVAILABILITY	FIX RATE **	FIX DIMENSION	CAPACITY	AMBIGUITY
Public Safety Urban Police, EMS Rural Police, EMS State Police	250 ft. 1000 ft. 1000 ft.	Urban Area County State	99.7%	1 sec. 1 sec. 1 sec.	Two	Unlimited	Resolvable with 99.9% Confidence
Transportation Urban Buses Taxi Delivery Truck Truck (Hazardous Cargo)	500 ft. 500 ft. 1000 ft. 10000 ft.	Urban Area Urban Area Urban Area Nationwide	99.7%	1 sec. 1 sec. 1 sec. 1 sec.	Two	Unlimited	Resolvable with 99.9% Confidence
Highway Safety Planning (Traffic Records, Highway Inventory, Highway Main.)	100 ft.	State	99.7%	1 sec.	Two	Unlimited	Resolvable with 99.9% Confidence
Resource Management	100 ft.	Nationwide	99.7%	1 sec.	Two	Unlimited	Resolvable with 99.9% Confidence

- * Requirement under study, values noted are current estimates.
- ** Fix Rate of navigation system, user update rate dependent on application and characteristics of communication link.

LAND USE REQUIREMENTS FIGURE 4

References:

1. "Federal Radionavigation Plan" (U.S. Department of Defense Ref. No. DOD-4650.4-P-1 and U.S. Department of Transportation Ref. No. DOT-TSC-RSPA-81-12-1 Mar 1982), Vol III.
2. Ibid, Vol II, Chapt 3
3. Internal DOT memo of 23 May 1983.
4. "Federal Radionavigation Plan" (U.S. Department of Defense Ref. No. DOD-4569.4-P-1 and U.S. Department of Transportation Ref. No. DOT-TSC-RSPA-81-12-1 Mar 1982), Vol II, Chapt 2.
5. Ibid, Vol II, Chapt 4
6. "Differential OMEGA Station" (Sercel France), p.3
7. Pealer, Nevin A. "Status of Civil Marine Radionavigation Systems" Proceedings of the Surface Transportation Users Conference (U.S. Department of Transportation Report DOT-TSC-RSPA-83-1, Apr 1983), p.35
8. Martel, John "Status of DOD Radionavigation Systems" Proceedings of the Surface Transportation Users Conference (U.S. Department of Transportation, Report DOT-TSC-RSPA-83-1, April 1983), p.13
9. Dick, William G. "Radionavigation Economic Planning Model Scenario Evaluation Report" U.S. Department of Transportation, Transportation Systems Center July 1983, p.2-9.

SESSION TWO SPEAKERS



Leo Fehlner



Vern Johnson



Marty Poppe and Per Enge



David Wells



CDR Tony Pealer

SESSION THREE

CHAIRMAN

Cdr D Clements
Coast Guard Pacific Area

DESLOT: AN ACCEPTABLE ALTERNATIVE?

LTJG R.H. Orr
U.S. Coast Guard
COMMANDANT (G-NRN)
U.S. Coast Guard Headquarters
2100 2nd Street, S.W.
Washington, D.C. 20593

ABSTRACT

Before January 1982, all standby transmitters at tube-type Loran-C stations were "powered-up." In January of 1982 the Coast Guard began an experiment to determine the potential energy savings at Loran stations and the effect on operation of the Loran program by securing the standby transmitter completely. Five Loran-C transmitting stations have received the DESLOT modification, although the program is still considered experimental. At risk is the Coast Guard's impressive Loran signal availability percentage. This paper describes and discusses DESLOT (De-Energized Standby Loran Transmitter) - its pros and cons.

DESLOT

The acronym DESLOT stands for De-energized Standby Loran Transmitter. Before DESLOT, all tube type Loran-C transmitting stations operated with the standby transmitter "powered-up." That is, all filaments and biases were on with only plate voltages off. If the operate transmitter failed, the "Transmitter Automatic Controller" (TAC) would sense the off air, switch transmitters, and apply B+ to the standby transmitter. The wisdom of keeping the standby "hot" was not questioned until recently. In early 1981 we received a proposal from our Fourteenth District office in Hawaii for a modification which would leave the standby transmitter "cold," resulting, hopefully, in lower fuel and electricity costs. The modification would enable the TAC to start the standby, warm it up, and apply B+ after 90 seconds. The initial reaction was interesting. It was suggested that the originator of this idea should be labeled a heretic and burned at the stake. There was much discussion about "reduced filament/tube life," "filament stress," "gassey tubes," "condensation," "thermal shock," and the possibility of increased bad time. There were many opinions, but there would be no way to tell whether or not it would work if we didn't try it somewhere. Since at the time we were unable to otherwise obtain an engineering evaluation of DESLOT, in December 1981 the Office of Navigation authorized installation of the modification at the CENPAC (4990) LORSTAS Upolu Point, Johnston Island, and Kure Island.

DESCRIPTION

The DESLOT modification itself is actually quite simple. It consists of a few relays and switches which allow the standby transmitter to be completely de-energized while still fully controllable from the TAC. The cost of the modification per station is about 450 dollars, and can be accomplished by two technicians in a few hours.

A front panel switch allows selection of the "DESLOT" or "Non-DESLOT" mode of operation. In the Non-DESLOT position, the transmitter operates as it did prior to the mod. In this mode, if the TAC senses an operate transmitter failure or power below 50%, it will initiate and complete a trans-

mitter switch in 40 to 60 seconds. In the DESLOT mode, in the case of an operate transmitter failure, the standby is automatically warmed up and placed on air 90 seconds from the time of failure. If the "switch xmtr" button on the TAC is depressed, the switch is completed in 60 seconds as before.

DISCUSSION

Obviously, this 90 second potential off air has become a point of controversy, especially among those of us who know what it was like to stand bleary-eyed in front of an oscilloscope presentation of the pulse for eight hours at a time, writing on chart recorders 24 hours a day, always shooting for that elusive 100%. Of course, if we went off air for 60 seconds or less, it wasn't really bad time. No blink was required, so we could pretend nothing really happened. Now it has been proposed to go over that magic 60 seconds, and blink (that dirty word!) is inevitable.

Let us consider some operational realities. First of all, the DESLOT mod is only being used in the unique situation of an operate transmitter failure. How often does this occur? Once a month? Twice? There are a lot of other ways to buy 90 seconds of bad time. Second, we're not really talking about 90 seconds, only the extra 30. The operate transmitter would have failed anyway. And finally, the most important factor: DATA. One simply cannot come to a conclusion concerning an hypothetical situation without experiment and observation.

DATA:

The Data received so far from the first four stations to receive the mod indicate no increase in unuseable time due to DESLOT. Indeed, there appears to actually be an improvement not only in availability, but in other areas such as generator efficiency, transmitter maintenance requirements, tube life, and most importantly, energy costs at both generator powered and shore powered stations.

1. The energy savings at CENPAC alone for the first year was over \$112,000, a savings of 18-20%.

2. Energy savings at Yap, an AN/FPN-45 transmitter station, which generates its own power and has a significantly larger power demand than the CENPAC AN/FPN-42's, have been about \$82,000 or about 19%.

3. Generator efficiency at Yap has increased by about 8%. More kW per gallon are being produced because of the lighter load.

4. A review of monthly reports has shown equal or better performance at all LORSTAS concerned since installation.

5. Component failure analysis has shown no increase of failure due to DESLOT. In fact it appears that tube life has increased due to the reduction of filament hours.

6. Preventive maintenance manhours have decreased approximately 15% apparently due to the decrease in operating time and the lower levels of dirt entering the transmitter via the cooling system.

7. No adverse effect on pulse shape/signal parameters.

a. For a hot standby, the amount of ECD change was normally about .1 microseconds.

b. For a cold standby (DESLOT), ECD change has been about .1 to .2 microseconds.

c. In both cases, ECD stabilizes within 1/2 hour.

8. Condensation was a predicted problem. Not only has condensation not increased, but previous condensation problems have disappeared.

IMPLEMENTATION:

Although we had already collected a large amount of data from the CENPAC and Yap installations, we were not ready to recommend blanket modification of all tube type transmitters in the field before a few more questions were answered. So far, the stations that had received the mod were all in similar climates. Hokkaido was the next station chosen because of its location and the fact that it is a dual rated AN/FPN-45. Hokkaido's installation was completed in mid-June, 1983. We have not yet received a 6-month report on Hokkaido's operation.

In July, 1983 it was decided that our Engineering Center in Wildwood, New Jersey would take over evaluation of the modification, with the possibility in mind of expanding DESLOT to all CONUS tube-type stations. Two stations were chosen for this engineering evaluation because of their location and configuration: Tok, Alaska, an AN/FPN-44, which was installed in September, and Baudette, Minnesota, a cold-climate AN/FPN-42, which will be modified in October or November.

CONCLUSIONS:

We expect the final engineering evaluation by April or May 1984, with a recom-

mendation of whether or not to proceed with DESLOT as a field change for all AN/FPN-42, 44, 44A, and 45 transmitting stations. If the program continues to return the kind of results we have seen thus far, we are probably looking at implementation Coast Guard wide. The applicability of DESLOT to our AN/FPN-39 transmitters in Europe has not yet been formally addressed, but will probably be discussed seriously in the near future.

AUTOMATIC AIRCRAFT/VESSEL TRACKING SYSTEMS

A. William Marchal
Vice President
Offshore Navigation, Inc.

Positive air traffic control in the U. S. national Air Space has been a routine matter for decades with ground radar covering all but some remote overland areas for enroute, terminal, and approach operations. Such is not the case, however, for the offshore helicopter operations in the Gulf of Mexico.

The Gulf Coast offshore IFR route structure consists of a number of radials from each of several coastal VOR's along Louisiana and Texas. In the absence of shore based radar coverage for the 3000-5000 ft. altitudes of helicopter IFR flights, the Houston Air Traffic Control Center has had to rely on periodic verbal position reports from the pilots. With this limited information, the FAA uses altitude separation with 10 to 20 miles between aircraft on a given radial.

In 1979, ONI proposes a joint program to the FAA to evaluate an automatic flight following concept based on telemetering the aircraft position derived from the on-board navigation system (Loran-C in this case) to a base station where the position would be displayed along with aircraft ID and altitude on a high resolution TV monitor, which would emulate an air traffic control radar presentation. The idea was accepted, and ONI worked jointly (but not under contract) with the FAA to develop the airborne equipment and the computer controlled base station display system. ONI developed and manufactured the FLITE-TRAK 100 airborne telemetry system to be compatible with the FAA specification for the signal in space, and a commercial version of the base station designated the FLITE-TRAK 600. DOT's Transportation System Center in Cambridge, Massachusetts was tasked with the development of the first generation LOFF (Loran Flight Following) base station for the Houston Center. This coincided with the expansion of the FAA's Gulf Coast VHF radio network to include a number of offshore stations, which were relayed ashore to the Houston Center via microwave/land line links. It was decided to share the FAA voice channel with the LOFF data for evaluation purposes, recognizing that ultimately, a separate data channel would be required.

Referring to Figure 1, the airborne telemetry unit accepts latitude/longitude position information from the onboard navigation system and transmits it along with the aircraft ID and altitude from an encoding altimeter over either an existing aircraft radio or a dedicated VHF transceiver in the FLITE-TRAK 100 Computer Unit automatically at a pilot

selected interval (nine steps from 15 to 300 seconds). The base station processes the received message for display on the color monitor screen with appropriate map overlays, and lists the information for each aircraft including ID, lat/lon, altitude, speed, heading, and flight plan on the system control/listing terminal.

Since the message from the aircraft included the automatic transmission interval, the base station will automatically alert the controller/dispatcher if one or more messages are missed. Once an aircraft is in the system (the first message automatically starts tracking in the base station), an aircraft cannot get out of the system without an alarm, unless it is closed out by the dispatcher. A MAYDAY button on the airborne control panel will send a message with a special format five times at two second intervals if activated by the pilot. The special format is recognized by the base station computer, and both visual and audible alarms are given.

Whereas the Houston Center LOFF base station display was designed to emulate ATC radar, ONI's FLITE-TRAK 600 was designed primarily for the aircraft operators where both the safety and efficiency of operations could be greatly improved with an automatic flight following system. The first FLITE-TRAK 600 systems installed were for Gulf Coast helicopter operations. The graphic display incorporates operator selected overlays, including the coastline, VOR's, bases, airports, offshore platforms, military training routes, radio coverage areas, pipelines, flight plans, and prestored search patterns for search and rescue operations. The operator's terminal used for system control lists all of the information on each aircraft. Additional features are incorporated to assist in dispatching such as listing along with distance and magnetic bearing the five closest objects on a given type to a specific aircraft. For example, the five closest platforms to an aircraft in trouble. Stored lists include fuel locations, hospitals, airports, platforms. Others can be specified by the customer. Gulf Coast FLITE-TRAK customers include Transcontinental Gas Pipeline Co. in Houston, Mobil Oil Co. in Morgan City, LA and Chevron Oil Co. in New Orleans. The Chevron system has two remote operator terminals at other Louisiana bases.

In February, 1984, the FAA replaced the first generation LOFF equipment in the Houston Center with a specifically modified FLITE-TRAK 600 base station with a color graphic

display. Although the evaluation period for the LOFF program is not over, people associated with the operations in the FAA's Southwest Region indicate unofficially that they expect the equipment to be required for offshore IFR helicopters within the next two years. The concept of non-radar dependent surveillance is getting a serious look by other regions for special areas not covered by radar.

In other areas of the world, Shell U.K. is installing a system offshore in the East Shetland Basin of the North Sea this spring to enhance their search and rescue capability. The Shell system will also eventually track suitably equipped vessel providing a complete transportation information system. In addition, Aramco is installing a FLITE-TRAK 700 system (see Figure 2) in Saudi Arabia in 1984. The 700 system utilizes the FLITE-TRAK 600 flight following as a front end with real time two-way digital communication, and feeds this information into a large data base system for complete aviation management, including aircraft and crew scheduling, cargo and passenger manifests, maintenance, inventory, and personnel records. The Aramco system will feature 16 remote terminals and handle over 40 rotary and fixed wing aircraft. Both the FLITE-TRAK 600 and 700 systems are customized for client requirements.

While the systems on the Gulf Coast utilize Loran-C as a position input, the FLITE-TRAK 100 will accept navigation data from a number of systems such as VLF/Omega, INS, or Decca over an ARINC 429 data bus. The present one-way capability will be expanded to incorporate ACARS two-way air/ground and ground/air data not limited to navigation and flight following. The FLITE-TRAK 100 will include HF operation as an option late in 1984.

Since the concept was first discussed in 1979, automatic aircraft position reporting has gained widespread acceptance as a very cost effective alternative to radar for aircraft surveillance. The British CAA is in the process of deciding on a specification for the VHF and HF signals in space for North Sea usage. Other governmental agencies have expressed an interest in the concept to supplement existing radar coverage or to provide position information where none exists. It is evident that the near future will see increased use of automatic aircraft position reporting systems.

The same concept of automatic position reporting used in the FLITE-TRAK system for aircraft is being utilized in a vessel collision avoidance warning system (CAWS) in New Orleans, LA. The Lake Pontchartrain Causeway is a twenty-four mile bridge connecting New Orleans with the North Shore. Since the first of the twin spans were completed in 1956, the bridge has been knocked down more than ten times by tug/barge traffic resulting in a number of deaths. As a result, the State of Louisiana contracted with ONI in 1983 to provide a Loran-C based warning system.

Referring to Figure 3, the mobile equipment consists of a portable unit containing a Loran-C receiver, VHF transceiver, a micro-processor controlled telemetry interface, and power supply with four hour battery backup. The Loran-C receiver and VHF transceiver share a common five whip antenna utilizing a specially designed coupler.

The unmanned base station located at the south end of the Causeway is depicted in Figure 4. Remote terminals are located at the Causeway administration building at the south end of the Causeway and at the Department of Wildlife and Fisheries Commission office at the New Orleans Superdome. The CAWS system is operated under the jurisdiction of the Wildlife and Fisheries in accordance with a state law that requires all tugs and self-propelled dredges to be equipped with a CAWS mobile unit when operating in the lake.

The CAWS base station has a map of the lake (Figure 5) stored in memory along with the Causeway, and two buffer zones with safety fairways for bascule crossings. The shipboard unit also has a map of the lake in memory and whenever it enters the lake, it automatically logs in with the base station. The base station polls all active units at a variable rate depending on their distance from the Causeway. If one of the vessels equipped with CAWS enters a buffer zone, the base station sends a signal to the vessel which activates an audible alarm on the bridge. This alarm can be silenced with the acknowledge button but if the vessel is still in the buffer zone when it is polled again, the alarm will again be sounded. In addition to the mobile unit alarm, the base station uses a computer driven voice synthesizer to broadcast a collision alert on the Causeway police radio frequency including vessel ID, point of impact, north or south-bound span, and time to collision. The police will then stop traffic at the appropriate point.

Once the shipboard unit is installed and power applied, no human action is required at either the mobile units or base station. The mobile unit cannot be turned off if the vessel is in the lake since the "ON/OFF" switch merely signals the base station with a request to turn off. The base station determines if the vessel is in the lake before sending a "PERMISSION GRANTED" signal to the vessel.

The Lake Pontchartrain CAWS system is the first such system ever implemented. Similar applications of the concept of automatic positioning of vessels are already being evaluated in areas such as Tampa Bay where Loran-C may again be used to protect life and property.

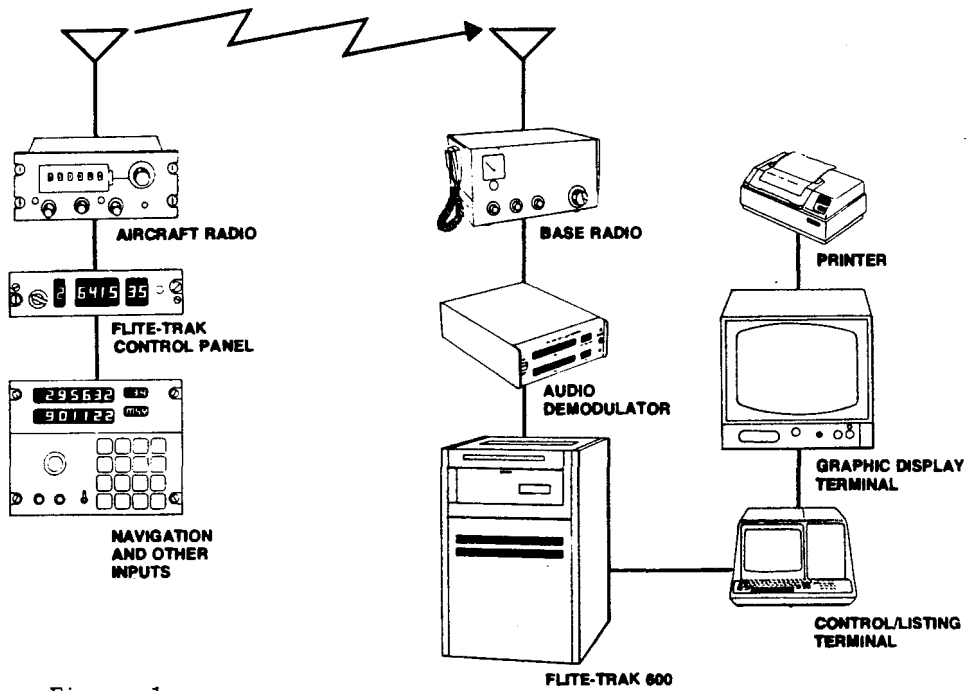


Figure 1

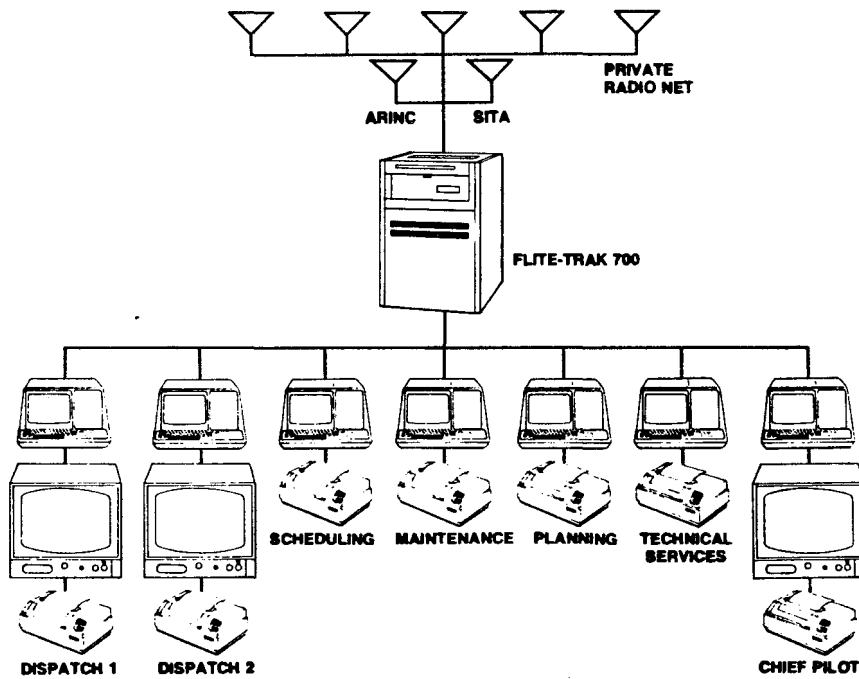
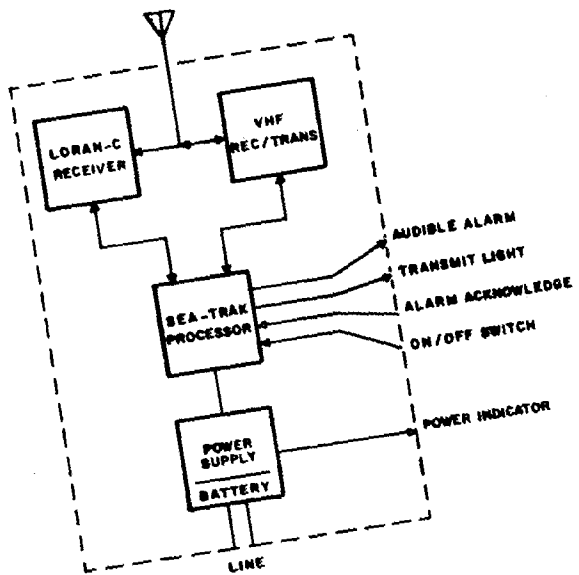
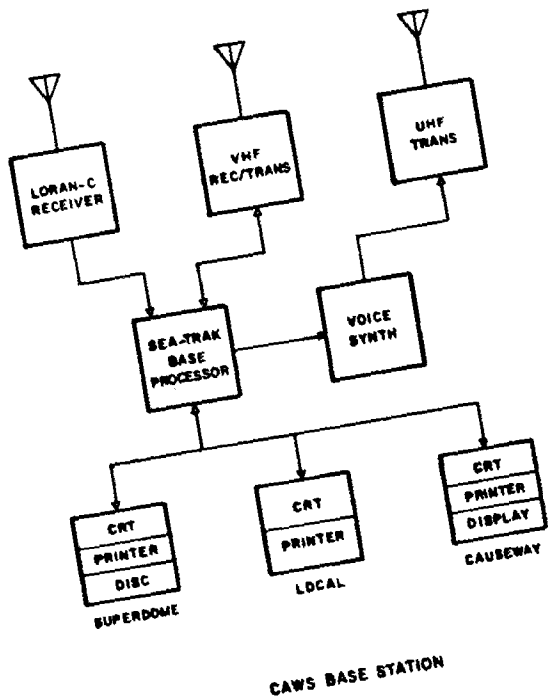


Figure 2



CAWS MOBILE STATION

Figure 3



CAWS BASE STATION

Figure 4

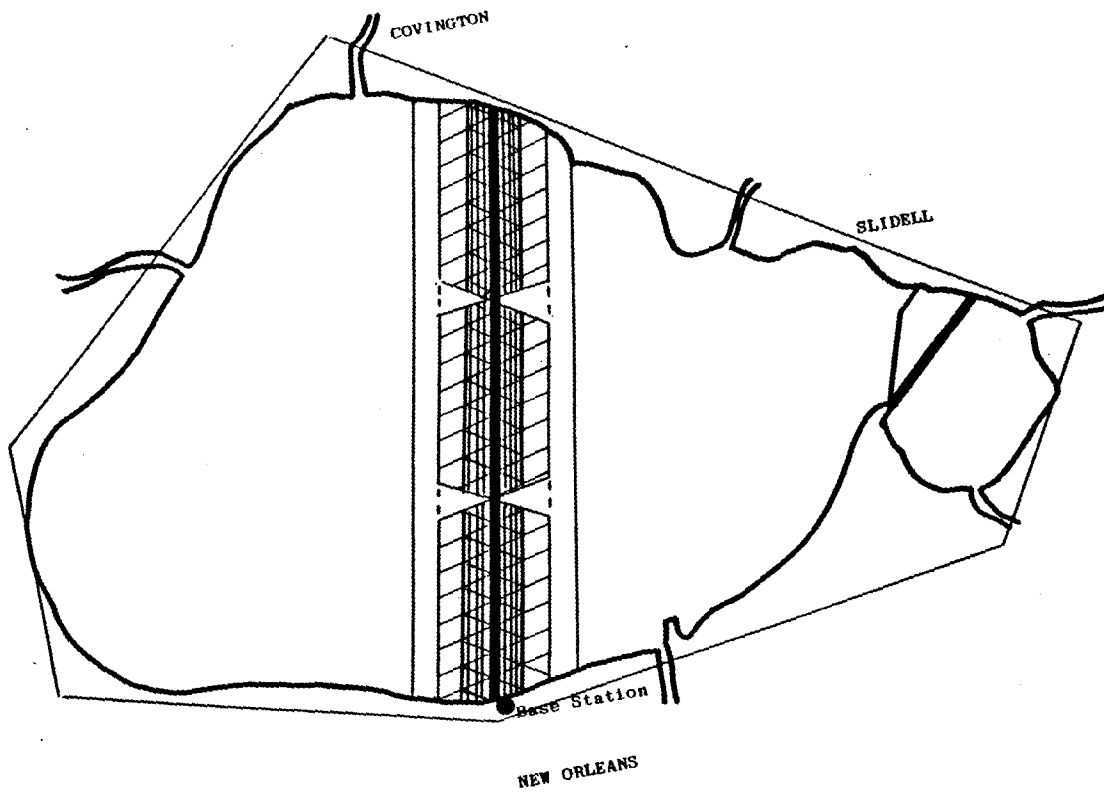


Figure 5

Laura G. Charron
Carl F. Lukac

U. S. Naval Observatory
34th Street and Massachusetts Avenue, N. W.
Washington, D. C. 20390

ABSTRACT

The problem of relating timed pulses of a Loran-C chain to the U. S. Naval Observatory (USNO) time scale is being gradually alleviated. Beginning in the 1960's, the USNO monitored the East Coast Loran-C chain at Washington, D. C. However, for those chains whose groundwave coverage does not include the Observatory, various methods had to be used to synchronize a chain to the USNO Master Clock (USNO MC). Portable clock visits to Loran monitoring stations have been a mainstay for years. However, their infrequent occurrences necessitated the need for devising analytical techniques which could reliably provide the difference USNO MC minus Loran to within half a microsecond. The advent of time transfers using the Defense Communication Agency satellites to calibrate cesium clocks at monitoring stations supplemented the analytical techniques. Today data from one of the most sophisticated navigation systems (Global Positioning System) is used as a calibration tool. This paper discusses the steps in the evolutionary process which have led to the current USNO program of remote time scale formation for Loran-C timing.

INTRODUCTION

The U. S. Naval Observatory (USNO) has been involved since its founding in providing time "to all who avail themselves thereof" as stated in its mission statement. As part of the Department of Defense (DoD) Directive 5160.51 of 31 August 1971, the Observatory was also required to provide means of traceability to the USNO Master Clock (USNO MC) for other DoD agencies and contractors. One means of doing this was by the publication of corrections to systems capable of providing a timing pulse. Such a system is the Loran-C system of the U. S. Coast Guard. The techniques used to determine the difference USNO MC minus Loran-C have evolved over the years. Figure 1 is a simplistic diagram of the steps in this evolutionary process of monitoring and calibrating the times of emission for Loran-C.

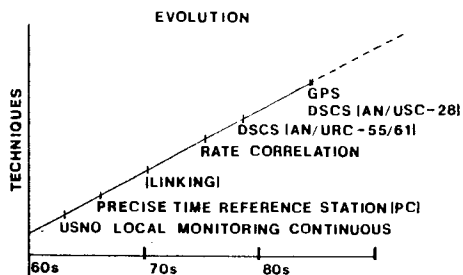


Figure 1. Progressive development of Loran-C calibration methods

This paper will discuss the steps which led to the current techniques for determining remote time scales for Loran-C chains and for calibrating those time scales.

DIRECT MONITORING

Beginning 1 June 1961, and since then without interruption, the USNO has monitored daily the East Coast Loran-C transmissions from Carolina Beach, North Carolina. At first the measurements were made manually. In the late sixties, these daily time-of-arrival (TOA) measurements against the USNO MC began to be published in a weekly "bulletin" now known as Time Service Announcement Series 4. Within a few years, requirements for such corrections to other Loran chains were apparent. Being outside of groundwave coverage of most chains, the Observatory turned to methods other than direct monitoring. Before discussing these different techniques, consideration is given to the improvements in the monitoring capabilities at USNO.

One of the first steps in improving the quality of available data was the establishment of automatic readings of TOA several times per day for several receivers by the Data Acquisition System (IBM 1800). These data from the different receivers were compared and an averaged difference of the value USNO MC minus the Loran-C chain was determined. By this time, delays due to propagation, receiver, antenna, etc. were being subtracted from the TOA data so that Time-Of-Emission was being published.

The next step in this upgrading was an improvement in the Data Acquisition and Control (DAC) system itself. The IBM 1800 was replaced by an IBM Series 1, backed up by a Hewlett-Packard (HP) 1000. The HP 1000 began making automatic hourly readings which could be evaluated.

The installation of an automatic Austron 2100 Loran-C receiver, combined with hourly readings initiated by the HP 1000 DAC currently provides time differences for the Northeast USA (LC/9960), Southeast USA (LC/7980), Great Lakes (LC/8970) and the East Coast Canada (LC/5930) Loran-C chains. (Automatic systems have also been installed in sites such as the Naval Astronautics Group, Hawaii, the Naval Observatory Substation, Florida, and the Satellite Communication Terminal Camp Roberts, California. The hourly readings are transmitted to USNO by a telephone call initiated by the HP 1000. No measurements between USNO MC and the primary cesiums at these sites were readily available, until recently, other than by portable clock visits.) The improvements cited here provided better traceability to the USNO MC through the Loran-C chains which were monitored in Washington. But what of other chains such as the European chains?

LINKING

Greatly influencing the desire to have precise time differences available between USNO and the North Atlantic, Norwegian Sea, and the Mediterranean Sea, was the need to establish and maintain better timing coordination between the Observatory/laboratories of North America and those of Europe. At that time the link was maintained by HF and VLF monitoring and portable clock visits. Improvement in this link was required so that the atomic clock data provided by the laboratories of the Western Hemisphere to the Bureau International de l'Heure (BIH) at the Paris Observatory, France could be better utilized in the formation of International Atomic Time (TAI). As may be seen in Figure 2 (reference 1), the means

As an illustration (Figure 4) of this technique, Loran data for the National Research Laboratory of Metrology (NRLM) located in Japan, has been subtracted from that obtained at NASA in Guam, Tokyo Astronomical Observatory (TAO), and Radio Research Laboratory (RRL), Japan. A change in frequency is clearly evident during July which is attributed to NRLM - the station common to all three differences.

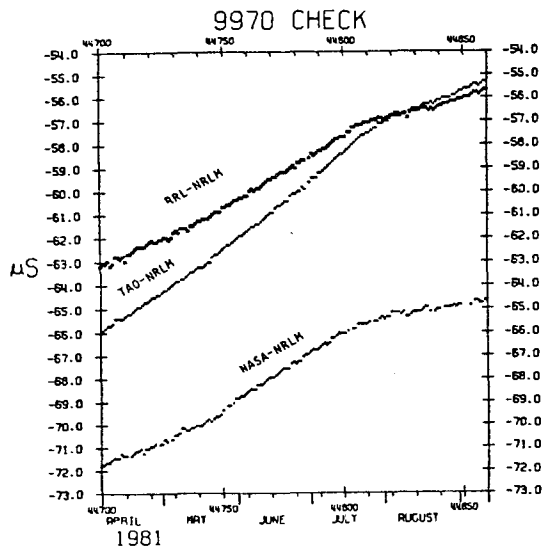


Figure 4. Differences in rates between pairs of cesiums can detect a rate change in a single clock.

Once being able to determine which cesium has changed frequency (X, Y, or Z), it is possible to formulate a time scale for X, Y, and Z which may be combined with the Loran-C TOA data measured at each station. Each portable clock measurement of USNO MC minus X, Y, or Z must equal the value formulated. A delay (propagation, receiver, etc) is computed for each station and this value plus a constant 't' which has been empirically chosen so that consistency in the values of USNO MC minus Loran-C via each station are equal at a calibration point (such as at a portable clock measurement) is subtracted from each station's TOA data.

An averaged or mean value of USNO MC minus Loran-C is formed from the differences USNO - Loran-C via X, Y, and Z. (Details are given in reference 3). While this technique was an improvement over the earlier methods, reliance still had to be placed upon the infrequent portable clock trip. In the early 70's, time transfers using the Defense Satellite Communication System (DSCS) were initiated.

DEFENSE SATELLITE COMMUNICATION SYSTEM (DSCS)

The procedures and techniques described above necessitated the accumulation of TOA data from various monitoring sites - an expansion of the PTTI data base log book into a machine readable data base. In conjunction with the accumulation of this Loran-C data, the establishment of a system of time transfers via the DSCS also necessitated the requirement for a data base for easier access and analysis of the multitudinous time comparisons. As seen in Figure 5, time transfers were performed between several terminals (only those involved with Loran-C monitoring are shown). It should be noted that the time transfers at Kwajalein and Iceland have been temporarily suspended.

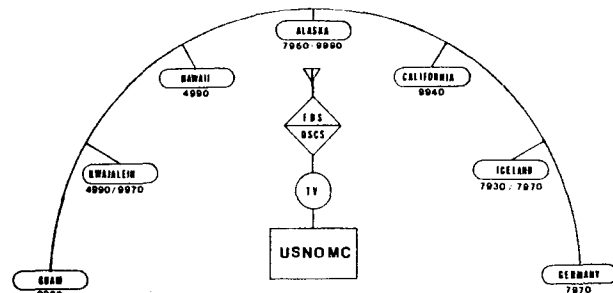


Figure 5. Defense Satellite Communication System (DSCS) terminals which also monitor a Loran-C signal. Their link to the USNO MC is via television transfer between the Ft. Detrick, Maryland (FDS) terminal and USNO.

Each terminal transmits to the Observatory its measured data, e.g., the time transfers, the intercomparisons between on-site cesiums and its TOA data. These data were (and still are) sent by teletype in a special format which can be read by a program on the IBM Series 1 DAC. The information is processed and stored on a data base at the mainframe computer (an IBM 4341) for later analysis.

In trying to improve the determination of the differences USNO MC minus Loran-C, a methodology was developed which used the time comparison data from all available sources. As a test of the validity of applying the DSCS time transfers to Loran-C measures, the time difference data from Alaska were first examined.

At Elmendorf (ELM) Air Force Base, Alaska, the Defense Communication Agency had established a terminal with the capability of obtaining a time difference between ELM and the terminal at Ft. Detrick, Maryland (See Figure 5 above). As can be seen, this immediately provided a calibration point to ELM whenever a time transfer could be performed, usually weekly. For greater detail concerning the relationships between USNO, DSCS and Loran-C, see reference 4.

While the DSCS terminal, ELM, was engaged in obtaining weekly satellite time transfer data, the Elmendorf PTRS was daily monitoring the North Pacific (LC/9990) and the Gulf of Alaska (LC/7960) Loran-C chains, obtaining comparisons between their on-site cesiums and measuring the time differences between their primary cesium and the cesium at ELM. By forming a remote time scale from these data, calibrating the scale using ELM satellite time transfers and then combining these values with the TOA data, an averaged value of USNO MC minus Loran-C was determined (references 3, 4, and 5) which was independent of that obtained by the PTRS. It was found that approximately a 10 microsecond difference (i.e., discrepancy) existed between the Elmendorf PTRS values and the remote time scale calibrated by satellite time transfer values as can be seen in Figure 6 below.

In December 1978, a portable clock team was sent to Alaska to calibrate all the cesiums at each site known to be monitoring either of the Alaskan Loran-C chains, to determine in a systematic manner any delays that would influence the TOA data and to verify procedures used in obtaining data. The cesiums at the ELM site were also calibrated. Upon analysis of the measurements obtained by the portable clock team, the feasibility of time scale methodology calibrated through DSCS satellite time transfers was verified. This technique was adopted and the time differences subsequently published for the USNO MC vs. Gulf of Alaska (LC/7960) and the USNO MC vs. North Pacific (LC/9990) chains were based on the satellite time transfer methodology rather than on the infrequently calibrated PTRS clocks.

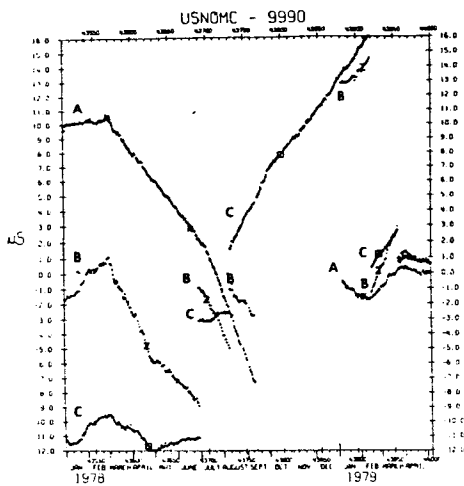


Figure 6. The trace labelled, A, is the difference between values determined at a PTRS (Trace B) and those obtained from the time scale method (Trace C).

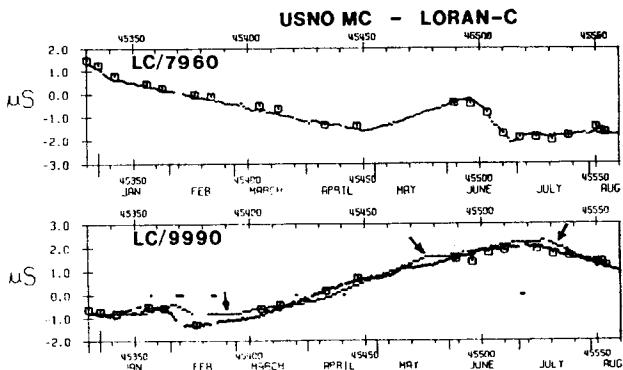


Figure 7. Time comparisons for Alaskan Loran-C chains based on satellite time transfers (indicated by the square symbols) and analytical techniques. Published values of their differences are also shown for LC/9990. When not coincident with the analytical determination, the published values are indicated by an arrow.

Figure 7 illustrates the values as determined via (a) the time scale and (b) satellite time transfers. The third trace in the plot for LC/9990 represents the published values. It must always be remembered that the differences are constantly being redetermined as more data are received. Therefore, it is possible that a difference may occur between time scale determination and the value published. These differences are usually quite small - if some large change occurs at the Loran-C transmitter as may be seen about June in the Gulf of Alaska chain, it may take several days or weeks to accurately determine the chain's difference with respect to USNO MC. The personnel at the U.S. Coast Guard have been extremely helpful in isolating these changes and in determining the causes.

Shortly after the adoption of this technique it was expanded to include the Northwest Pacific area to complement the rate correlation method described earlier.

In August 1983, testing of time transfers using an improved modem, the USC-28, was begun. A terminal is designated as NET CONTROL. Every other terminal in the "net" can monitor the time of the NET CONTROL and obtain the difference between its own primary cesium clock and that of the NET CONTROL terminal.

In this discussion, the data from the station at Elmendorf (ELM) AFB, are used. Figure 8 shows the difference between USNO MC minus the primary cesium clock (Serial No. 0533) via the time scale for LC/9990 and the satellite time transfers.

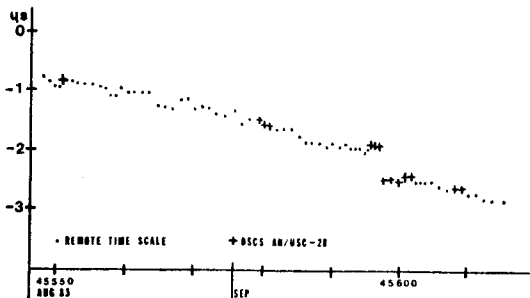


Figure 8. USNO MC - DSCS/ELM/0533

Time transfers (indicated by the + symbol) and time scale determination for the Elmendorf (ELM) DSCS terminal using the USC-28 modem.

Agreement is extremely good after removing an apparent systematic bias of 0.4 microsecond. A bias between DSCS time transfers and portable clock measurements was first reported in reference 6.

Once having determined USNO MC minus ELM/0533 (A), a series of computations are made. To (A) is added the difference between ELM/0533, the cesium clock at the satellite terminal, and the primary cesium clock which monitors LC/9990 at the PTRS Elmendorf, giving a value of USNO MC minus PTRS via time transfer. To this value is added the TOA data minus an adopted delay. A daily calibrated value is thus obtained for USNO MC minus LC/9990. These satellite time transfers permit still further improvement in providing reliable data to the Loran-C timing community. These calibration points must still supplement the analytical technique described earlier -- it would be a step backward to place complete and sole reliance upon the data available from one station.

GLOBAL POSITIONING SYSTEM

For approximately one and a half years, the USNO has been publishing the differences between USNO MC and the various GPS satellite clocks. (Further information of GPS may be found in reference 7.) Receivers are being deployed world-wide. It is possible to compute the times during which each GPS satellite will be visible to two or more stations having GPS receivers. When such a satellite pass is received by both stations during this period of common-view, it is possible to determine the time difference between stations with a high degree of accuracy. Figure 9 shows some of the stations currently monitoring GPS.

GLOBAL POSITIONING SYSTEM

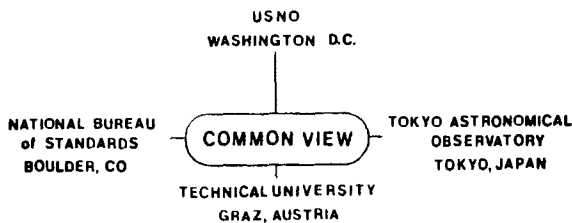


Figure 9. Some stations monitoring GPS transmissions in common-view with USNO.

As the values for the Northwest Pacific (LC/9970) Loran-C chain have been discussed using the rate correlation method and then calibrated via the DSCS time transfer data, this chain serves as a useful tool to show how the common-view GPS data from TAO and USNO may be used as a further calibrating method for Loran-C.

In January 1983, TAO began a program to determine the difference between the TAO time scale and GPS time. These data, as well as the time of arrival data, are available on a weekly basis to USNO in the RC28 catalog of the General Electric Mark III computer system. Additional information concerning this computer system is available in reference 8.

When the TAO minus GPS data, combined with the common-view data of USNO MC minus GPS, was first used in conjunction with the remote time scale method of determining Loran-C data, there was agreement to within 50 nanoseconds. Figure 10 demonstrates the close agreement.

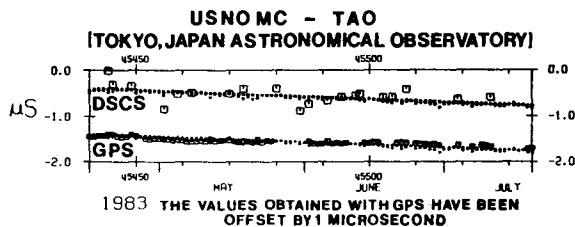


Figure 10. TAO time scale comparisons against DSCS time transfers and GPS common-view data. The square symbol designates the satellite values.

In equation form,

$$\frac{\text{USNO MC} - \text{GPS}(X) - (\text{TAO} - \text{GPS}(X))}{\text{USNO MC} - \text{TAO}} \quad \text{via GPS}(X)$$

where X is a particular satellite monitored at both stations during a period of common-view.

To the value USNO MC minus TAO is added the difference TAO minus LC/9970 to give a difference of USNO MC minus LC/9970 via the Tokyo GPS data. An empirical correction of 4 microseconds has been added to these values to maintain the consistency discussed earlier.

Since the mid-70's, several other stations such as the National Metrology Laboratory, Korea and the Shanxai Observatory, Peoples Republic of China (reference 9), contribute their TOA's to the USNO data base. As each station is added to the system, a constant delay is empirically adopted to retain consistency of the system. The TAO has recently announced that they have modified their adopted delay which will necessitate a decrease in the 4.0 microseconds empirical correction. Since all the Japanese laboratories had established internal consistency, the redetermination of the TAO adopted delay, will necessitate a change in the other laboratories. The National Radio Metrology Laboratory (NRLM) has already published such a revision. Figure 11 illustrates the values of USNO MC minus LC/9970.

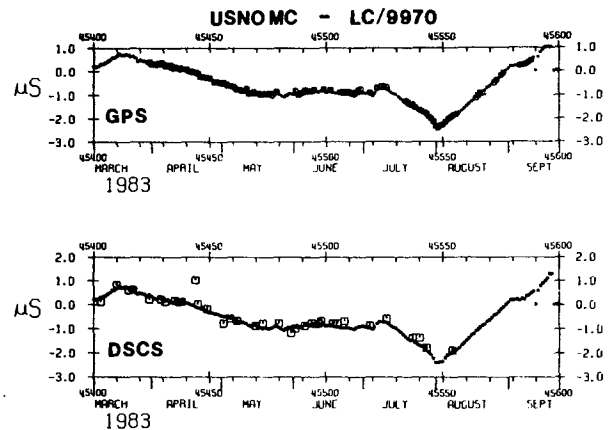


Figure 11. Time scale for the Northwest Pacific (LC/9990) Loran-C chain compared to GPS and DSCS time transfers. The square designates the satellite value.

These satellite calibration points, when used in conjunction with the analytical techniques, ensure the quality of the published Loran-C time differences.

SUMMARY

In its efforts to upgrade the quality of its data, the USNO has substantially improved its own monitoring capabilities by acquiring newer Loran monitoring equipment, increasing the frequency of its monitoring efforts, and upgrading the primary and secondary data acquisition systems. Further evolution in the methodology of determining differences between USNO MC and Loran-C is anticipated concurrent with investigation into other time synchronization techniques.

REFERENCES

1. Bureau International de l'Heure, "Time Links Used for Establishing TAI in 1982," Annual Report for 1982, Figure 3, B-65.
2. Private Communication between L. Charron, NAVOBSY, and Cdr. David Clements, USCG, Government Island, Alameda, California, August 3, 1983.
3. Lukac, Carl F., "Loran-C Prediction Problems," Proceedings of the Thirteenth Annual Precise Time and Time Interval (PTTI) Applications and Planning Meeting, December 1981, Washington, D. C.

4. Charron, Laura G., "Relationships Between U. S. Naval Observatory, Loran-C and The Defense Satellite Communication System," Proceedings of the Thirteenth Annual Precise Time and Time Interval (PTTI) Applications and Planning Meeting, December 1981, Washington, D. C.
5. Lukac, Carl F., and Charron, Laura G., "Timing a Loran-C Chain," Journal of the Institute of Navigation, Vol. 29, No. 3, Fall 1982.
6. Fisher, Laura Charron, "Precise Time and Time Interval Data Handling and Reduction," Proceedings of the Fifth Annual Precise Time and Time Interval (PTTI) Applications and Planning Meeting, December 1973, Washington, D. C.
7. (a) Janiczek, P.M., Editor, Global Positioning System, Papers published in NAVIGATION, Institute of Navigation, 1980 (ISBN 0-936406-00-3).

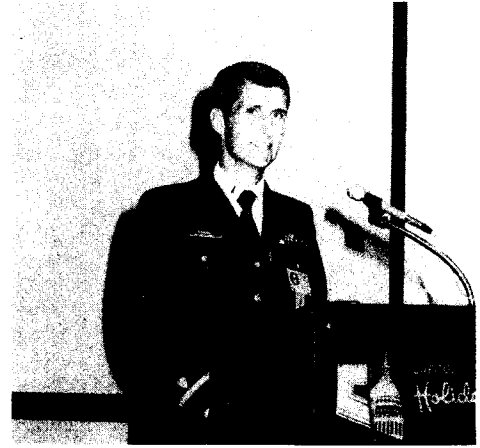
(b) "Session V, Synchronization, Radiation Studies and Quartz Technology," Proceedings of the Fourteenth Annual Precise Time and Time Interval (PTTI) Applications and Planning Meeting, December 1982, Washington, D. C.

(c) "Session II --- GPS Time Transfer," Proceedings of the Fifteenth Annual Precise Time and Time Interval (PTTI) Applications and Planning Meeting, December 1983, Washington, D. C.
8. Withington, F. N., "G.E. Mark III RC28 Catalog User's Guide for MERIT, World Data Center A and Other Time Applications," May 1983 (to be published as TSA Series 18).
9. Yung-wei, Miao and Xiao-pei, Pan, "Timing Accuracy of LF and TV Synchronization Techniques," Proceedings of the Fifteenth Annual Precise Time and Time Interval (PTTI) Applications and Planning Meeting, December 1983, Washington, D. C.

SESSION THREE SPEAKERS



LT Robin Orr



ENS Bruce Serinis



Ed Bregstone



Gerald Sage



Laura Charron



Bill Marchal

SESSION FOUR

CHAIRMAN

Larry Sartin
ASEC

NAVIGATION AVIONICS INTEGRATION WITH LORAN-C

J.I. Leighton and R.S. Warren
The Analytic Sciences Corporation
One Jacob Way
Reading, Massachusetts 01867

ABSTRACT

Loran-C has gained increased acceptance by aircraft pilots in recent years as a supplement to VOR/DME for use in the National Airspace System. This acceptance has been spawned by the development of airborne Loran-C receivers/navigation systems and by the FAA's certification of this equipment for enroute/terminal flight. Among the reasons that Loran-C has not gained total acceptance, including certification for non-precision approach, are concerns over grid warpage/instability and cycle identification/slippage. Recognizing that most aircraft are equipped with VOR and DME, it is natural to ask the question: Can limited data from these radionavigation aids be integrated with Loran-C data to improve Loran-C accuracy and confirm proper tracking in areas of marginal Loran-C coverage?

The objective of this paper is to present the expected performance of an algorithm for integrating Loran-C with VOR or DME in the cockpit. Considerable synergism is embodied in this avionics suite and a properly-designed algorithm should be capable of realizing a significant improvement in Loran-C navigation accuracy.

INTRODUCTION

The primary civil radionavigation systems for aircraft are VHF Omnidirectional Range (VOR) and Distance Measuring Equipment (DME). These systems satisfy the accuracy requirements given in Advisory Circular 90-45A (1) and are considered minimum instrumentation for aircraft certified to fly using Instrument Flight Rules (IFR). VOR/DME coverage is limited to line-of-sight ranges of approximately 200 nm and the ground equipment is relatively expensive to install and maintain. Therefore, many small airports do not support VOR/DME and are limited to Visual Flight Rules (VFR).

The relatively wide-area coverage provided by Loran-C has prompted the development of several airborne Loran-C navigation systems which has required the FAA to address certification of Loran-C for enroute/terminal and non-precision approach. Airborne Loran-C

equipment is currently receiving IFR certification for enroute/terminal phases of flight and the FAA is developing procedures/requirements in support of Loran-C certification for non-precision approach. Features which make Loran-C particularly attractive to airborne users include:

- Wide-area continuous coverage with an associated reduction in pilot workload
- Greater range than the present civil navigation systems (VOR/DME), allowing coverage of many airports which are too small to maintain radionavigation equipment
- Cockpit display of aircraft latitude and longitude
- Relatively low cost.

Areas of concern to the FAA in the certification of Loran-C for non-precision approach at all airports include:

- Grid instability and warpage which, combined with geometric effects, give rise to variations in accuracy over the coverage area
- Undetected cycle-slip during flight or during the cycle identification procedure.

Loran-C equipment manufacturers are employing grid calibration/error compensation techniques to reduce grid warpage effects, along with multi-chain/master-independent navigation algorithms to optimize the available geometry, expand the coverage region, and reduce the possibility of undetected cycle slip. The FAA is addressing grid instability problems by considering the potential use of pattern monitors. It should be possible to compensate for most of the local grid warpage effects through determination of grid bias corrections at airports (3). All of these items will reduce the operational problems associated with Loran-C in the airborne environment and serve to accelerate the process of obtaining certification of Loran-C for non-precision approach.

The current trend toward digital avionics in a technological environment of increasing computational power and decreasing cost is prompting manufacturers to consider the development of hybrid integrated navigation systems. The U.S. Air Force is currently supporting the development of all-digital integrated avionics, and increased levels of integration are appearing in the cockpits of commercial aircraft.

The integration of individual navigation sensor/system outputs with appropriate software can produce a navigation system with accuracy, coverage, and operational features that represent significant improvements over performance levels achievable with each of the constituent systems individually. A single, best estimate of current aircraft position which is contiguous through all phases of flight can be provided by an integrated system. Accuracy can be improved by exploiting the synergism of available sensors/systems through error estimation/correction algorithms. Further, a properly-designed integration algorithm can be used to rapidly detect anomalous effects (e.g., Loran-C cycle slip or station outage) and alert the pilot or correct the display of navigation information, thereby improving the reliability of available data.

It is anticipated that there will be a trend over the next decade toward integrated navigation systems for General Aviation, and Loran-C is a prime candidate for integrated avionics. Integrated systems which embody Loran-C are not new (6). There are operational military systems which incorporate Loran-C, and selected commercial houses have incorporated various levels of multisensor integration within their equipment. Hybrid systems may embody "light integration" which may package two or more sensors in the same box with manual or semi-automatic selection/switching. Alternatively, "heavy integration" may be used which includes some type of algorithm or filter (e.g., Kalman filter) that models and estimates the errors associated with the individual sensors/systems.

This paper is directed at quantifying the expected performance of an integrated Loran-C navigation system which is aided by VOR or DME. A Kalman filter is used to achieve the integration, and linear covariance analysis (2) is employed to assess the expected accuracy of the integrated system. Wide-area coverage combined with the highly-repeatable position-fix capability of Loran-C complements the higher absolute accuracy associated with range- and bearing-only data from DME and VOR, respectively. Loran-C provides the "interpolation" between discrete (limited availability) fixes, and these discrete updates can be used to detect Loran-C position error effects due to grid warpage and cycle slip. The resulting integration algorithm

used here is only one of many possible realizations and is not the primary topic of the paper. Rather, the intent of this paper is to provide insight into the accuracy characteristics of candidate hybrid systems and to show the potential for on-line calibration of Loran-C grid warpage in support of non-precision approach accuracy requirements at thousands of small airports which do not currently have an IFR capability.

INTEGRATION ALGORITHM

Aviation Requirements

Airborne equipment error requirements for operation in the U.S. National Airspace System are given in FAA Advisory Circular 90-45A (1). The requirements for enroute, terminal, and non-precision approach flight phases are presented in Table 1. The AC-90-45A requirements are limits on the 95-percent confidence (2σ) error. Enroute and terminal accuracy requirements are typically satisfied by Loran-C without grid calibration, a fact acknowledged by the FAA issuance of a Supplemental Type Certificate for enroute/terminal use of the Texas Instruments TI-9100 receiver.

TABLE 1
AC-90-45A AIRBORNE EQUIPMENT
ERROR REQUIREMENTS

FLIGHT PHASE	95% CONFIDENCE (2σ) (CROSS-TRACK OR ALONG-TRACK ERROR)
Enroute	1.5 nm, 9200 ft
Terminal	1.1 nm, 6600 ft
Non-precision Approach	0.3 nm, 1800 ft

While studies (3) have shown that grid instability/warpage and geometry effects do not preclude the use of Loran-C for non-precision approach with the primary Loran-C triad, selection and use of another triad as a result of operator error or Loran-C transmitter outage may not satisfy position accuracy requirements for non-precision approach.

Radionavigation Aids

VOR equipment provides magnetic bearing between the aircraft and the ground VOR beacon, which is typically located near the center of the airfield. DME provides line-of-sight range between the aircraft and DME transponder. When DME is available, it is usually collocated with VOR. Table 2 summarizes the typical accuracy of these radionavigation aids (4,5) and contrasts them to Loran-C. Since both VOR and DME operate at relatively high frequency, they are limited to line-of-sight range, about 200 nm at high altitude. Of primary interest is VOR- or DME-aiding of Loran-C to potentially enable non-precision approach to airports which do

not maintain VOR or DME (airports which have VOR or DME can already provide non-precision approach), but are within range of other VOR or DME equipment.

TABLE 2
SUMMARY OF PRIMARY RADIONAVIGATION
SYSTEM CHARACTERISTICS

RADIO-NAVIGATION AID	TYPE INFORMATION	USEFUL RANGE (nm)	TYPICAL ACCURACY (2σ)
VOR	Magnetic Bearing	200*	3.5 deg
DME	Slant Range	200*	0.1 nm
Loran-C	Latitude Longitude	700	0.25 nm geodetic 0.05 nm repeatable

*Limited to line-of-sight

System Mechanization

A system mechanization for integrating Loran-C with each of the radionavigation aids summarized in Table 2 is shown in Fig. 1. The integration algorithm is a Kalman-type filter which requires inputs that are differences of whole value quantities, in this case either bearing or range. The objective of the Loran-C/Relative Navigation Aid integration algorithm is to develop a single algorithm that will utilize data from either or both of the radionavigation aids. The dashed box shown in Fig. 1 indicates the functional software blocks required to implement a complete integration algorithm. The equipment shown outside the box, with the possible exception of the Loran-C receiver, is currently available on most aircraft.

Integration of a VOR-derived bearing with Loran-C position requires some preprocessing to develop consistent measurements. With the VOR, the integration algorithm input is the difference between the VOR and Loran-C implied bearing from the aircraft to the VOR beacon. Loran-C implied bearing to the VOR can be computed using the Loran-C indicated position and the local VOR location. The

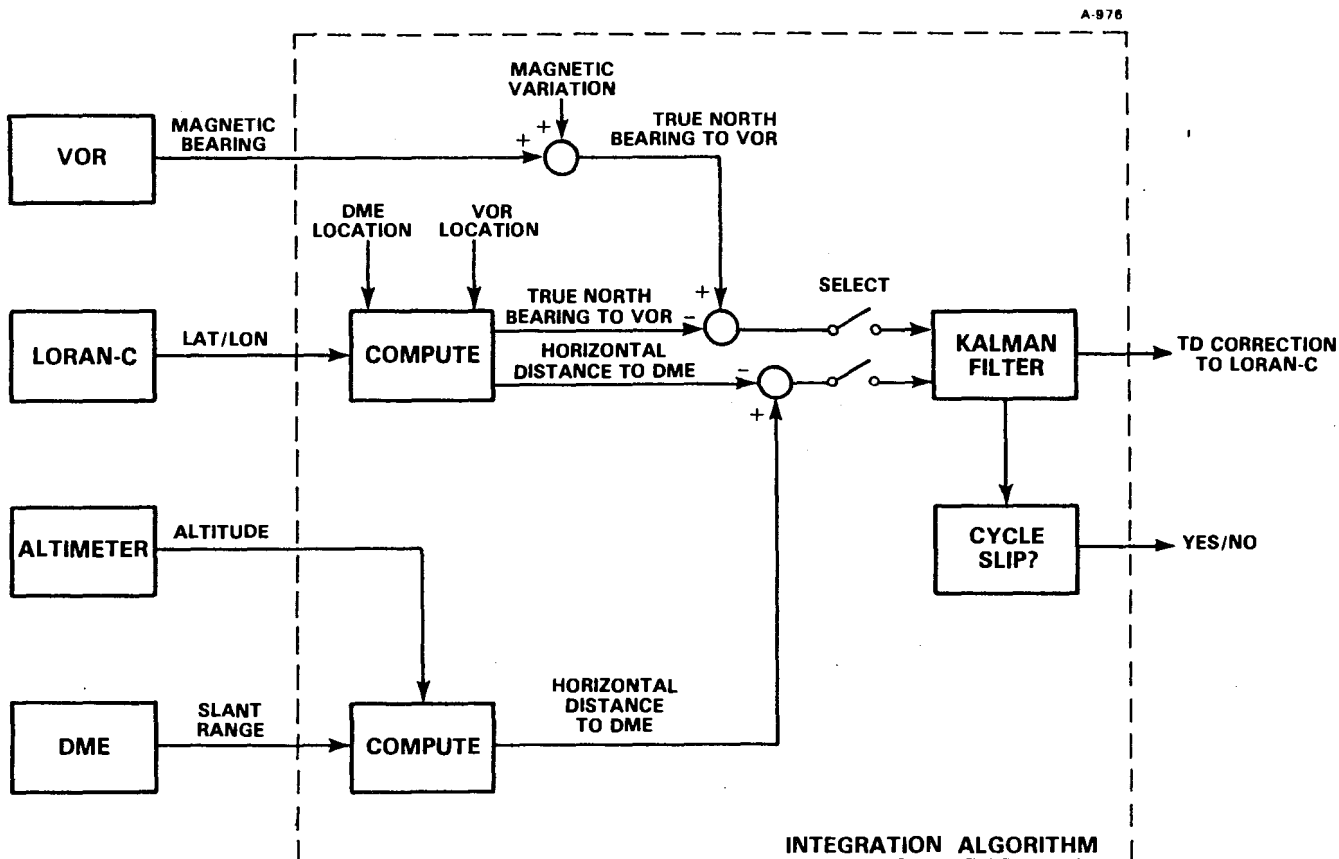


Figure 1. Loran-C Relative Navigation Aid Integration Algorithm Mechanization

divergence between these two indicated bearings is used as the input to the integration algorithm.

The integration algorithm input for the Loran-C/DME mechanization is different than the Loran-C/VOR mechanization. The fundamental DME measurement is slant range from aircraft to DME. Using the altimeter output, DME-indicated slant range is transformed to horizontal range. Loran-C indicated distance to the DME transponder is computed based on the current Loran-C indicated position and the known DME transponder location.

The integration algorithm used in this evaluation is a ten-state Kalman filter. Seven states model the Loran-C errors, one state models the VOR angular error, and two states are used to characterize the DME range measurement error. The output of this integration algorithm includes both an assessment of whether the Loran-C receiver is tracking the correct cycle and time delay (TD) corrections. The cycle slip identification feature is an independent verification of correct cycle tracking by comparison of Loran-C position with data from either the VOR or DME. The output is a YES/NO assessment of correct cycle tracking and could be used to blank or flash the Loran-C TD/Lat-Lon display. The primary outputs of the integration algorithm are TD corrections, which effectively removes Loran-C grid instability/warping. This is accomplished by exploiting the local VOR or DME measurements to "calibrate" the Loran-C grid within a region.

ACCURACY EVALUATION METHODOLOGY

Approach

Covariance analysis (2) is used to quantify the expected performance of an integrated VOR- or DME-aided Loran-C system. Figure 2 shows the functional block diagram of the simulation used to generate the results presented here. The components of this simulation include error models for each of the radionavigation aids, a trajectory generator, and the integration algorithm. The output of the simulation provides an estimate of the improved position fix accuracy obtained through VOR- or DME-aiding of Loran-C. A trajectory generator produces the geometry scenarios summarized in the Operating Scenarios section.

Truth Models

The error models for each radionavigation aid used in the simulation capture the expected error in the fundamental measurement produced by that aid. Characteristics for these models are derived from Refs. 3,4,5. Table 3 summarizes the significant error sources modeled for each of the three radionavigation aids. The indicated Loran-C errors are modeled for each of the three time-of-arrival

(TOA) measurements which are transformed to TD errors.

ACCURACY PROJECTIONS

Operating Scenarios

Position fix accuracy of any hyperbolic radionavigation aid, including Loran-C, is a strong function of the aircraft geometry relative to the transmitter locations (3). Geometric Dilution of Precision (GDOP) can vary from very good (GDOP=1) to poor (GDOP=5) by selecting different Loran-C stations within the same chain. To provide best and worst case performance predictions, GDOP=1.3 and GDOP=5.1 Loran-C geometry scenarios are simulated.

Three 200 nm aircraft flight paths are simulated. These geometry scenarios are summarized in Table 4. Scenarios 1 and 2 correspond to an aircraft which is initially 100 nm away from the radionavigation aid, and having a flight path nearly over the aid and continuing for another 100 nm beyond the aid. Scenario 3 is a fly-by geometry with an aircraft initially 140 nm from the radionavigation aid, and having a straight line flight path which flies-by the aid with a point-of-closest-approach of approximately 75 nm. This scenario is of interest to the pilot who wants to make a non-precision approach to an airport that does not support VOR/DME but is within range (<100 nm) of an airport that does support VOR/DME. All three scenarios assume a constant aircraft ground speed of 200 kt at an altitude of 20,000 ft.

The Loran-C geometry conditions are selected GDOP/flight path combinations that exist in the area of Atlantic City, NJ and are representative of conditions that could exist in other regions with Loran-C coverage. While unaided Loran-C utilizing GDOP=1.3 should meet the non-precision approach requirements (3) listed in Table 1 if the grid warpage is not excessive, evaluation of both GDOP=1.3 and GDOP=5.1 scenarios (Northeast Loran-C chain MXY and MWX triads, respectively) provide best- and worst-case geometry conditions for integration algorithm evaluation.

Loran-C/DME Integration

Simulation results for Loran-C/DME Scenario 1 are shown in Fig. 3, corresponding to different times along the flight path. The error ellipse shown at time T=0 corresponds to the unaided Loran-C nominal position fix accuracy. After only one DME measurement at time T=1 min, when the aircraft is 100 nm away from the DME transponder, a significant reduction in the error ellipse minor axis is observed. The error component in the major axis is unchanged, however this is consistent with the DME providing range measurements along the aircraft's flight path. Notice, however, that there is little change in the

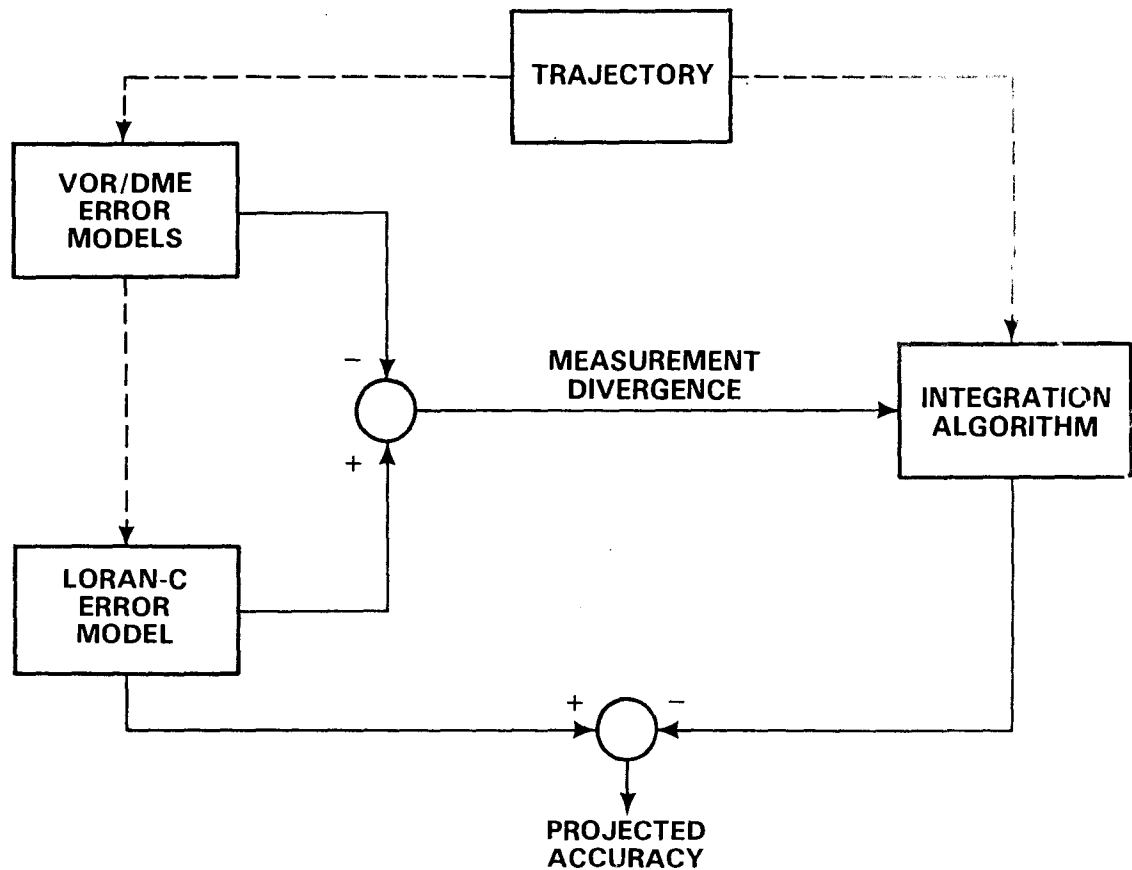


Figure 2. Simulation Block Diagram

TABLE 3
TRUTH MODEL CHARACTERISTICS

INSTRUMENT	ERROR
VOR	Receiver and ground station bias; receiver measurement noise
DME	Transponder timing bias; receiver timing bias; receiver measurement noise
Loran-C	TOA propagation bias and spatial decorrelation; receiver measurement noise

TABLE 4
LORAN-C/AVIONICS GEOMETRY SCENARIOS

SCENARIO NUMBER	LORAN-C GDOP	AIRCRAFT FLIGHT PATH RELATIVE TO RADIONAVIGATION AID
1	1.3	Fly-over
2	5.1	Fly-over
3	5.1	Fly-by

error ellipse at T=30 min. This is due to the relative insensitivity of the DME error to distance. Integrated Loran-C/DME position fix errors do not reduce to an arbitrarily small value due to the spatial decorrelation of Loran-C errors along the flight path. The final error ellipse at time T=60 min, with the aircraft again 100 nm away from the DME, is nearly the same as at time T=30 min. Table 5 summarizes the position fix improvements along the error ellipse minor axis as a function of time.

Scenario 2 simulation results, utilizing poor Loran-C geometry (GDOP=5.1) are shown in Fig. 4. At time T=0, the unaided Loran-C error ellipse is significantly larger than in Scenario 1. After only one DME measurement at time T=1 min, the orientation of the error ellipse is changed so that the minor axis is nearly aligned with the flight path. The major axis is correspondingly reduced so that it is within the unaided Loran-C error ellipse. The 2σ along-track position error is reduced by 60 percent to 1000 ft. Slight improvements in the integrated Loran-C/DME error ellipse continue until the aircraft passes over the DME. These improvements, however, are less significant than those observed in Scenario 1. This is due to the

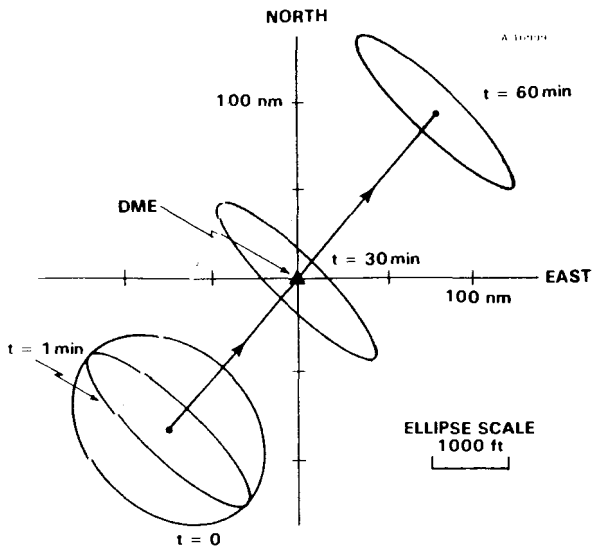


Figure 3 Scenario 1 Loran-C/DME 2σ Position Error Ellipse

TABLE 5
POSITION FIX IMPROVEMENT DUE TO
LORAN-C/DME INTEGRATION
IN SCENARIO 1

TIME (min)	PERCENT IMPROVEMENT IN POSITION FIX ALONG FLIGHT PATH	2σ POSITION FIX UNCERTAINTY ALONG FLIGHT PATH (ft)
0	0	1100
1	60	450
30	73	300
60	70	325

measurement geometry for Loran-C in this test case.

Simulation results for Loran-C/DME Scenario 3 are shown in Fig. 5. This represents the largest change in measurement geometry of the three scenarios evaluated. Both range and bearing to the DME change over the flight path with a net change in bearing angle of approximately 100 deg. As shown in Fig. 4 for Scenario 2, a single DME measurement provides significant position fix improvements over the unaided Loran-C error ellipse. Note that the orientation of the integrated Loran-C/DME error ellipse rotates with the aircraft to DME line-of-sight (LOS). The change in bearing angle provides increased observability of both North and East Loran-C position errors.

Each of the three scenarios produces results which are consistent with the particular Loran-C/flight path geometry being evaluated. These scenarios also demonstrate that

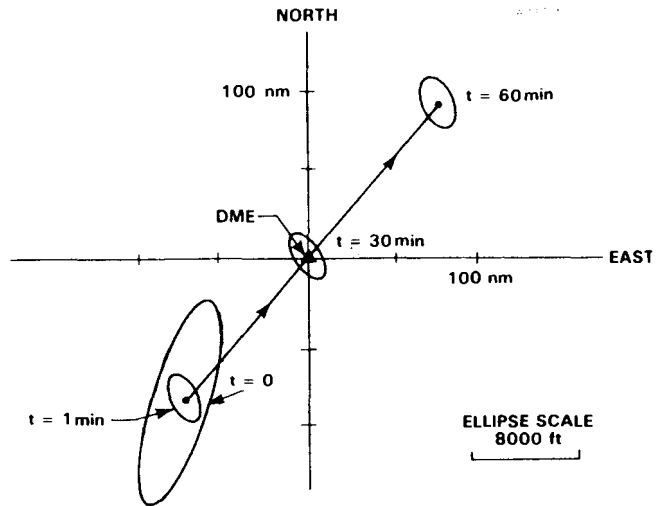


Figure 4. Scenario 2 Loran-C/DME 2σ Position Error Ellipse

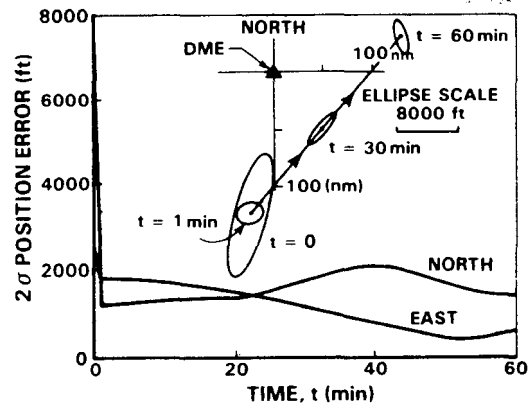


Figure 5. Scenario 3 Loran-C/DME 2σ Position Error Ellipse

Loran-C/DME integration can provide significant position fix improvements over unaided Loran-C.

Loran-C/VOR Integration

Position error simulation results for Loran-C/VOR Scenario 1, utilizing GDOP=1.3 and corresponding to different times along the flight path, are given in Fig. 6. The error ellipse shown at time $T=0$ is the same unaided Loran-C nominal position fix accuracy used in Loran-C/DME Scenario 1. In contrast to the integrated Loran-C/DME Scenario 1 results, Loran-C/VOR position accuracy slowly improves as the aircraft approaches the VOR (not shown in Fig. 6). The accuracy improvement is in the direction of the error ellipse major axis associated with unaided Loran-C, which corresponds to the flight path cross-range direction for this geometry scenario. The reason for the slowly improving position accuracy is that cross-range position error

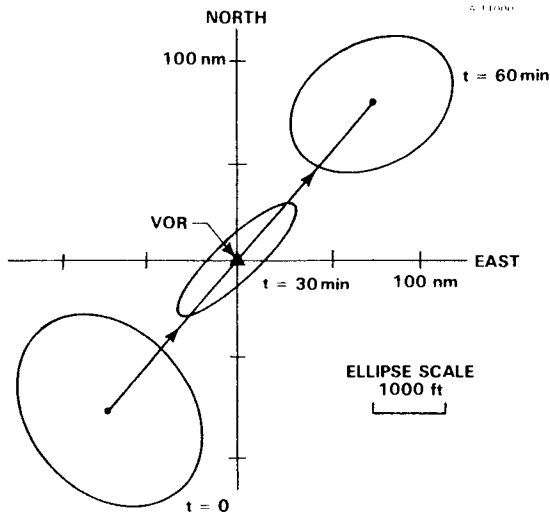


Figure 6. Scenario 1 Loran-C/VOR
2 σ Position Error Ellipse

measurements derived from the VOR angle measurements are range dependent. At short distances, the cross-range position error is small compared to the cross-range position error associated with the same VOR angle measurement error observed at a greater distance. At time T=30 min, the error ellipse exhibits the minimum cross-range error that can be achieved.

As shown in Fig. 6, the position fix accuracy degrades as the aircraft moves away from the VOR beacon due to the spatial decorrelation of the Loran-C error and the lower quality cross-range information associated with bearing measurement error at longer range. The final error ellipse at time T=60 min, with the aircraft 100 nm away from the VOR, is, however, smaller than the unaided Loran-C error ellipse at time T=0, for which the aircraft is also 100 nm away from the VOR beacon. This position fix improvement is the result of the gradual calibration of Loran-C using improved VOR measurements as the aircraft approaches the VOR beacon, followed by the reliance of the Kalman filter on this calibrated Loran-C model as the aircraft moves away from the VOR beacon. If the Loran-C error is a pure bias offset over the flight path, then the growth in the Loran-C/VOR error estimate after time T=30 min will not be observed. Table 6 summarizes the position fix improvements in the aircraft cross-range axis as a function of time.

Figure 7 shows Loran-C/VOR simulation results corresponding to Scenario 2, utilizing Loran-C GDOP=5.1. The improvement in position fix accuracy is significant in the cross-track direction. The characteristic decrease/increase in aircraft cross-track position

TABLE 6
POSITION FIX IMPROVEMENT DUE TO
LORAN-C/VOR INTEGRATION IN SCENARIO 1

TIME (min)	PERCENT IMPROVEMENT IN POSITION FIX IN AIRCRAFT CROSS-RANGE	2 σ POSITION FIX UNCERTAINTY IN AIRCRAFT CROSS-RANGE (ft)
0	0	1400
18	30	980
30	80	250
42	60	540
60	45	780

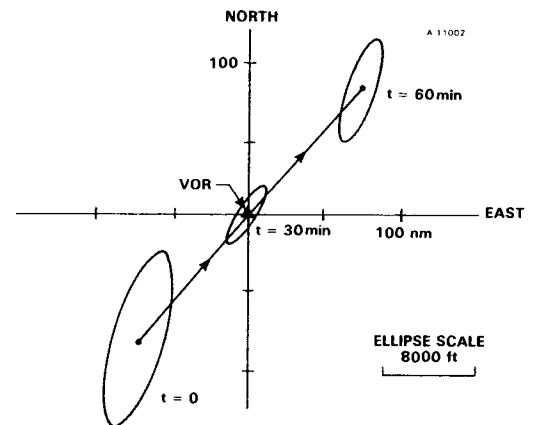


Figure 7. Scenario 2 Loran-C/VOR
2 σ Position Error Ellipse

error is not as large as in Scenario 1 because the unaided Loran-C position error is very large and is not aligned with the flight path. The overall reduction in the error ellipse is due primarily to the realignment of the error ellipse to be minimized along the aircraft cross-track direction. Integrated Loran-C/VOR position fix accuracy at time T=30 min results in a 50-percent reduction in Loran-C cross-track position error.

Simulation results of integrated Loran-C/VOR Scenario 3 are shown in Fig. 8. The characteristic decrease/increase in position fix error is partially observed in this geometry scenario. Initially, when the unaided Loran-C error ellipse is aligned with the aircraft-to-VOR LOS, the position fix accuracy improves as a result of both changing geometry and reduced aircraft-to-VOR range. Integrated Loran-C/VOR position fix accuracy does not degrade substantially between T=30 and T=60 min due to the relatively small change in aircraft-to-VOR LOS (with respect to the unaided Loran-C position error ellipse). The change in aircraft-to-VOR range is relatively insignificant in comparison to the major axis of the unaided Loran-C error ellipse which is the primary observation axis.

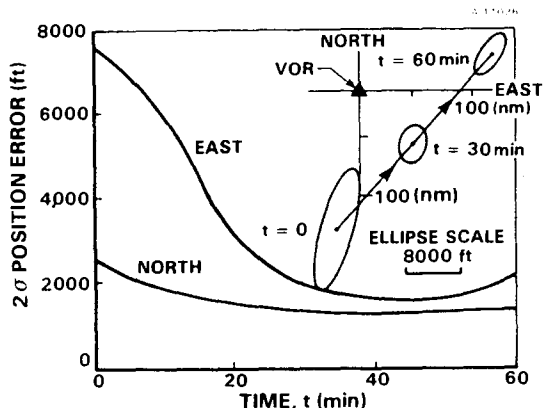


Figure 8. Scenario 3 Loran-C/VOR
2 σ Position Error Ellipse

The three Loran-C/VOR scenarios produce simulation results which are consistent with the simulated geometry. Based on these simulation results, Loran-C/VOR integration produces significant position fix accuracy improvements over unaided Loran-C. These improvements are most significant when the aircraft is closest to the VOR beacon.

Integrated Loran-C/Avionics Discussion

Integrated Loran-C/DME position fix data is superior to integrated Loran-C/VOR due to the range sensitivity inherent in VOR bearing measurements. Improvements in Loran-C/DME position fix accuracy are along the aircraft to DME LOS, while improvements in Loran-C/VOR position fix accuracy are normal to the aircraft to VOR LOS. Clearly, if both VOR and DME are available, integration with Loran-C will produce the smallest position error ellipse which is bounded by the intersection of the error ellipse for each radionavigation aid used alone.

Multiple Loran-C/Radionavigation Aid fixes at different bearing angles along the flight path can, however, provide increased observability of Loran-C errors, resulting in better integrated position fix accuracy. If the correlation distance of the Loran-C errors is relatively long compared to the flight path and substantial changes in the aircraft to radionavigation aid LOS bearing angle are experienced, a two-dimensional Loran-C position error calibration can be obtained with one-dimensional DME (range-only) or VOR (bearing-only) measurements. Of course, more complicated flight paths may be postulated, such as a circle around the VOR/DME, which will provide even greater observability of Loran-C error. However, the fly-by scenario is representative of a typical flight path and serves to illustrate the expected performance of an aided Loran-C navigation system.

Another approach to providing two-dimensional calibration of Loran-C error is to

process multiple fixes from more than one DME (or VOR) at different bearing angles. This means that more than one DME (or VOR) must be in range of the aircraft. However, it is not necessary to simultaneously interrogate the available transponders. The high correlation of Loran-C error over the several minutes it may take to process the fixes from several radionavigation aids allows the integration algorithm to establish two-dimensional calibration of Loran-C.

As an added benefit of the Loran-C/Radionavigation Aid integration algorithm, monitoring of proper Loran-C cycle tracking can be performed. A cycle-slip detection algorithm can use the outputs of the Kalman filter to identify the large position errors associated with cycle-slip. Because cycle-slip may occur in any of the three Loran-C stations being used for navigation, it is not possible to ensure cycle-slip detection for all signals with a single-geometry measurement (VOR or DME). A combined VOR/DME fix or DME fixes at multiple Loran-C/Radionavigation Aid geometries can, however, be used to provide the required observability of Loran-C error in each of the received TOA measurements. Relatively simple logic can be used to correct the indicated cycle-slip or modify the TD/Lat-Lon display to alert the pilot of a possible problem.

CONCLUSIONS

Integration of Loran-C with DME or VOR provides a navigation system which can satisfy the aircraft non-precision approach accuracy requirements given in AC 90-45A (i.e., 1800 ft along-track and cross-track) for all but some of the most severe Loran-C geometry scenarios (GDOP=5.1). Loran-C/DME integration offers rapid calibration of Loran-C errors in the relative direction defined by the aircraft-to-DME LOS. Simulation results indicate that unaided Loran-C position fix error can be reduced by up to 80 percent based on the geometry scenarios evaluated herein.

Integrated Loran-C/VOR position fix accuracy is strongly range (aircraft to VOR) dependent since the relative bearing angle is the fundamental measurement. However, the resulting Loran-C calibration accuracy is approximately equal to that associated with using DME measurements when the aircraft flies over (or within a few miles) of the VOR.

The major advantage of radionavigation aid integration is to provide a non-precision approach capability at airports which do not support VOR/DME equipment but are in the vicinity (e.g., within ~ 50 to 100 nm) of VOR/DME equipment and have good Loran-C coverage. Fixes-of-opportunity from a VOR and/or DME can be used to calibrate the Loran-C error within a local region. However, the integrated Loran-C accuracy attained is geometry

dependent, that is, dependent on aircraft-to-VOR/DME geometry and the associated relative geometry of the Loran-C chain.

ACKNOWLEDGEMENT

The results presented in the paper were obtained as part of a TASC Independent Research and Development Program effort. The authors acknowledge the technical support provided by Dr. Leon DePalma.

REFERENCES

1. "Approval of Area Navigation Systems for Use in the U.S. National Airspace System," Federal Aviation Administration, Advisory Circular AC-90-45A, February 1975.
2. Gelb, A. (Editor), Applied Optimal Estimation, MIT Press, Cambridge, MA, 1974.
3. DePalma, L.M., Creamer, P.M., and Erikson, R.G., "Loran-C Grid Calibration Requirements for Aircraft Non-Precision Approach," Proceeding of the Position, Location and Navigational Symposium (Atlantic City, NJ, December 1982).
4. Kayton, M. and Fried, W.R. (Editors), Avionics Navigation Systems, Wiley, New York, NY, 1969.
5. "Federal Radionavigation Plan," U.S. Departments of Defense and Transportation, Report No. DOD-NO.4650.4-P/DOT-TSC-RSPA-80-16, July 1980.
6. Sage, G.F. and Luse, J.D., "Integration of Transit, Omega and LORAN-C for Marine Navigation," Navigation: Journal of the Institute of Navigation (Vol. 30, No. 1, Spring 1983).

THE HISTORY OF LORAN-C CHARTING
AT THE NATIONAL OCEAN SERVICE

Jeffrey S. Stuart
Marine Chart Branch
Charting and Geodetic Services
National Ocean Service, NOAA
Rockville, Maryland 20852

For the past 10 years the National Ocean Service (NOS) has been engaged in a continuing effort to provide the public with accurate LORAN-C charts that keep abreast of the changing and expanding LORAN-C network. From the beginning this project has been dependent on the support of the U.S. Coast Guard (USCG) and the Defense Mapping Agency Hydrographic/ Topographic Center (DMAHTC).

While LORAN-C has been available for commercial use since 1958, the lines of position were not shown on NOS nautical charts until 1973. Prior to that time, the high cost of receivers limited interest in the use of LORAN-C to the military and scientific research and survey groups. There was no wide spread demand for LORAN-C charts. The existing LORAN-A system met most civilian need for a radio-navigational aid. The LORAN-A lines of position were already overprinted on many NOS charts. But by the late 1960's, advances in microelectronics made it possible for manufacturers to produce and sell LORAN-C receivers at a price within the range of commercial users. Low cost receivers and anticipated expansion of the LORAN-C system resulted in increased interest in LORAN-C charts.

In December 1971, the USCG requested that NOS', Marine Chart Branch print a limited issue of NOS chart 13009, Gulf of Maine and Georges Bank, with a LORAN-C grid overlay. The purpose of this special issue chart was to facilitate a USCG evaluation of the accuracy of LORAN-C in nearshore areas. Using LORAN-C overlays produced by DMAHTC, NOS overprinted LORAN-C lines on the existing chart base, and 300 copies were forwarded to the USCG early in 1972.

In a follow-up request in November 1972, USCG asked NOS to overprint LORAN-C lattices on seven more NOS base charts for USCG use. This second USCG request involved several more NOS nautical charts of the east coast as well as Aleutian Island charts 16006 and 16012. DMAHTC once again provided the necessary LORAN-C overlays for each chart base. Two hundred copies of the latest edition of each of these seven charts with LORAN-C overprinted were forwarded to USCG headquarters by September 1973.

Fiscal constraints prevented NOS from complying with further USCG requests for special purpose LORAN-C charts. But in early summer 1973, USCG requested NOS to overprint LORAN-C on the next regularly scheduled editions of each of the seven charts for which limited issue LORAN-C editions had previously been prepared. The USCG also contracted with DMAHTC for the production of LORAN-C overlays to fit eight more NOS base charts being considered for future public issue.

The 19th edition of NOS chart 16006, Bering Sea-Eastern Part, dated September 8, 1973, was the first regular issue chart to show LORAN-C lines overprinted. This chart, 1:1,500,000 in scale, was a prototype and the basis for discussions concerning the overprinting of LORAN-C lines on future charts. The lines of position were generated based on assumed all seawater path with no correction for overland signal propagation delay referred to as Additional Secondary Factor (ASF) corrections.

LORAN-A lines were already overprinted on NOS charts. Discussions with USCG and DMAHTC produced a general agreement that the most practical method for charting both LORAN-A and LORAN-C in a common area would be to print two versions of the same chart, back to back, with existing LORAN-A coverage on one face and LORAN-C lines of position on the other. Marine Chart Branch Cartographic Order, dated December 13, 1973, formally authorized the overprinting of LORAN-C lines on NOS charts and outlined general charting policy.

The Department of Transportation (DOT) endorsed LORAN-C as the primary government provided radionavigation system for the Coastal Confluence Zone (CCZ) of the United States in May 1974. Concurrent plans for the phasing out of LORAN-A service and growing public acceptance of the LORAN-C system increased the demand for LORAN-C chart coverage.

With several LORAN-C charts already on issue NOS, USCG, and DMAHTC finalized plans for future LORAN charting in May 1975. NOS agreed to overprint LORAN-C lattices reflecting existing LORAN-C coverage on approximately 150 charts of scales of 1:80,000 and smaller during Fiscal Years 1975 and 1976. East coast charts were given highest priority. NOS chart printing schedules were tentatively adjusted to accommodate this effort. Copies of these adjusted schedules were forwarded to DMAHTC and USCG.

Tentative plans were also developed to provide future chart coverage of several planned west coast and Alaskan chains during Fiscal Year 1977. USCG desired that these NOS charts be on issue prior to the proposed operational dates for these chains which were scheduled to begin service in 1977. NOS printing schedules for affected west coast charts were also revised.

Still further charting plans were outlined involving the charting of the lines of position for two more new chains designed to provide new coverage on the east and gulf coasts. These chains were scheduled to begin service in 1978 and 1979.

To facilitate this charting effort, DMAHTC agreed to provide NOS with accurate master and slave station positions for each chain based on the NOS charting datum (North America Datum of 1927, NAD 1927) and other necessary data. In addition, DMAHTC agreed to provide NOS with ASF corrections for each lattice charted. These adjustments were necessary to bring the charted lattices within the $\frac{1}{4}$ -nautical mile accuracy (95 percent, 2 drms) criteria established by the USCG. Classified prior to 1978, these corrections were to be incorporated in the construction of the lattices but the amount and direction of the adjustment was not to be made public.

DMAHTC agreed to provide these ASF corrections for all charts between 1:80,000 and 1:875,000 scale that were to have LORAN-C overprinted. For charts smaller in scale than 1:875,000, DMAHTC determined on a chart-by-chart basis whether or not a single correction could bring a particular lattice within the 1/4-nautical mile accuracy criteria over the entire area of chart coverage. They supplied corrections for those charts where they were deemed applicable. On charts of 1:1,500,000 scale and smaller, ASF corrections were not considered significant. The USCG agreed to keep DMAHTC and NOS advised of system changes and to set priorities and to monitor the overall charting effort. All three agencies were to be involved in collection system calibration data.

There was also a consensus between NOS, USCG, and DMAHTC that LORAN-C lines would not be shown on harbor or harbor entrance charts larger than 1:80,000 scale and that the lattices should not be shown in most inshore areas or inland waters on smaller scale charts. The primary charting area of concern was the CCZ. The inner limit of that zone had been defined by DOT as the harbor entrance.

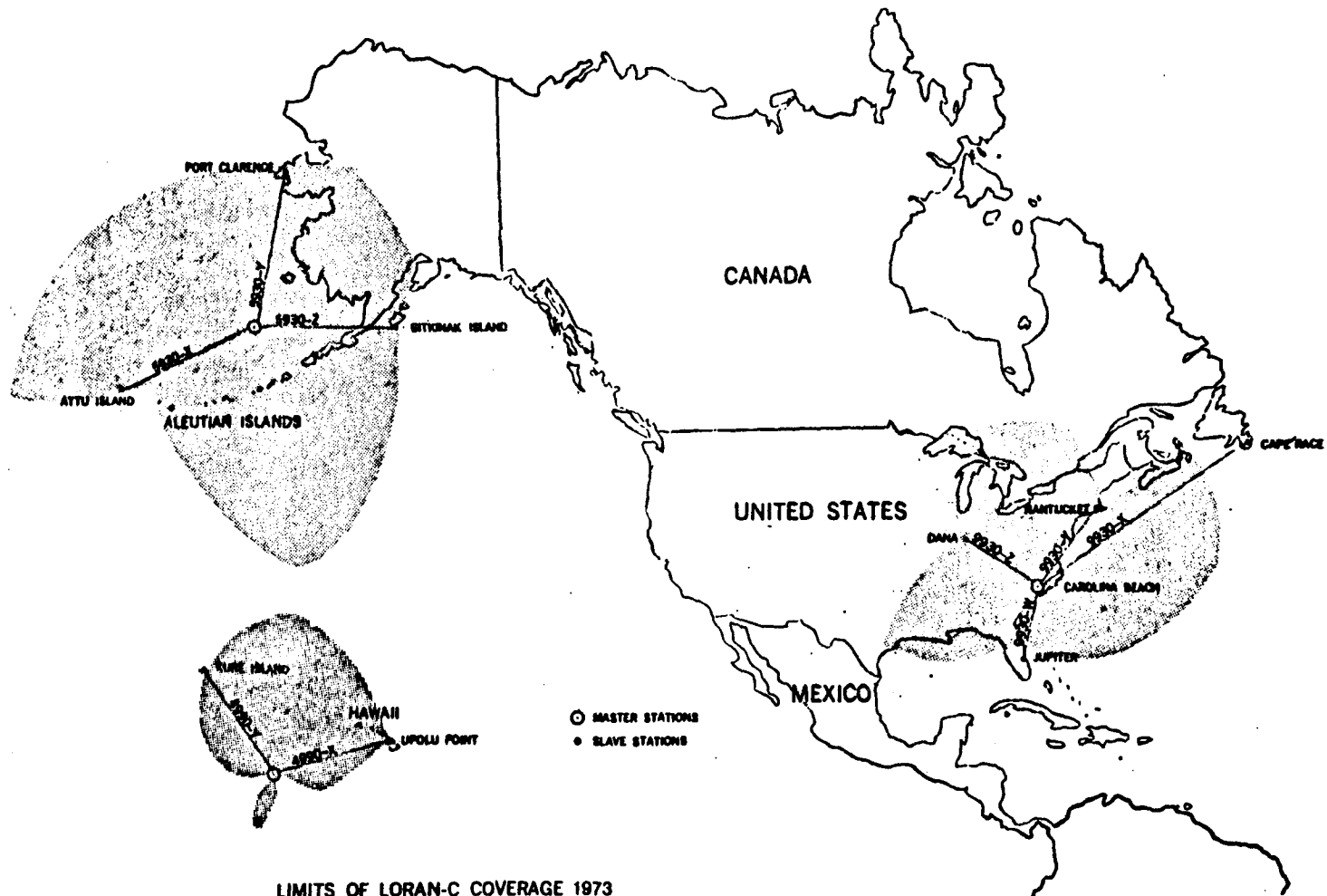
Based on these general interagency agreements, NOS began to add LORAN-C lines of position to nautical charts. This was scheduled and accomplished in five basic phases:

Phase 1 - Charting of Lines of Position for U.S. LORAN-C Coverage Existing as of January 1, 1973.

LORAN-C overlays for the first seven charts overprinted by NOS had been prepared by DMAHTC for the earlier special purpose issues of these charts requested by the USCG. The DMAHTC overlays for all seven of these charts were constructed based on an assumed all seawater path with no adjustment for overland signal transmission delay (ASF). These overlays were adequate as constructed for overprinting the first two NOS LORAN-C charts on public issue. Both charts covered the Aleutian Islands were smaller than 1:1,000,000 scale and ASF corrections were not considered significant. Chart 16006 was issued in September 1973 and chart 16012 was issued in February 1974.

The remaining five charts for which DMAHTC had prepared LORAN-C overlays were east coast charts varying in scale between 1:200,000 and 1:500,000. At these larger scales, accuracy of the lines of position was a primary concern. On the lattices for these charts some adjustment for overland signal delay (ASF) was required in order to meet the 1/4-nautical mile accuracy criteria.

On each overlay of these charts, DMAHTC indicated the distance in millimeters in the north-south direction and the distance in millimeters in the east-west direction that the corners of the overlay would have to be shifted to adjust the lattice for ASF. This had the effect of shifting the entire lattice by a constant amount representing an average ASF correction for the area of chart coverage. The 18th edition of NOS chart 11520, Cape Hatteras to Charleston, dated March 30, 1974, was the first NOS chart printed with lattices adjusted for ASF.



LIMITS OF LORAN-C COVERAGE 1973

GROUNDWAVE COVERAGE: 95% FIX ACCURACY (20RMS) OF 1500 FEET WITH A STANDARD DEVIATION OF 0.1 MICROSECOND, 1:3 SIGNAL-TO-NOISE RATIO USING VALUES NOT EXCEEDED MORE THAN 95% OF THE TIME THROUGHOUT THE YEAR.

OUTLINE OF NOS LORAN-C CHARTING PROJECT

PHASE 1 - CHARTING OF LINES OF POSITION FOR U.S. LORAN-C COVERAGE EXISTING AS OF JANUARY 1, 1973

<u>CHAIN MASTER</u>	<u>SLAVE PAIRINGS</u>	<u>NUMBER OF CHARTS OVERPRINTED</u>	<u>CHARTING SCHEDULE</u>	<u>SYSTEM OPERATIONAL DATE</u>
9930 CAROLINA BEACH, NC	9930W JUPITER INLET, FLA 9930X CAPE RACE, NEWFNDLND 9930Y NANTUCKET, MASS 9930Z DANA, INDIANA	107*	MARCH 1974-DEC 1976	JAN 1969**
5930 ST PAUL ISLAND, AK	5930X ATTU I, ALASKA 5930Y PORT CLARENCE, AK 5930Z SITKINAK I, AK	38***	SEPT 1973-JAN 1977	1962****
4990 SAND I, JOHNSTON I	4990X UPOLU PT, HAWAII 4990Y KURE I, MIDWAY I	20	OCT 1975-JAN 1978	JAN 1961

* INCLUDES 8 SMALL SCALE CHARTS OF GREAT LAKES

** SERVICE TERMINATED ON SEPT 30, 1979

*** ONLY 8 CHARTS ACTUALLY OVERPRINTED DUE TO TERMINATION OF SERVICE

**** SERVICE TERMINATED FEB 28, 1977

PHASE 2 - CHARTING OF LINES OF POSITION FOR NEW WEST COAST AND ALASKAN CHAINS

<u>CHAIN MASTER</u>	<u>SLAVE PAIRINGS</u>	<u>NUMBER OF CHARTS OVERPRINTED</u>	<u>CHARTING SCHEDULE</u>	<u>SYSTEM OPERATIONAL DATE</u>
9990 ST PAUL ISLAND, AK	9990X ATTU I, ALASKA 9990Y PORT CLARENCE, AK 9990Z NARROW CAPE, AK	46	JULY 1976-JULY 1986	MARCH 1, 1977
9940 FALLON, NEVADA	9940W GEORGE, WA 9940X MIDDLETOWN, CA 9940Y SEARCHLIGHT, NEV	21	JULY 1976-JAN 1977	APRIL 26, 1977
7960 TOK JUNCTION, AK	7960X NARROW CAPE, AK 7960Y SHOAL COVE, AK	43	JULY 1976-JAN 1977	JUNE 28, 1977
5990 WILLIAMS LAKE, BRITISH COLUMBIA, CANADA	5990X SHOAL COVE, AK 5990Y GEORGE, WA 5990Z PORT HARDY, VANC*	16	JULY 1976-JAN 1977	SEPT 5, 1977 NOV 20, 1980

* 5990Z RATE ADDED TO THOSE CHARTS SHOWING THE 5990 CHAIN IN 1980, 1981 AND 1982 AS THEY CAME UP IN REGULAR PRINTING CYCLE

PHASE 3 - CHARTING OF LINES OF POSITION FOR RECONFIGURED EAST AND GULF COAST CHAINS

<u>CHAIN MASTER</u>	<u>SLAVE PAIRINGS</u>	<u>NUMBER OF CHARTS OVERPRINTED</u>	<u>CHARTING SCHEDULE</u>	<u>SYSTEM OPERATIONAL DATE</u>
9960 SENECA, NY	9960W CARIBOU, MAINE 9960X NANTUCKET, MASS 9960Y CAROLINA BEACH, NC 9960Z DANA, INDIANA*	47	JUNE 1977-OCT 1979	SEPT 9, 1978 MAY 1, 1979
7980 MALONE, FLA	7980W GRANGEVILLE, LA 7980X RAYMONDVILLE, TEX 7980Y JUPITER INLET, FLA 7980Z CAROLINA BEACH, NC**	64	JUNE 1977-OCT 1979	DEC 27, 1978 DEC 1, 1978 DEC 1, 1978 OCT 1, 1979

* 7980Z RATE ADDED TO CHARTS BEGINNING IN 1979 AS THEY CAME UP IN REGULAR PRINT CYCLE

** 9960Z RATE ADDED TO CHARTS BEGINNING IN 1979 AS THEY CAME UP IN REGULAR PRINT CYCLE

PHASE 4 - CHARTING OF LINES OF POSITION FOR NEW CHAINS ON GREAT LAKES CHARTS

<u>CHAIN MASTER</u>	<u>SLAVE PAIRINGS</u>	<u>NUMBER OF CHARTS OVERPRINTED</u>	<u>CHARTING SCHEDULE</u>	<u>SYSTEM OPERATIONAL DATE</u>
9960 SENECA, NY	SAME AS ABOVE	22	JAN 1980-JAN 1983	SEE ABOVE
8970 DANA, INDIANA	8970W MALONE, FLA* 8970X SENECA, NY 8970Y BAUDETTE, MINN	31	FEB 1980-JAN 1983	MARCH 31, 1980

* 8970W RATE NOT CHARTED BECAUSE IT IS USED PRIMARILY FOR OVERLAND LORAN-C APPLICATIONS

PHASE 5 - CHARTING OF LINES OF POSITION FOR CANADIAN EAST COAST CHAIN

<u>CHAIN MASTER</u>	<u>SLAVE PAIRINGS</u>	<u>NUMBER OF CHARTS OVERPRINTED</u>	<u>CHARTING SCHEDULE</u>	<u>SYSTEM OPERATIONAL DATE</u>
5930 CARIBOU, MAINE	5930X NANTUCKET, MASS 5930Y CAPE RACE, NEWFNDLND	14	FEB 1982-JUNE 1983	APRIL 30, 1980

The corner shift method was used to adjust DMAHTC-generated LORAN-C overlays for ASF on the first several charts overprinted. This technique, however, proved cumbersome. Lines had to be extended on two adjacent chart edges to fill the void caused by the shift and painted out on the opposite edges where they extended beyond the chart limits.

In trying to find a simpler method of adjusting the lattices for ASF, NOS ran some test plots of its own in 1974. By altering the coding delay used as input in the generation of each lattice by the amount of correction for ASF provided by DMAHTC in microseconds, NOS was able to produce overlays that resulted in the identical placement of the lines of position as had been obtained using corner shifts.

From this point on DMAHTC furnished ASF correction data to NOS in terms of microseconds. If the ASF correction for a LORAN-C rate was negative, it was added to the coding delay. If the correction was positive, it was subtracted from the coding delay.

This technique of altering the coding delay was used to construct the lattices for the remaining Phase 1 charts for which ASF corrections were required. For each rate, a single correction was used representing an average of ASF correction data in the area of chart coverage. These corrections were theoretically derived by DMAHTC. But they were based on a relatively large volume of observed data collected over a period of years.

Largely completed by June 1976, the charting of existing LORAN-C chains provided coverage for the east and gulf coasts, the Great Lakes, Alaska, and Hawaii.

Phase 2 - Charting Lines of Position for New West Coast and Alaskan Chains

Prior to 1977 there was no operational LORAN-C service on the west coast. With LORAN-C chart coverage of much of the remaining U.S. coastal area available by June 30, 1976, the charting of the lines of position for the proposed west coast and Alaskan chains was scheduled to be completed July 1, 1976, and January 1, 1977. NOS revised its normal printing schedule in order to accommodate this charting effort and to make it possible for LORAN-C charts of these areas to be available when these new chains became operational.

A problem developed concerning the first west coast charts on issue showing the lines of position for the 9940 chain. Single ASF lattice shifts provided by DMAHTC were again incorporated in the construction of each lattice. But the theoretically derived ASF corrections furnished for the first west coast charts did not prove sufficient to bring the lattices within the 1/4-nautical mile accuracy standard over the entire area of chart coverage.

The land and sea interface on the west coast was very different from other areas where calibration data for operating LORAN-C chains had been collected, and the Fallon, Nevada, master station was much farther inland than existing master stations. Moreover, the 9940 chain and other new west coast chains had been

operational on an experimental basis for a short period of time. There was very little reliable calibration data available upon which DMAHTC could base predicted ASF corrections.

As a result, the initial LORAN-C editions of southern California charts 18746, 18720, 18721, 18765, and 18740 were inaccurate. These charts were in error by 2 microseconds or more in some cases. This resulted in positioning errors of up to 2 1/2-nautical miles. The five southern California charts overprinted with LORAN-C lines were originally printed between March 19, 1977, and October 23, 1977.

In response to this problem, the NOAA Ship RAINIER conducted a calibration survey in the affected area which was completed in September 1977. The data collected were forwarded to DMAHTC for evaluation. Correction items for the charts in question were broadcast and published in DMAHTC and USCG Notices to Mariners in December 1977.

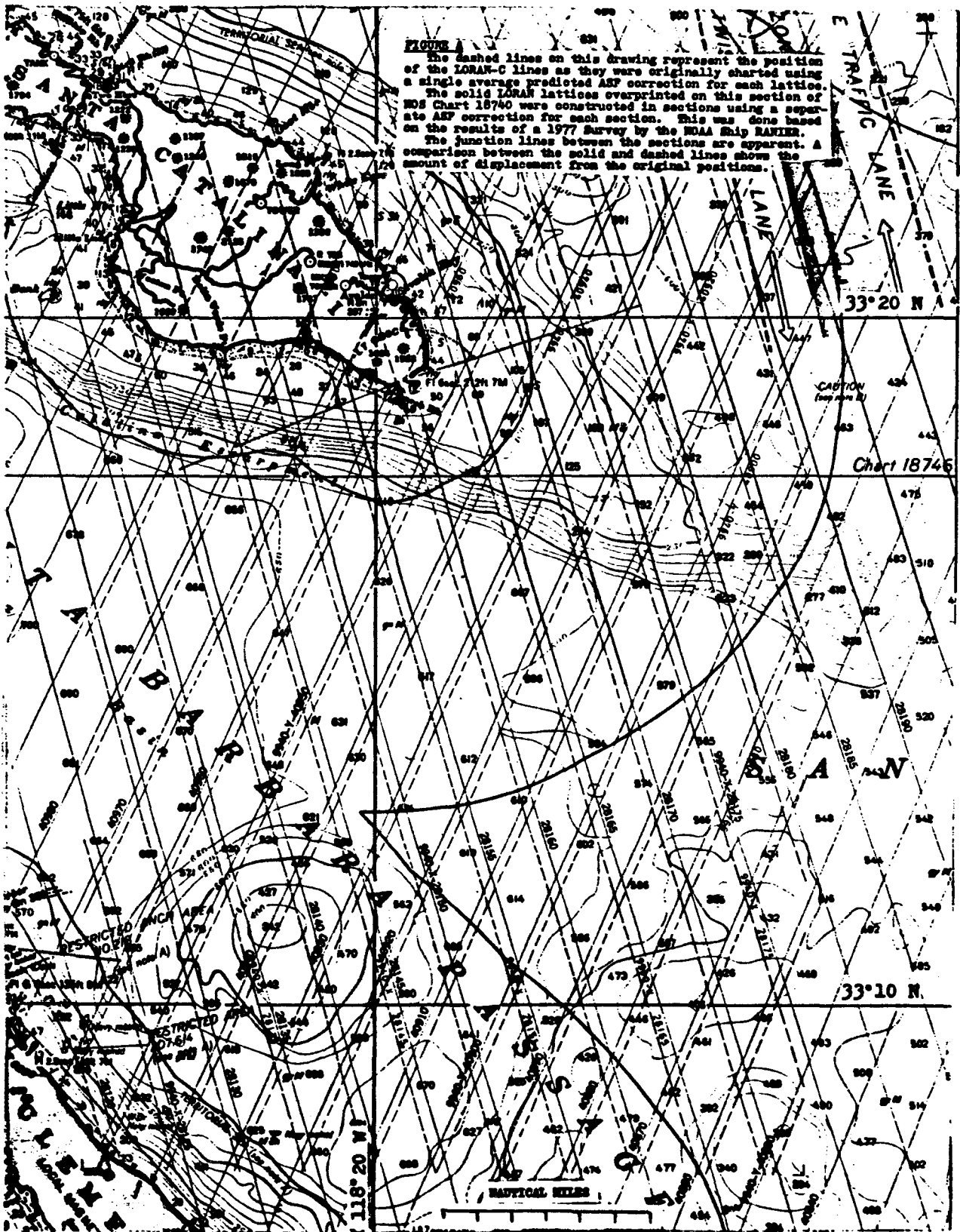
By November 1978, DMAHTC had forwarded revised lattice shifts concerning these charts to NOS. The single lattice correction technique was again used in the reconstruction of these LORAN-C overlays. But in order to meet the established accuracy criteria, it was necessary to divide some of the charts into as many as four separate sections. A single microsecond correction was incorporated in the construction of the lattices for each of these sections. A different correction was used for each section. Where the chart sections junctioned, corresponding lines of position were arbitrarily connected. These short junction lines were particularly noticeable on the revised edition of chart 18740 (see figure A). New editions of all five charts with corrected lattices were printed between May 1, 1978, and June 2, 1979.

Another charting problem affecting the accuracy of the lines of position developed concerning the new 9990 Alaskan chain. This chain was a reconfiguration of the previous 5930 chain. The original master station on St. Paul Island was retained along with slave stations located at Port Clarence and on Attu Island. The previous 5930 slave station on Sitkinak Island was abandoned in favor of a new slave station at Narrow Cape.

The first NAD 27 data sheet for the Alaskan chain received by NOS from DMAHTC was dated March 5, 1976. Positions for the St. Paul master station and slaves at Attu Island and Port Clarence were carried forward from a previous data sheet furnished by DMAHTC for the original 5930 chain dated April 20, 1966. A revised DMAHTC data sheet dated June 23, 1980, placed the St. Paul master station more than 2 seconds north and 7 seconds west of the original coordinates.

Complications involved in the original geodetic survey location of the St. Paul tower led to this discrepancy. The revised positions received in 1980 resulted in the need to revise or reevaluate the printed lattices on approximately 40 charts with particular attention given to larger scale charts. Because many Alaskan charts are reissued infrequently, at 3- to 8-year intervals, the problem of revising the lattices was compounded.

In scheduling the overprinting of LORAN lines of position for the new west coast and Alaskan chains, DMAHTC recommended that 19 charts be removed from the printing schedule and that the overprinting of LORAN-C lines on these charts be



postponed until a later date. The coverage area of these charts contained land and water in such mixture that charting techniques available at that time could not bring the lattices within the required 1/4-nautical mile accuracy.

Phase 3 - Charting of the Lines of Position for the Reconfigured East and Gulf Coast Chains

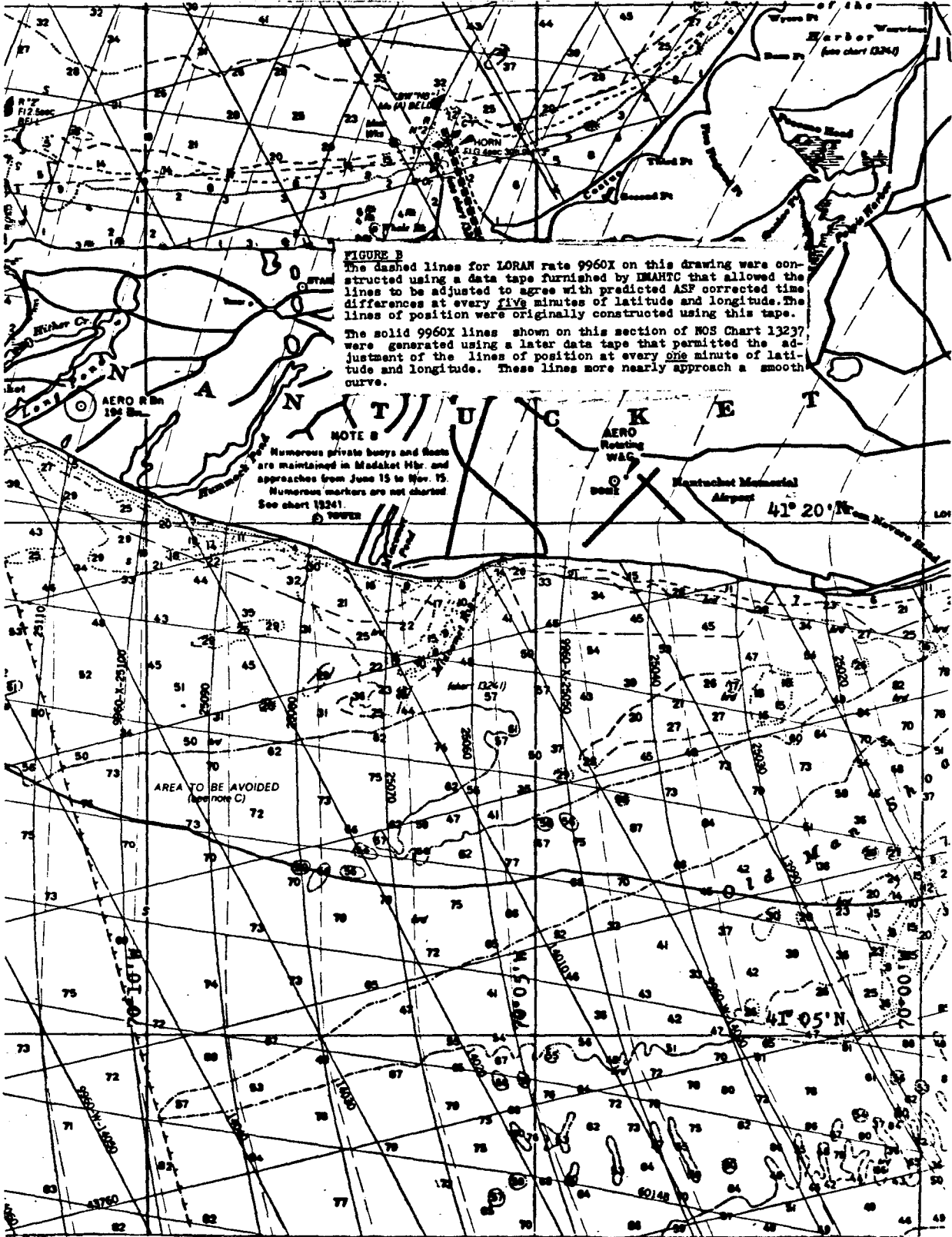
The experience gained in charting the LORAN-C lattices on west coast charts caused the USCG, DMAHTC, and NOS to reevaluate existing charting methods. Before the charting of lines of position for the proposed east and gulf coast chains began in June 1977, it was determined that a single average correction would not be sufficient to bring the lattices within 1/4-nautical mile accuracy on coastal charts 1:100,000 scale and larger. Charting of the lattices on these charts was deferred until an adequate charting method was available. For charts of smaller scales, however, the single lattice correction technique continued to be used.

At the request of USCG, DMAHTC forwarded to NOS a computer program to be used to construct the lattices on the large-scale charts. Added as an option to the existing NOS LORAN plotting, the program produced contoured lines of position that were in agreement with ASF corrected time difference predictions provided at every 5 minutes of latitude and longitude in the area of chart coverage. Data tapes furnished by DMAHTC containing the corrected time differences were used in conjunction with this program to construct the lattices on all east and gulf coast charts 1:80,000 to 1:100,000 scale.

The lines of position generated using these 5-minute data tapes were not smooth in areas where the curvature of the lines of position was very pronounced. The lines of position for rate 9960X on NOS chart 13237, Nantucket Sound and Approaches, were very segmented as originally charted using a 5-minute data tape (see figure B). In these instances, DMAHTC provided data tapes with ASF corrected time differences predicted at every minute of latitude and longitude. The lines of position constructed based on these 1-minute data tapes more nearly approached a smooth curve.

NOS attempted to have LORAN-C chart coverage for the new east and gulf coast chains on issue prior to the operational dates for those chains. This led to an unavoidable charting error concerning the 7980Y lines of position. Based on the results of experimental operation of the gulf coast chain, USCG revised the proposed coding delay for the 7980Y rate from 41000 to 43000. Several small-scale charts were already overprinted and on issue before this change. Therefore the numeric labels for the 7980Y lines of position on these charts were 2,000 microseconds in error. Correction items were published in Notices to Mariners for the charts involved in November 1978.

Originally issued with 7980 lines of position between March 4, 1978, and September 23, 1978, all 11 charts were corrected and reprinted between May 1, 1979, and October 31, 1979. The original DMAHTC data tapes for use in constructing the lattices overprinted on 1:80,000-scale gulf coast charts were also 2,000 microseconds in error. However, the lattices overprinted were correctly labeled when the charts were issued.



The deferral of charting LORAN-C lines on large scale charts until NOS could adapt the DMAHTC warped lattice program delayed the entire charting schedule by a few months. Therefore, a few charts were not overprinted with the new 7980 and 9960 lines of position prior to the termination of the old 9930 service on September 30, 1979, and the start of the new service on October 1, 1979. This resulted in considerable inconvenience to mariners. In the Charleston, South Carolina, area, for example, shrimpers and commercial fisherman were left without current LORAN-C charts to use during a busy part of their working season. The charted 9930 lines were obsolete.

In order to avert serious economic loss in the Charleston area, NOS responded to an inquiry from Senator Ernest Hollings of South Carolina by rapidly generating several hundred mylar LORAN-C overlays and distributing them to mariners in the Charleston vicinity within 2 weeks of the operational date of the new LORAN service. These overlays were to be used in conjunction with NOS chart 11520, Cape Hatteras to Charleston; NOS chart 11521, Charleston Harbor and Approaches; and NOS chart 11009, Cape Hatteras to Straits of Florida. Though the 9960 lines of position were shown on chart 11520 at this time, part of the chart coverage area was at the limit of acceptable ground wave coverage for the 9960 chain. The mylar overlay generated for that chart showed the 7980 lines which were indicated to be more useful in the Charleston area.

As a follow-up to this remedial action, a new edition of chart 11521 covering the immediate Charleston area was printed showing the 7980 lines of position. This new edition was dated February 23, 1980. The next editions of chart 11520 and chart 11009 also reflected appropriate LORAN-C additions and revisions.

Unexplained anomalies affecting the 7980W rate in the western Gulf of Mexico were discovered as a result of a verification survey conducted by the USCG in that area in October 1978. There were significant differences between the predicted grid values and actual survey observations for the 7980W rate in the coastal area between Galveston and Brownsville, Texas. Predicted data at specified points were approximately 0.8 microseconds higher than the observed values. DMAHTC predicted values for the 7980W rate in the coastal area east of the Mississippi River were found to be acceptably accurate. No survey information was collected in the area between the Mississippi River and Galveston but the predicted values in this area were treated as suspect, and the charting of the lines of position for the 7980W rate on the 1:80,000 scale coverage in that area was deferred until an adequate survey was conducted.

Although DMAHTC data tapes with predicted time differences at every 5 minutes of latitude and longitude were used to construct the lattices for the 7980X, 7980Y, and 7980Z rates on the 1:80,000 scale charts between Galveston and Brownsville, the 7980W lines were constructed using single lattice corrections furnished by DMAHTC after evaluation of USCG survey data.

The 7980 lattice on NOS chart 11300, Galveston to Rio Grande, covering the entire western gulf area was revised on the 23rd edition issued July 5, 1980. In order to bring the lines of position into agreement with the USCG survey data, the lattice was reconstructed in two sections with single ASF corrections used to adjust the lines in each section. Where the sections junctioned, the lines were arbitrarily connected using shore junction lines as was done on several west coast charts.



Navigation System Decommissioned

By WILLIAM MATTHEWS

NC OCT 16 1979 Staff Reporter

In an effort to make a highly accurate ocean navigation system even more precise, two federal agencies have put it temporarily out of commission.

New radio signal transmitters installed this month by the Coast Guard were intended to increase the distance covered by the Long Range Aid to Navigation system.

But charts that would enable navigators to interpret the new signals will not be printed by the National Oceanic and Atmospheric Administration until December.

The lack of charts to interpret the signals has resulted in "a navigational blackout" between Charleston and the North Carolina border, according to U.S. Sen. Ernest F. Hollings, D-S.C.

Now fishermen are unable to locate good fishing spots, out-of-state boaters are getting lost and people who depend on accurate navigation for a living are losing money, according to Hollings, and "all of it was avoidable," he said.

Capt. James Fournier, Coast Guard congressional affairs officer, said the problem resulted because NOAA failed to produce new charts on schedule.

But he said the temporary loss of the LORAN-C system should pose no safety hazard to navigators. "There are a number of ways to navigate beside LORAN-C," he said. Fishermen and other navigators can use celestial navigation, fathom meters, radio beacons, sea buoys and common sense to survive without LORAN-C signals, he said.

The Phoenicians navigated 5,000 years ago without the aid of electronics, he said.

According to Capt. Albert S. Lachicotte Jr., port captain for the state Department of Wildlife and Marine Resources, the lack of intelligible LORAN-C signals is "a big inconvenience" but is unlikely to cause experienced navigators major difficulties.

"With LORAN-C you can get within 50 yards of the mark you want" even when out of sight of land, Lachicotte said. Without it, coming that close is very difficult, he said.

Many fishermen will resort to using a compass and time coordinates for navigation, he said. But for many it will be much harder to find specific fishing spots.

Long-line fishermen may have trouble locating their lines without LORAN-C signals, he said. "But the average person with experience with the sea won't have a problem" getting home safely, he said.

The absence of LORAN-C so far has not created safety problems, a spokesman from the Charleston Coast Guard base said Monday.

A spokesman from Hollings' office said a limited number of new charts will be available this week at the Custom House for fishermen, commercial navigators and others who may suffer economically from the loss of accurate navigation capability.

The 7980W lines of position were later added to the 1:80,000 scale charts between Mississippi and Galveston using 5-minute data tapes furnished by DMAHTC that reflected the latest survey data. The 7980X and 7980Y lines of position were evaluated at the same time and revised if necessary.

The 7980W lattice on NOS chart 11340, Mississippi River to Galveston, was revised on the 45th edition issued January 29, 1983. The lattice was originally added to the 37th edition dated June 10, 1978.

Because the 9960Z and 7980Z rates were scheduled to become operational 8 to 10 months after the other rates in the reconfigured east and gulf coast chains, the overprinting of lines of position for these rates was deferred until they became operational. This reduced the initial workload and facilitated the overprinting of LORAN-C on a large number of charts prior to the operational dates for the remaining rates. When the 7980Z chain became operational, the 7980X lines of position were removed from east coast charts. Except in a few cases, 7980Z lines of position were not shown on large-scale charts west of the Mississippi River. The lines for that rate have been removed from those western gulf charts where it had been initially charted.

Phase 4 - Charting Lines of Position for New Chains on Great Lakes Charts

Following the termination of the original 9930 LORAN-C service on September 30, 1979, the Great Lakes region was without LORAN-C chart coverage for a few months. Small scale chart coverage for each of the lakes was not available until early 1980.

On the eastern lake charts, Erie and Ontario, the lines of position for the existing 9960 chain were overprinted. Both the 9960 and 8970 lines of position were overprinted on the Lake Huron chart because Lake Huron is in the ground wave coverage area for both chains. On the western lake charts, Michigan and Superior, the lines of position for the 8970 chain were the only lattices overprinted. The ground wave coverage for the 8970 chain extended to the eastern lakes but the signal strength from the 8970Y Baudette, Minnesota, slave was weak except in the northern part of Lake Erie.

The lines of position for the 8970W rate were not shown on NOS charts. The baseline extension for the 8970W pair runs through the western lakes region resulting in poor gradients. This pairing of the Dana, Indiana, master with the Malone, Florida, slave was designed primarily for overland LORAN-C applications.

The 1:100,000-scale coastal charts covering Lake Erie and Lake Ontario were the first large-scale lake charts overprinted with the new LORAN lattices. Since the old 9930 lines of position were not overprinted on lake coastal charts, this represented the first large-scale LORAN-C chart coverage in the lakes area.

DMAHTC data tapes were used to construct the LORAN lattices for all the large-scale lake charts. Eastern lake charts were overprinted first because the 9960 chain had been in operation for about a year, and NOS and USCG calibration surveys had been conducted in Lake Erie and Lake Ontario. Predicted time differences that were provided for these charts by DMAHTC were based, in part, on this preliminary survey data.

Because the 8970 chain was not operational until March 1980, the LORAN-C lattices for the western lake coastal charts were constructed based on predicted time differences that did not incorporate calibration survey data. These charts have not yet been revised to reflect the results of survey data collected after the initial printings.

Phase 5 - Charting of Lines of Position for the New Canadian East Coast Chain

Operating with the master station at Caribou, Maine, and slaves on Nantucket Island, Massachusetts, and Cape Race, Newfoundland, the 5930 Canadian East Coast (CEC) chain was originally scheduled to be overprinted on NOS charts between December 1978 and November 1979 as part of the general charting agreement with USCG and DMAHTC concluded in 1975. But the Caribou system did not become operational until April 20, 1980. The addition of the 5930 lines of position to northeast coastal charts was therefore deferred.

In response to a letter from the USCG received in April 1980, NOS added the 5930 lines of position to the 9960 lines already overprinted on NOS charts 13260, 13009, 13203, and 13204. This provided small-scale chart coverage of the CEC chain in the Georges Bank area. The 34th edition of NOS chart 13009, Gulf of Maine and Georges Bank, 1:500,000 scale dated August 30, 1980, was the first NOS chart on issue showing the 5930 lines of position.

As a result of another letter from the USCG received in October 1981, NOS chart coverage of the 5930 chain was expanded to include chart 13006, West Quoddy Head to New York, and nine 1:80,000-scale coastal charts covering the area from Nantucket Island to the Canadian border. DMAHTC again furnished 5-minute data tapes for use in overprinting the lattices on the large-scale charts. The predicted time differences on these data tapes were based on recent and extensive survey calibration data in the area.

The 9960 lines of position were already overprinted on all of these charts, but the crossing angles and gradients for these rates in the northeast coastal area were generally poor. In that area, the 5930 rates gave improved coverage.

Editing and Evaluation of Existing NOS LORAN-C Charts

During a fairly intensive charting effort, the primary concern of NOS was the rapid overprinting of accurate lines of position on a large number of charts in order to provide the public with accurate LORAN-C nautical chart coverage as quickly as possible. These overprinted charts and established chart specifications are now in the process of being evaluated in terms of both chart accuracy and clarity.

Chart clutter has always been a major concern but it has not always been avoidable. When the first LORAN-C charts were issued, the LORAN-C lines were overprinted on many charts already showing LORAN-A lattices. In the interest of chart clarity, the LORAN-A and LORAN-C lattices were initially printed back to back on separate faces of the same chart. But the results of a LORAN chart evaluation questionnaire distributed to all attendees at a LORAN-C users

conference convened in Portland, Oregon, in December 1975, indicated that a majority of chart users desired that LORAN-A and LORAN-C lines be shown on the same chart base. This would facilitate conversion from the one system to the other.

Therefore, NOS abandoned back-to-back printings and began to print both systems on the same face of the chart. To reduce clutter, all LORAN-A lines were printed in a subdued gold color to differentiate them from LORAN-C lines. This was done except in cases where the total number of LORAN-A and LORAN-C lattices to be overprinted was more than six. When the combined number of lattices was more than six, the LORAN-A rates were shown on one face of the chart and the LORAN-C lines on the other.

When the need arose to overprint the lines of position for the new east and gulf coast and Great Lakes chains on charts already showing existing LORAN-C and LORAN-A lattices, the chart clutter problem became more serious. It became necessary to use the back-to-back printing method again showing the new LORAN-C lines and the old LORAN-C lines on one side of the chart and the new LORAN-C lines and LORAN-A lines on the other. This facilitated the conversion of old LORAN-C positions and LORAN-A positions to new LORAN-C coordinates.

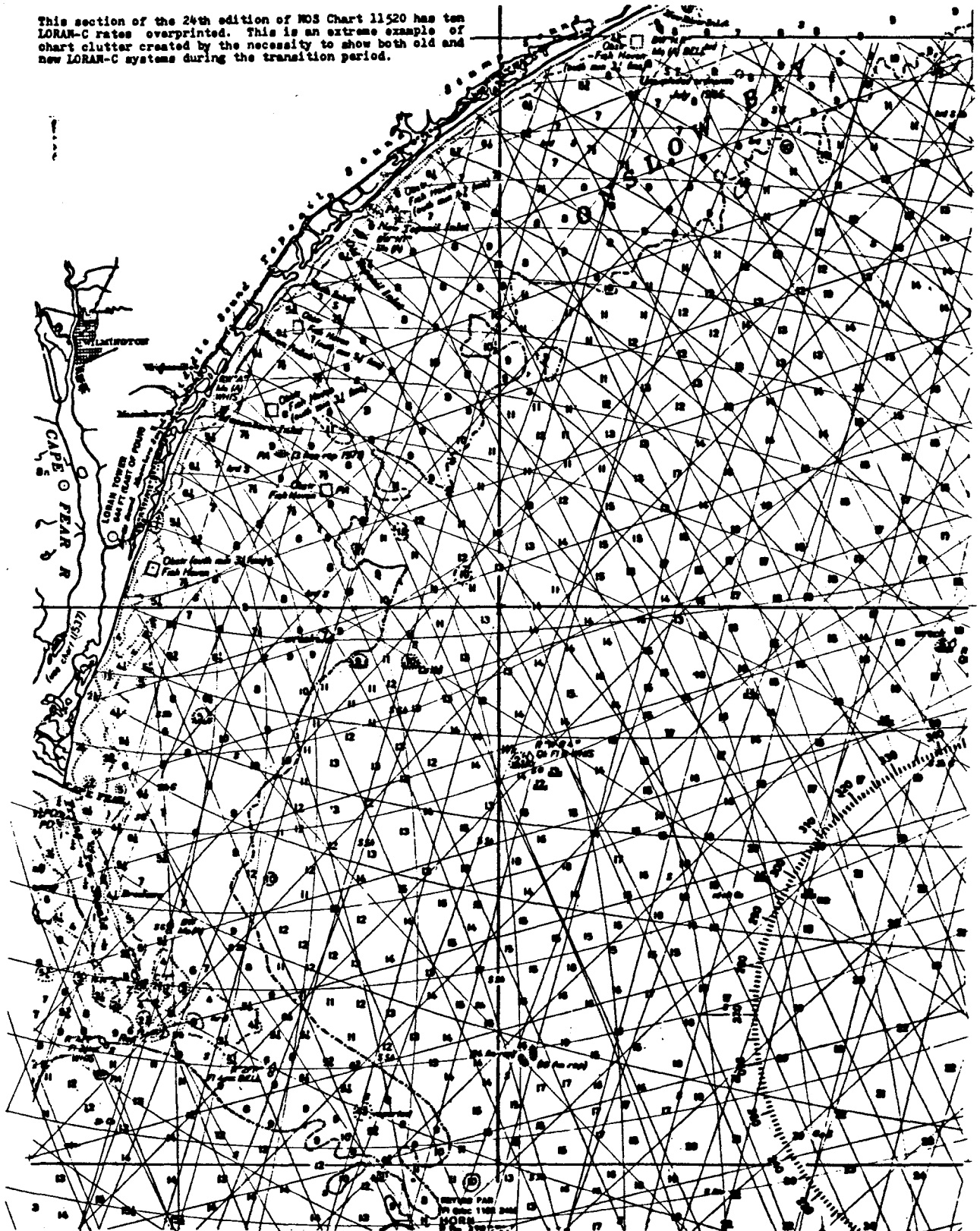
This procedure resulted in considerable chart clutter on a number of charts. There was a total of 10 lattices overprinted on NOS chart 11520, Cape Hatteras to Charleston, 24th edition, dated December 8, 1979. By agreement with the USCG, however, NOS continued to show the lines of position for the old 9930 lines of position for at least one printing of each chart involved after the termination of 9930 service on September 30, 1979. NOS similarly continued to show LORAN-A lattices for a transition period following the termination of all LORAN-A service in U.S. coastal waters on December 31, 1980. When these lattices began to be removed, the chart appearance improved significantly.

In some instances the number of overprinted lattices continues to be a problem. Chart 11520 still shows seven lattices even with three old 9930 lattices removed. That chart is in an area of overlap between the 7980 and 9960 chains. Chart 14860, Lake Huron, shows six overprinted lattices on a single face being in an overlap area between the 8970 and 9970 chains.

Spacing between the lines of position on the lattices remaining on NOS charts is being reevaluated on a chart-by-chart basis. In constructing the lattices, line spacing between 1/2 inch and 1-1/4 inches apart was the accepted criteria based on DMAHTC specifications. On some charts it is now felt that the 1/2-inch minimum spacing criteria is too close. This is particularly true on charts with a large number of lattices overprinted and on charts where the hydrography and other detail are very heavy.

In the interest of chart accuracy, the lines of position for some rates have been deleted. Poor gradients in the area of the baseline extension and poor signal strength reported can result in the deletion of a rate. Lines of position can also be added if it is determined that an uncharted rate is more suitable in a given area than those already charted. On charts that fall in the area of overlap between LORAN-C chains and charts covering the fringe areas of groundwave coverage for existing chains, the question of which rates to show is being reexamined. As more survey data are analyzed, the overprinted lattices on NOS charts will continue to be examined.

This section of the 24th edition of NOS Chart 11520 has ten LORAN-C rates overprinted. This is an extreme example of chart clutter created by the necessity to show both old and new LORAN-C systems during the transition period.



Future LORAN-C Charting

The NOS LORAN-C charting effort as outlined in the 1975 agreement with USCG and DMAHTC is nearly complete. As more survey data are processed, the lattices on all overprinted charts are subject to revision. A list of NOS LORAN-C charts scheduled to be printed during a specific fiscal year is forwarded to DMAHTC. DMAHTC will then supply NOS with necessary data for those charts on which the lattices may need to be revised. The final decision to revise the lattices will be made by NOS in consultation with USCG. In most instances, revision of the lines of position should concern charts 1:100,000 scale and larger. The lattices on smaller scale charts should prove adequate. Discrepancy reports from all sources will be examined in making a decision to revise the overprinted lines of position.

Charts remaining to be overprinted include a few large-scale charts of Lake Michigan and Lake Erie. Also, 19 west coast and Alaskan charts were removed from the original charting schedule because they depicted land and sea in such mixture that a single ASF correction for each lattice could not bring the lattices within the 1/4-nautical mile accuracy criteria. The Straits of Juan de Fuca and Puget Sound charts included in this list have the highest priority.

At the time lattices were overprinted on large-scale charts of the west coast and Alaska, the DMAHTC "warped lattice" program using data tapes to correct the lines of position at every 5 minutes of latitude and longitude was not available for NOS use. The single lattice correction technique was used to construct the lattices on all these charts. The lattices may eventually need to be reconstructed using the "warped lattice" method.

The addition of LORAN-C lines of position to harbor charts of scales 1:40,000 and larger is a future possibility. However, more extensive data collection and evaluation will be necessary before this is considered. While fairly constant offshore, the ASF corrections in nearshore and inland waters are more irregular. Improved charting techniques dealing with ASF may have to be developed before the lines can be overprinted on these charts.

There will be a future need to construct LORAN-C lattices for all new charts where they are appropriate. A proposed datum shift on NOS charts from NAD 27 to NAD 83 will also be a future consideration affecting the LORAN-C lattices.

The existing LORAN-C network serving U.S. coastal waters should remain stable for the near future. A proposal to build a new station at Yakutat, Alaska, for incorporation into the 7960 Tok Junction chain has been cancelled and there are no other major revisions planned in the short term.

Supplemental LORAN-C Charting and Support Projects

In addition to the scheduled overprinting of NOS charts, the Marine Chart Branch has provided many mylar LORAN-C overlays upon request in support of NOAA hydrographic and bathymetric surveys and other research projects. LORAN-C plotting overlays have been provided on several occasions for NOAA's Atlantic Oceanographic and Meteorological Laboratories in Miami. And a series of approximately 50 mylar LORAN-C plotting sheets were ruled for NOAA's Data Buoy

Center, National Space Technology Laboratories, NSTL Station, Mississippi. These were used to plot data buoy migrations. Another set of overlays was ruled for the Field Research Office, NOAA Air Resources Laboratory, Idaho Falls, Idaho. These overlays were used to track particle emission dispersal from the Mt. St. Helens' eruption.

In response to requests from outside NOAA, the Marine Chart Branch has processed a number of other overlays to facilitate buoy positioning by the USCG and to support commercial fishing and diving interests and another needs. In addition to providing overlays, the Marine Chart Branch has provided other services related to LORAN-C, including converting LORAN-A coordinates to LORAN-C coordinates and LORAN-C coordinates to latitude and longitude coordinates. For example, 100 pairs of coordinates for intersecting lines of position shown on NOS chart 12304, Delaware Bay, were converted to geographic positions for Ichthyological Associates, an ecological research and consulting firm. The distance between these positions was then calculated in meters. These conversions and calculated distances facilitated the company's biological impact study of the Salem Nuclear Power Plant on the Delaware River conducted in 1981.

NOS was also an active participant in the 1980 Radio Technical Commission for Marine Services panel discussions concerning minimum performance standards for automated LORAN-C coordinate converters.

Evolution of Charting Techniques and Specifications

The major changes in the preparation of LORAN-C overlays since 1973 have concerned the method used to adjust the lattices for ASF. For the first several Phase 1 charts, the lattices were constructed by DMAHTC based on assumed all seawater paths and adjusted for ASF by physically shifting them using the corner shift technique. Subsequent LORAN-C lattices were constructed by NOS and incorporated ASF adjustments in the automated construction of each lattice using one of two methods.

The single lattice correction technique used by NOS to construct the lattices on all charts in the Phase 1 and Phase 2 stages of the NOS LORAN-C charting effort involves altering the theoretical coding delay assigned to each LORAN-C rate. The coding delay for each rate is altered by a different amount depending on the ASF corrections given for each chart.

The basic NOS HYLOT plotter program used to generate magnetic tapes that direct the automated plotters in the construction of the lattices does not take into account seawater delay, referred to as the Secondary Phase Factor (SF) or overland signal delay (ASF). The coding delay used as input to the HYLOT program is adjusted for both SF and ASF. The seawater (SF) corrections for each rate is computed. The overland (ASF) corrections are furnished for each chart by DMAHTC.

The formula for computing this altered coding delay used as input in the generation of a lattice is:

$$CD' = CD + SF - ASF$$

FIGURE D

LORAN-C CONSTANTS---EAST COAST, U.S.A.
(2 May 1969)

Item:

- a. LORAN-C pair designations: 9930(SS7)-W, 9930(SS7)-X, 9930(SS7)-Y, 9930(SS7)-Z
- b. Transmitting station locations (NAD-27)

<u>Pair</u>	<u>Location</u>	<u>*Latitude</u>	<u>*Longitude</u>	<u>Station Letter</u>
9930-W (SS7)	Cape Fear, North Carolina (Master)	34° 03' 45.61" N	77° 54' 47.20" W	H
	Jupiter Inlet Florida (Slave)	27° 01' 57.32" N	80° 06' 53.71" W	J
9930-X (SS7)	Cape Fear, North Carolina (Master)	34° 03' 45.61" N	77° 54' 47.20" W	H
	Cape Race, Newfoundland (Slave)	46° 46' 32.70" N	53° 10' 31.76" W	R
9930-Y (SS7)	Cape Fear, North Carolina (Master)	34° 03' 45.61" N	77° 54' 47.20" W	H
	Nantucket Island, Massachusetts (Slave)	41° 15' 11.98" N	69° 58' 40.51" W	V
9930-Z (SS7)	Cape Fear, North Carolina	34° 03' 45.61" N	77° 54' 47.20" W	H
	Dana, Indiana (Slave)	39° 51' 07.48" N	87° 29' 11.51" W	D

* North American Datum: (1927) --- Clarke Spheroid 1866 --- Parameters of reference ellipsoid - Item 9b. of the General Specifications.

- c. Coding delay: (assigned)

<u>Pair</u>	<u>Microseconds</u>
9930-W	11,000
9930-X	28,000
9930-Y	49,000
9930-Z	65,000

FIGURE D

LORAN-C CONSTANTS--EAST COAST, U.S.A.--NAD 1927 (2 May 1969)

d. Coding delay, CD, + computed baseline time, Bc, which includes the secondary phase correction for all seawater path:

Pair 9930-W: $CD + Bc = 11,000 + 2,695.48 = 13,695.48$ microseconds
Pair 9930-X: $CD + Bc = 28,000 + 8,389.57 = 36,389.57$ microseconds
Pair 9930-Y: $CD + Bc = 49,000 + 3,541.27 = 52,541.27$ microseconds
Pair 9930-Z: $CD + Bc = 68,000 + 3,560.68 = 69,560.68$ microseconds

e.

<u>Pair</u>	<u>Computed Baseline Distance in Meters</u>	<u>Angle of Intersection of Baselines at Master Station</u>
9930-W	807,401.8214	114°04'10.2480"
9930-Z	1,066,532.1075	89°05'11.9902"
9930-Y	1,060,720.7462	9°30'54.9395"
9930-X	2,512,789.6513	147°19'42.8223"
9930-W	807,401.8214	

CD' is the altered coding delay used as input to the plotter program. CD is the theoretical coding delay as assigned to that rate. SF is the seawater adjustment and ASF is the overland correction. The formula for computing SF for any LORAN-C rate is given as:

$$SF = Bc - (Bd/P)$$

Bc is the computed one-way baseline time which includes SF. Bd is the baseline distance in meters and P is the signal propagation velocity. Values for Bc, Bd, and P can be obtained from information sheets for each chain furnished by DMAHTC (See figure D).

For example, calculating SF for rate 9930-Z:

$$\begin{aligned} Bc &= 3,560,68 \text{ microseconds} \\ Bd &= 1,066,532.1075 \text{ meters} \\ P &= 299.693 \text{ meters/microsecond} \\ SF &= 3,560 - \frac{1,066,532.1075 \text{ meters}}{299.693 \text{ meters/microsecond}} \\ &= 3,560.68 - 3,558.75 \\ &= 1.93 \text{ microseconds} \end{aligned}$$

For NOS chart 12300, the ASF correction in microseconds for rate 9930Z is - 2.78. Therefore, computing the altered coding delay used in the construction of that lattice:

$$\begin{aligned} CD' &= 65000.00 + 1.93 - (2.78) \\ &= 65000.00 + 1.93 + 2.78 \\ &= 65004.71 \text{ microseconds} \end{aligned}$$

In following these computations, consider that the coding delay for a given rate is a constant and that the entire lattice is being shifted by a constant amount.

The coding delay is the starting microsecond value for the lines of position beginning at the slave station baseline extension. The microsecond values for the lines of position increase moving toward the master station. For example, the lines of position for rate 9930Z constructed at 20-microsecond intervals would have a value of 65000 at the baseline extension (See figure E). The first curves moving away from the baseline would have values of 65020, 65040, 65060 and so on.

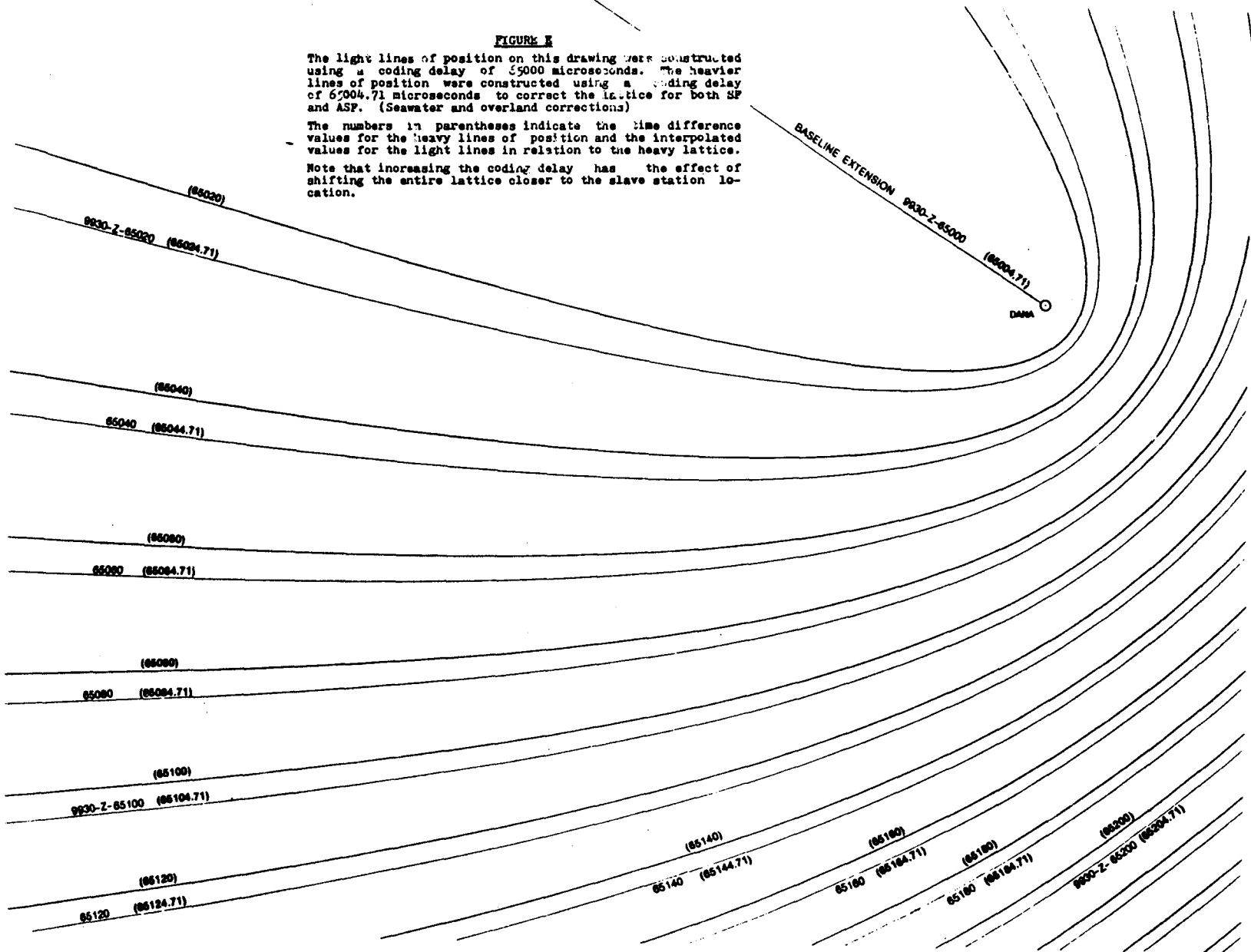
By altering the coding delay according to the sample calculation for rate 9930Z, the baseline would have an effective value of 65004.71 and the values for the first curves moving away from the baseline would increase accordingly to 65024.71, 65044.71, and so on. But curves are not charted at uneven intervals. The dashed lines (figure E) represent the position of the even 20-microsecond curves based on the altered coding delay. These interpolated lines of position are closer to the baseline than the theoretical 20 microsecond curves. Increasing the coding delay has the effect of shifting the entire lattice closer to the slave station. Decreasing the coding delay used in the construction of a lattice would have the effect of shifting the entire lattice farther away from the slave station.

FIGURE E

The light lines of position on this drawing were constructed using a coding delay of 5000 microseconds. The heavier lines of position were constructed using a coding delay of 65004.71 microseconds to correct the lattice for both SP and ASP. (Seawater and overland corrections)

The numbers in parentheses indicate the time difference values for the heavy lines of position and the interpolated values for the light lines in relation to the heavy lattice.

Note that increasing the coding delay has the effect of shifting the entire lattice closer to the slave station location.



The second technique NOS uses to adjust the lattice for ASF relies on data tapes furnished by DMAHTC that provide corrected time differences at every 5 minutes of latitude and longitude. This method was used to construct the lattices on all charts larger than 1:100,000 in scale during the Phase 3, Phase 4, and Phase 5 stages of the NOS LORAN-C charting project. It was adopted for use on large-scale charts following the difficulties encountered with the first charted lattices on southern California coastal charts that were constructed using a single lattice correction for each rate.

The lattices produced using this technique are contoured to bring them into agreement with the time differences predicted by DMAHTC. The program interpolates between these gridded values to construct lines of position at specified microsecond intervals. The DMAHTC predicted values are adjusted for both SF and ASF.

The geographic limits of the LORAN-C chart overlays produced using these 5-minute data tapes are the nearest 5-minute intervals of latitude and longitude beyond the latitude and longitude coordinates of the chart neatline. On these oversized plots, the lines of position must be deleted where they extend beyond the chart neatline.

DMAHTC data tapes that provide predicted time differences at every 1 minute of latitude and longitude were used to construct lattices in areas where there was a sharp curvature to the lines of position (See figure B). An alternative approach to the use of 1-minute data tapes to produce accurate smooth lines of position when the lines constructed using 5-minute tapes are erratic is to use a series of single lattice corrections for the same rate.

The NOS HYLOT program allows the user to plot up to nine separate rates on one plot. This option can be used to plot up to nine separate sections of the same rate. By using a different coding delay adjustment in generating the lines for each section, it is often possible to shift a single line of position or several lines to make them agree with the DMAHTC predicted time differences. Use of this technique results in smooth lines of position that are tangent at several locations to the corresponding erratic lines constructed using a 5-minute data tape.

This method is particularly adaptable when the lines of position are nearly parallel to either the north-south or east-west chart axis. If the gridded ASF correction values increase or decrease in a compatible manner, this technique can be used effectively.

In adding LORAN-C lines of position to nautical charts of 1:100,000 to 1:80,000 in scale and in a few instances to even larger scale charts, NOS was a pioneer. The first editions of these charts overprinted with LORAN-C represented the largest scale LORAN-C coverage available to the general public. In deciding to add LORAN-C lines to large scale charts, NOS was concerned about the accuracy of the LORAN-C lattices constructed using predicted ASF corrections that were not verified by field calibration. This concern was shared by the Canadian Hydrographic Service (CHS) who did not show LORAN-C on charts larger than

1:125,000 in scale. In consultation with the USCG and DMAHTC, the following caution note was added to NOS charts in order to alert users to possible LORAN-C inaccuracies:

The LORAN-C lines of position overprinted on this chart have been prepared for use with groundwave signals and are presently compensated only for theoretical propagation delays which have not yet been verified by observed data. Mariners are cautioned not to rely entirely on the lattices in inshore waters.

Revised versions of this note will indicate that the lines of position shown on a chart are based only on predicted ASF or that they are based on ASF corrections that incorporate the results of field calibrations.

All LORAN-C lattices for NOS charts were constructed either on NAD 27 or on Old Hawaiian Datum. The base charts for several Pacific Ocean charts were constructed on one of several Astro Datums. Because Astro Datum coordinates for LORAN-C towers could not be obtained, the lattices for these charts were constructed on Old Hawaiian Datum.

NOS chart 19480, Gambia Shoal to Kure Island, was constructed based on Astro Datum. The 4990Y lattice constructed for that chart based on Old Hawaiian Datum was not in proper relation to the charted Kure Island slave station for that rate. Therefore, the lattice was shifted to bring it into agreement with the charted position of the slave station.

In August 1978, NOAA Ship TOWNSEND CROMWELL investigated a discrepancy reported by the USCG concerning the charted LORAN-C lattices constructed on Old Hawaiian Datum for chart 19441, Maro Reef, and the base chart constructed on Astro Datum. The results of this investigation indicated that the LORAN-C lattices agreed very closely with the charted projection grid and that the position of the charted hydrography and topography relative to that grid were in error. The discrepancy was believed to have been caused by errors in the original positioning system.

Obviously the timely development of high-speed plotters greatly facilitated the NOS LORAN-C charting project. The old manual method used in constructing many LORAN-A overlays would have been totally inadequate and the early automated plotters were too slow to accommodate the workload. Although NOS has used a Raster laser drum plotter to generate positive LORAN-C overlays for a few charts, most chart lattices have been constructed using one of two CALCOMP flatbed plotters. The volume of work and the necessity to adjust the size of the overlays to compensate for small distortions in sizes of existing chart negatives made the use of the flatbed plotters more practical.

LORAN-C lattices have generally been scribed, and positives made photographically from these scribes have been used to label the lines of position in preparation for overprinting. The automated plotters did not construct the baseline extensions for LORAN-C rates. Points along the baseline were computed using a programmable calculator. These positions were then plotted on overlays where the baseline extension was shown and a smooth line constructed and scribed through the plotted points.

After some initial experimentation, NOS adopted most DMAHTC LORAN-C charting specifications and guidelines. Lattices were constructed with general spacing between the lines of position no less than 1/2 inch nor greater than 1 1/2 inches. For all LORAN-C chains, the W lines of position were printed in blue, the X lines in purple, the Y rates in screened black, and the Z rates in green. These general specifications for line spacing and color were also adopted by CHS.

NOS did not adopt the DMAHTC practice of printing bold index lines of position at regular intervals and decided not to dash the lines of position in inshore areas or in areas beyond the limits of the CCZ.

GLOSSARY

Secondary Phase Factor (SF) -- Signal delay in microseconds as the transmitted LORAN-C signal travels over an assumed all seawater path. The primary phase factor is the theoretical velocity of the transmitted signal in free space.

Additional Secondary Phase Factor (ASF) -- Additional signal delay in microseconds due to differing land conductivity of the varied terrain in the path of the transmitted signal. ASF corrections are separate from and do not include SF corrections.

Baseline -- The great circle line connecting the master transmitting station and a secondary transmitting station.

Baseline Extension -- The extension of the baseline beyond either the master or secondary transmitting station.

Chain -- A LORAN-C network consisting of a master transmitting station and two to four secondary transmitting stations.

Coastal Confluence Zone (CCZ) -- The outer boundary of the CCZ is defined as 50 nautical miles offshore or the edge of the Continental Shelf (100 fathom curve), whichever is greater. The inner boundary of the CCZ is defined as the harbor entrance. The 1974 Department of Transportation National Plan for Navigation designated LORAN-C as the primary radionavigation system for the CCZ.

Definitions for SF, ASF, and CCZ are based on a 1977 paper entitled, "Applications of Overland Propagation Corrections to LORAN-C Charts within the CCZ" by Edwin O. Danford and David M. Somerville of the Defense Mapping Agency Hydrographic/Topographic Center. Other definitions are taken from the U.S. Coast Guard "LORAN-C Users Handbook" published in May 1980.

ACKNOWLEDGEMENTS

The author would like to acknowledge the following people for their contributions to the NOS LORAN-C charting project and to this paper:

National Ocean Service: Capt. Donald R. Tibbit, NOAA (Ret.); R. Adm. Richard H. Houlder, NOAA (Ret.); Capt. Lavon L. Posey, NOAA; Mr. Frank W. Maloney; Mr. Maxwell M. Rogers, Mr. Dennis J. Romesburg; Mr. Norman E. Banks; Mr. James E. Gearhart; Mr. Norman D. Smith; Lt. Cdr. Richard A. Schiro, NOAA; Ms. Rosemary E. Riodan; and Mr. Jack L. Wallace.

U.S. Coast Guard: Lt. Cdr. John F. Weseman, USCG; Lt. Cdr. Richard Kirkman, USCG; CWO Mark Crabill, USCG; and the late Cdr. Brent Mills, USCG.

Defense Mapping Agency Hydrographic/Topographic Center: Mr. John E. Hanna, Mr. W. M. Swartwood, Mr. Edwin O. Danford, and Mr. John J. Speight.

FREQUENCY AND TIME DOMAIN CHARACTERIZATION OF LORAN-C SIGNALS
IN THE NEAR FAR FIELD

Authors:

Francis W. Mooney, Senior Project Engineer
Systems Evaluation Division, DTS-52
Transportation Systems Center
Kendall Square
Cambridge, MA 02142

Albert D. Frost
Electrical Engineering Department
University of New Hampshire
Durham, NH 03824

ABSTRACT

In 1982, the Coast Guard commissioned the Transportation Systems Center (TSC) with the task of measuring and documenting the transmission signatures of Loran-C stations. Equipment for measuring frequency domain characteristics was assembled and tested in 1982. Supplemental equipment for measuring the time domain signature was procured and integrated into the suite in 1983. The resultant ensemble makes it possible to characterize the station signature in two working days; previously it required a week for the USCG to make similar type measurements. This paper will describe the equipment suite and present the results obtained at LORSTA Seneca.

INTRODUCTION

Measurements of Loran-C signals have always been a complex process because of the pulsed nature of the system. While the allowed spectrum for Loran-C has been established as the frequency band 90-110 kHz for many years, the principal use of the system is in the time domain, so emphasis has been maintained on time domain parameters. Precise measurement of Loran-C transmissions in either time or frequency domain has remained difficult through the years due to instrumentation limitations. In 1982, the Coast Guard commissioned TSC to assemble an equipment suite which would permit measurement of Loran-C signals in the frequency domain. The objective was two fold; first, to establish that Loran-C stations were meeting CCIR requirements regarding in-band power and harmonics, and second, to have a mobile capability that would permit signal analysis throughout the service area so that the Coast Guard could assure users that signals were meeting specifications. Introduction of a new generation of time domain sampling equipment by Hewlett Packard in late 1982 also facilitated making time domain measurements

and this capability was added to the equipment suite in 1983. This paper will address development of the measurement capability for signals in each domain separately, then present results of station measurements.

FREQUENCY DOMAIN

Challenges exist to making measurement of Loran-C signals in the frequency domain in the form of the sensors, the measurement equipment, computation of in-band energy and separation of harmonics from interference or background noise. When TSC initiated this project, the Coast Guard had already resolved most of the challenges, but each will be briefly considered.

The standard sensor at a Loran-C transmitting station is a wide band, Pearson current transformer. The Pearson is adequate for near-band measurements, but its frequency response is less desirable for harmonic observations. To make field measurements, the Coast Guard procured Austron loop antennas and developed a series of wide band and stop band filters to facilitate observations. Each loop, transmission line and filter were tested at EECEN and are maintained as an integrated unit. Frequency response curves for each package are provided with a set.

For many years, frequency measurements in the low frequency range were made with the Hewlett Packard 310 frequency selective voltmeter. Frequency measurements were laborious since the meter was hand tuned. In the '70s, a series of spectrum analyzers were produced which permitted making rapid measurements throughout the LF band, but precise measurements of individual frequency components were difficult because results were taken off a CRT. When Hewlett Packard introduced the 3585 Spectrum Analyzer, it became possible to make precision measurements at all frequencies as was done with the 310, but rapidly scan for spectral shape and interference. TSC engineers programmed the 3585 with a Tektronix 4052 graphics computer. In this way, gathering spectral information and on-line analysis became easier by an order of magnitude.

The equipment interconnection for gathering basic spectrum information is shown in Figure 1. Measurements are made as follows:

(1) The loop antenna is oriented to achieve a peak signal. It is terminated by a wide band filter for in band measurements, and by a stop band (100 kHz notched) filter for harmonic measurements.

(2) The 4052 steers the 3585 through the frequency band 76-124 kHz in 1 kHz steps, with the IF bandwidth set at 300 Hz. Data is taken at each frequency and measurements are compensated for the response of the loop/filter.

(3) In-band energy is then calculated based on Simpson's rule (this computation procedure was previously established by the Coast Guard). The number of data points necessary to provide accurate observations was established through joint TSC/Coast Guard efforts. The observation is semi-automatic in that the operator sets up the equipment, then the 4052 controls measurements. Program results are shown in Figures 2 through 6. The quality of data is clearly shown in Figure 3, where variability of measurements at each frequency is considerably less than 1%.

For harmonic information, the equipment interconnection is shown in Figure 7. On an oscilloscope which is triggered by a Loran-C rate generator, the IF output of the spectrum analyzer is observed. Loran-C energy is clearly synchronized on the oscilloscope and peak/peak readings are made at each harmonic frequency. A representative example is shown in Figure 8.

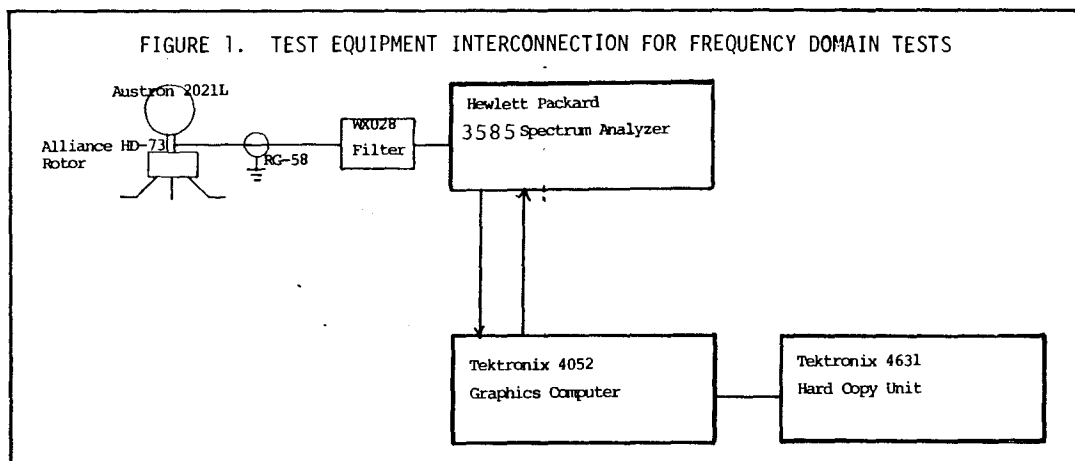


FIGURE 2. SAMPLE SPECTRUM RECORD IDENTIFICATION

DOT/TSC LORAN-C Signal Analysis		PGM 012
RECORD IDENTIFICATION	ns1H2	
RANGE	-15.0 DBM	
RBM	300 HZ	
SELECT FILE NO.2		
FILE CONTAINS	NAH012	25-JUL-83 15:20 CONTINUE ? YES
TAPE ASSIGNED		TSCXX1 FILE2
INPUT LORSTA ID	NANTUCKET	
MEASUREMENT SITE ID	TN2XNTR24	
NUMBER OF SAMPLES IN AVERAGE	Emax 53 ?	5
SPECTRUM SAMPLE SPACING (KHZ)	1	

FIGURE 3. SAMPLE FREQUENCY SPECTRUM OBSERVATIONS
PAGE 1 OF 5

naTN2		ALL SAMPLES		
100	-50.40	101	-50.50	99 -50.20 ← Numbers are in dB
	-50.50		-50.40	-50.50
	-50.40		-49.60	-50.30
	-50.50		-50.50	-50.30
	-50.60		-50.40	-49.40
		102	-50.30	98 -50.00
			-50.30	-50.10
			-50.30	-50.10
			-50.30	-50.10
			-50.30	-50.10
		103	-50.10	97 -49.60
			-50.10	-49.50
			-50.10	-49.50
			-50.20	-49.40
			-50.20	-49.50
		104	-50.00	96 -48.00
			-50.00	-48.00
			-50.10	-48.70
			-50.00	-48.00
			-50.00	-48.00
		105	-50.20	95 -48.15
			-50.20	-48.15
			-50.10	-48.05
			-50.20	-48.15
			-50.10	-48.35

FIGURE 4. EXAMPLE FREQUENCY SPECTRUM SAMPLES

naTN2		AVE. OF 5 SAMPLES		
100	-50.61	101 kHz	-50.40	99 -50.25 ← Numbers are in dB
		102	-50.43	98 -50.21
		103	-50.27	97 -49.63
		104	-50.15	96 -48.91
		105	-50.29	95 -48.29
		106	-51.13	94 -48.20
		107	-53.22	93 -49.09
		108	-56.27	92 -53.10
		109	-59.97	91 -57.24
		110	-64.25	90 -61.50
		111	-68.40	89 -65.73
		112	-72.60	88 -70.15
		113	-75.00	87 -75.10
		114	-76.98	86 -80.73
		115	-76.70	85 -83.30
		116	-76.72	84 -83.65
		117	-76.75	83 -81.71
		118	-76.86	82 -81.02
		119	-77.81	81 -80.39
		120	-78.48	80 -79.03
		121	-78.77	79 -80.88
		122	-80.54	78 -81.16
		123	-82.04	77 -82.71
100	-50.41	124	-83.53	76 -81.24

FIGURE 5. EXAMPLE OF AN/FPN-42 SPECTRUM ENVELOPE AT LORSTA NANTUCKET

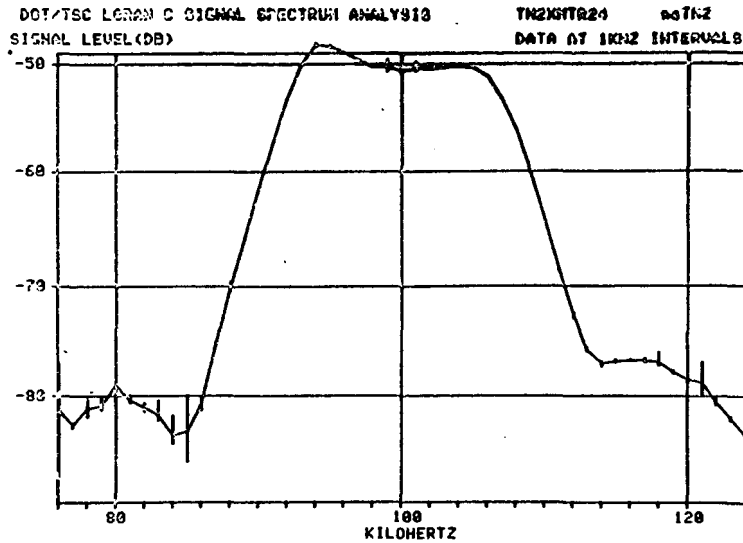


FIGURE 6. EXAMPLE OF IN BAND POWER COMPUTATION

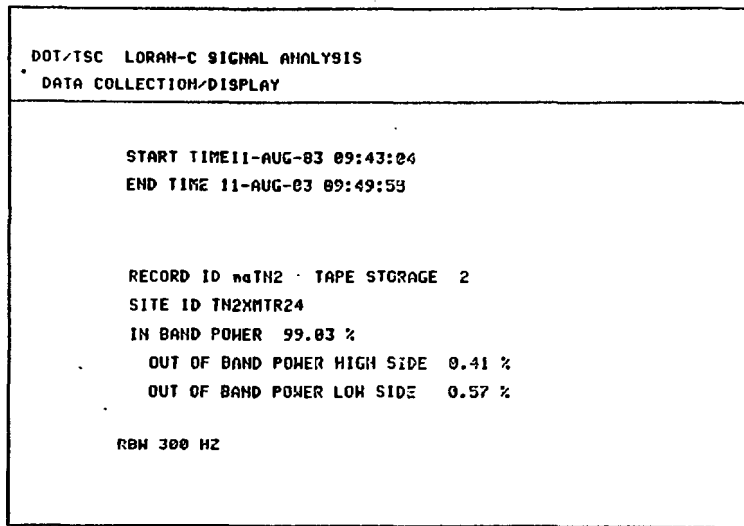
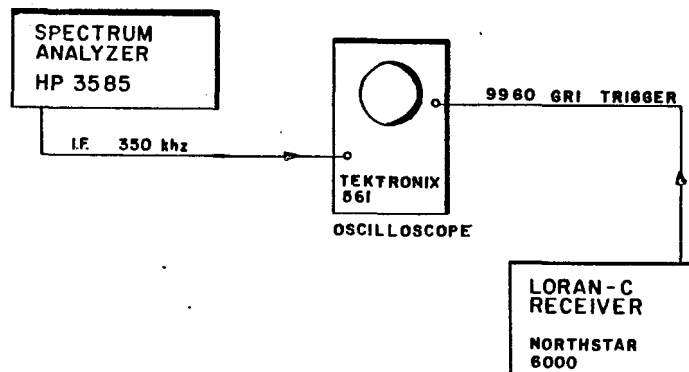
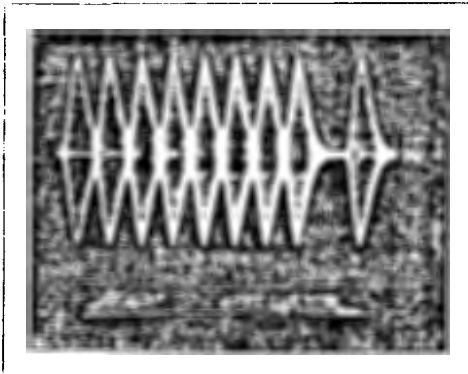


FIGURE 7. IN BAND HARMONIC MEASUREMENT - TYPICAL EQUIPMENT INTERCONNECTION



TIME DOMAIN

FIGURE 8. EXAMPLE OF HP 5385A IF OUTPUT DURING HARMONICS MEASUREMENT

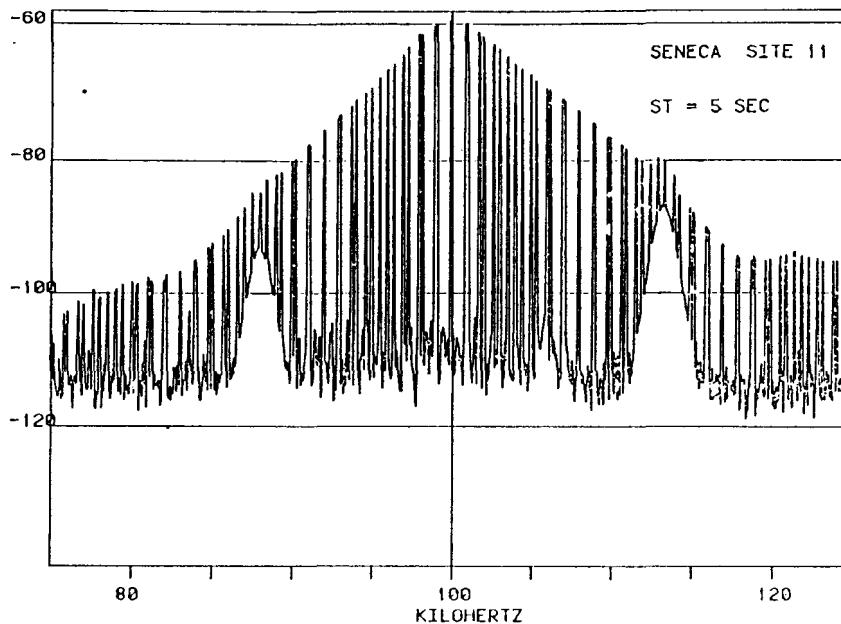


Interfering frequencies are identified through operator control of the spectrum analyzer. When scanning with a sweep time of 5 seconds, Loran-C transmissions are seen on the analyzer as vertical lines. Interfering frequencies are shown as voids in display. Observations throughout a band are first done with a rapid, continuous scan. Exact frequency identification of any interfering signal is accomplished by manual adjustment of a cursor. Figure 9 shows observations made at LORSTA Seneca where a near band signal at 113.2 kHz was laying under the local signal. The interference does not have the bandwidth indicated. This a phenomenon introduced by the combination of sweep time and analyzer bandwidth setting.

Time domain specifications for Loran-C pulses are identified in great detail in "Specification of the Transmitted Loran-C Signal (COMDTINST M16562.4)." The Coast Guard has assembled a limited number of instrumentation packages which are used, on a rotational basis, to evaluate Loran-C stations. They are called Loran-C Data Acquisition units (LORDAC). These units interface directly with LORSTA timing equipment and make precise measurements of the signals. Timing/synchronization signals are obtained in such a fashion that the LORDACs are operated only at LORSTAs.

In the fall of 1982, Hewlett Packard introduced the 5180A waveform recorder. This piece of stand alone test equipment featured a 60 dB dynamic range analog to digital convertor with memory storage of 16,384 bytes (partitionable from 1 to 32 sections). The bandwidth of the 5180A was 20 MHz, adequate for Loran-C. A decision was made to procure a waveform recorder, interface it with the 4052 and develop a time domain analysis capability which was independent of station equipment.

FIGURE 9. EXAMPLE OF INTERFERING FREQUENCIES UNDER LORAN-C SPECTRUM



The capability to analyze time domain performance of a Loran-C station using the 5180A has been achieved. Use of the 5180A provides a fresh look at Loran-C pulses because the instrument literally takes a "snapshot" rather than average a number of samples as is done by the LORDAC. Simply stated, the 5180A is triggered to look at either a group of Loran-C pulses or a sequence of the same pulse in 16 consecutive Group Repetition Intervals (GRIs).

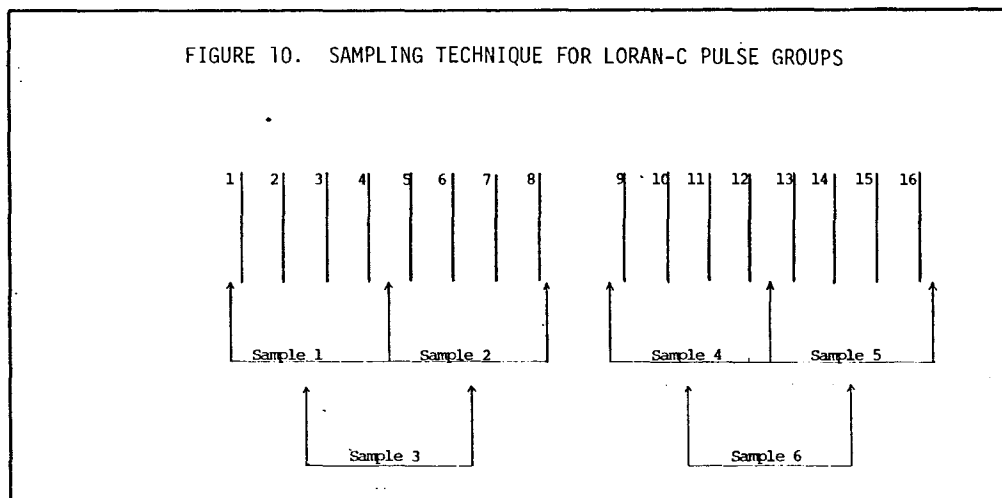
After various sampling experiments, it was determined that a sample spacing of 200 ns produced no discernable error. Two critical items in the development of the time domain analysis capability were the establishment of a synchronous GRI trigger and the creation of control programs which permitted on-site data acquisition and analysis.

Turn-on and sample times in the 5180A permit taking samples sets no oftener than 5 ms. With no partition of the memory, this permits examination of 4 consecutive pulses when a 200 ns sample space is used. In order to measure pulse-to-pulse spacing for all pulses in two phase code intervals, six sample sets must be taken. Initiating the sample is done by a special purpose trigger generator, driven by two GCF-W-541-B Loran-C Cross Rate Blankers. The overlapping sample sequence is illustrated in Figure 10. The sampling problem is made considerably more complex at a double-rated Loran-C station. It was found at LORSTA Nantucket that samples taken near cross-over were different than those taken where the transmitter is less stressed. The simple sample statement regarding pulse samples made earlier reflects several months of experimentation.

The 4052 graphics computer features 32 k RAM with a tape drive storage cassette capable of approximately 300 k bytes. Analyzing all the pulse parameters contained in COMDTINST 16562.4 proved to require more program than can be currently hosted in the 4052, therefore a program was prepared to identify and print peak values of half cycles, zero crossovers and to compute the Envelope to Cycle Difference (ECD). Analysis of pulse-to-pulse spacing, droop, etc. is done post mission on the 4052 with off line programs.

The block diagram of time domain analysis equipment is shown in Figure 11. The RF source for the waveform recorder can be a Loran-C simulator, a receiver, an output from the station current transformer or the loop antenna used for frequency analysis. All of these sensors have been tested and the effect of the coupling network is quite striking. Figure 12 is a Loran-C pulse obtained from an EPSCO 4010-50 Loran-C Simulator. ECD for this pulse is 0.37 microseconds, but the effective frequency, obtained by doing a curve fit to zero crossings, is 98.6 kHz.

Figure 13 shows a Loran-C pulse as shown in the RF section of a Loran-C receiver. ECD analysis using the Coast Guard's algorithm is not possible for this waveform because the slope is outside the range of convergence. A Loran-C pulse, as taken off the current transformer at LORSTA Nantucket, is shown in Figure 14. Analysis of this pulse gives an ECD of +0.339 microseconds, with an rms error for half cycle peaks of 0.437%.



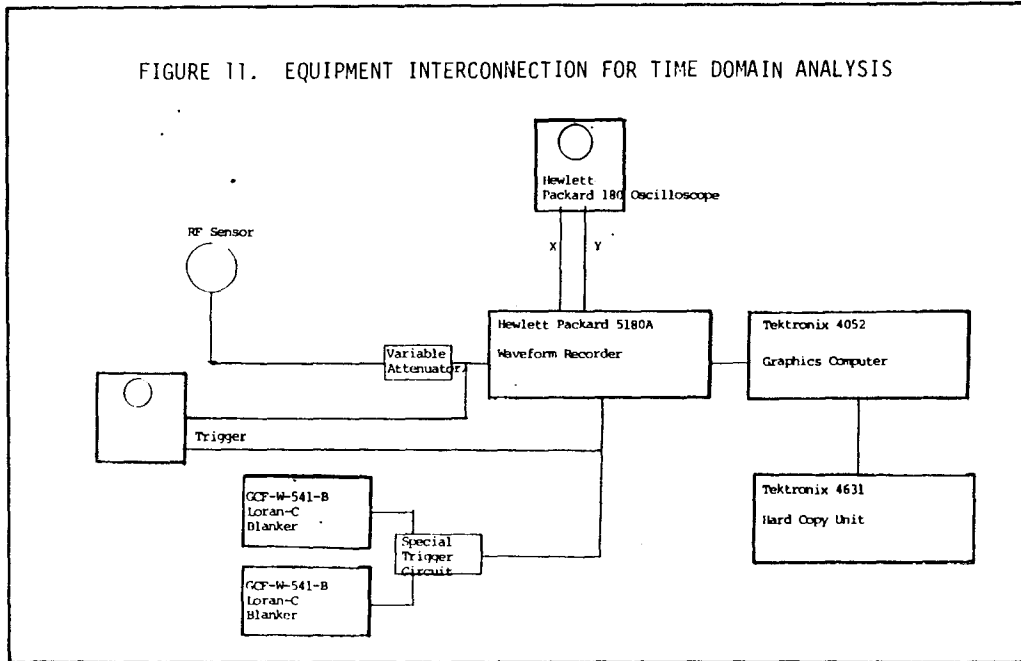
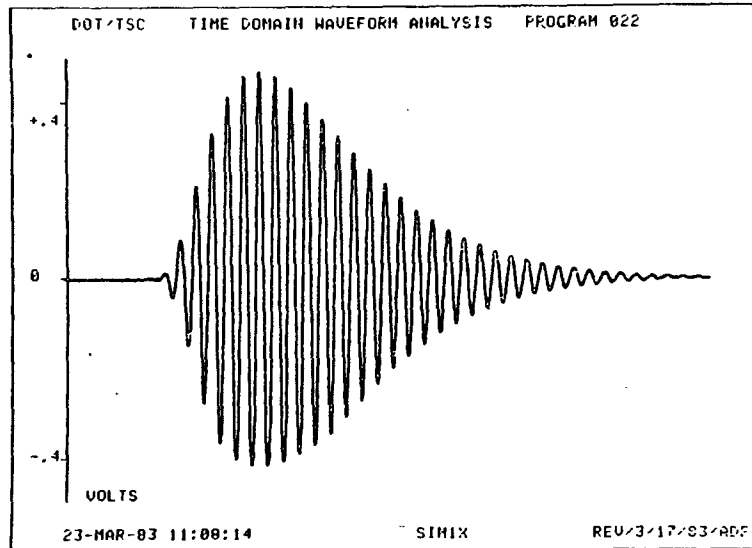


FIGURE 12. LORAN-C PULSE FROM EPSCO 4010-50 SIMULATOR AS RECEIVED BY H.P. 5180A WAVEFORM RECORDER



MOBILE TEST FACILITY (MTF)

TSC maintains a MTF for various field projects. Through the years, the size and shape has changed. The current MTF is a Plymouth window van, coupled with a small utility trailer. The window van houses all test equipment and an AC line conditioner, while the trailer houses 2, 4 kW gasoline generators. Only one generator is used at a time, but experience has shown that redundancy in prime power sources is necessary.

Table 1 lists the equipment suite used in making the Loran-C measurements discussed in this paper. In addition to the frequency and time domain equipment already discussed, two Loran-C receivers, a NORTHSTAR 6000 and an AUSTRON 5000 provide a continuous status monitor of the Loran-C system when in the field. They are also used when making interference measurements in the service area.

FIGURE 13. LORAN-C PULSE FROM A LORAN-C RECEIVER'S RF STRIP

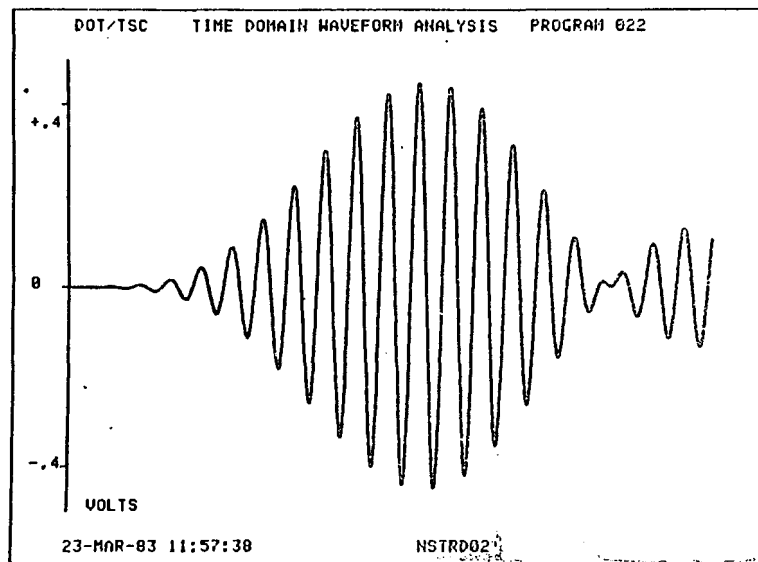
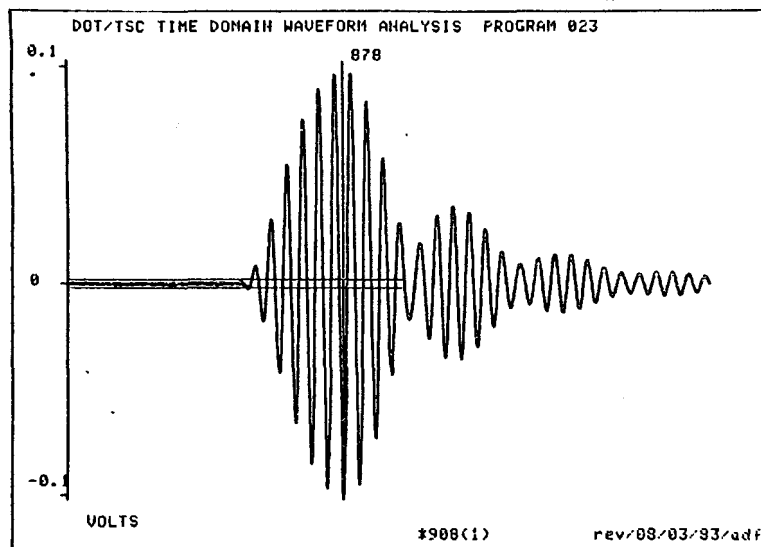


FIGURE 14. LORAN-C PULSE OBSERVED AT LORSTA NANTUCKET



A rubidium frequency standard, with its attendant distribution amplifier and battery backup completes the equipment suite. Use of the rubidium standard for all test equipment assures that all equipment has a common, stabilized oscillator throughout any test program. The rubidium is kept in continuous operation while individual equipments, such as the waveform recorder, are secured at night.

MEASUREMENTS AND RESULTS

Frequency Domain

Characterization of signals in the frequency domain at a station requires that observations be made at a minimum of 5 sites. Comparison of data from the sites discloses whether any signal distortion is present due to a local anomaly. When possible, 3 sites, equidistant from the station on 120 degree radials, are used to measure spectrum. This orientation also permits radiation pattern verification. Harmonic transmissions from

the stations disappear at increasing radial distances into the test equipment background noise level and therefore are measured between 1-2 km from the station. A complete round of frequency measurements; spectrum, harmonics, interference, etc. can be made within one hour at a site.

Time Domain

Measurement of signals in the time domain is accomplished at the transmitting site and at 1-2 km from the station. Measurements at a greater distance are not possible due to disappearance of the first half cycle into test equipment background noise. Observations of signals from one rate, one transmitter, can be accomplished in approximately one hour. Data verification is limited to that necessary to ensure that all equipment is operating satisfactorily. Major analysis is done post mission.

TABLE 1. MOBILE TEST FACILITY EQUIPMENT SUITE USED FOR LORAN-C MEASUREMENTS

FREQUENCY DOMAIN :

- 2021L AUSTRON LOOP ANTENNA
- HD-73 ALLIANCE ROTOR
- CG-WX028 FILTER
- 3585A H.P. SPECTRUM ANALYZER
- 4052 TEKTRONIX COMPUTER
- 4631 TEKTRONIX HARD COPY UNIT

TIME DOMAIN :

- 355D H.P. VARIABLE ATTENUATOR
- 5180A H.P. WAVEFORM RECORDER
- 4052 TEKTRONIX COMPUTER
- GCF-W-541A-B LORAN-C CROSS RATE BLANKERS
- SELECTIVE TRIGGER CIRCUIT
- 4631 TEKTRONIX HARD COPY UNIT
- 180 H.P. OSCILLOSCOPES

OTHERS :

- 304D TRACOR RUBIDIUM FREQUENCY STANDARD
- 312C TRACOR STANDBY POWER SUPPLY
- 525 TRACOR FREQUENCY DISTRIBUTION UNIT
- AUSTRON 5000A LORAN-C RECEIVER
- DIGITAL FDP8 COMPUTER
- T.I. 700 ASR TELEPRINTER
- NORTHSTAR 6000 LORAN-C RECEIVER

TABLE 2. IN BAND POWER MEASUREMENTS AT LORSTA SENECA

DOT/TSC LORAN-C SIGNAL ANALYSIS			LORSTA SENECA			
CT	8 59	9 5	98.96	0.55	0.49	17 AUG 82
1	9 53	10 0	98.96	0.69	0.42	17 AUG 82
2	11 50	11 58	99.15	0.57	0.29	17 AUG 82
3	12 41	12 47	98.97	0.71	0.32	17 AUG 82
4	13 22	13 31	99.01	0.64	0.36	17 AUG 82
5	15 50	16 6	98.95	0.72	0.33	17 AUG 82
6	16 45	16 51	98.81	0.84	0.35	17 AUG 82
7	17 28	17 34	98.98	0.71	0.31	17 AUG 82
8	9 13	9 19	98.92	0.74	0.34	18 AUG 82
9	10 45	10 52	98.81	0.93	0.28	18 AUG 82
10	11 50	11 57	98.97	0.70	0.33	18 AUG 82
10A	13 13	13 20	98.89	0.76	0.35	18 AUG 82
11	14 7	14 14	98.88	0.75	0.37	18 AUG 82
11A	15 41	15 48	98.82	0.77	0.41	18 AUG 82

X POWER IN-BAND (98 - 110 kHz)
 X POWER (ABOVE 110 kHz)
 X POWER (BELOW 98 kHz)

SITE START TIME : EDT END TIME : EDT DATE

Results

TSC has completed field trips to LORSTAs Seneca, Nantucket and Caribou. The results are being documented in a series of reports to the Aids to Navigation Division (G-NRN-1) at Coast Guard Headquarters. The report for Seneca is complete. Those for Nantucket and Caribou will be delivered in October and November 1983. Only data for Seneca has been completely processed and will be addressed in this paper.

At LORSTA Seneca, observations of in-band power were made at 14 sites, at distances ranging from the current transformer on-site to 33 km. A summary table is presented in Table 2. The mean value of power in-band is effectively 99%, with out-of-band power split 0.3% to the low side, 0.7% to the high side. Repeatability of observations is remarkable, and a superposition of the spectrum envelope of the current transformer data plus that from Sites 11 and 12, is shown in Figure 15 to illustrate this observation.

Harmonics observed at Seneca are summarized in Table 3. COMDTINST M16562.4 does not address allowable harmonic levels, so those published in the Wild Goose Association "Loran-C System Characterization" are also shown for reference purposes.

SUMMARY

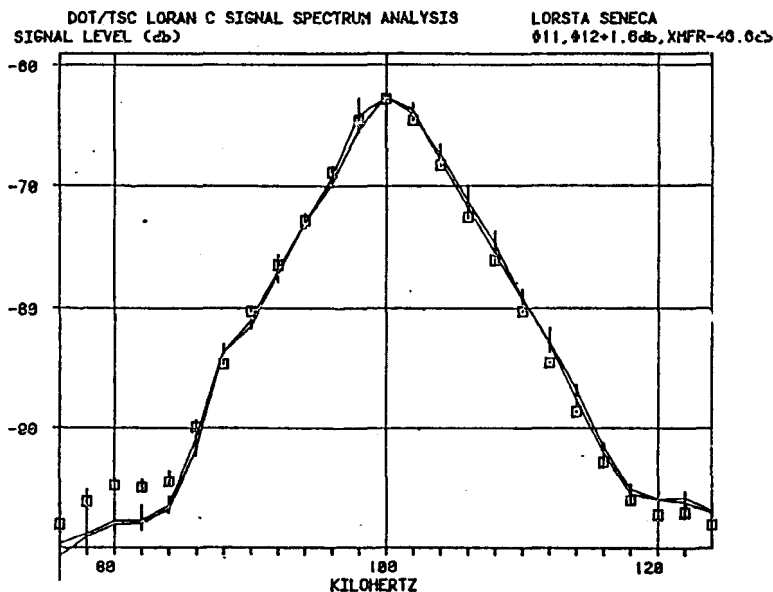
The ability of TSC to measure and analyze the signals from Loran-C transmitting stations has been developed and is an on-call capability for use by the Coast Guard. Three stations have been visited to date and trips to six more are planned for FY84. As the number of visits grows, the Coast Guard will have ready reference material regarding performance of each station. The information can, in turn, be used to make further refinements to operations procedures and as a basis for system improvements.

TABLE 3. OBSERVED LORAN-C HARMONICS AT LORSTA SENECA

HARMONICS	OBSERVED	REFERENCE LEVELS
2nd	< 130 dB*	-70 dB
3rd	-109 dB	-80 dB
4th	< 130 dB	-85 dB
5th	-115 dB	-90 dB
6th or GREATER	< 130 dB	

* 130 dB is dynamic range of equipment

FIGURE 15. SUPERPOSITION OF THE SPECTRUM ENVELOPE AT LORSTA SENECA



CONCLUSIONS

Signals from Loran-C stations can be measured with the equipment ensemble described in this paper. Interfering signals also can be measured and quickly compared to those from Loran-C stations. While not an "instant" response, the capability now exists to quickly isolate the cause of RF interference to Loran-C receivers at a given location within the Loran-C coverage area. The Coast Guard now has the capability to provide empirical assurance to users that the signals in space do meet requirements of COMDT INST M16562.4.

U.S. BUREAU OF THE CENSUS
INVESTIGATION OF LORAN-C APPLICATION TO THE 1990 CENSUS

Patricia A. Angus
Geography Division
Bureau of the Census
Washington, District of Columbia 20233

David C. Burnham
Transportation Systems Center
Kendall Square
Cambridge, Massachusetts 02142

Albert D. Frost
Electrical Engineering Department
University of New Hampshire
Durham, New Hampshire 03824

ABSTRACT

The Bureau of the Census, U.S. Department of Commerce, is conducting a program to evaluate the possible use of Loran-C and other radionavigation systems to determine the location of rural residences in the 1990 Decennial Census. In cooperation with the Transportation Systems Center, U.S. Department of Transportation, requirements of the Census Bureau for a rural residence location system were developed and refined. In response to these criteria, a first phase test program using Loran-C was designed and implemented within an area defined by the U.S.G.C. Georgetown, Massachusetts 7.5 minute quadrangle map to measure Loran-C repeatable accuracy. Using the data collected by TSC during the first phase of the test program, the Bureau will attempt to develop a data base for the evaluation of advanced geocoding techniques and the absolute accuracy of Loran-C. Results are discussed from the analysis of data recorded at eight repeatable accuracy reference points. Measurements were made at an additional seventy sites throughout the test area to study local Loran-C grid anomalies, signal strength variations, and interference phenomena.

INTRODUCTION

The Bureau of the Census, United States Department of Commerce, is considering the possible use of radionavigation systems to locate rural residences in the 1990 Census. The Transportation Systems Center (TSC) of the U.S. Department of Transportation (DOT) has been commissioned by the Census Bureau to conduct a series of studies and measurements to evaluate the potential of various systems to meet Bureau requirements. Although all navigation systems are being examined at this time for their applicability to the decennial census, efforts to date have been focused on Loran-C, mainly because of its availability now and its extensive coverage in the continental U.S. An added inducement to close study of Loran-C has been the recent and rapid advances in re-

ceiver technology which, particularly in the demanding airborne field, has seen the capabilities of units expanding greatly while retail prices have plummeted toward the thousand dollar range. No decisions have been made at the present time, however, concerning which radionavigation system, if any, would best suit the needs of the Census Bureau.

In order to add empirical data to the analytical information which has been generated during the past year, a test program was outlined to measure the repeatable accuracy of Loran-C in rural environments. Repeatable accuracy is important for census operations because it is an indicator of how well an enumerator can return to rural residences for follow-up interviews or data collecting. Absolute accuracy is equally important for census operations because it is an indicator of how well geographic classification codes can be assigned to residences. This paper, however, discusses only the repeatable accuracy, not the absolute accuracy of Loran-C.

A phased measurement program was suggested in which the field environment would become increasingly difficult for Loran-C functions. The first phase was conducted in an area just north of Boston, Massachusetts within an area defined by the U.S. Geological Survey Georgetown quadrangle map. This convenient location near the Transportation Systems Center facilitated test system development and checkout in addition to providing a good Loran-C signal area. This paper is basically a report of our test experience in the Georgetown environments.

Before we discuss the test operations and results, perhaps it would be beneficial to outline the operations involved in gathering data for a decennial census, especially those activities that could be aided by current position location technology.

The decennial census operations of the Bureau of the Census include three major activities that might be improved in rural areas by the use of a radionavigation system.

- a) Prelist Operation - Before a decennial census can be carried out, address lists for all dwellings must be obtained or generated. In rural and small town areas the prelist operation is carried out by census employees termed "enumerators" who visit all dwellings in an assigned area. If each dwelling visited were coded with coordinates from a radionavigation receiver, it would be possible to validate the prelist data, identify duplicate data, and verify that all areas were covered.
- b) Follow-Up Operation - On decennial census day, census forms are sent to all dwellings. Approximately two weeks later census workers visit those dwellings from which no census form has been received. The follow-up operation might be expedited by using a radionavigation receiver to locate and identify a dwelling whose coordinates had been entered during the prelist operation.
- c) Geocoding - The current prelist procedures result in a crude map spotting of each dwelling unit location within each census block. This map is not accurate enough to identify dwelling location if an invisible boundary, such as a congressional district border, were to pass through the block. Radionavigation coordinates might be used to geocode residence locations so that invisible boundaries can be defined as desired.

A radionavigation receiver intended for Census Bureau use must satisfy a variety of requirements. The receiver unit must be inexpensive, small, lightweight, portable, and easily used by an unsophisticated operator. Some kind of guidance indicator is needed for the follow-up operation. The accuracy required depends somewhat upon the mode of operation. The follow-up mode requires good repeatable accuracy, perhaps as good as 50 feet for distinguishing between closely spaced dwellings. The geocoding function could require predictable accuracy as good as 30 feet to precisely locate closely spaced buildings and to assure unique coordinates for each dwelling. Poorer accuracy values do not necessarily preclude using a specific radionavigation system, but may require procedures which overcome the inherent inaccuracy of the

system. A radionavigation system to be used for the 1990 Decennial Census must be available by the end of 1986 to allow both for trial use before the actual census and for the development of sound operational procedures. The system must be available continuously through the day and coverage is needed for the continental United States, Hawaii, Alaska, Puerto Rico, and other U.S. territories and possessions.

In 1982 the DOT Transportation Systems Center began a program to assess the capabilities of available radionavigation systems, and Loran-C in particular, to meet the decennial census needs of the Bureau of the Census. An analysis of the Bureau of the Census requirements indicated that accuracy, both predictable and repeatable, in the rural environment is a potential limiting factor for Loran-C use. The program reported here was designed to measure the Loran-C accuracy achievable in a rural area with high signal-to-noise ratios and good geometry. This paper will discuss only repeatable accuracy.

DATA COLLECTION

Site Selection

The location selected for the tests was north of Boston in the area defined by the Georgetown quadrangle map. This site met the following selection criteria:

- a) Good Loran-C signal strength and geometry.
- b) Both small towns and rural areas.
- c) Reasonably flat terrain.
- d) Conveniently located to TSC.

A preliminary site survey was carried out by TSC to characterize the different areas on the map and to identify promising test points, especially surveyed benchmarks. The quadrangle was then visited by Census Bureau personnel in order to finalize the detailed plans for the tests. The specific test sites were selected mutually by the Bureau of the Census and TSC. A number of different types of points were defined, two of which are:

- a) Monitor - A standard Coast Guard Loran-C harbor monitor was installed in the tower of the Topsfield Municipal Building. It continually recorded data on shifts in the Loran-C grid throughout the three-week test period in June and July 1983.
- b) Repeatable Accuracy Points - Eleven points were selected for the analysis of repeatable accuracy. Three were the benchmarks, the other eight were

selected from a variety of situations; many of them were located on Interstate 95 overpasses.

Equipment

Mobile Test Facility (MTF). TSC maintains a mobile test facility (MTF) to facilitate field tests of radionavigation systems. It consists of a window van and a special purpose trailer which houses power generators. The van contains only necessary test equipment and thus its contents vary significantly from program to program. For the Census Bureau Loran-C tests, major equipment included two Austron 5000 Loran-C monitor receivers, one Northstar 6000 Loran-C receiver and a Tektronix 4052 graphics computer.

Austron 5000 Loran-C Monitor Receiver. The Austron 5000 is the receiver used by the U.S. Coast Guard for both system control and precision surveys. It is the recognized standard in the Loran-C technical community for use when full characterization of all signals is necessary. The principal differences between the 5000 and other survey receivers lie in the areas of accuracy, (0.010 microseconds over a wide dynamic range), envelope-to-cycle delay (ECD) readout (provides accurate envelope numbers for each station tracked with a range of + 4.0 microseconds from the standard track point of 0.0 microseconds), RF bandwidth (70 kHz when used as a monitor, 25 kHz when used as a navigator), variable tracking loop constants and multi-chain operation (up to 4 chains). For the Census Bureau tests the 5000 was configured as a monitor receiver and only three stations in the Northeast Loran-C chain were tracked. In the monitor mode the 5000 provided more accurate values of ECD with a tradeoff in decreased ability to track Loran-C signals in areas with excessive wide-band noise, such as might be experienced near power lines. This configuration was selected because the primary test goal was to evaluate the limits of Loran-C accuracy and repeatability, rather than to assess operation in a noisy environment. Loran-C information is recorded at preprogrammed intervals on a Texas Instruments teleprinter. The cycle tracking loop constant was set at 400 (nominally 0.25 Hz) which provides an effective averaging time of 10 seconds. Samples were taken at 30-second intervals, thus ensuring that each observation was statistically independent.

Northstar 6000 Loran-C Receiver. The Northstar 6000 receiver was designed for general purpose marine applications but its tracking loops permit use in vehicles at speeds approaching 50 mph. This re-

ceiver was the industry standard for several years because of its excellent performance. One particular attribute is its ability to acquire Loran-C signals quickly and accurately (correct cycle lock). During the tests, information from the Northstar 6000 receiver was used to verify that the Austron 5000 had not jumped cycles when moving between sites. Time difference and signal-to-noise information was logged at each site.

Tektronix 4052 Graphics Computer. The 4052 is the standard instrument controller, data storage and data analysis tool in the MTF. Data from the Austron 5000 was hand keyed into the 4052 and analyzed using special analysis programs prepared for the tests. The programs computed statistical averages of Loran-C time difference (TD) readings and converted TD variations into standard Cartesian x,y variations.

Fixed Loran-C Monitor. A base monitor was installed in the Topsfield Municipal Building during the tests. It consisted of an Internav 404 Loran-C receiver and a Texas Instruments 700 teleprinter. The 404 is a survey quality Loran-C receiver with 0.010 microsecond resolution. The Coast Guard routinely uses this receiver for monitoring Loran-C signal stability and the actual equipment for this test was borrowed from and installed by the Coast Guard. The monitor provided continuous time difference and signal quality information throughout the tests.

Methodology

The daily test schedule was designed to meet the different goals of the tests with an efficient use of equipment and personnel. Each day started at the Topsfield Municipal Building where, except for weekends, the TSC mobile test facility (MTF) van was parked at night. A Loran-C reading was taken at the parking place before beginning the test sequence for the day. This initial reading checked the operation of the equipment and also supplied one of the repeatable accuracy points. Each day about half the repeatable accuracy points were visited. Each repeatable point had a well defined mark so that the MTF could be exactly positioned where it had been on previous measurements.

DATA ANALYSIS

At the selected test sites field measurements were made of the relative time delay of signals from the Loran-C station pair of Seneca NY (master M) and Caribou ME (secondary W) and the pair of Seneca

NY (Master M) and Nantucket MA (secondary X). These time differences, expressed in microseconds, are designated TDA (M - W) and TDB (M - X). These stations are part of the Northeast U.S. chain and operate at a group repetition interval of 99600 microseconds.

The Austron 5000 receiver system described above was used as the basic receiver for the field tests. Measurements were taken after receiver and signal status values indicated that both signal pairs had been satisfactorily tracked and any transient effects had died away. The acquired TDA and TDB values were recorded at 30-second intervals for a period of five minutes, providing 10 readings of each position coordinate at each site. Each data point represents a 10-second signal average provided by the internal time constants of the Austron tracking loops. These TD values as well as information relating to the circumstances of each test site visit were transcribed to a site visit log sheet.

Repeatable Accuracy

Each repeatable accuracy site was visited from 4 to 10 times. Overall average values for TDA and TDB were computed for each site. Using the local values of the orientation and gradient of the TDA and TDB contour lines, it is possible to compute an indicated x, y position, relative to the mean value, for each pair of TD measurements. Figure 1 illustrates one application of these computations. This figure presents a scale map plot of the predicted relative position of the test vehicle on each of the seven TD data sets collected at that site between 22 June and 1 July. In this case the five-minute average values for TDA and TDB were used. A 100-foot radius circle is drawn for comparison. If instead, the individual (30 seconds) data pairs are used, then the point distribution is as shown in Figure 2 which displays a total of 70 measurements. A wider scatter about the mean is evident with a shorter integration time. As with Figure 1, the center of the coordinate axes is the overall average of all observations. The data summary presented in Table 1 for site #2 presents standard deviations of TDA and TDB values and estimates of consequent 2 DRMS position scatter relative to the group mean, for averaging intervals of 30 seconds, 1 minute, 2.5 minutes and 5 minutes. The assumption is made that the TDA and TDB errors have a Gaussian distribution. The cumulative distribution in computed site location relative to the mean has been plotted

in Figure 3 for this same data set. The percentage of all measurements falling within a radius r is plotted as a function of r . For site #2, 65% of all points lie within 35 feet of the mean position while 95% are within 60 feet.

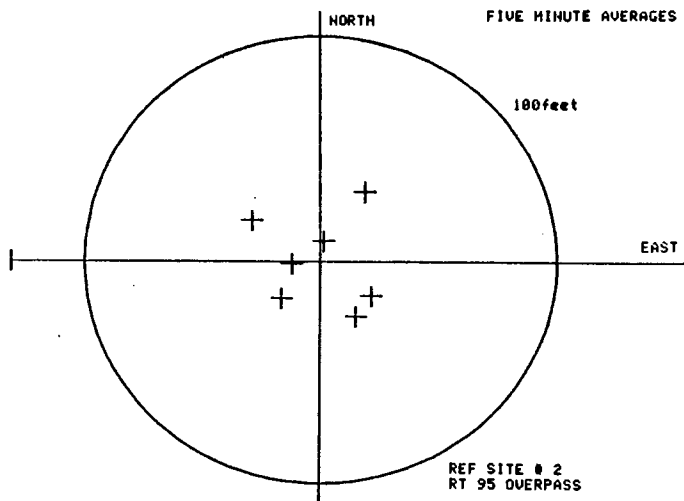


FIGURE 1. REPEATABLE ERROR PLOT FOR SITE 2 SHOWING ONE FIVE-MINUTE AVERAGE POINT FOR EACH SITE VISIT

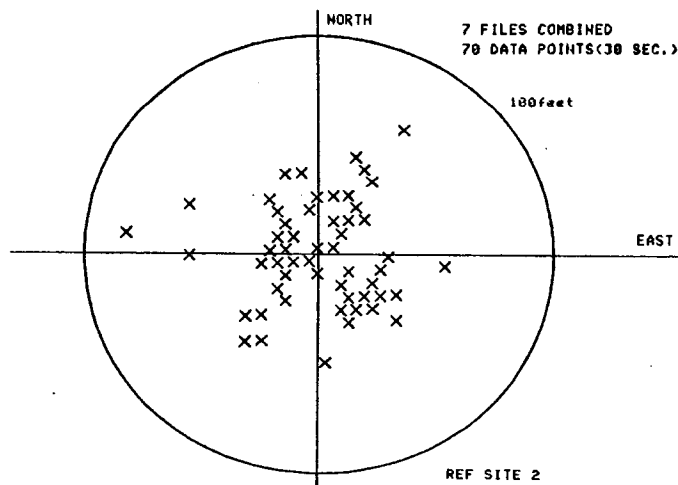


FIGURE 2. REPEATABLE ERROR PLOT FOR SITE 2 SHOWING ALL DATA POINTS

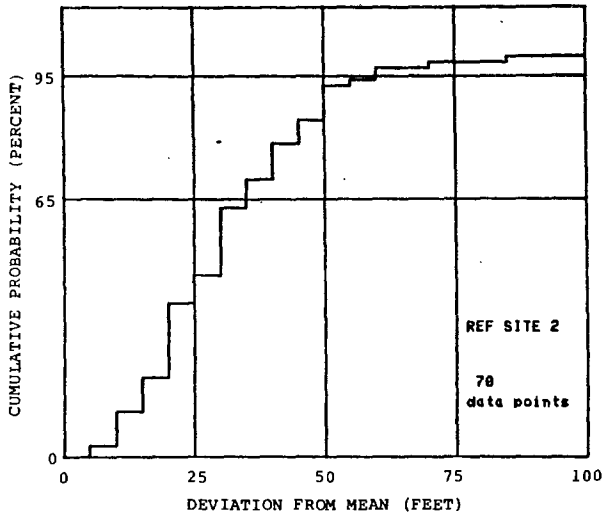


FIGURE 3. MEASURED CUMULATIVE REPEATABLE ERROR DISTRIBUTION FOR SITE 2

TABLE 1. CALCULATED REPEATABLE ACCURACY FOR SITE 2: ROUTE I95 OVERPASS

AVERAGE TDA (M-W) = 13938.81 microseconds			
AVERAGE TDB (M-X) = 25950.97 microseconds			
AVG. TIME (min)	ACCURACY 2 DRMS (feet)	STANDARD DEV. (microseconds)	
		TDA	TDB
0.5	73.7	0.040	0.039
1.0	68.0	0.036	0.036
2.5	62.5	0.031	0.035
5.0	59.2	0.029	0.034

A complete recapitulation of all repeatable site data (a total of 460 points from 11 sites) is presented in Table 2 and Figure 4. The latter shows that 95% of all data values are within 60 feet of the mean value for each measurement site. Since this result is based on 30-second data, further improvement would be expected for moderate averaging periods of 2 to 5 minutes.

Grid Shift Correction

Using Loran-C monitor data, daily and hourly averages of the grid shift were calculated. The daily averages included only times when field data were being collected. The maximum variations in

daily averaged TDA and TDB were about 50 and 30 nanoseconds respectively. On most days the hourly variation was less than 0.040 microseconds during the work day. In all cases the variation was less than 0.100 microseconds. There was no consistent daily pattern in the grid shifts.

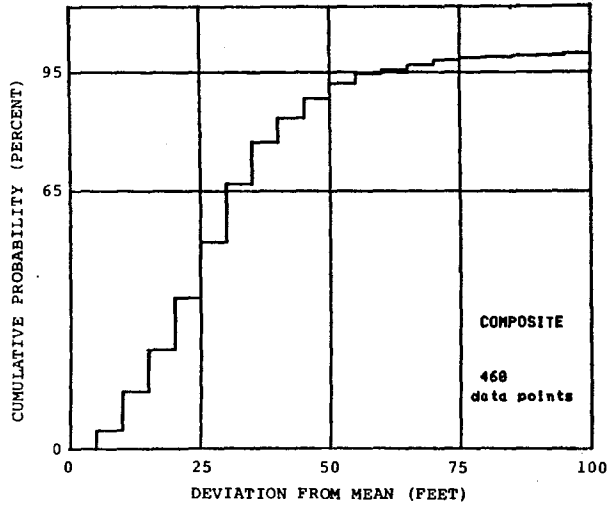


FIGURE 4. MEASURED CUMULATIVE REPEATABLE ERROR DISTRIBUTION FOR ALL SITES

TABLE 2. CALCULATED REPEATABLE ACCURACY FOR ALL SITES (2, 11A, 11B, 23, 47, 75, 82, 88, 100, 106, 112): 460 POINTS

AVERAGING TIME (minutes)	ACCURACY 2 DRMS (feet)
0.5	69.9
1	59.3
2	52.1
5	47.5

The repeatable accuracy evaluation above ignored any shifts in the Loran-C grid. Table 3 shows how much the standard deviation of the time difference measurements is improved if the five-minute-average data points are corrected by the average grid shift for the day on which the measurements were made. In order to have the best chance of seeing the effect of grid corrections, two sites were selected which had a small amount of scatter and data collected on the day

when the largest TDA shift was noted. Even under these conditions the observed improvement was marginal. If no systematic grid shifts exist, the additional variation introduced by subtracting the reference data would be expected to increase the standard deviation, as is noted in one case (site 2, TDB). The small improvement noted in the other three cases indicates that the grid shift variation is slightly larger than the effect of the reference measurement variation.

CONCLUSIONS

The repeatable accuracy of Loran-C is 60 feet (2 DRMS error) in land areas with good signal-to-noise ratios, good Loran-C geometry, and using the equipment described in this paper. These results cannot be generalized to apply to the typical census environment nor do they predict the results that could be obtained in other areas of the country. A typical rural environment is likely to have some sites where Loran-C signals can be swamped by local interference.

TABLE 3. EFFECT OF GRID SHIFT CORRECTIONS ON REPEATABLE ACCURACY

STANDARD DEVIATION (microseconds)			
SITE	TD	UNCORRECTED	CORRECTED
2	A	.030	.030
2	B	.011	.018
88	A	.038	.031
88	B	.025	.022

A form of differential Loran-C method has been suggested for Census Bureau use in order to eliminate the seasonal shifts in the Loran-C grid. In this method an enumerator would return periodically to a reference point and all measured TD's would be corrected by the TD changes observed at the reference site. A significant operational question is how often the reference site must be visited. A daily check has been suggested. The measured grid shift data showed that a single reference check in the morning would have been adequate on most of the days of the tests. The limited effectiveness of grid shift corrections shown in Table 3 would suggest that a reference measurement every two weeks would be adequate in June/July. Since the grid shifts are seasonal, more frequent checks may be required at other times of the year.

Noise Interference

Sites with extremely noisy Loran-C signals were excluded from the analysis of repeatable accuracy. Most of the streets and roads in the quadrangle are lined with power lines which appeared to be a source of noise interference which prevented Loran-C signal acquisition at several sites selected for repeatable accuracy evaluation. Interference problems would have an adverse impact on census use of Loran-C and will be discussed in more detail in the final report on this project.

The Austron 5000 Loran-C receiver used for the test is a survey quality receiver which has excellent time resolution and is therefore suited for measuring the small time difference variations which define the repeatable accuracy of Loran-C. The Austron 5000, however, was not optimized for tracking and noise rejection and therefore did not provide the overall performance which would be expected from state-of-the-art Loran-C receivers. In particular, the effects of interference would be expected to be larger for the Austron 5000 than for an optimized receiver.

In several ways the tests reported here do not characterize how the Census Bureau would operationally employ a radionavigation receiver. First, the Austron 5000 receiver is not the type of equipment which would be suitable. Equipment designed for census purposes would need to be portable, lightweight, and relatively inexpensive. Second, the Loran-C readings would be taken only once at each site, not taken repeatedly as in this test. Third, the single Loran-C reading would use a shorter averaging time, probably less than two minutes, rather than the five minutes used in this test.

The Census Bureau is continuing to investigate the use of a variety of radionavigation systems. No decision has been made about which system, if any, can meet Bureau needs. Additional studies need to be done.

LORAN-C: 1983 and Beyond

BY LCDR W.J. THRALL

U.S. COAST GUARD
COMMANDANT (C-NRN)
U.S. COAST GUARD HEADQUARTERS
2100 2ND STREET, S.W.
WASHINGTON, D.C. 20593

ABSTRACT

Loran-C has been called steady-state. We, within the Office of Navigation, consider Loran-C as much more than steady-state. This paper discusses present and future plans to further improve the Loran-C system, while reducing operational costs and implementing personnel reductions. Topics include: the Solid-state Transmitter (SSX) procurement and installation, the Remote Operating System (ROS), the De-energized Secondary Loran Transmitter (DESLOT), present day costs of mid-continent stations, development of the Loran-C database, updating and improving the Loran-C Engineering Course, and joint FAA/USCG efforts.

INTRODUCTION

Atta Boy, Team!

Many of you have been the prime movers and shapers of Loran-C over the past 25 years, designing, improving, and constantly striving for that elusive 100% signal availability. Today, thanks to your past efforts, Loran is easily providing better than 99.7% signal availability Loran-wide. In fact, Loran is providing better than 99.9%, approaching and occasionally reaching 99.97% availability. Thirteen chains located in more than half a dozen countries all coordinated by the common goal of providing perfect Loran-C service. I feel it's been, and continues to be, a team effort, and I'm proud to be a part of the team.

TODAY

Malicious Rumors

Lately, we have heard Loran-C is dead, dying, status-quo or steady-state. We all realize it is not dead. Nor (to the chagrin of GPS supporters) is it dying or steady-state. It may not be expanding like it was; it may not require the same kind of design engineering effort of the past, but it is not aground. It is, however, under attack by the four P's of new and emerging navigation systems...Promise, Potential, PR, and Politics.

Holdin' Down the Fort

Those of us involved with Loran today are energetic, enthusiastic, and open-minded. We're looking for alternatives, finding improvements, and solving new problems. We are seeing the possibilities of the future

and preparing to meet those challenges through planning, fact accumulation and documentation. True, some of the problems we face today are not new, but they're new to us. We're over-coming our limitations of experience with energy and enthusiasm for this dynamic program.

Promises and Risks

Many of you have had the opportunity to read, listen, discuss, or debate our present attempts to lower operating costs through Remote Operations (ROS) and by De-energizing the Standby Loran Transmitter (DESLOT) at tube-type stations. To many of you this is heresy, a shunning of our responsibility and obligation as the Loran Program Manager because it puts Loran's 99.9+% signal availability at risk.

We aren't attempting these budget reductions without good reason. The Loran program has historically justified the purchase of new equipment and the cost of improvements (to the then existing Loran equipment) based upon a promise to reduce future operating costs. ROS at SSX stations is a fulfillment of that promise. ROS at tube-type stations is an attempt to benefit from the reliable and redundant equipment previously installed by utilizing today's integrated circuit technology. How successful will ROS be? Only time and prudent monitoring will tell.

ROS allows semi-automated and remote operations. We're trying to use computers as tools to solve our dwindling knowledge pool. It frees five or more billets from each ROS'd station. Do operations and availability suffer? Not yet. They may for a short period. We will monitor each individual ROS station closely to ensure that Loran's signal availability of 99.9% and 99.99% is not jeopardized. Eventually, we expect to achieve improved operation and availability due to less opportunities for human error. Will it work? At FPN-44A and FPN-45 stations we think so. At SSX stations such as Raymondville and Port Hardy, it works and works well.

Loran station Searchlight has had an experimental ROS installed and operating under an evaluation phase. We, the Program Manager, PacArea, and the 11th Coast Guard District, are not satisfied with the results at present. Certain recommended changes will have to be incorporated before the Searchlight test can be further evaluated. We are confident that EECEN Wildwood will overcome the hardware and software

limitations of the present ROS and that the future tube-type ROS will provide very favorable operations. If, at first, the ROS at Searchlight, Fallon and George do not provide the necessary availability, it will be improved/modified so that it will. Operational availability will not be compromised.

ROS is working successfully at the Canadian Loran station Port Hardy and at our own Loran station Raymondville. True, there are some (I emphasize some) manned FPN-42 stations doing better than these ROS'd SSX stations. Why? Because we're lucky enough to still have a few "old timers" around to make a few transmitters sit-up and take orders, but overall performance data shows that the SSX/ROS station out-performs and costs less to operate than FPN-42 stations. It was this factual argument that helped convince Congress to allow us to replace our aging FPN-42 transmitters with new Solid State Transmitters; that is providing we reduce crew manning to four or less. ROS allows successful reduced manning.

The economic advantage of replacing aging FPN-42's with SSX's is apparently slight by the year 2000. However, the risk of not being able to continue successful Loran operations to the year 2000 is removed. And if we are required (by Congress and their constituents) to maintain Loran-C operations beyond the year 2000, we are certain we will be able to, and, as we do, we will save money in comparison to trying to continue to run the aging FPN-42.

More Promise...More Risk

DESLOT is not new. The idea has, apparently, been around for some time. When the 14th Coast Guard District requested an on-air experiment of DESLOT at Upolu Point, I gave operational approval. Why? Why not? I had heard opinions--many opinions on thermal shock, decreased tube life, condensation and moisture buildup in the transmitters, etc.; I shared many of these same good opinions not to DESLOT, but...not one hard fact or substantiating collection of data existed pro or con.

I don't want to run a program on opinions. I need and want data and facts. That's what I ordered. That's what I received. To date, all of CENPAC and part of NWPAC have been outfitted with the DESLOT modification, and their performance is being monitored and documented by the 14th Coast Guard District. Loran station TOK has just been outfitted and Baudette is to follow. Both of these stations are being monitored by EECEN Wildwood to collect more data and facts. To date, the DESLOT programs at CENPAC and NWPAC have been very successful. Both show a tremendous savings in operating costs. Additionally, through the introduction of the DESLOT modification, we're experiencing the benefit of ensuring all transmitters have only authorized field changes, that the field changes are all installed correctly, and that unauthorized field changes are removed. Also, certain long standing problems not directly related

to the transmitters have been discovered and corrected.

Tube usage hasn't skyrocketed. The predicted catastrophic failures have not come to pass. True, long term trends haven't had time to develop, but short term evidence is positive.

There is one major area of concern to those of us monitoring both ROS and DESLOT. That is signal availability. As I mentioned previously, we're experiencing 99.9+% availability, system-wide. We do not intend to lower our goals nor our expectations.

DESLOT represents an increase of about one minute of bad time for every automatic transmitter switch occurring. Abnormally high amounts of these switches indicate transmitter problems. We want those problems corrected. Then we want to compare what we've gained versus what we may have lost.

A Need for Speed

I have spoken about data. Facts. We within the Program Manager shop are sponsoring the development of a database management package that will contain all kinds of general station information as well as signal and availability data. This data base will allow us to be more accurate and responsive to many queries; e.g., when a particular station came on-line, or compare operations between 42's and 44's or SSX's, or Lorsta George to Lorsta Yap, or the number of momentaries, off-air conditions, equipment failures, different costs related to operations, manning levels and who's the new CO and what's the Loran station's phone number. What has taken embarrassingly long to research and report, will be available in minutes or seconds at the touch of a few key strokes.

Continuing Education

Realizing that the Loran experience pool is shrinking within the Coast Guard, we have begun working with our Area Managers, the Loran Branch of the Electronic Systems Division, the Coast Guard Academy and other Support Managers and individuals to update and improve the Loran-C Engineering Course. We are attempting to develop not just a relevant and accurate course, but also a reference text of information and history regarding Loran-C. This two week course is available to Host Nation personnel as well as other Federal Agency employees.

But all of this is today...1983. What about beyond?

THE FUTURE

I am hopeful that over the next couple of years Loran-C will again be seen in the correct context it deserves...a mature but improving program, offering many diversified jobs and challenges to those willing to join the team.

Changes

Starting in January 1984 the North Atlantic Chain will cease operations...In its place will be the new Icelandic and Labrador Sea Chains.

We have heard about the Saudi Arabian Chain, the French Rho-Rho system, and the Norwegian desire for more Loran coverage. We know about the Suez Loran Operations. But is there a need for a mid-continent U.S. chain? Definitely not from a mariner point of view. But what about the FAA? Aviation users are pushing the use of Loran for enroute navigation and non-precision approaches where Loran-C is available. Apparently, aviation users of Loran are growing rapidly and strongly advocating Loran. Additionally, we've been led to understand that the FAA is not willing to accept the proposed 18 satellite constellation of GPS. Can a joint Coast Guard and FAA agreement be developed for the construction and operation of a mid-continent chain? Right now, I don't know, but we have to find out. To that end I have inflated the actual construction costs of Lorsta Raymondville to the present. I have determined that a similar station would cost between \$4.5M and \$5.5M (not including land acquisition or geographic cost factors). Is that estimate accurate? or reasonable? or enticing? Is anyone interested? I'm sure we'll find out.

Are there uses encompassing not just the marine and aviation users, but, also, terrestrial users? U.S. Loran construction and expansion is over without a new, expanded charter or mandate from Congress. There appears to be both room and a necessity for a mid-continent chain, but facts and data will have to be presented to the Commandant, the Department of Transportation, GAO and the Congress. Data like that accumulated and presented by LCDR Bob Wenzel and CWO Dan Slagel of the U.S. Coast Guard, showing a system providing better than 40 meter accuracy is the kind of data we're in need of. We need data showing where our present coverage really ends... not theoretical boundaries, but real limits based upon received signals. We believe that the users require actual LOPs based upon actual not theoretical data. We have a great system that isn't yet as good as it could be.

If the system is to be expanded anywhere, then it must come about because of a grassroots demand from the user community for increased Loran coverage. Not just in the mid-continent, but in other areas where there is a need for the precision navigation capability of Loran-C. Without a vocal demand from constituents and manufacturers to their elected officials and supported by factual needs, there is little chance of Loran-C expansion. That is not necessarily bad. If there's no need, let's not spend tax dollars needlessly. However, the bushel basket stifling application and growth has to be removed from the Loran

program. I believe that today that bushel basket has been removed.

Continued Operations

Loran coverage of the Coastal Confluence Zone (CCZ) will be around until the year 2000. It may be around beyond 2000, but, as yet, we have no definite word. The Coast Guard presence in support of Loran operations in Europe is expected to be removed starting in 1992. We anticipate much of the coverage to remain the same due to Host Nation operations. The historical DOD chains of CENPAC and NWPAC, operated by the U.S. Coast Guard, may not last beyond 1992. However, we perceive a need for future discussions with the Japanese regarding continued operations of NWPAC as a Host Nation operation.

As for CENPAC, is it DOD or is it CCZ? Initially, back in 1975, it was presented as a DOD chain not a CCZ chain. As a part of the review process of the Federal Radionavigation Plan (FRP), we will be asking DOD for a reassertion of their need for either NWPAC or CENPAC beyond the GPS operational date (whenever that is--1988 to 1996). Further, we will be accelerating an ongoing review of the need for CENPAC to the civil user beyond 1992 as a result of the availability of GPS. As of today, we have no evidence of any overwhelming need for CENPAC other than DOD requirements.

In Summary

We are operating in an atmosphere of honesty and budget justification. In an attempt to reduce operating costs to the Coast Guard and to maintain, if not increase, our credibility to the Congress, we are looking at providing coverage only where coverage is needed and wanted at a reduced cost...hence, SSX, ROS, and DESLOT.

Loran is here and now. The promise of Loran has been met, but there is a continued need for input from users. We are working on a study of users of all radionavigation systems--Omega, Radiobeacon and Loran-C. What we hope to find is not just how many users there are, but how they are using the system(s), what would make the system(s) better for their application, and, from their point of view, where is/are the system(s) deficient. We are attempting to be more responsive to the real user, not just to our perceptions of the users need. I want to know how the user perceives a momentary signal loss, an off-air for five minutes, ten, and so on. I want to know when they use Loran-C. If they use Loran-C. Where they can and where they can't. I want to hear about those that require and are not obtaining the desired repeatable accuracy. My staff and I want to know so we can explore solutions and request necessary funding. In short, so we can plan effectively.

These tasks of the Program Manager will have a significant impact on Loran-C for the future. The tasks, briefly mentioned, will take time. They will be accom-

plished...The results will be based on honest facts and data obtained. We will continue to keep an open mind and an energetic spirit. We realize that Loran-C is here, is now and will continue to be, long after we've moved on. It is imperative that we leave our successors with a clear and well defined path, along with the tools necessary, to reach successfully into the year 2000 and beyond.

LORAN-C CALIBRATION

Jack M. Ligon
Office of Command, Control and Communications
U.S. Coast Guard
Washington, D.C.

ABSTRACT

The Loran-C coordinate conversion process is usually based upon a Coast Guard provided calibration factor called emission delay. Data taken from the Coast Guard Loran-C harbor monitors documents significant seasonal variations in emission delay, particularly in northern latitudes where there is land in the propagation paths. On the other hand, data taken at the controlling monitors indicates that the controlling time-differences are typically being maintained to within 20 nanoseconds. This paper recommends that calibrations be based upon controlling monitor location and time-differences instead of emission delay, a parameter which is neither observed nor controlled. It concludes by examining the implications of the change in calibration philosophy upon concepts relating to operation.

THE MYTH OF IDEAL LORAN-C.

Almost every paper or article on Loran-C contains some "boiler plate" with at least a few words paying tribute to the Loran-C ideal. After the necessary 100kHz, pulsed, hyperbolic, groundwave, phase-coded, etc., descriptives, the authors usually, perhaps unknowingly, pass on the myth to the next generation of readers. The myth goes something like this: "The master station transmits its signal. The secondary station receives the master signal, waits the prescribed coding delay, and then transmits its own signal. The time interval between the master and secondary transmissions is called emission delay." This Ideal Loran-C system is well-described in many articles, books and papers. We can all relate to the ideal, and we are comfortable with it.

LORAN-C AS WE OPERATE IT.

Fortunately, as we shall see later, we have not been operating the Loran-C system in accordance with that ideal for a long time. Until the mid-1960's, the Coast Guard attempted to operate ideal Loran-C by synchronizing the secondary transmitters to the received master signals. The coding delay was held constant in accordance with the ideal. However, monitor receivers in the service area and at the master stations observed time-difference variations when the secondaries were supposedly holding the emission-delay constant. There were two major contributors to these variations: the master-secondary propagation time was not constant, and the receiving conditions at a secondary station were perhaps less than ideal. In addition, the secondaries

were only attempting to hold the coding delay constant, not the emission delay. When the cesium frequency standards were installed at the Loran-C transmitting stations, it became practical to control the chains from the System Area Monitors (SAMs). In this method of operation, the SAM time-differences are held constant. This removes any dependency upon the master-to-secondary path, but it does cause the time-difference at any point in the coverage of a Loran baseline to be dependent not only upon the transmitter-to-user propagation paths but also upon the transmitter-to-SAM paths. Controlling the baselines at the SAMs greatly improved the stability within the service area because most of the propagation variations were common-mode for both the users and the SAM.

SEASONAL VARIABILITY OF THE LORAN-C SYSTEM.

The propagation velocity of the Loran-C groundwave is decreased by moisture in the air and poor soil conductivity. Both of these are affected by the weather, and particularly its seasonal variations. The Coast Guard Office of Research and Development has set up Loran-C Harbor Monitors in most of the major U.S. harbors to collect data to assess the potential of the presently-existing Loran-C signals to provide all-weather harbor and river radionavigation⁽¹⁾. Data is also collected from the SAM receivers to fill out the entire picture. This R&D data provides a representative cross-section of the stability from the warm, perpetually-humid Gulf of Mexico to the north central U.S. which has significant seasonal changes from cold, dry winters to hot, humid summers. The R&D data shows that the SAMs do a very good job of controlling the baselines to maintain the Control Standard Time Differences (CSTDs). They are well within 20 nanoseconds of the CSTDs more than 95% of the time. The data shows the coverage to be relatively stable in the south, and more sensitive to weather conditions in the north. Long-term seasonal variations, linked to changes in ground conductivity, and rapid variations in both directions, linked to changes in the atmosphere can be observed in the data. Estimates of the peak-to-peak seasonal variations in propagation velocity range from something less than .006% in the Gulf of Mexico, to more than .12% in the north central U.S.⁽²⁾.

CONTROL PHILOSOPHY.

Once we have located the transmitting and monitor stations, the shape of the field of loran signals on the face of the earth is purely in the hands of mother nature. We

have no control over propagation velocity. The only parameter we can control is the time of emission. This dictates that we can only hold the time-difference constant at a single location. We can control coding delay, or emission delay, or CSTD by selecting the monitor location, but we can only choose one. If we control coding delay, the area of the coverage with the most stable grid will be the secondary baseline extension (a useless portion of the service area). If we control emission delay, the area with the most stable grid will be the locus of points propagationally equidistant from the Master and Secondary transmitters (wherever that is). If we control CSTD, the area with the best stability will be in the vicinity of the SAM. For a warm-weather, all-seawater baseline, the performance distinctions among controlling coding delay, or emission delay, or CSTD tend to disappear. In colder climates, and in the presence of land masses, a controlled CSTD will cause significant variations in transmitted emission delay. The current Coast Guard Loran-C control policy calls for maintaining constant CSTDs at the Alpha-1 System Area Monitor (SAM), and this SAM is usually located in the neighborhood where the most stable and accurate coverage is desired⁽³⁾. We have learned to accept the weather-related variations which exist throughout the rest of the chain.

LORAN-C OF COORDINATE CONVERSION.

So far, two different Loran-C systems have been discussed: The ideal one, and the one we actually operate. There are really three different Loran-C systems. The third system is the Loran-C of coordinate conversion. This is perhaps the most difficult Loran-C system to deal with because it attempts to relate the real earth to real groundwave radio propagation when neither have a simple, precise, and accurate mathematical model⁽⁴⁾. Most coordinate conversion currently relies upon the WGS72 spheroidal model and a simplified groundwave propagation model. The greatest current flaw in our method of coordinate conversion though is its dependence upon the ideal Loran-C model and not the model of how we actually operate the system.

The Chain Data in the Loran-C Signal Specification is preceded by a page of what are called General Specifications. In these General Specifications, nine parameters are listed which determine the baseline length. These parameters define a standard all-seawater coordinate conversion process. The complete set of parameters of relevance to the Loran-C of coordinate conversion are:

Global model (WGS-72) (a set of constants),

Locations of transmitters on the global model, (constants),

Propagation Model (a set of coefficients which are assumed constant), and

Emission Delay (assumed constant).

The Defense Mapping Agency uses these parameters and some empirical ground-conductivity models to predict the positions of the Loran-C lines-of-position on the nautical charts. They also publish tables of Additional Secondary Phase (ASF) corrections for the Coastal Confluence Zone. Current policy requires that the measured emission delay be identical to the emission delay coefficient in the coordinate conversion model. There is much very good material describing coordinate conversion for an ideal homogeneous all-seawater earth⁽⁵⁾⁽⁶⁾. The addition of land to the propagation paths makes the coordinate conversion problem much more complicated. The traditional means, of handling this problem, Millington's Method, is very cut-and-try and doesn't leave one comfortable that the art of coordinate conversion is all that it could be. Some of the more successful designers of coordinate converters have even abandoned the classical model altogether. The major point to be made here, however, is that the current Loran-C of coordinate conversion is related to ideal model of Loran-C, and not to the Loran-C system we actually operate.

LORAN-C CALIBRATION.

In the final analyses, we cannot calibrate the Loran-C system we operate. We can only calibrate coordinate converters.

In general, the purpose of calibration is to adjust the coefficients of the coordinate conversion model to fit in some way, the measured reality. The Loran-C Signal Specification, takes a much more restrictive view and defines the purpose of calibration as "insuring that the emission delay (ED) of each secondary station is set to the value published by the U.S. Coast Guard." The remainder of this paper will attempt to justify a change in calibration policy to "insuring that the primary monitor (Alpha-1 SAM) control standard time-difference (CSTD) for each station is set to the value published by the U.S. Coast Guard." It will also highlight our control philosophy's impact upon the coordinate conversion process.

Let us first examine the effects of propagation velocity changes using a simplified homogeneous model.

In the ideal Loran-C model, the time-difference (TD) at any point in the coverage of a loran baseline can be defined as :

$$TD = \frac{1}{v} [MS + SP + B*v - MP]$$

Where v is the velocity of propagation (assumed constant),

MS is the great-circle distance from the Master to the Secondary (a constant),

SP is the great-circle distance from the Secondary to the Point (a constant),

B is the coding delay (another assumed constant), and

MP is the great-circle distance from the Master to the Point (a constant).

In ideal Loran-C, the Secondary receives the Master signal, waits the prescribed coding delay and then transmits its own signal. The time between the emission of the Master and Secondary signals as viewed by a common clock is called emission delay (ED).

$$ED = \frac{1}{v} [MS + B*v]$$

and, substituting,

$$TD = \frac{1}{v} [SP - MP] + ED$$

Although emission delay is defined here as a constant, it is a function of the propagation velocity along the Master-Secondary baseline, which is known to vary with changes in the weather.

The SAM's observed time-difference can be expressed as:

$$TDO = \frac{1}{v} [SO - MO] + ED$$

where TDO is the Observed SAM time-difference, which is maintained a constant (+/- some tolerance).

SO is the great-circle distance from the Secondary to the SAM (a constant).

MO is the great-circle distance from the Master to the SAM (a constant).

ED must be a variable to compensate for fluctuations in v.

Re-arranging:

$$ED = \frac{1}{v} [v*TDO + MO - SO]$$

In the Loran-C system that we operate, the TD at a point in the operating area is then:

$$TD = \frac{1}{v} [SP - MP + MO - SO + v*TDO]$$

As v changes, the TD can vary at points throughout the service area except at SAM, and variations in TD will be larger the greater the hyperbolic separation (SP - MP + MO - SO) between the SAM and the point. In reality, we are operating a differential Loran-C system with the SAM as the reference point, and our calibration should take this reality into account.

EMISSION DELAY DETERMINATION.

Because the current calibration policy is tied to the emission delay parameter, some discussion is required. There are three basic techniques for determining a parameter which has the name emission delay: direct measurement of emission delay, measurement of baseline extension time differences, and estimation using service area time-difference data. Direct measurement relates to the ideal model, baseline extension measurements relate to the system as we operate it, and estimation using service area data relates to the system of coordinate conversion.

Emission delay measurement.

There are several possible techniques for measuring emission delay:

In the recent past, Loran-C chains have been calibrated by using the portable clock emission delay technique of Section 3.A of the Signal Specification.

Time recovered from GPS or some other satellite system could also be used to provide the reference for direct measurement of emission delay. This is also a possible alternate control method.

Theoretically, a single time-difference measured at the electrical mid-point of the baseline could provide a direct measurement of emission delay.

Baseline extension time-difference measurement.

The emission delay can be calculated using time-differences measured with a receiver at the extensions at each end of a baseline. The TD at the Secondary end should be the coding delay, B; the TD at the Master end should be twice the baseline propagation time added to the coding delay, $2 MS/v + B$. The emission delay can be found by adding these two TDs together and dividing by 2. This is the classical method of determining the transmitted emission delay. Because of Secondary Phase, the time-difference is not constant along real baseline extensions. However, it is probably close at distances greater than 35 miles from the nearest transmitter.

Emission delay estimation.

Given an ensemble of TD measurements in the service area and a coordinate conversion model, parameters such as

propagation velocity, emission delay and ground conductivities can be mathematically estimated. This technique, along with Millington's method and with baseline extension measurements was used for calibrations during the early days. It was very labor intensive and time-consuming because of the measurements required and because of the art involved in properly assigning ground conductivities.

The measurement methods should all be effective for determining the transmitted emission delay. Their real value in providing a calibration reference is doubtful given the variability of the actual emission delay. The baseline extension time-difference method has the advantage of not requiring special equipment or techniques. A semi-skilled user could walk or drive to the baseline extension or a pilot could fly the baseline extension to get the measurements. The flying clock technique seems to be overkill when a number that is certainly as "good as any" can be obtained with a simple Loran-C receiver. In addition, since the baseline CSTD is the controlled parameter, there is no way of guaranteeing that the baseline is at the same state when both of the flying clock measurements are being taken. However, the flying clock emission delay measurement technique represents an ingenious solution to the problem of overcoming the Secondary Phase problems on baseline extensions. It also overcomes any problems with radio interference. Baseline extension time-difference measurements are certainly more economical than a flying clock exercise, and less risky because there is no need to keep time during the travelling, or recover time should the Master station have a casualty. Time-difference measurements are always preferred to time-of arrival measurements of any sort.

The estimation method can probably be broadened to permit many coordinate conversion models, each perhaps having a different value for the parameter we call emission delay. Certainly, there is no requirement that the estimated emission delay equal the actual transmitted or measured emission delay.

CALIBRATION BY ASSIGNING CSTDs.

The Coast Guard is currently committed to a program of improving the Loran-C charts, starting with the small scale charts and progressing to the larger scale harbor approach charts. This program is ultimately doomed to failure unless the "middle man" is eliminated and the Loran-C system of coordinate conversion is linked directly to the Loran-C system we actually operate. The explosion of Loran-C into the aviation community also forces us to take a closer look at the whole calibration question.

The process for calibrating Loran-C can be compared to the process of calibrating a voltmeter. A voltmeter attempts to relate

an artificial quantity (the meter scale deflection) to a physical quantity (the voltage applied to the probes). In the Loran-C System, the coordinate conversion process attempts to relate an artificial quantity (latitude and longitude) to a physical quantity (time-differences). The three factors which enter into voltmeter calibration: zeroing, full-scale deflection, and scale characteristic, are analogous to setting the coordinate converter to indicate the SAM latitude and longitude when the Control Standard time-Differences (CSTDs) are entered, assigning coordinate converter velocities of propagation based upon the observed time-differences at the ends of the baselines, and selecting the model used in coordinate conversion.

In reality, the information in sections 3A and 3B of the Loran-C Signal Specification is tightly-coupled and cannot be neatly separated. Calibration for a baseline should be a four-step process:

- (a) Assign the desired ideal or nominal emission delay to the DMA model.
- (b) Using the DMA model, predict the TD at the Latitude/Longitude for the Alpha-1 SAM.
- (c) Assign this predicted TD as the CSTD for the Alpha-1 SAM.
- (f) For reassurance only, measure the TDs on the extensions of the baseline, or make an emission delay measurement.

Step (d) can be eliminated once confidence is built-up.

The measured emission delay probably will not be the same as the nominal emission delay, but if the primary users and the Alpha-1 SAM cannot tell the difference, who else can? Certainly, a user is not going to navigate on the baseline extensions.

The nominal emission delay for a baseline for any coordinate converting algorithm should simply be that number required by it to produce the CSTDs at SAM (or to produce reference TDs at any reference location). This is basically emission delay by estimation based upon a single measurement.

The user community should be advised via the Signal Specification and the Radionavigation Systems Booklet⁽⁷⁾ that the Coast Guard neither observes nor controls emission delays. Users should simply be told the Latitude and Longitude for the transmitters and the SAM(s) and Alpha 1 SAM CSTDs.

Perhaps the process that has recently been called "calibration" might more accurately be termed "setting," and "calibration" should be reserved for alignment of some standard coordinate conversion model.

IMPLICATIONS OF PROPAGATION VARIATIONS
UPON OPERATIONS.

Monitor location, control, coverage, and charting should be re-examined in the light of our knowledge about seasonal propagation variations and out method of control.

Monitor Location.

The Alpha-1 monitor should be located in the area where the most stable coverage is desired. If there are two or more of these areas, then obviously some compromise is required. The simplest solution is to have one primary coverage area, and provide some sort of seasonal corrections for the others. The lines-of-position over the entire coverage area are best-behaved when the monitor is located toward the middle of the baseline. Care must be taken to insure that the Alpha-1 SAM Loran-C signals are representative of the primary coverage area.

Multiple Monitors.

If there is more than one monitor site, the information from the multiple sites can be combined to provide control. However, it can be shown that the multiple sites could be replaced with a single monitor located at the point as determined by the combining model. We only have one degree of freedom.

Monitor Relocation.

The Alpha-1 SAM defines the baseline as we operate it. If we move the Alpha-1 SAM, we start operating a different baseline. In this case, the new CSTDs should not be determined by a short-term correlation, but rather by the method described above. If data were available for correlation over a full year, it would be possible to transfer the mean emission delay between the two baselines.

Control.

When control is shifted to the Alpha-2 SAM for a short duration, this SAM should probably maintain the average time-differences it was observing just prior to the shift. Assigned Alpha-2 CSTDs would make a baseline bi-stable and cause unnecessary shifts in the LOPs when control is shifted.

Coverage.

Propagation variations, acting through our present control method, create shifts in LOPs, and these shifts increase with hyperbolic separation from the SAM. The accuracy limitation at the

fringe of Loran-C coverage, at least in northern latitudes where there is land in the propagation paths, is probably not poor signal-to-noise-ratio acting through geometry, but rather propagation variations coupled through control and acting through geometry. A new method of calculating coverage diagrams based upon the hyperbolic distance from the SAM and peak seasonal variations will eventually have to be developed.

Charting.

The earth's surface is not homogeneous, so there are spatial variations in the lines of position from the coordinate conversion models. Over the course of a year, the lines of position that are hyperbolically close to the Alpha 1 SAM are very stable; the baseline extension LOPs can vary by a mi crosecond or more. The seasonal variations that have been observed make chart improvements using field measurements somewhat difficult. A method must be devised to separate the seasonal variations from the spatial variations in this field data. One solution is to take measurements several times during the year. The R&D harbor monitor data and the modelling they are doing may provide a means of isolating the temporal from the spatial variations. Certainly, field TD measurements are the only way to learn anything about the coordinate conversion process.

CONCLUSIONS.

Our present chain control philosophy and methods are probably adequate for a majority of the marine users.

Calibrations should be by assignment of CSTDs. They should be specified in terms of the alpha-1 SAM CSTD's and WGS-72 Latitudes and Longitudes for all transmitters and monitors.

The coordinate converter manufacturers and user Community should be better informed on the method we actually use to control the system and its effect upon coordinate conversion.

Emission delay is neither monitored nor controlled by the Coast Guard. It can vary seasonally 0.5 micro-seconds or more.

If emission delays are officially mentioned by the

Coast Guard, they should carry some caveat on their variability. They certainly should not be published with a 0.01 microsecond resolution and accuracy.

Because our current control philosophy permits wide variations in emission delay, it has very little value as a calibration parameter.

There could be a benefit to measuring the Loran-C TDs at known locations in the service area to improve the coordinate conversion methods. However, some means must be devised for taking into account the seasonal variations.

REFERENCES

- (1) TAGGART, D., "THE COAST GUARD'S HARBOR MONITOR PROJECT", Proceedings of the Wild Goose Association Twelfth Technical Symposium, Oct 1983 (to be published)
- (2) WENZEL, R. J. and SLAGLE, D.C., "LORAN-C SIGNAL STABILITY STUDY: NEUS/SEUS," USCG R&D REPORT CG-D28-83 (to be published)
- (3) "SPECIFICATION OF THE TRANSMITTED LORAN-C SIGNAL", USCG COMDTINST M16562.4, JULY 1981
- (4) "MINIMUM PERFORMANCE STANDARDS (MPS) AUTOMATIC COORDINATE CONVERSION SYSTEMS" Report of RTCM Special Committee No. 75, Radio Technical Commission for Marine Services, RTCM Paper 378-81/DO-10, Nov 1981
- (5) NEWMAN, J. N. "LORAN NAVIGATION WITH A HAND CALCULATOR", collected papers of The New England Sailing Yacht Symposium, March 1980
- (6) McCULLOUGH, J.R., IRWIN, B. J., and BOWLES, R.M., "LORAN-C LATITUDE-LONGITUDE CONVERSION AT SEA: PROGRAMMING CONSIDERATIONS", Proceedings of the Wild Goose Association Eleventh Technical Symposium, Oct. 1982.
- (7) "RADIONAVIGATION SYSTEMS" Commandant (G-NRN) USCG, Washington, D.C. (published periodically).

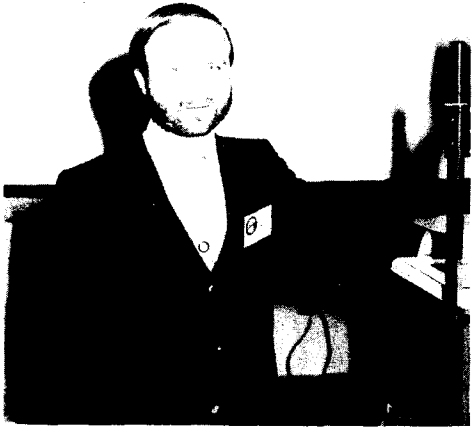
SESSION FOUR SPEAKERS



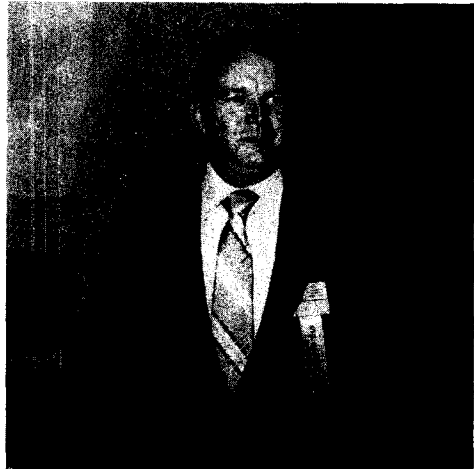
LT Jim Iverson



Jim Leighton



Jeff Stuart



Bill Mooney



David Burnham and Al Frost



LCDR Bill Thrall

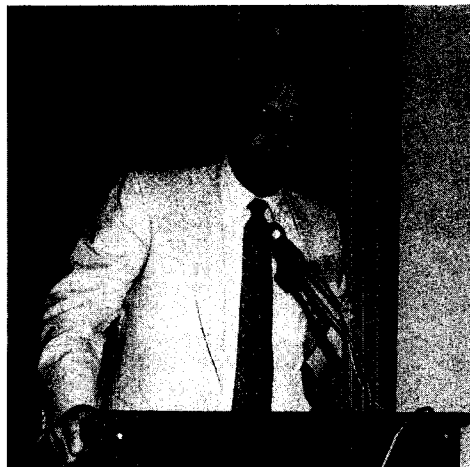
SESSION FIVE
CALIBRATION ASF & PREDICTABILITY



BOB TILL, MODERATOR



PANEL DISCUSSION



JACK LIGON



President Carl Andren



General Chairman Bob Schellhase



Technical Chairman Hal Sherman

CONVENTION SCENE AND AWARDS

GUEST SPEAKERS



James Constantino
Transportation Systems Center



RADM Al Manning, USCG Headquarters



David Julyan, Navigation Sciences Inc



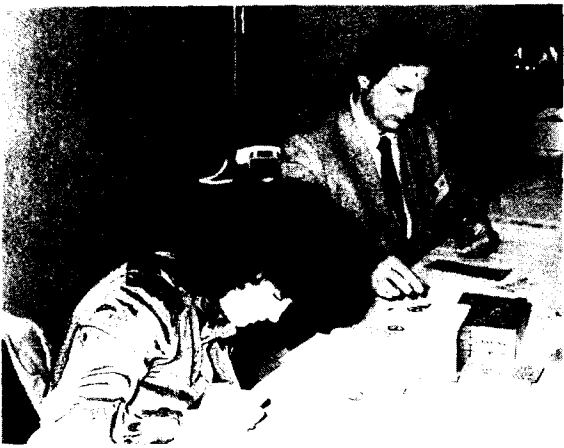
Mike Eaton receiving the Medal of Merit



Dave Carter being presented with the Service Award



Best Paper Award: Jim McCullough, Barry Irwin and Robert Bowles (McCullough accepting)



REGISTRATION



CONCENTRATION



CONVERSATION



RELAXATION

REGISTERED ATTENDANCE
WILD GOOSE ASSOCIATION 12th ANNUAL TECHNICAL SYMPOSIUM
WASHINGTON, D.C
OCTOBER 12-14, 1983

Tom Jerardi, APL/JHU
10852 Green Mtn. Ct.,
Columbia MD 21044

Robert M. Bowles, US Geological Survey
Quissett Campus,
Woods Hole MA 02543

Lorraine Pinette, Megapulse
8 Preston Ct,
Bedford

James R. McCullough, Woods Hole
37 Saconneset Rd.,
Falmouth MA 02543

Robert Lobecker, SAI
379 Thames,
Newport RI 02840

Martin A. Lettis, USCG
22 Fieldview Dr.,
North Cape May NJ 08204

Robert McKeown, ITT Avionics
500 Washington Ave.,
Nutley

David Wells, 538 Squires St.
Fredericton NB,
Canada E3B3VA

Michael W. DuBose, USCG COCO/SEUS
USCG LORSTA,
Malone FL 32446

Frank Cassidy, Datamarine International
53 Portside Dr.,
Pocasset MA 02559

Vester Scott, Technical Writer
1375 Barnes Dr. East,
Columbus Ohio 43229

Doug Taggart, USCG R&D Center
Avery Pt.,
Groton CT. 06340

Larry Sartin, ASEC
Old Concorde Rd.,
Burlington Mass.

Capt. Richard H. Wight, USCG
USCG R&D Center,
Avery Point Groton CT 06340

Paul Johannesen, Megapulse Inc.
8 Preston Ct.,
Bedford Mass. 01730

Gerald Sage, Navigation Tech
2327 Double O Mine Trail,
Cool CA 95614

Mortimer Rogoff, Navigation Science Inc.
6900 Wisconsin Ave. Suite 301,
Bethesda MD 20815

F. W. Mooney, TSC
2 Surf St.,
Marblehead MA 01945

Frank McMullan, Kaman Tempo
1613 University Blvd. NE,
Albuquerque NM 87110

Robert C. Imler, USCG EECEN
USCG EECEN,
Wildwood NJ 08260

John McKeever, USCG
G-TES-4,
Washington DC 20593

Paul Arnstein, USCG
G-TES-4,
Washington DC 20593

Ed Bregstone, USCG
2607 Central Ave.,
Alexandria VA 22302

Fred Garland III, USCG
12416 Parkton St.,
Ft. Washington MD 20744

Robert Erikson, FAA Technical Center
Atlantic City Airport,
Atlantic City NJ 08405

Tony Pealer, DOT / RSPA
Room 8409: 400 7th St.SW,
Washington DC 20590

P.D. Gibbs, Foster Airdata Systems Inc.
7020 Huntley Rd.,
Columbus Ohio 43229

J.P. Van Etten, ITT Avionics Div.
500 Washington Ave.,
Nutley NJ 07110

John J. Speight, Defence Mapping Agency HTC
6500 Brookes Ln.,
Washington DC 20315

Lewis C. Phillips, Defence Mapping Agency HTC
6500 Brookes Ln.,
Washington DC 20315

Edward Danford, Defence Mapping Agency HTC
6500 Brookes Ln.,
Washington DC 20315

G.R. Westling, USCG Academy
USCG Academy,
New London CT 06320

Hatcher E. Chalkley, Texas Instruments
PO Box 405 MS 3439,
Lewisville TX 75067

Leo Fehlner, JHU / APL
118 Quaint Acres Dr.,
Silver Spring MD 20904

Vernon I. Weihe, WGA
4133 N. 33rd Rd.,
Arlington VA 22207

Edward Antuowiak, Bowditch Navigation
40 Pleasant St.,
Portsmouth NH

Capt. James F. Culbertson, U.S. Coast Guard
15781 Exeter St.,
Westminster CA 92683

Tom Nolan, Maritime Institute
5700 Hammonds Ferry Rd.,
Linthicum Hts. MD 21090

Jimmie L. Toms, Advanced Navigation Inc.
621 Lofstrand Ln.,
Rockville MD 20850

Bruce O. Francis, Advanced Navigation Inc.
621 Lofstrand Ln.,
Rockville MD 20850

Charles J. Baltzer, Advanced Navigation Inc.
621 Lofstrand Ln.,
Rockville MD 20850

Bill Marchal, Offshore Navigation Inc.
Box 23504,
New Orleans LA 70183

Martin Poppe Jr., Cambridge Engineering Inc.
Box 66,
Cambridge VT 05444

William Garmany Jr., ITT Avionics Div.
500 Washington Ave.,
Nutley NJ 07110

W.M. Swartwood, Defense Mapping Agency
6500 Brookes Ln.,
Washington DC 20315

Cdr. Roger W. Hassard, USCG R&D Center
Avery Point,
Groton CT 06340

Joseph Hersey, U.S. Coast Guard
3901 Oaklawn Rd.,
Oxon Hill MD 20744

James D. Kelly, TASC
1 Jacob Way,
Reading MA 01867

Robert D. Till, FAA Technical Center
Atlantic City Airport,
Atlantic City NJ 08405

Larry Cortland, Teledyne Systems
19601 Nordhoff St.,
Northridge CA 91324

Bill Burgin, SI-TEX Marine Electronics
Box 6700,
Clearwater FL 33518

T. Fujino, SI-TEX Marine Electronics
Box 6700,
Clearwater FL 33518

Jeffrey S. Stuart, National Ocean Service
128 Spring St.,
Gaithersburg MD 20877

Jack Ivers,
17 Oxford Terrace,
Westwood MA 02090

Mike Evans, Western Research
PO Box 2469,
Houston TX 77252

R.E. Burke Jr., USCG EECEN
6 New Vernon Ave.,
Ocean View NJ 08230

J. Ralph Johler, CRPLi
PO Box 1056,
Boulder CO 80306

Alan R. Cook, CRPLi
PO Box 1056,
Boulder CO 80306

John M. Beukers, Beukers Laboratories Inc.
Flowerfield Building #7,
St. James NY 11780

Mike Eaton, Canadian Hydrographic Service
PO Box 1006,
Dartmouth NS Canada B2Y 4A2

Capt. John Maloney, USCG
U.S. Coast Guard (G-TD/64),
Washington DC 20593

Edward L. McGann, Megapulse Inc.
8 Preston Court,
Bedford MA 01730

Carl S. Andren, Megapulse Inc.
Suite 400 Walker Bldg. 734 15th St. NW,
Washington DC 20005

Carl E. Faflick, Megapulse Inc.
8 Preston Court,
Bedford MA 01730

Herbert L. Brown, Megapulse Inc.
8 Preston Court,
Bedford MA 01730

Robert D. Bronson, II Morrow Inc.
PO Box 13549,
Salem OR 97309

Bahar Uttam, Jaycor
205 S. Whiting St. Suite 607,
Alexandria VA 22304

David C. Scull, DOT / RSPA
400 7th St. SW,
Washington DC 20590

David A. Carter, Jaycor
300 Unicorn Park Dr.,
Woburn MA 01801

Charles M. Kenney, ITT Avionics Div.
500 Washington Ave.,
Nutley NJ 07110

William G. Walker, Navigation Sciences Inc.
6900 Wisconsin Ave. Suite 301,
Bethesda MD 20815

Robert Weaver, USCG EECEN
USCG EECEN,
Wildwood NJ 08260

Bob Schellhase, USCG
G-NRN-1,
Washington DC 20593

Capt. D.G. Currier, USCG
G-NRN,
Washington DC 20593

Cdr. Jack Lang, USCG
G-NRN,
Washington DC 20593

LCDR R.A. Kirkman, USCG
G-NRN-3,
Washington DC 20593

LCDR Robert Swart, USCG
G-NRN-2,
Washington DC 20593

LCDR William Thrall, USCG
G-NRN-1,
Washington DC 20593

LT R.L. Gazlay, USCG
G-NRN-3,
Washington DC 20593

LT Hathaway Cornelius, USCG
G-NRN,
Washington DC 20593

LT James Iversen, USCG
G-NRN-1,
Washington DC 20593

LTJG J.A. Budde, USCG
G-NRN-3,
Washington DC 20593

LTJG J.Y. Noblet, USCG
G-NRN-2,
Washington DC 20593

LTJG Robin Orr, USCG
G-NRN-1,
Washington DC 20593

ENS Bruce Serinis, USCG
G-NRN-1,
Washington DC 20593

CWO2 R.J. Gill, USCG
G-NRN-2,
Washington DC 20593

CWO2 G.D. Ziemer, USCG
G-NRN-3,
Washington DC 20593

LT D.J. Houghton, USCG
G-NRN-2,
Washington DC 20593

LT M.P. Selavka, USCG
G-NRN-3,
Washington DC 20593

Dan Andrusiak, USCG
G-NRN-1,
Washington DC 20593

Guy P. Clark, Pharologic Ltd.
1377 K St. NW Suite 841,
Washington DC 20005

Walter N. Dean, ARNAV Systems Inc.
P.O. Box 7078,
Salem OR 97303

Ronald S. Warren, TASC
One Jacob Way,
Reading MA 01867

Leon DePalma, TASC
One Jacob Way,
Reading MA 01867

Dave Clements, US Coast Guard
COMPACAREA (Pt1) Govt. Island,
Alameda CA 94501

Robert Janes, Internav
P.O. Box 1261,
Sydney N.S. Canada

Martin Rothblatt, GEOSTAR
1001 22nd St. NW,
Washington DC 20037

Jack Ligon, USCG
2100 Second St. SW,
Washington DC 20590

Joseph A. Walsh, Maritime Adm.
400 Seventh St. SW (MAR-930),
Washington DC 20590

Michael Butler, USCG
USCG EECEN,
Wildwood NJ 08260

Laura G. Charron, NAVOBSY
34th Mass. Ave.,
Washington DC

Bernard Ambroseno, Epsco Inc.
411 Providence Hgwy,
Westwood MA 02090

Russell A. Doughty, USCG
3604 Northwick Pl.,
Bowie MD 20716

David Underwood, Motor Boating & Sailing Magazine
Box 310 CARP,
Ontario Canada KOA 1L0

Stephen C. Hung, DOT/St. Lawrence Seaway
800 Independence Ave. SW,
Washington DC 20591

R. G. Roll, APL/JHU
3804 Kelsey St.,
Silver Spring MD

K. L. Fuller, RACAL-DECCA Ltd.
118 Burlington Rd.,
New Malden Surrey UK

Daniel H. Tillotson, ARINC Research
2551 Riva Rd.,
Annapolis MD 21401

Capt. W.H. Hayes, USCG EECEN
USCG EECEN,
Wildwood NJ 08260

Kurtis L. Maynard, John E. Chance & Assoc.
P.O. Box 52029,
Lafayette LA 70505

William O'Halloran, Jaycor
300 Unicorn Park Drive,
Woburn MA 01801

Robert L. Frank, Consultant
30795 River Crossing,
Birmingham MI 48010

Vernon L. Johnson, ITT Avionics
500 Washington Avenue,
Nutley NJ 07110

W.C. Beanland,
4515 Willard Ave. Apt. 2214 So.,
Chevy Chase MD 20815

Lloyd D. Higginbotham, Consultant
4 Townsend Rd.,
Acton MA 01720

Albert D. Frost, Electrical Engr. Dept.
UNH Dept. of Electrical and
Computer Engr.,
Durham NH 03824

Capt. Phillip J. Kies, USCG
ICAF,
Ft. McNair

Ed Cooper, ARNAV Systems
4740 Ridge Dr. NE,
Salem OR 97303

Per Enge, Megapulse
8 Preston Ct.,
Bedford MA 01730

David Gray, CDN. Hydrographic
615 Booth St.,
Ottawa Canada

Kenn Zemejda, Applied Physics Lab.
Johns Hopkins Rd.,
Laurel MD

Doc Ewen,
60 Beaver Rd.,
Weston

Patricia Anne Angus, Census Bureau
Bureau of Census,
Washington DC

James I. Leighton, TASC
1 Jacob Way,
Reading MA 01867

J.C. Rennie, Canadian Cost Guard
FL5 TWR A Place de Ville,
Ottawa Canada K1A0N7

John C. Fuechsel, N.O.I.A.
1050 17th St. NW Suite 700,
Washington DC 20036

Harold T. Sherman, ITT Avionics Div.
500 Washington Avenue
Nutley NJ 07110



"They told me Boston is north.
Now I wonder which"

ACKNOWLEDGEMENTS

SUPER SPONSORS

ITT Avionics Division

Jaycor

Megapulse, Inc

SPONSORS

Advanced Navigation Inc

ARNAV Systems

ASEC

Beukers Labs

Cambridge Engineering

Dahl Loran Service

EPSCO

Micrologic

Offshore Navigation Inc

Singer/Kearfott

TASC

Texas Instruments

BOOSTERS

Robert L. Frank, Consultant

Kaman - Tempo

The Wild Goose Association extends thanks and appreciation to ITT Avionics Division, Nutley NJ for publishing these Proceedings